

Inorganic solid state aspects of coordination
polymers: synthesis, structure and properties
of new transition metal complexes.



PhD thesis submitted to the
Faculty of Mathematics and Natural Sciences
of the Christian Albrechts University of Kiel

for the degree of
Doctor rer. nat.

submitted by

Gaurav Vikram Bhosekar, M.Sc.

Kiel, December 2007.

Examiner:

PD Dr. Christian Näther

Co-examiner:

Prof. Dr. Wolfgang Bensch

The Dean

Affirmation

I declare that the work presented here was performed by myself, under the supervision of my scientific tutor, only using the devices, resources and media mentioned in the thesis. The PhD thesis is solely submitted to the University of Kiel.

Gaurav Vikram Bhosekar

Kiel, December 2007.

Content

1	Introduction	1
1.1	Goals and problems in the area of coordination polymers, inorganic-organic hybrid compounds and metal organic frameworks.....	1
1.2	Thermal decomposition reactions as an alternative procedure for the preparation of coordination compounds and polymers.....	2
1.3	Starting point: Synthesis, structures and properties of coordination polymers based on copper(I) halides and N-donor ligands.....	2
1.4	Major goals of the thesis: Investigations on Zn(II) halide coordination compounds.....	18
1.5	References.....	23
2	Publications	31
2.1	On the Preparation of Coordination Polymers by Controlled Thermal Decomposition: Synthesis, Crystal Structures and Thermal Properties of Zinc Halide Coordination Polymers..... Gaurav Bhosekar, Inke Jeß and Christian Näther..... <i>Inorg. Chem.</i> , 2006, 43, 6508-6515.....	31
	Supplemental material.....	39
2.2	Preparation of stable and metastable coordination compounds: Insight into the structural, thermodynamic and kinetic aspects of the formation of coordination polymers..... Christian Näther, Gaurav Bhosekar and Inke Jeß..... <i>Inorg. Chem.</i> , 2007, 46, 8079-8087.....	57
	Supplemental material.....	66
2.3	Synthesis, crystal structures and thermal properties of new ZnBr ₂ (Pyrimidine) coordination compounds..... Christian Näther, Gaurav Bhosekar and Inke Jeß..... <i>Eur. J. Inorg. Chem.</i> , 2007, in press.....	90
	Supplemental material.....	97
2.4	Dibromo-bis(pyridazine-κN)zinc(II)..... Gaurav Bhosekar, Inke Jeß and Christian Näther..... <i>Acta Crystallogr.</i> , 2006, E62, m1859-m1860.....	113
	Supplemental material.....	115

2.5	Diiodo-bis(pyridazine- κ N)zinc(II).....	118
	Gaurav Bhosekar, Inke Jeß and Christian Näther.....	
	<i>Acta Crystallogr</i> , 2006, <i>E62</i> , m2073-m2074.....	
	Supplemental material.....	120
2.6	Structures and Properties of three Polymorphic Modifications based on tetrahedral Building Blocks of Dichloro-bis(pyridazine-N) zinc(II).....	123
	Gaurav Bhosekar, Inke Jeß, Zdenek Havlas and Christian Näther.....	
	<i>Cryst. Growth & Des.</i> , 2007, in press.....	
	Supplemental material.....	131
2.7	Two Polymorphic Modifications of Dibromo-bis(acetonitrile-N)-zinc(II).....	147
	Gaurav Bhosekar, Inke Jeß and Christian Näther.....	
	<i>Z. Naturforsch.</i> , 2006, <i>61b</i> , 721-726.....	
	Supplemental material.....	153
2.8	A redetermination of (acetonitrile- κ N)diiodozinc(II).....	157
	Gaurav Bhosekar, Inke Jeß and Christian Näther.....	
	<i>Acta Crystallogr.</i> , 2006, <i>E62</i> , m315-m316.....	
	Supplemental material.....	159
2.9	Synthesis, Crystal Structure and Thermal Reactivity of [ZnX ₂ (2-chloropyrazine)] (X = Cl, Br, I) Coordination Compounds.....	162
	Gaurav Bhosekar, Inke Jeß, Nicolai Lehnert and Christian Näther.....	
	<i>Eur. J. Inorg. Chem.</i> , 2007, in press.....	
	Supplemental material.....	169
3	Contribution to conferences.....	188
3.1	Synthesis, Crystal Structures and thermal Behavior of Zn(II) halide Pyrimidine Coordination Polymers.....	188
	Gaurav Bhosekar, Inke Jeß and Christian Näther.....	
	13 th Meeting of the GDCh Section "Solid State Chemistry": Modelling in Solid State and Material Chemistry 2006, Aachen.....	
3.2	Thermal Decomposition Reactions for the Discovery and preparation of New stable and metam stable ZnI ₂ (pyrimidine) Coordination compounds.....	189
	Gaurav Bhosekar, Inke Jeß and Christian Näther.....	
	9 th Meeting of the North German Universities, 2006, Warnemünde.....	
3.3	Synthesis, Crystal Structures and thermal Behavior of Zn(II) halide Pyrimidine Coordination Polymers.....	190
	Gaurav Bhosekar, Inke Jeß und Christian Näther.....	

	36 th National Seminar on Crystallography held at Department of Chemistry, Anna University, Chennai, India from 22-24 January 2007.....	
3.4	Investigations on the trimorphism of dichlorobis(pyridazine-N)zinc(II)..... Gaurav Bhosekar, Inke Jeß and Christian Näther..... 4 th Meeting of the German Crystallographic Society, 2007, Bremen.....	191
3.5	Polymorphic modifications of dichloro-bis(pyridazine-N) zinc(II)..... Gaurav Bhosekar, Inke Jeß and Christian Näther..... 10 th Meeting of the North German Universities, 2006, Bremen.....	192
4	Summary.....	193
5	Appendix.....	202
5.1	List of publications.....	202
5.2	Contribution to conferences.....	204
5.3	Scientific lectures.....	205
5.4	Resume	206
5.5	Acknowledgement.....	207

1. Introduction

1.1 Goals and problems in the area of coordination polymers, inorganic-organic hybrid compounds and metal organic frameworks

In the last few years, the preparation of new coordination polymers, inorganic-organic hybrid compounds or metal organic frameworks has become of increasing interest [1-3]. One major goal in this area is the preparation of compounds with desired physical properties [4-6] like conducting [7-9], porous [5, 9-21], magnetic [22-29], catalytic [30-34] or NLO materials [35] and luminophores [36-41]. However, to reach this goal several problems have to be overcome: First of all structure-property relationships must be investigated in detail, which is frequently difficult to achieve. Furthermore, strategies for a more directed design of the structures of these solids must be developed, in order to influence their physical properties in a desired way [42-56]. This is a real challenge in this area and needs a specific knowledge of the interactions in crystals and their interplay [57]. In this context one has to be aware of the phenomenon of polymorphism or isomerism which is frequently found in such compounds and which makes "Crystal Engineering" so difficult [57-64].

Moreover, for any characterization or application of a new compound the preparation of large and pure amounts of this materials is required, which is very often difficult to achieve. In most cases such compounds are prepared in solution [65-66] and there are only some examples where coordination compounds are prepared in the solid state [67-69]. Because in solution different species are in equilibrium, isolating of the solids very often leads to mixtures of different compounds, which only in some cases can be separated by hand. However, there is absolutely no doubt, that manual separation is an unacceptable method for the preparation of larger amounts of a compound, especially if these materials should be used for any further application. Therefore, much synthetic effort must be spend afterwards to overcome this problem, which in some cases might be unsuccessful. Furthermore, in some cases thermodynamically metastable compound can be overlooked or cannot be prepared if the synthesis is performed in solution. Therefore, additional methods for the preparation and the discovery of new or known, metastable or stable coordination compounds would really be helpful.

1.2 Thermal decomposition reactions as an alternative tool for the preparation of coordination compounds

One interesting method for the discovery or pure preparation of coordination polymers can be thermal decomposition reactions of suitable precursor compounds, which was shown by Näther et al [70-94]. As this is a typical solid state method it is normally not used in coordination chemistry. However compared to other synthetic approaches, this method has several advantages.

In this method a ligand rich compound is heated until the ligand vaporizes. In most cases ligand deficient intermediate compounds can be isolated before all ligands are removed. The intermediate compounds thus obtained are very pure and with 100% yield. Because the ligand is irreversibly removed, the equilibrium is shifted completely in the direction of the ligand deficient phases, which in most cases is not possible if compounds are prepared in solution. Therefore, also metastable compounds can be discovered and prepared.

One disadvantage is that part of the ligands used in the synthesis get lost during preparation. However, in some cases ligand rich precursor compounds can be prepared that contain additional solvent which is used in the synthesis. In this case only this solvent is removed and the stoichiometry of the ligand deficient phase is predefined. It is also obvious that this method depends on the thermal stability of the ligands and therefore, not all ligands can be removed. However, we showed that a large number of different ligands can be used and that the outcome of such experiments can strongly be influenced by the experimental conditions.

1.3 Starting point: Synthesis, structures and properties of coordination polymers based on copper(I) halides and N-donor ligands

One class of coordination polymers is based on copper(I)halides and N-donor ligands [70-164]. These compounds are very often red to yellow colored with some of them showing luminescence and thermoluminescence. The crystal structures of these coordination polymers are based on inorganic CuX substructures (X = halide or pseudo halide) which are linked by the organic ligands into multidimensional coordination polymers. Depending on the copper(I) halide or pseudo halide and the nature of the organic ligand, different CuX substructures e. g. monomers [95-102], dimers [103-117], zig-zag- or helical single chains [118-127], double chains [128-147], 6-membered rings [148-149], 8-membered rings and cubes [150-155] or more complicated CuX substructures [156-162] are observed (figure 1). The compounds with helical chains are of special interest because several of them crystallize in chiral space groups and therefore, are promising candidates for e. g. non-linear optical properties.

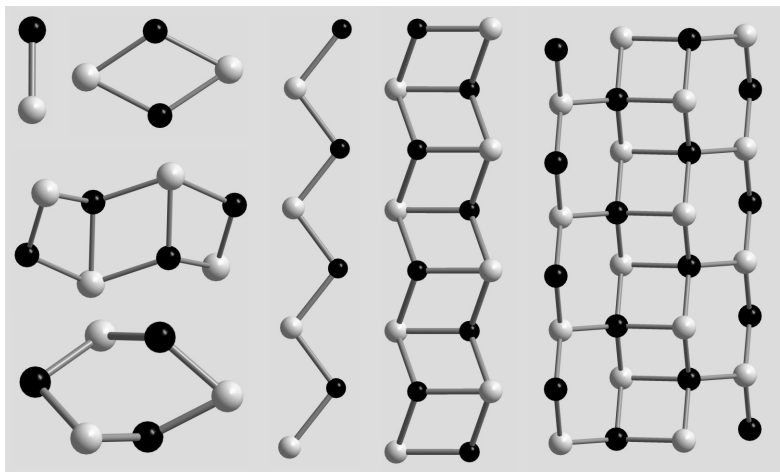


Figure 1: Examples for different CuX-substructures in CuX coordination polymers (X = Cl, Br, I) with N-donor ligands.

The dimensionality of the coordination network can be influenced predominantly by the coordination properties of the organic ligands. If donor ligands with only one nitrogen donor atom are used, 1-dimensional coordination networks are commonly observed (figure 2: left), whereas for a bidentate ligand a layer-like coordination network is mainly found (figure 2: right).

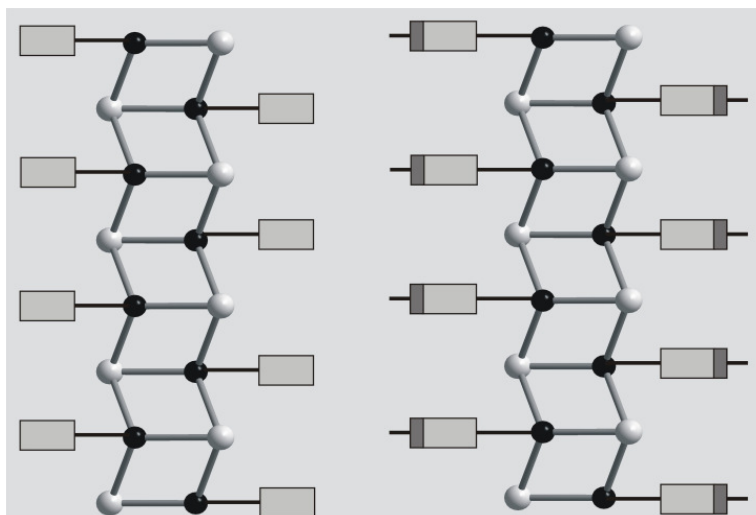


Figure 2: Examples for a 1-dimensional (left) and a 2-dimensional (right) coordination network in CuX coordination polymers with N-donor ligands.

For one definite copper(I) halide or pseudo halide and one specific ligand, frequently several compounds are found, which differ in terms of ratio between the inorganic and organic part. Therefore, e. g. 1:2, 1:1; 3:2, 2:1 or 4:1 compounds are found, which are called in the following ligand rich and ligand deficient compounds. Which compound is obtained in the

synthesis depend predominantly on the temperature and the stoichiometry of the reactants. In several cases only mixtures of different compounds are obtained or one specific compound cannot be prepared in solution. However, during the investigations on the thermal properties of such compounds it was found that most of the ligand rich CuX compounds can be quantitatively transformed into ligand deficient compounds via controlled thermal decomposition [70-94]. In the beginning this was found for the CuX coordination polymers with pyrazine [70].

With pyrazine two different compounds based on copper(I)chloride were described independently [121-122, 136]. At first, both compounds were obtained by accident in extremely complex reactions and were only characterized by X-ray diffraction. The structure of the ligand rich 1:1 compound poly[CuCl(μ_2 -pyrazine-N,N')] consists of "zig-zag"-like CuCl single chains which are connected via μ -N,N' coordination into layers (figure 3: left) [121-122]. In the ligand deficient 2:1 compound poly[(CuCl) $_2$ (μ_2 -pyrazine-N,N')] CuCl double chains are found which are linked into layers by the pyrazine ligands (figure 1: right) [136]. The crystal structures of the 1:1 compound with CuBr [126] and of the 2:1 compound with CuBr [140] and CuI [143] were also characterized and showed a similar topology of the coordination network as the 1:1 and the 2:1 compounds with CuCl.

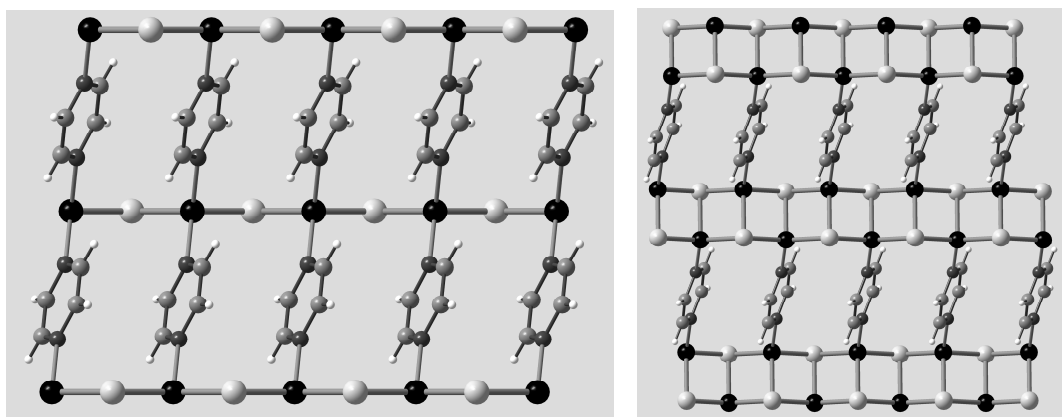


Figure 3: Crystal structure of poly[CuCl(μ_2 -pyrazine-N,N')] (left) and poly[(CuCl) $_2$ (μ_2 -pyrazine-N,N')] (right).

All the compounds can be easily prepared by the direct reaction of the copper(I)halides with pyrazine in different solvents. If the reaction is performed in solution the ligand 1:1 compounds with CuCl and CuBr can be obtained in large amounts and very pure, whereas the corresponding ligand deficient 2:1 compounds are always obtained as mixtures of the 1:1 and the 2:1 compound. If pyrazine is reacted with CuI, only the ligand deficient 2:1 compound is obtained pure, whereas the ligand rich compound cannot be prepared.

However, if the compound with CuCl is heated in a simultaneous DTA-TG apparatus two mass steps are observed in the TG curve which are accompanied with two endothermic events in the DTA curve (figure 4: top left). The experimental mass loss of each step is in good agreement with that calculated for the loss of half of the pyrazine ligands. The residue of this reaction was identified as pure copper(I)chloride. If the residue after the first TG step is investigated by elemental analysis X-ray powder diffraction it is proven that a very pure ligand deficient 2:1 compound poly[(CuCl)₂(μ₂-pyrazine-N,N')] is formed. (figure 4: top: right). Temperature dependent X-ray powder diffraction measurements gave no hint for additional phases and shows that the 2:1 compound decomposes to CuCl on further heating (figure 4: bottom).

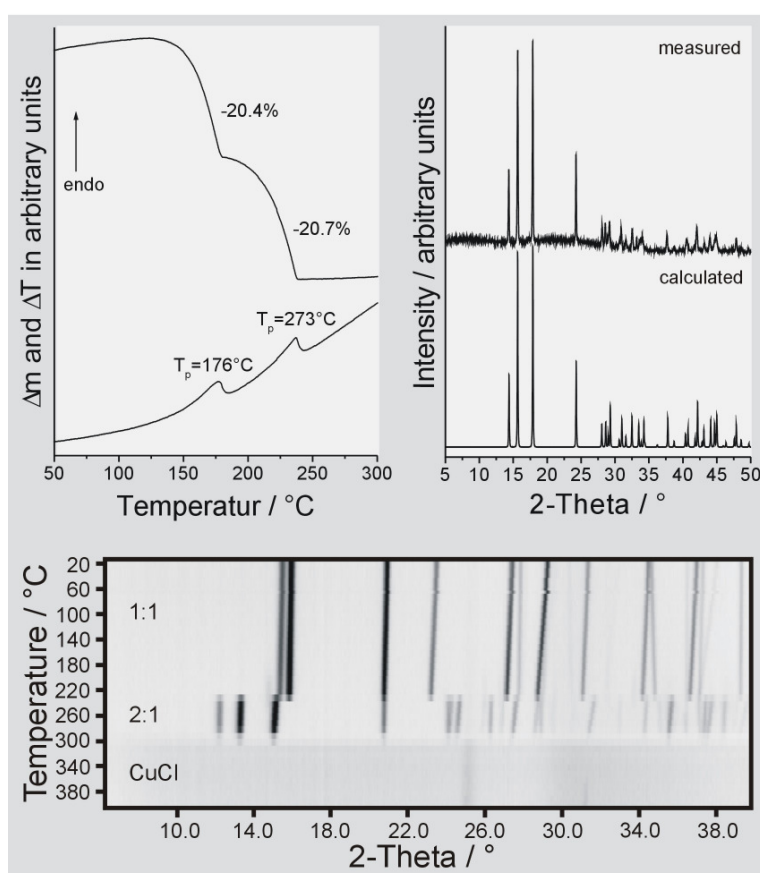


Figure 4: DTA-TG curve for the 1:1 compound poly[CuCl(μ₂-pyrazine-N,N')] (top left), experimental X-ray powder pattern for the residue obtained after the first TG step in the measurement of poly[CuCl(μ₂-pyrazine-N,N')] and calculated pattern for the 2:1 compound poly[(CuCl)₂(μ₂-pyrazine-N,N')] (top right) as well as results of the temperature dependent X-ray powder measurements for poly[CuCl(μ₂-pyrazine-N,N')] (bottom).

In further investigations it was shown that the 1:1 compound with CuBr reacts in a similar way. This was a very helpful reaction, because for the first time the ligand deficient 2:1 compounds with CuCl and CuBr were prepared pure which is not possible in solution. These

results clearly show that new CuX coordination polymers can be prepared by thermal decomposition and that this method is an adequate alternative to the preparation in solution.

Starting from these findings systematic investigations on the synthesis, crystal structures and thermal properties of CuX coordination polymers were started in the group of Näther et al.

Investigations on the thermal properties of CuX(4,4'-bipyridine) coordination polymers

To prove if this method is useful only for the preparation of the CuX(pyrazine) coordination polymers or could also be used for the preparation of different CuX coordination polymers, Näther et. al. studied CuX coordination polymers with the linear ligand 4,4'-bipyridine [82].

The ligand rich 1:1 compounds poly[CuX(μ_2 -4,4'-bipyridine-N,N')] (X = Cl [105], Br [137] and I [142-143]), shows a CuX substructure and a topology of the coordination network which is completely different to those of the ligand rich 1:1 compounds with pyrazine (figure 5: left). (CuI)₂ dimers are found as the substructure which are connected by the 4,4'-bipyridine ligands into a pseudo-hexagonal layer structure (figure 5: left).

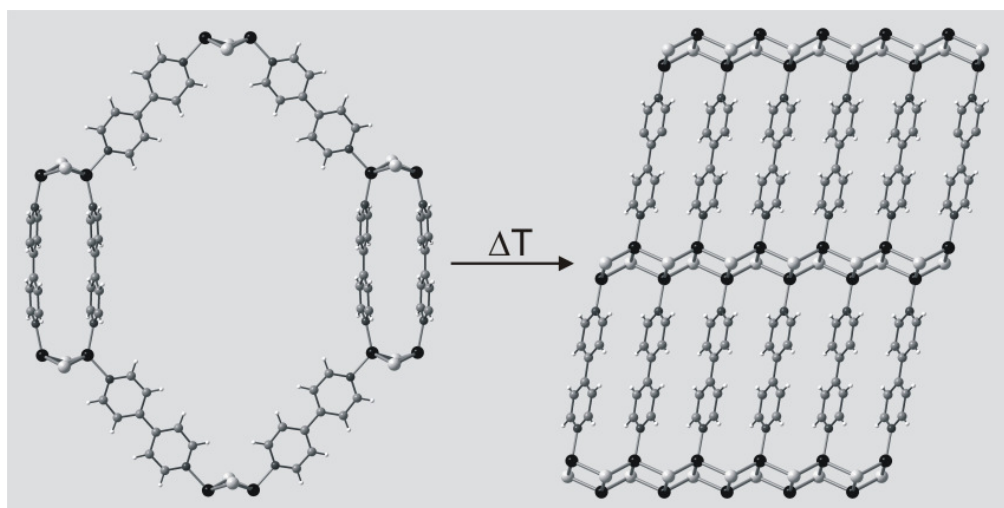


Figure 5: Structural changes during the thermal decomposition of the ligand-rich 1:1-compounds poly[CuX(μ_2 -4,4'-bipyridine-N,N')] into poly[(CuX)₂(μ_2 -4,4'-bipyridine-N,N')].

In contrast, the crystal structures of the ligand deficient 2:1 compounds poly[(CuX)₂(μ_2 -4,4'-bipyridine-N,N')] (X = Cl [137], Br [137, 142] and I [82]) shows a coordination topology which is identical to those in the ligand deficient 2:1 compounds with pyrazine. CuX double chains are found which are connected into layers by the 4,4'-bipyridine ligands (figure 5: right).

On heating the ligand rich 1:1 compounds with 4,4'-bipyridine it transforms quantitatively into the ligand deficient 2:1 compounds before decomposition into copper(I) halides is observed [82]. This result shows clearly that this method can also be used for the preparation of other coordination compounds and is not limited to the preparation of pyrazine coordination polymers. These investigations also show that there is no simple relationship between the structure of the starting and the final compound and their thermal reactivity.

Thermal properties of structural related CuX coordination polymers with 2-methylpyrazine and 2-chloropyrazine

In the investigations described above the thermal behavior of CuX compounds with 4,4'-bipyridine were studied in which the structure of the ligand rich compound is completely different from that of the CuX compounds with pyrazine. In further investigations ligand rich compounds were investigated which forms an identical topology of the coordination network. In this context one suitable ligand is 2-methylpyrazine. The CuX (X = Cl, Br, I) compounds were previously structurally characterized [120]. As expected the 1:1 compounds with CuCl and CuBr shows structures in which the coordination topology is identical to those of the compounds with pyrazine (compare figure 3: left and figure 6: left). In contrast to the pyrazine compounds, in the 2-methylpyrazine compounds the relative orientation of the 2-methylpyrazine ligands alternates leading to a doubling of one crystallographic axis. The structures of the 2:1 compounds with CuBr and CuI are also similar to those with pyrazine. CuX double chains occur which are connected into layers by the ligand (compare figure 3: right and figure 6: right). As in the 1:1 compounds the relative orientation of the methyl groups alternate. Unfortunately the structure of the 2:1 compound with CuCl is not known.

On heating the ligand rich 1:1 compounds with CuX (X = Cl, Br, I) and 2-methylpyrazine, decompose into the ligand deficient 2:1 compounds, which reacts on further heating resulting in the copper(I) halides [81]. Even if the structure of the 2:1 compound with CuCl is not known these investigations clearly shows that it is formed during the reaction. The thermal reactivity of the 2-methylpyrazine compounds is not very surprising because their structures are comparable to those of the compounds with pyrazine.

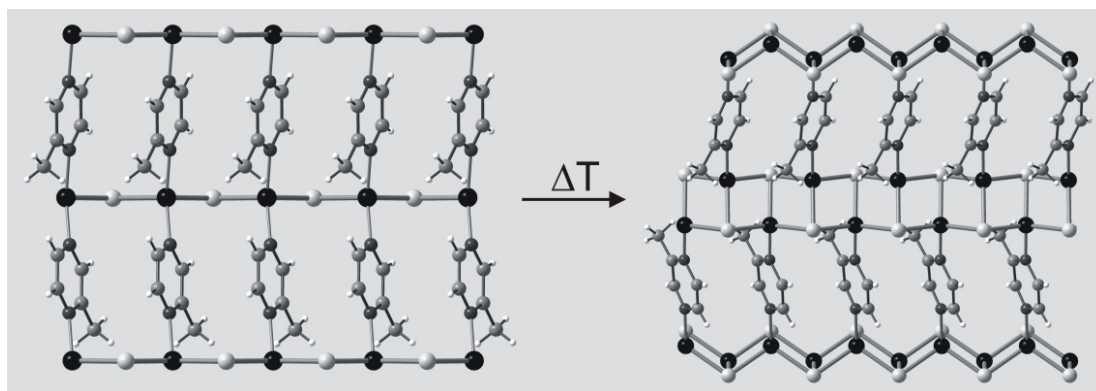


Figure 6: Structural changes during the thermal decomposition of poly[CuX(μ_2 -2-methylpyrazine-N,N')] (X = Cl, Br) (left) into poly[(CuCl) $_2$ (μ_2 -pyrazine-N,N')] (X = Br, I) (right).

In further studies the properties of the coordination polymers with 2-chloropyrazine were studied due to the following reason. If a methyl group in the ligand is exchanged by a chloro atom similar crystal structures are expected. In several cases isotopic compounds are obtained which is known as the chloro-methyl exchange rule [57]. The reason for this behaviour can be regarded to similar van der Waals radii of a methyl group and a chloro atom and the fact, that methyl groups or chloro atom very often behave isotropic in crystal structures.

If the copper(I) halides are reacted with 2-chloropyrazine 1:1 compounds are obtained, which in the case of CuCl and CuBr are isotopic. As expected their crystal structures are similar to those of the corresponding compounds with 2-methylpyrazine but they are not isotopic (figure 7: left). In contrast to the coordination polymers with 2-methylpyrazine, in the 2-chloropyrazine compounds the arrangement of the chloro atom is slightly different and does not alternate.

Surprisingly the crystal structure of the CuI compound with 2-chloropyrazine is completely different. CuI double chains occur and the 2-chloropyrazine ligand does not act as a bridging ligand (figure 7: right). However, it is frequently found in such compounds that the structures of the CuCl and CuBr coordination polymers are similar whereas the CuI compounds shows completely different crystal structures or a different topology of the coordination network.

The thermal behaviour of poly[CuX(μ_2 -2-chloropyrazine-N,N')] (X = Cl, Br) is completely different from that of the 2-methylpyrazine coordination polymers [74, 81]. On heating, both compounds decompose directly to the copper(I) halides without the formation of a ligand deficient intermediate phase (figure 7: top and mid) [74]. In contrast, the ligand rich 1.1 compound catena[CuI(2-chloropyrazine-N)] which exhibit a completely different structure transform into the new ligand deficient 2:1 compound poly[CuI(μ_2 -2-chloropyrazine-N,N')] [74] (figure 7: bottom).

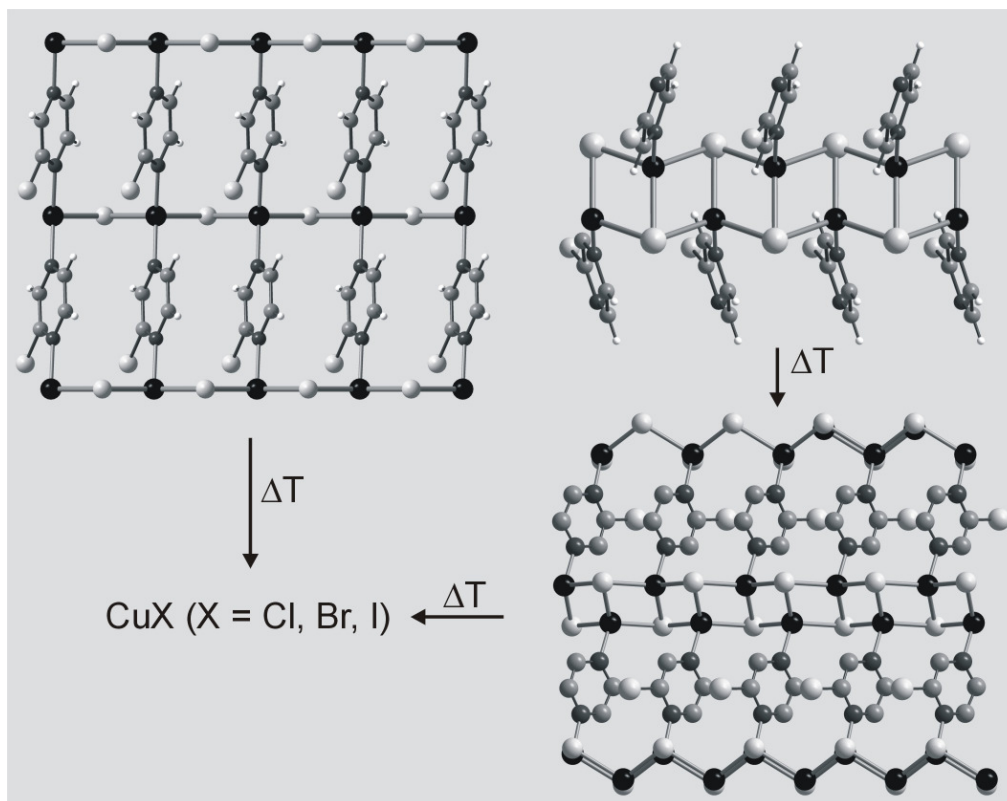


Figure 7: Structural changes during the thermal decomposition of poly[CuX(μ_2 -2-chloropyrazine-N,N')] (X = Cl, Br) (left) and catena[CuI(μ_2 -2-chloropyrazine-N)] (right).

Several intermediate phases during a thermal decomposition: CuX coordination polymers with 2,5-dimethylpyrazine

In all of the reactions mentioned above only the decomposition of a ligand rich 1:1 into a ligand deficient 2:1 compound is observed before the copper(I) halides has formed, which means that only one ligand deficient intermediate phase is observed in these cases. However, in some cases several ligand deficient intermediate phases can be obtained, which was observed for the coordination polymers with 2,5-dimethylpyrazine [75].

Altogether four different compounds were structurally characterized. In the 1:1 compounds poly[CuCl(μ_2 -2,5-dimethylpyrazine-N,N')] and poly[CuBr(μ_2 -2,5-dimethylpyrazine-N,N')] dimers occur which are connected by the 2,5-dimethylpyrazine ligands into layers (figure 8: top). Both compounds are not isotypic but show an identical coordination topology. The 1:1 compound with CuI cannot be prepared. The ligand deficient 2:1 compounds poly[(CuX) $_2$ (μ_2 -2,5-dimethylpyrazine-N,N')] where X = Br and I are isotypic and consists of CuX double chains which are connected by the 2,5-dimethylpyrazine ligands into layers (figure 8: bottom:

left). On heating only two mass steps are observed for the CuCl compound of which the first correspond to the formation of the ligand deficient 2:1 compound and the second to the formation of CuCl (figure 8: bottom right.)

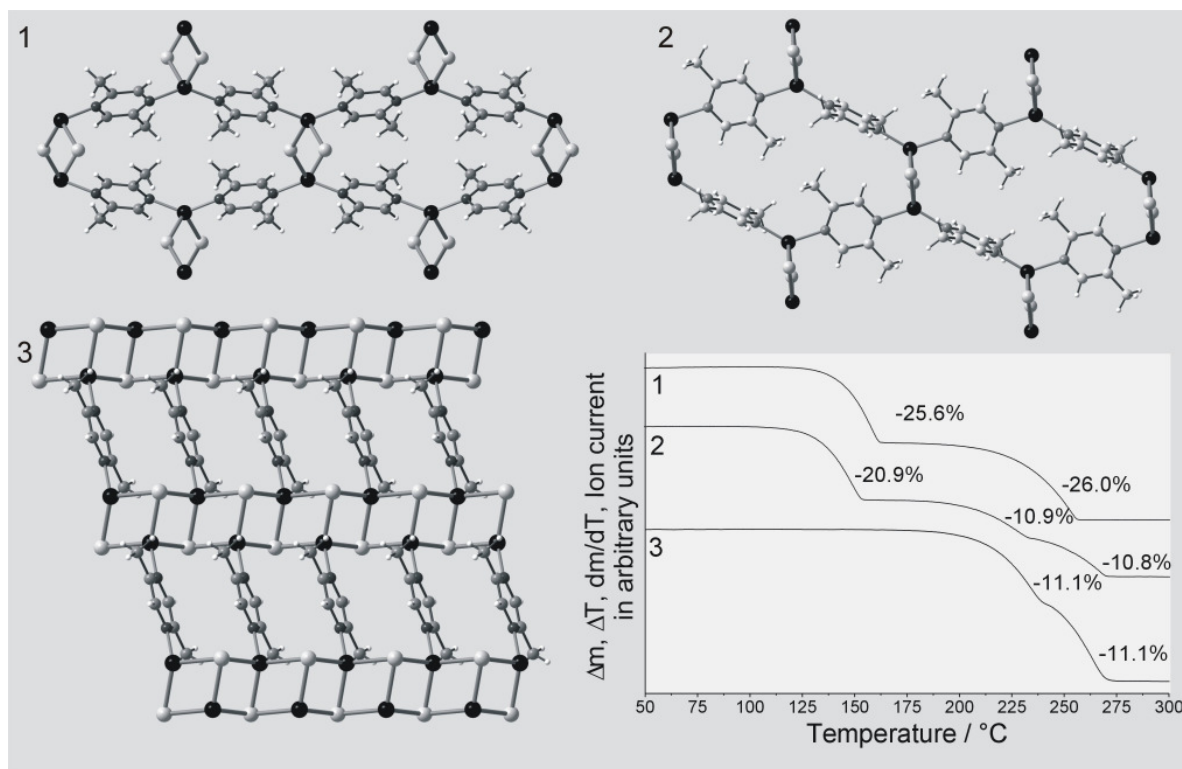


Figure 8: Crystal structures of poly[CuCl(μ_2 -2,5-dimethylpyrazine-N,N')] (1) (top left), poly[CuBr(μ_2 -2,5-dimethylpyrazine-N,N')] (2) (top right), poly[(CuX) $_2$ (μ_2 -2,5-dimethylpyrazine-N,N')] (X = Cl (3), ; bottom left) and TG curves for compounds 1, 2 and 3 (bottom right).

If the compound poly[CuBr(μ_2 -2,5-dimethylpyrazine-N,N')] is heated, one additional mass step is observed after the formation of the 2:1 compound which corresponds to the formation of a new 4:1 compound (figure 8: bottom right).

Influence of the kinetic of the thermal decomposition reaction on product formation: CuX coordination polymers with 2-ethylpyrazine

The investigations performed for the CuX coordination polymers with 2-methylpyrazine and 2-chloropyrazine has shown that the thermal reactivity of two very similar compounds can be completely different. In this context the question arises, which parameter affects the occurrence of different phases in a thermal decomposition reaction. It can be assumed that

the kinetics of all reactions involved could play an important role, which can be investigated by heating rate dependent TG measurements.

If CuCl is reacted with 2-ethylpyrazine, the corresponding ligand rich 1:1 and ligand deficient 2:1 compound can be prepared [77]. If the ligand rich compound is investigated using slow heating rates, two mass steps are observed. The first step corresponds to the formation of the ligand deficient 2:1 compound and the second to the formation of CuCl (figure 9). If the heating rate is successively increased the value of the first mass step decreases to a value which corresponds to the formation of a 3:2 compound of composition $(\text{CuCl})_3(\text{2-ethylpyrazine})_2$ (figure 9).

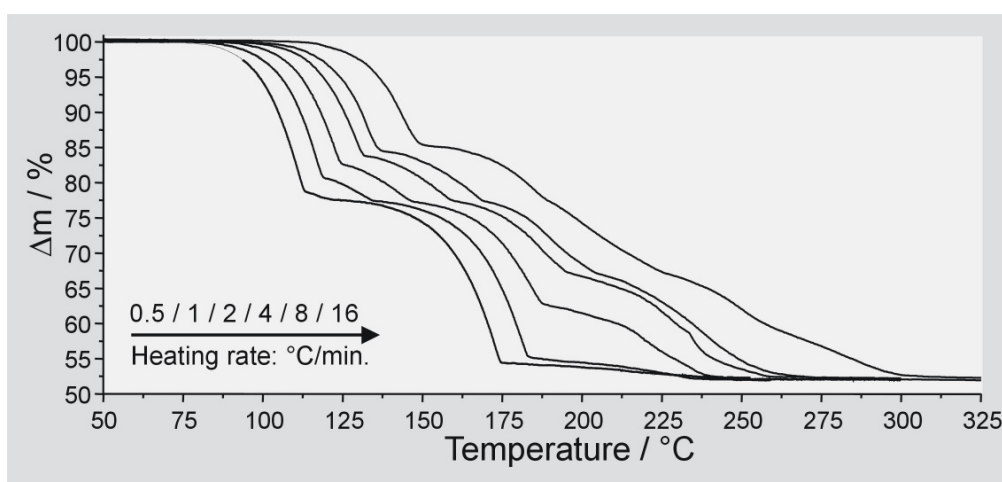


Figure 9: Heating rate dependent TG measurements for ligand rich 1:1-compound $\text{poly}[\text{CuCl}(\mu_2\text{-2-ethylpyrazine-N,N'})]$.

If the residue formed at fast heating rates is isolated and investigated using elemental analysis and X-ray powder diffraction it can be proved that a new 3:2 compound has formed. A small amount of single crystal of this compound can be prepared in solution but they are always contaminated with a large amount of crystals of the 2:1 compound. Because all three compounds were characterized by single crystal X-ray diffraction, one can follow the structural changes during the thermal transformation. The 1:1 compound consists of $(\text{CuCl})_2$ dimers which are connected by the 2-ethylpyrazine ligands into layers (figure 10: left). In the 3:2 compound $(\text{CuCl})_3$ 6-membered rings are found which are connected by the ligands into a one-dimensional coordination network (figure 10: mid). The 2:1 compound shows a coordination topology which is frequently found in such ligand deficient compounds. CuCl double chains are found which are connected into layers by the ligands (figure 10: right).

These investigations prove that the thermal reactivity and the product formation depends on the kinetics of all reactions involved. In the present case it was proven that the reaction sequence consists of consecutive and not of parallel reactions.

For the corresponding compounds with CuBr only a 3:2 and a 2:1 compound can be prepared of which the former one transforms into the ligand deficient 2:1 coordination polymer on heating [76]. The coordination polymers with CuI and 2-ethylpyrazine will be discussed in the following section.

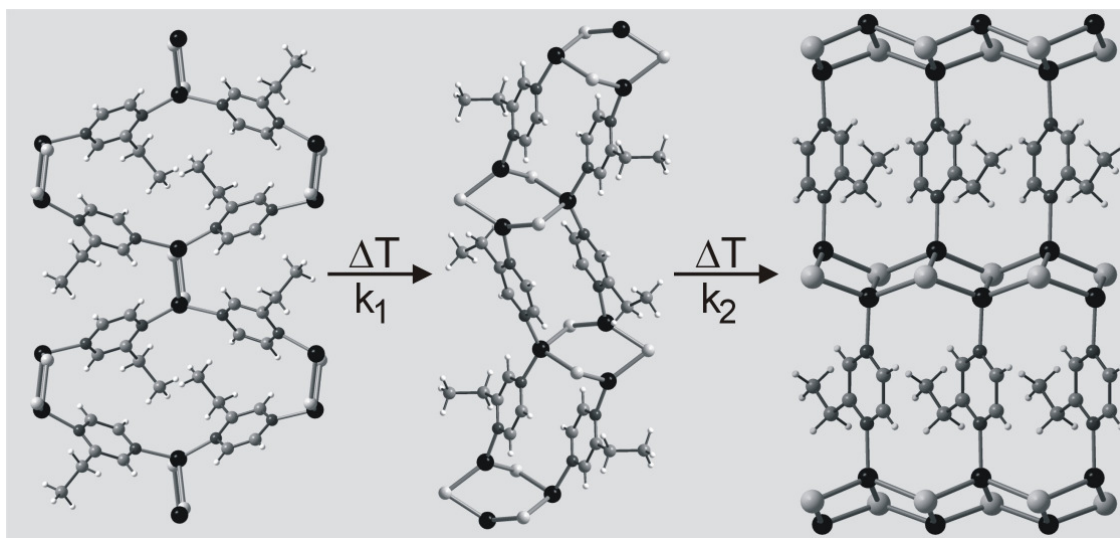


Figure 10: Structural changes during the thermal decomposition of the ligand rich 1:1-compounds $\text{poly}[\text{CuCl}(\mu_2\text{-2-ethylpyrazine-}N,N)]$ (left) to 3:2 $\text{catena}[\text{Cu}_3\text{Cl}_3(\mu_2\text{-2-ethylpyrazine-}N,N)_2]$ (mid) to 2:1 $\text{poly}[\text{Cu}_2\text{Cl}_2(\mu_2\text{-2-ethylpyrazine-}N,N)]$ (right).

More complicated reactions: Structures and reactivity of copper(I)iodide(2-ethylpyrazine) coordination polymers

Compared to the reactions described above the thermal decomposition reactions can be more complex. This was observed for the CuX coordination polymers with copper(I)iodide and 2-ethylpyrazine. Altogether three different compounds are observed with two of them show dimorphism [83].

If CuI is reacted with an excess of 2-ethylpyrazine discrete molecular complexes of the ligand rich 1:2 compound $[(\text{CuI})_2(2\text{-ethylpyrazine-}N)_4]$ (1) occurs which consists of $(\text{CuI})_2$ dimers in which each copper atom is coordinated by two 2-ethylpyrazine ligands. If this compound is heated in a thermobalance a mass loss is observed which correspond to the transformation in a ligand deficient 2:1 compound. If the reaction is investigated with temperature dependent X-ray powder diffraction it can be shown that the 1:1 compound $\text{poly}[(\text{CuI})_2(\mu_2\text{-2-}$

ethylpyrazine-N,N')₂] (2) occurs as an intermediate before the decomposition in the 2:1 compound is observed (Figure 11).

Using slightly different reaction conditions crystals of two different 1:1 compounds can be prepared. The crystal structure of poly[(CuI)₂(μ₂-2-ethylpyrazine-N,N')₂] (2) contains (CuI)₂ dimers which are connected by the 2-ethylpyrazine ligands into layers(3), whereas poly[(CuI)₂(μ₂-2-ethyl(μ₂-lpyrazine-N,N')-(2-ethylpyrazine-N))] (4) consists of 8-membered CuI rings, which are connected by the 2-ethylpyrazine ligands into layers. The most stable compounds are the 2:1 compound poly[(CuI)₂(μ₂-2-ethylpyrazine-N,N')] which is always formed at room-temperature independent of the stoichiometry between CuI and 2-ethylpyrazine. In this compound CuI double chains are connected by the ligands into layers. The crystal structure of the second modification of the 2:1 compounds is very similar to that the first. The main difference is found in the orientation of the ethyl groups.

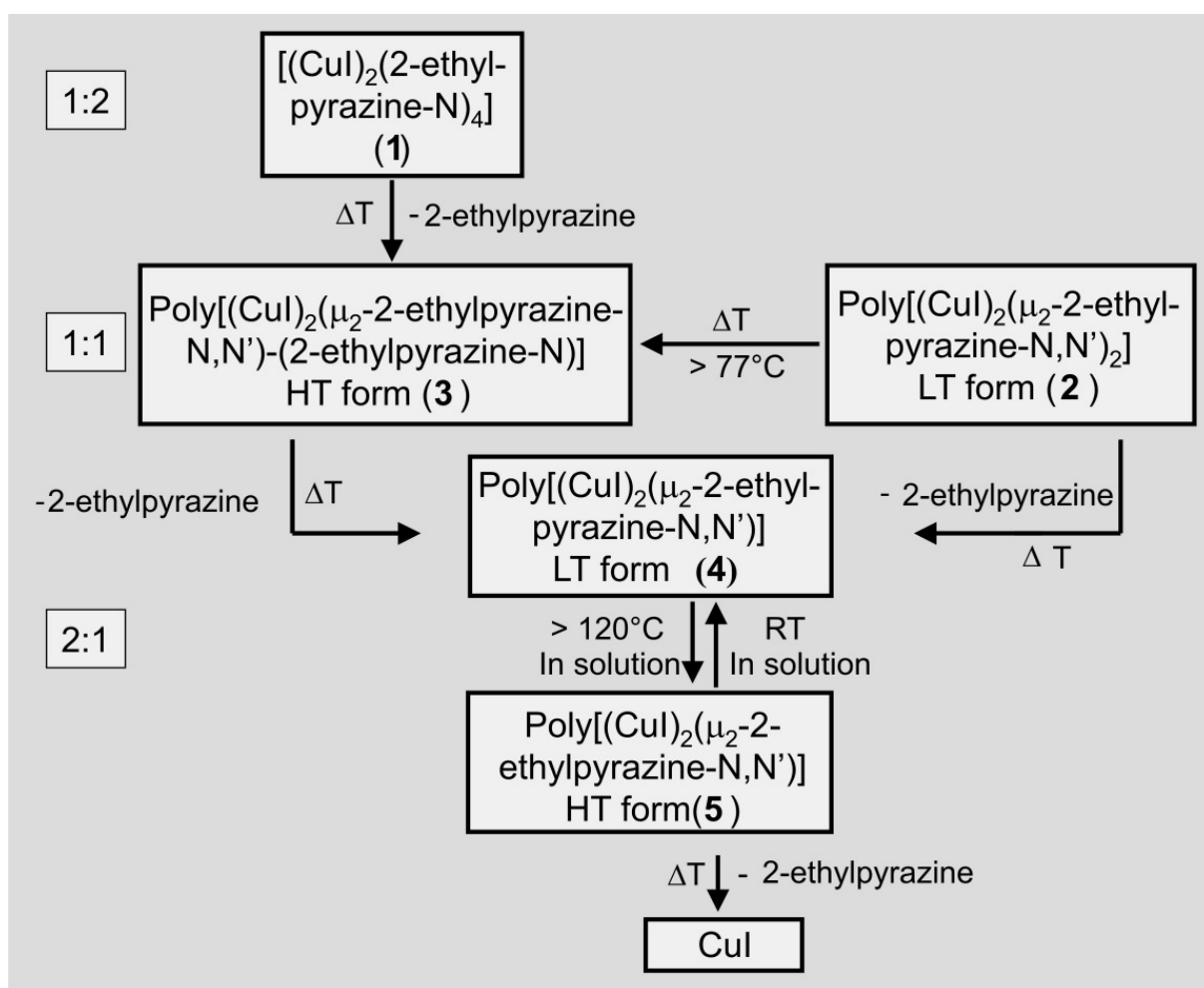


Figure 11: Schematic representation of the transformations of the different coordination polymers of copper(I)iodide(2-ethylpyrazine).

The thermal behaviour of all compounds was investigated using TG-DTA-MS measurements, differential scanning calorimetry and temperature dependent X-ray powder diffraction measurements. It was shown that the ligand rich 1:2 compound 1 transforms into the 1:1 compound 2 (figure 11). This modification is also formed if the second modification 3 is heated which shows that compound 2 is more stable at higher temperature (figure 11). On further heating compound 2 transforms into the 2:1 modification 4 which is the most stable form of all these coordination polymers. However, if CuI is reacted with 2-ethylpyrazine in a molar ratio of 2:1, in the beginning the red coloured form 5 occurs which transforms within seconds into form 4. This clearly shows that form 4 is the thermodynamic most stable modification at room-temperature whereas form 5 is metastable. If a saturated solution of form 4 is heated above 120°C it transforms into form 5, which shows that this modification is the thermodynamic most stable form above this temperature (figure 11). Single crystal of form 5 was obtained by crystallization from a saturated solution in the temperature range between 150 and 120°. On cooling, the crystals of this modification have to be separated from the solution, otherwise the retransformation into compound 4 is observed.

Polymorphism and isomerism in CuX coordination polymers.

During the investigations described above also polymorphic modifications are obtained. The term “polymorphism” is defined as the ability of a compound of the same composition to exist in more than one crystalline modification. This phenomenon is important for several reasons. First of all the structural aspects of polymorphism provide information on intermolecular interactions in crystals and therefore, can be used for a more rational crystal design. Moreover, investigations on the thermodynamic and kinetic aspects e. g. of polymorphism provide important information about the stability of each modification and their transformation behaviour.

We found different forms for the CuI(2-iodopyrazine) compounds. If copper(I)iodide is reacted with 2-iodopyrazine in the beginning a yellow coloured compound precipitates which transforms within minutes into a red compound [79]. In the yellow form CuI double chains are found in which the copper atoms are coordinated by three iodine atoms and one nitrogen atom of the 2-iodopyrazine ligand (figure 13). The ligand does not connect different copper atoms and therefore, a 1-dimensional coordination topology is observed (figure 13: top left). In the structure of red form CuI single chains are observed which are connected by the 2-iodopyrazine ligand into layers (figure 13: bottom left). Because the yellow form transforms into the red form, the latter should be the thermodynamic most stable form at room temperature.

Investigations using different differential thermoanalysis and thermogravimetry shows that none of the two modifications forms a ligand deficient intermediate phase and that they decompose directly into CuI (figure 12: top right). According to differential scanning calorimetry measurements the decomposition temperature of the red form is higher and that this form is more stable by about 19 kJ/mol (figure 12: bottom right). From temperature dependent X-ray powder diffraction measurements there are no indications for the transformation of one form into the other. Therefore, it is believed that the red form is the most stable form above the complete temperature range and that both the forms behave monotropic.

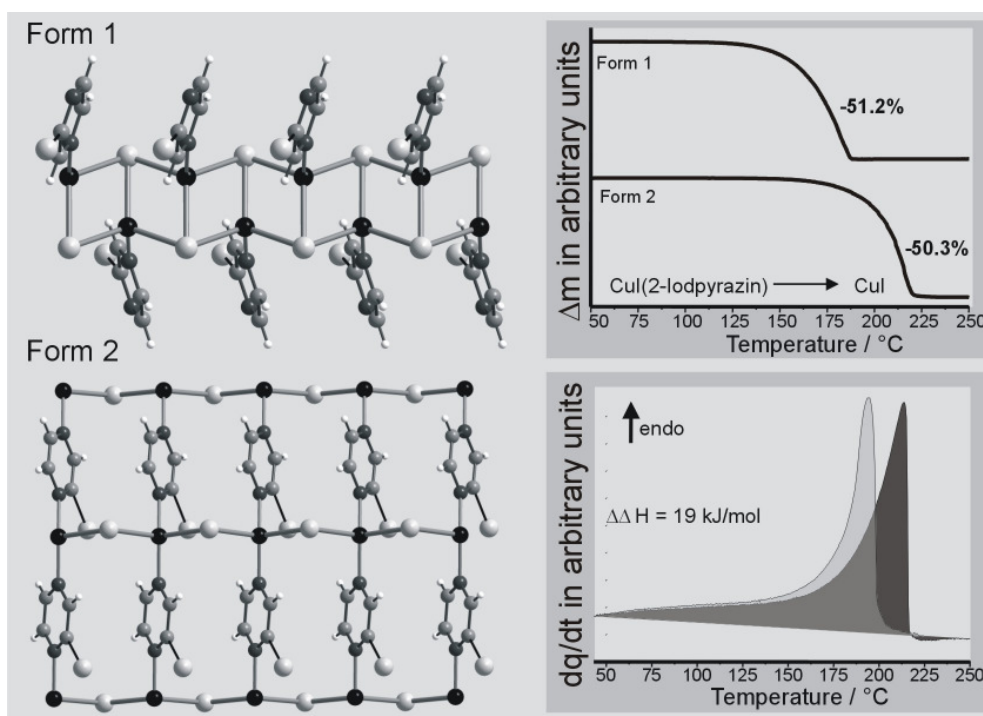


Figure 12: Crystal structure of the yellow (left) and the red modification of CuI(2-iodopyrazine) and the TG and DSC curves for both forms (right).

For the CuX coordination polymers with pyridiazine also two different modifications were isolated. The compound catena[CuCl(μ_2 -pyridazine-N,N)] (form L1) was described earlier by Sheldrick and coworkers [111]. In this form (CuCl)₂ dimers are found which are connected into chains by the pyridazine ligands (figure 13: right). Later it was shown that a second form (form 1) exists, in which CuCl single chains occur which are connected into double chains by the pyridazine ligands (figure 13: right) [80]. We have shown that our form is the thermodynamic most stable form at room temperature and that both forms behave enantiotropic. Whereas form 1 can be prepared in a pure state and in large amounts, form L1 is always obtained as a mixture of both forms.

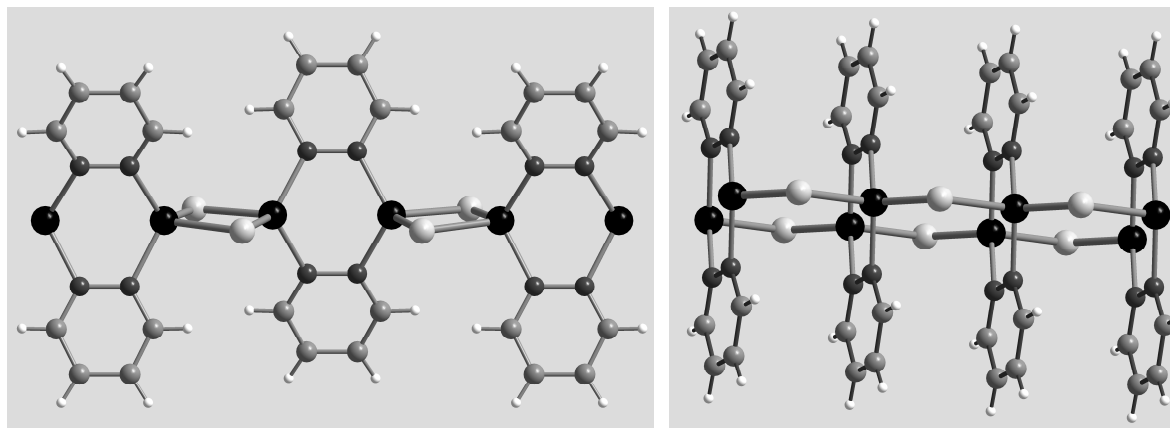


Figure 13: Crystal structure of form L1 (left) and form 1 (right) of $\text{catena}[\text{CuCl}(\mu_2\text{-pyridazine-N,N})]$.

Synthesis, structures and reactivity of CuX pseudohalide coordination polymers ($X = \text{SCN}$, CN).

The preparation of coordination polymers by thermal decomposition is not limited only to the preparation of copper(I) halides because also copper(I) pseudohalides reacts in a similar way. This was shown for the ligand rich copper(I) thiocyanate coordination polymers $\text{catena}[(\mu_2\text{-thiocyanato-N,S})\text{-}(1\text{-ethyl-2-methylpyrazine-N})]$ copper(I) [82]. Its crystal structure is composed of CuSCN double chains in which each copper atom is connected by two thiocyanate anions and two 1-ethyl-2-methyl-pyrazine ligands (Figure 14: left). In this compound only one nitrogen atom of the 1-ethyl-2-methyl-pyrazine ligand is involved in copper coordination. On heating this compound loses half of the ligands and forms the ligand deficient compound $\text{poly}[(\text{di-}\mu_2\text{-thiocyanato-N,S})\text{-}(\mu_2\text{-1-ethyl-2-methylpyrazine-N,N})]$ di-copper(I) as an intermediate. This reaction was investigated by DTA-TG-MS measurements and temperature resolved X-Ray powder diffraction. These investigations clearly shows that the new coordination polymers has formed very pure and in quantitative yields. The crystal structure of this 2:1 compound is very similar to those of several ligand deficient 2:1 copper(I)halide coordination polymers. It is composed of CuSCN layers that are connected by the N-donor ligands via $\mu\text{-N,N}'$ coordination into a three-dimensional coordination network (figure 14: right).

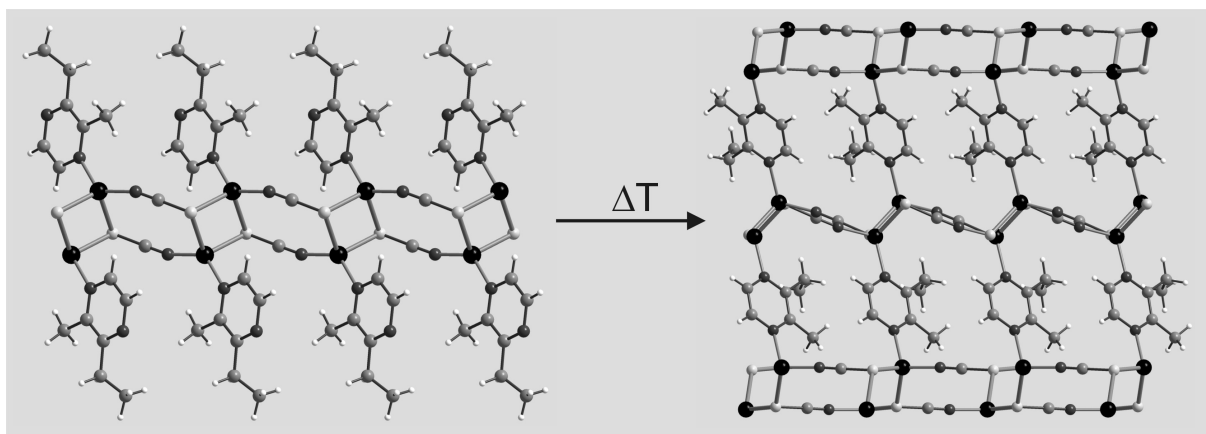


Figure 14: Crystal structure of catena[(μ_2 -thiocyanato-N,S)-(1-ethyl-2-methylpyrazine-N)] copper(I) (right) and poly[(di- μ_2 -thiocyanato-N,S)-(μ_2 -1-ethyl-2-methylpyrazine-N,N')] di-copper(I) (right).

In further investigations the thermal properties of copper(I)cyanide coordination polymers were investigated. In these investigations the 3:2 copper(I) cyanide coordination polymer poly[tri- μ_2 -cyano-C,N)-bis(μ_2 -2,3-dimethyl-pyrazine-N,N)] tricopper(I) was prepared by the reaction of copper(I) cyanide with 2,5-dimethylpyrazine in acetonitrile [89]. In its crystal structure a novel CuCN substructure is found, which is connected by the dimethylpyrazine ligands into a three-dimensional coordination network (figure 15: left). On heating this compound in a thermobalance two low resolved mass steps are observed which are accompanied by two endothermic events in the DTA curve (figure 15: right). If the reaction is performed at faster heating rates of 16 K/min both thermal events can be much better resolved which shows, that the kinetic must play an important role. However, if the intermediate formed in the first step is isolated and investigated using X-ray powder diffraction it can be shown that the ligand deficient 2:1 compound (CuCN)₂-(2,3-dimethylpyrazine) has formed.

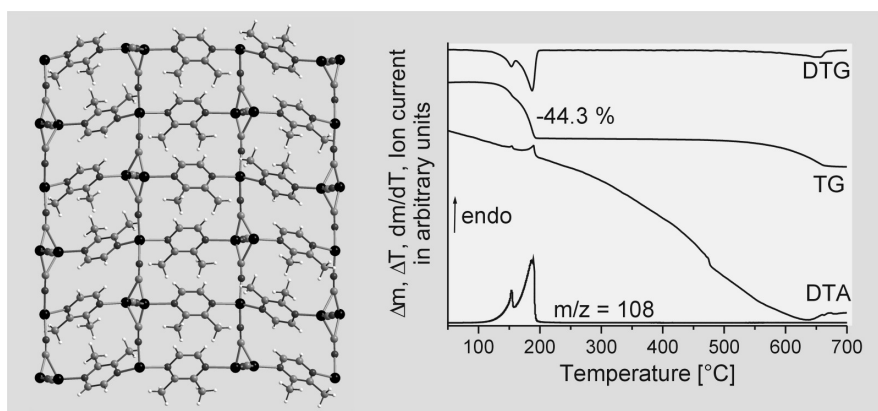


Figure 15: Crystal structure of poly[tri- μ_2 -cyano-C,N)-bis(μ_2 -2,3-dimethylpyrazine-N,N)] tricopper(I) (left) and DTA, TG, DTG and MS-trend scan curve for this compound (right).

1.4 Major goals of the thesis: Investigations on Zn(II) halide coordination compounds

In the investigations described above it was shown that new ligand deficient coordination polymers on the basis of copper(I) halides or pseudohalides and N-donor ligands can easily be discovered and prepared by thermal decomposition of suitable ligand rich precursor compounds. The intermediates obtained during the reaction are very pure and practically always formed in 100% yield. In addition, in a few cases also thermodynamic metastable compounds and polymorphic modifications can be obtained. Therefore, this method is an alternative tool to the preparation of such compounds in solution, especially in those cases where the products are always formed as mixtures or cannot be obtained at all.

Starting from these results the question arises if thermal decomposition reaction can only be used for the discovery and preparation of copper(I) coordination compounds or if this method can be expanded also to the preparation of other metal halide coordination compounds. Such investigations are the major part of this thesis, which deals with the preparation and characterization of coordination compounds based on zinc(II) halides and N-donor ligands. This includes investigations on the thermal reactivity of such compounds and the preparation of new thermodynamically stable and metastable zinc(II) halide coordination compounds and polymorphic modifications. Zinc(II) halide coordination compounds were selected because they show a large structural diversity and therefore, might be potential precursor compounds for the preparation of new ligand deficient compounds.

Compared to copper(I) halide or pseudohalide coordination compounds only a few zinc(II) halide coordination compounds are known and some representative examples are described in references [163-207]. Most of these contributions deal mainly with the crystal structures of such compounds and investigations on their thermal reactivity were not reported.

In contrast to copper(I) halide coordination compounds, in which the copper atoms are always tetrahedrally coordinated, in Zinc(II) halide coordination compounds tetrahedral [163-192] octahedral [193-196] and pentahedral [197-202] coordination is found (figure 16).

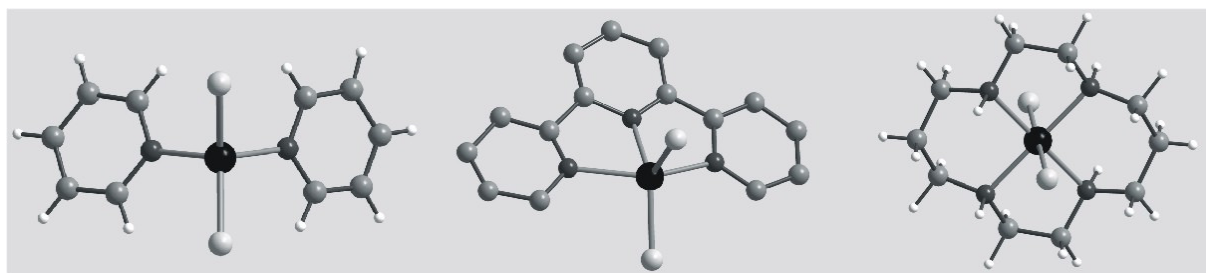


Figure. 16: Representative examples for tetrahedral (left) pentahedral (mid) and octahedral coordination of ZnX_2 halide ($X = Cl, Br, I$) coordination compounds.

This might be an advantage for the preparation of new ligand deficient compounds, because the occurrence of such intermediates will also depend on the structural diversity of the metal halide coordination compounds used in the thermal decomposition reaction. This is really needed because in contrast to copper(I) halides, zinc(II) halides do not show a large structural diversity of the metal halide substructure. Most of the zinc(II) halide coordination compounds consists of monomeric ZnX_2 units, in which the zinc is coordinated by two halide atoms and two donor atoms (figure 17) [163-214]. In some cases linear polymeric $(ZnX_2)_\infty$ chains are found, in which the zinc atoms are octahedrally coordinated by two donor atoms and four halide atoms (figure 17) [204-206]. In these compounds the octahedras sharing common edges with the neighbouring octahedra. In zinc(II) fluoride compounds also zig-zag-like single chains [203] or dimers [214] are found (figure 17). However, in these cases the ligands is negatively charged for charge compensation.

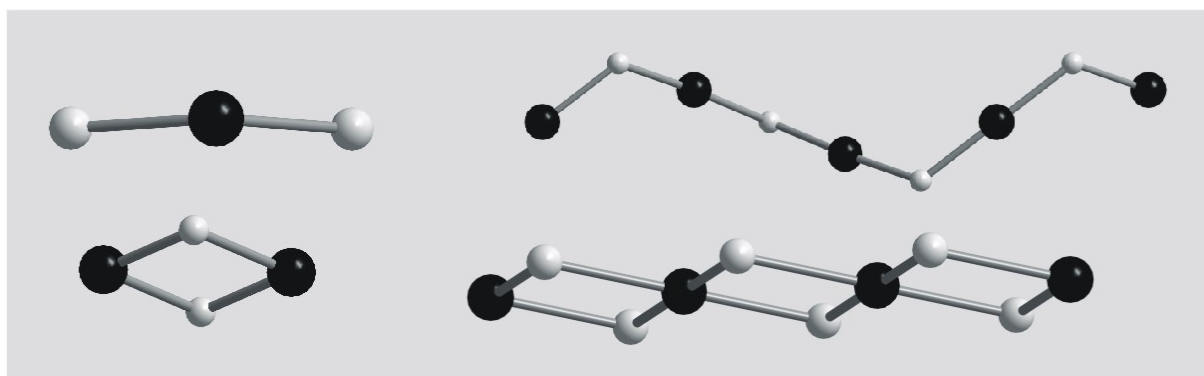


Figure. 17: Examples for different ZnX_2 -substructures in ZnX_2 coordination polymers ($X = F, Cl, Br, I$) with N donor ligands (The N donor ligands are omitted for clarity).

Dependent on the coordination behaviour of the ligands, the different ZnX_2 substructures mentioned above can further be connected into 1-, 2- or 3-dimensional coordination polymers, which to some extent are comparable to the networks observed in copper(I) halide coordination compounds.

For zinc(II) halide coordination compounds built up of monomeric ZnX_2 units this will lead to discrete complexes if the ligand exhibits only one N donor atom (figure 18: left) or to chains, if the ligand can connect two neighbouring Zn atoms (figure 18: right).

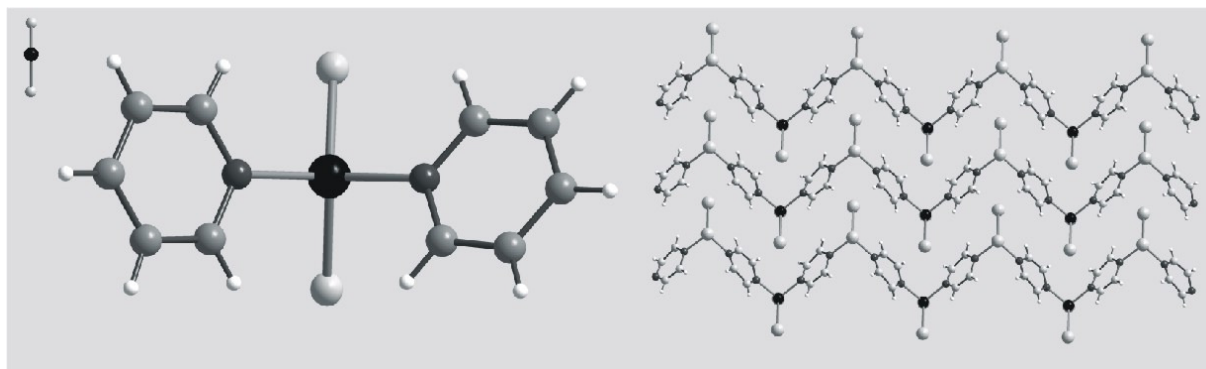


Figure. 18: Representative example for different coordination networks built up of ZnX_2 units and a non-bridging (left) and bridging (right) N donor ligand.

If the ZnX substructure consists of linear $[\text{ZnX}_2]_\infty$ chains, in which the zinc atoms are octahedrally coordinated structures are formed with bridging ligands in which the zinc(II)halide chains are connected into layers (figure 19). 1D coordination polymers with that substructure and nonbridging ligands are unknown.

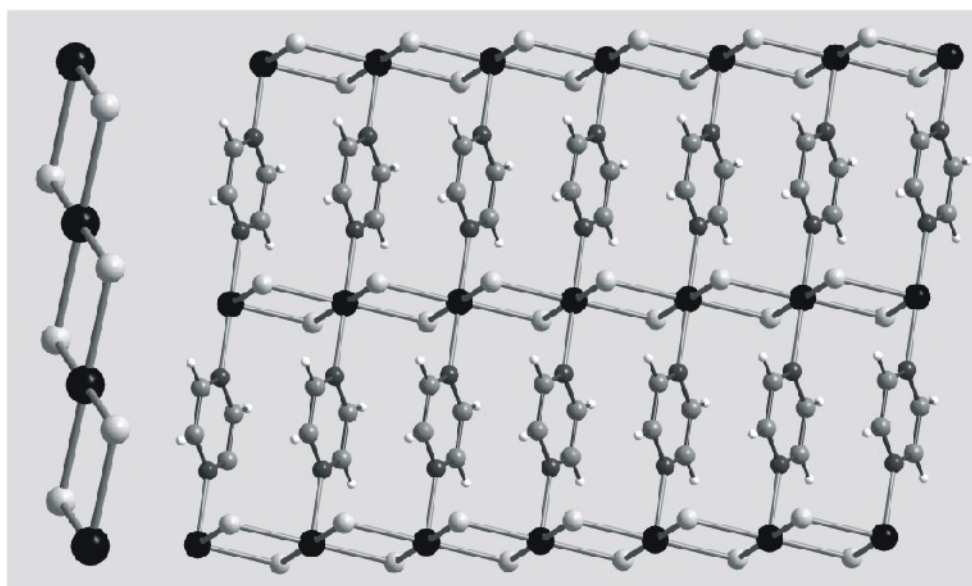


Figure. 19: Representative examples for a 2D coordination polymer built up of linear $[\text{ZnX}_2]_\infty$ chains and bridging N donor ligands.

As maintained above, in ZnF compounds in which the ligands are negatively charged also zig-zag-like single chains are obtained, which are connected into 2D layers by the ligands (figure 20).

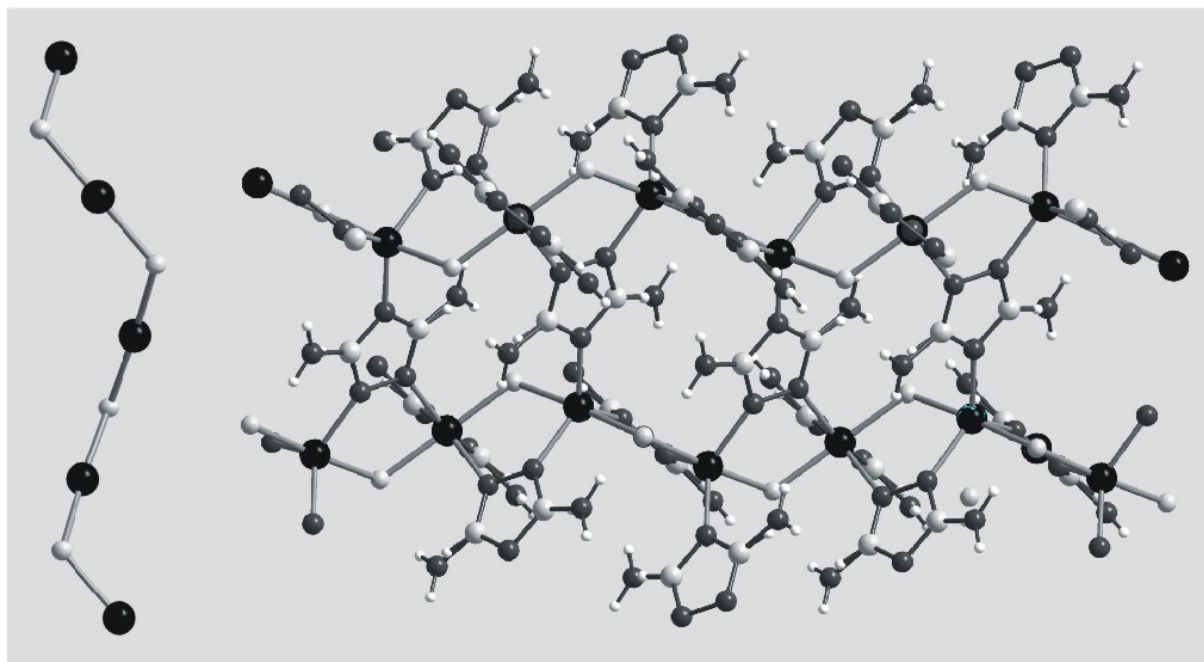


Figure. 20: Representative examples for ZnF zig-zag-like single chains which are connected into layers.

Finally, structures are known which consists of a $(\text{ZnF})_2$ substructure, in which the zinc is coordinated by two non-bridging ligands forming discrete molecular complexes (figure 21).

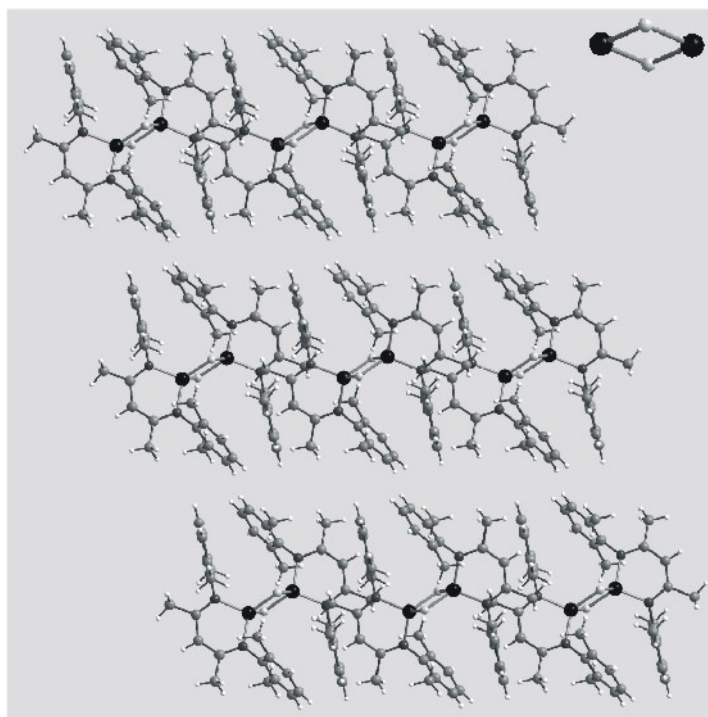


Figure. 21: Representative example for $(\text{ZnF})_2$ dimers which forms discrete molecular complexes.

Summarizing, also in zinc(II) halide coordination compounds a large structural diversity is found and therefore, such compounds might be good candidates for the preparation of new stable and metastable ligand deficient coordination compounds, which is investigated in this thesis.

For the preparation of the potential zinc(II) halide precursor compounds, the same ligands were used as for the preparation of the copper(I) halide coordination compounds described above (figure 22). In this case it can be expected that several compounds are obtained, in which the structures or especially the topology of the coordination networks are similar to those of the corresponding copper(I) halide compounds. In these cases the thermal reactivity can be much better compared to that of the copper(I) halide coordination compounds.

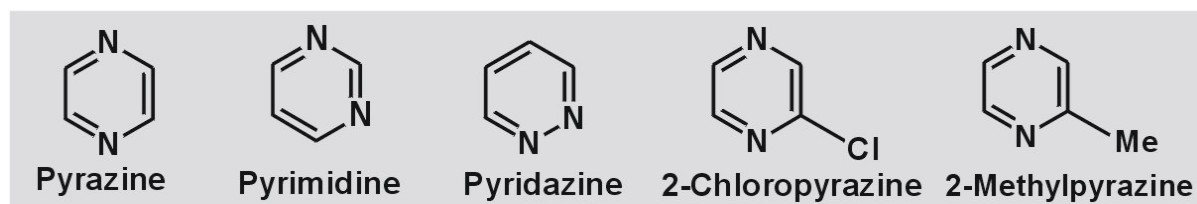


Figure. 22: Representative examples for ligands which were used in this thesis.

1.5 References

- [1] P. J. Hagrman, D. Hagrman, J. Zubieta, *Angew. Chem.* **1999**, *111*, 2798 and *Angew. Chem. Int. Ed. Engl.* **1999**, *38*, 2638.
- [2] S. L. James, *Chem. Soc. Rev.* **2003**, *5*, 276.
- [3] A. Y. Robin, K. M. Fromm, *Coord. Chem. Rev.* **2006**, *250*, 2127.
- [4] C. Janiak, *J. Chem. Soc. Dalton. Trans.* **2003**, 2781.
- [5] O. M. Yaghi, H. Li, C. Davis, D. Richardson, T. L. Groy, *Acc. Chem. Res.* **1998**, *31*, 474.
- [6] C.-T. Chen, K. S. Suslik, *Coord. Chem. Rev.* **1993**, *128*, 293.
- [7] Y. Zhao, M. Hong, Y. Liang, R. Cao, J. Weng, S. Lu, W. Li, *Chem. Commun.* **2000**, 39.
- [8] M. Hanack, S. Deger, A. Lange, *Coord. Chem. Rev.* **1988**, *83*, 115.
- [9] M. Eddaoudi, M. O'Keefe, O. M. Yaghi, *Nature* **1999**, *402*, 276.
- [10] M. Eddaoudi, J. Kim, N. Rosi, D. Vodak, J. Wachter, M. O'Keefe, O. M. Yaghi, *Science* **2002**, *295*, 469.
- [11] M. Eddaoudi, H. Li, O. M. Yaghi, *Y. Am. Chem. Soc.* **2000**, *122*, 1391.
- [12] J. L. C. Rowsell, O. M. Yaghi, *Microporous and Mesoporous Materials*, **2004**, *73*, 3.

- [13] N. L. Rosi, J. Kim, M. Eddaoudi, B. Chen., M. O'Keefe, O. M. Yaghi, *J. Am. Chem. Soc.* **2005**, *127*,1504.
- [14] H. K. Chae, D. Y. Siberio-Perez, J. Kim, Y. B. Go, M. Eddaoudi, A. J. Matzger, M. O'Keefe, O. M. Yaghi, *Nature*, **2004**, *427*, 523.
- [15] S. Noro, S. Kitagawa, M. Kondo, K. Seki, *Angew. Int. Ed.* **2000**, *39*, 2081.
- [16] A. P. Côté, G. K. H. Shimizu, *Coord. Chem. Rev.* **2003**, *245*, 49.
- [17] R. Kitaura, K. Fijimoto, S.-I. Noro, M. Kondo, S. Kitagawa, *Angew. Int. Ed.* **2002**, *41*, 133.
- [18] L. C. Tabares, J. A. R. Navarro, J. M. Salas, *J. Am. Chem. Soc.*, **2001**, *123*, 383.
- [19] C. Näther, J. Greve, I. Jeß, *Chem. Mater.*, **2002**, *14*, 4536.
- [20] C. Näther, J. Greve, I. Jeß, *J. Solid State Chem.* **2003**, *175*, 328.
- [21] S. Kitagawa, K. Uemura, *Chem. Soc. Rev.* **2005**, *34*,109.
- [22] S. R. Batten, K. Murray, *Coord. Chem. Rev.* **2003**, *246*,103.
- [23] S. Noro, H. Miyasaki, S. Kitagawa, T. Wada, T. Okubo, M. Yamashita, T. Mitani, *Inorg. Chem.* **2005**, *44*,133.
- [24] B. Moulton, J. Lu, R. Hajndl, S. Hariharan, M. J. Zaworotko, *Angew. Chem. Int. Ed.* **2002**, *41*, 2821.
- [25] G. J. Halder, C. J. Kepert, B. Moubaraki, K. S. Murray, J. D. Cashion, *Science* **2002**, *298*,1762.
- [26] C. Näther, J. Greve, *J. Solid State Chem.*, **2003**, *176*, 259.
- [27] J. L. Manson, A. M. Arif, J. S. Miller, *Chem. Commun.* **1999**, 1479.
- [28] S. Decurtins, H. W. Schmalke, P. Schneuwly, J. Ensling, P. Gütlich, *J. Am. Chem. Soc.* **1994**, *116*, 9521.
- [29] R. Sieber, S. Decurtins, H. Stoeckli-Evans, C. Wilson, D. Yufit, J. A. K. Howard, S. C. Capelli, A. Hauser, *Chemistry* **2000**, *6*, 361.
- [30] L.-X. Dai, *Angew. Chem. Int. Ed.* **2004**, *43*, 5726.
- [31] T. Sawaki, T. Dewa, Y. Aoyama, *J. Am. Chem. Soc.* **1998**, *120*, 8539.
- [32] T. Sawaki, Y. Aoyama, *J. Am. Chem. Soc.* **1999**, *121*, 4793.
- [33] T. Dewa, Y. Aoyama, *J. Mol. Catalysis* **2000**, *A152*, 257.
- [34] T. Dewa, T. Saiki, Y. Aoyama, *J. Am. Chem. Soc.* **2001**, *123*, 502.
- [35] O. R. Evans, W. Lin, *Acc. Chem. Res.* **2002**, *35*, 511.
- [36] D. Sun, R. Cao, J. Weng, M. Hong, Y. Liang, *J. Chem. Soc. Dalton Trans.* **2002**, 291.
- [37] R. Horikoshi, T. Mochida, N. Maki, S. Yamada, H. Moriyama, *J. Chem. Soc. Dalton Trans.* **2002**, 28.
- [38] C. Seward, N.-X. Hu, S. Wang, *J. Chem. Soc. Dalton Trans.* **2001**, 134.
- [39] B. Paul, C. Näther, B. Walfort, K. M. Fromm, B. Zimmermann, H. Lang, C. Janiak *Cryst. Eng. Commun.* **2005**, *7*, 309.

- [40] B. Paul, C. Näther, K. M. Fromm, C. Janiak, *Cryst. Eng. Commun.* **2004**, *6*, 293.
- [41] C. Näther, J. Greve, I. Jeß, C. Wickleder, *Solid State Sciences* **2003**, *5*, 1167.
- [42] R. Robson, B. F. Abrahams, S. R. Batten, R. W. Grable, B. F. Hoskins, J. Liu, In *Supramolecular Architecture*, ACS publications, Washington DC. **1992**, Chapter 19.
- [43] R. Robson, In *Comprehensive Supramolecular Chemistry*; Pergamon: New York 1996, Chapter 22, 733.
- [44] M. J. Zaworotko, *Chem. Soc. Rev.* **1994**, *23*, 283.
- [45] J. Y. Lu, *Coord. Chem. Rev.*, **2003**, *246*, 327.
- [46] M. Zaworotko, *Angew. Chem. Int. Ed.* **1998**, *37*, 1211.
- [47] S. R. Batten, R. Robson, *Angew. Chem.* 1998, *110*, 1558 and *Angew. Chem. Int. Ed.* **1998**, *37*, 1460.
- [48] L. Brammer, *Chem. Soc. Rev.* **2004**, *8*, 476.
- [49] D. Braga, L. Maini, M. Polito, L. Scaccianoce, G. Cojazzi, F. Grepioni, *Coord. Chem. Rev.* **2001**, *216*, 225.
- [50] Y. Zhou, M. Hong, X. Wu, *Chem. Commun.* **2006**, 135.
- [51] S.-L. Zheng, M.-L. Tong, X.-M. Chen, *Coord. Chem. Rev.* **2003**, *246*, 185.
- [52] A. Erxleben, *Coord. Chem. Rev.* **2003**, *246*, 203.
- [53] J. Y. Lu *Coord. Chem. Rev.* **2003**, *246*, 327.
- [54] A. N. Khlobystov, A. J. Blake, N. R. Champness, D. A. Lemenovskii, A. G. Majouga, N. V. Zyk, M. Schröder, *Coord. Chem. Rev.* **2001**, *222*, 155.
- [55] R. J. Puddephatt, *Coord. Chem. Rev.* **2001**, *216-217*, 313.
- [56] H. Zhang, X. Wang, K. Zhang, B. K. Teo, *Coord. Chem. Rev.* **1999**, *183*, 157.
- [57] G. R. Desiraju, *Crystal Engineering – The Design of Organic Solids*, Material Science Monographs, Elsevier, **1989**, *54* and literature cited therein.
- [58] B. Moulton, M. J. Zaworotko, *Chem. Rev.* **2001**, *101*, 1629.
- [59] S. R. Batten, K. Murray, *Aust. J. Chem.* **2001**, *54*, 605.
- [60] A. S. Barnett, A. J. Blake, N. R. Champness, *Chem. Commun.*, **2002**, 1640.
- [61] A. J. Blake, N. R. Brooks, N. R. Champness, M. Crew, A. Deveson, D. Fenske, D. H. Gregory, L. R. Hanton, P. Hubberstey, M. Schröder, *Chem. Commun.*, **2001**, 1432.
- [62] S. A. Barnett, A. J. Blake, N. R. Champness, C. Wilson, *Chem. Commun.* **2002**, 1640.
- [63] T. L. Hennigar, D. C. MacQuarrie, P. Losier, R. D. Rogers, M. J. Zaworotko, *Angew. Chem. Int. Ed.* **2003**, *36*, 972.
- [64] D. Braga, F. Grepioni, *Chem. Soc. Rev.* **2000**, *29*, 229.
- [65] S. Kitagawa, S. Noro, *Compreh. Coord. Chem.* **2004**, *7*, 231.
- [66] W. Clegg, *Compreh. Coord. Chem.* **2003**, *1*, 579.
- [67] D. Braga, F. Grepioni, *Angew. Chem., Int. Ed.* **2004**, *43*, 4002.
- [68] D. Braga, M. Curzi, M. Lusi, F. Grepioni, *Cryst. Eng. Comm* **2005**, *7*, 276.

- [69] D. Braga, M. Curzi, F. Grepioni, M. Polito, *Chem. Commun.*, **2005**, 2915.
- [70] C. Näther, J. Greve, I. Jeß, *Polyhedron*, **2001**, *20*, 1017.
- [71] C. Näther, I. Jeß, H. Studzinski, *Z. Naturforsch.* **2001**, *56b*, 997.
- [72] C. Näther, I. Jeß, *Monatshefte* **2001**, *132*, 897.
- [73] C. Näther, J. Greve, *Acta Cryst.* **2001**, *C57*, 377.
- [74] C. Näther, M. Wriedt, I. Jeß, *Z. Anorg. Allg. Chem.* **2002**, *628*, 394.
- [75] C. Näther, J. Greve, I. Jeß, *Solid State Sciences* **2002**, *4*, 813.
- [76] C. Näther, I. Jeß, *Z. Naturforsch.* **2002**, *57b*, 1133.
- [77] C. Näther, I. Jeß, *J. Solid State Chem.* **2002**, *169*, 103.
- [78] C. Näther, I. Jeß, *Acta Crystallogr.* **2002**, *C58*, m190.
- [79] C. Näther, M. Wriedt, I. Jeß, *Inorg. Chem* **2003**, *42*, 2391.
- [80] C. Näther, I. Jeß, *Inorg. Chem.* **2003**, *42*, 2968.
- [81] C. Näther, I. Jeß, M. Bolte, *Z. Naturforsch.* **2003**, *58b*, 1105.
- [82] C. Näther, I. Jeß, P. Kowallik, *Z. Anorg. Allg. Chem.* **2003**, *629*, 2144.
- [83] C. Näther, I. Jeß, N. Lehnert, D. Hinz-Hübner, *Solid State Sciences* **2003**, *5*, 1343.
- [84] C. Näther, I. Jeß, *Acta Crystallogr.* **2004**, *C60*, m153.
- [85] C. Näther, A. Beck, *Acta Crystallogr.*, **2004**, *E60*, m1008.
- [86] C. Näther, A. Beck, *Acta Crystallogr.* **2004**, *E60*, m1678.
- [87] T. Kromp, W. S. Sheldrick, C. Näther, *Z. Anorg. Allg. Chem.* **2003**, *629*, 45.
- [88] C. Näther, I. Jeß, *Eur. J. Inorg. Chem.* **2004**, 2868.
- [89] J. Greve, C. Näther, *Z. Naturforsch.* **2004**, *59b*, 1325.
- [90] C. Näther, M. Wriedt, I. Jeß, *Acta Crystallogr.* **2005**, *E61*, m329.
- [91] C. Näther, I. Jeß, *Inorg. Chem.*, **2006**, in press.
- [92] I. Jeß, P. Taborsky, J. Pospíšil, C. Näther *Dalton Trans.*, **2007**, *22*, 2263-2270.
- [93] I. Jeß, P. Taborsky, C. Näther, *Z. Naturforsch.*, **2007**, *62b*, 501.
- [94] I. Jeß, C. Näther, *Z. Naturforsch.*, **2007**, *62b*, 617.
- [95] Q.-Y. Cao, W.-F. Fu, Z.-L. Wang, *Acta Cryst.*, **2004**, *E60*, m987.
- [96] E. W. Ainscough, A. G. Bingham, A. M. Brodie, K. L. Brown., *J. Chem. Soc. Dalton Trans.* **1984**, 989.
- [97] M. M. Olmstead, T. E. Patten, C. Troeltzsch, *Inorg. Chim. Acta* **2004**, *357*, 619.
- [98] B. E. Green, C. H. L. Kennard, G. Smith, B. D. James, A. H. White, *Acta Cryst.* **1984**, *C40*, 426.
- [99] J. M. Dyason, L. M. Engelhardt, P. C. Healy, A. H. White, *Aust. J. Journal* **1986**, *39*, 1043.
- [100] J. P. Puzas, R. Nakon, J. L. Petersen, *Inorg. Chem.* **1986**, *25*, 3837.
- [101] P. G. Jones, E.-M. Zerbe., *Acta Cryst.* **2005**, *E61*, m106.

- [102] J. C. Dyason, L. M. Engelhardt, P. C. Healy, J. D. Kildea, A. H. White, *Aust. J. Chem.* **1988**, *41*, 335.
- [103] P. C. Healy, J. D. Kildea, A. H. White, *Aust. J. Chem.* **1989**, *42*, 137.
- [104] W. Hiller, *Acta Cryst.* **1986**, *42*, 149.
- [105] O. M. Yaghi, G. Li, *Angew. Chem. Int. Ed.* **1995**, *34*, 207.
- [106] B. Roßenbeck B, W. S. Sheldrick, *Z. Naturforsch.* **1999**, *54b*, 1510.
- [107] V. Schramm, A. Pierre, W. Hiller, *Acta Cryst.* **1984**, *C40*, 1840.
- [108] E. Bosch, C. L. Barnes, *New. J. Chem.* **2001**, *25*, 1376.
- [109] P. C. Healy, C. Pakawatchai, A. H. White, *J. Chem. Soc. Dalton Trans.* **1983**, 1917.
- [110] A. Habiyakare, E. A. C. Lucken, G. Bernardelli, *Z. Naturforsch (Phys. Sci.)* **1992**, *47a*, 106.
- [111] T. Kromp, W. S. Sheldrick, *Z. Naturforsch.* **1999**, *54b*, 1175.
- [112] E. Bosch, C. L. Barnes, *J. Coord. Chem.* **2003**, *56*, 329.
- [113] J. Y. Lu, B. R. Cabrera, R.-J. Wang, J. Li, *Inorg. Chem. Cryst.* **1999**, *38*, 4608.
- [114] R. H. Goeneman, J. L. Atwood, *Supramol. Chem.* **2001**, *12*, 353.
- [115] J. C. Dyason, L. M. Engelhardt, P. C. Healy, A. H. White, *Aust. J. Chem.* **1984**, *37*, 2201.
- [116] M. Munakata, T. Kuroda-Soaw, M. Maekawa, A. Honda, S. Kitagawa, *J. Chem. Soc-Dalton Trans.* **1994**, 2771.
- [117] J. A. Campbell, C. L. Raston, B. W. Skelton, A. H. White, *Aust. J. Chem.* **1977**, *30*, 1937.
- [118] M. A. S. Goher, T. C. W. Mak, *Inorg. Chim. Acta* **1988**, *141*, 323.
- [119] A. J. Graham, P. C. Healy, J. D. Kildea, A. H. White, *Aust. J. Chem.* **1989**, *42*, 177.
- [120] B. Roßenbeck, W. S. Sheldrick, *Z. Naturforsch.* **2000**, *55b*, 467.
- [121] J. M. Moreno, J. Suarez-Varela, E. Colacio, J. C. Avila-Roson, M. A. Hidalgo, D. Martin-Ramos, *Can. J. Chem.* **1995**, *73*, 1591.
- [122] R. Kuhlmann, G. L. Schimek, J. W. Kolis, *Polyhedron* **1999**, *18*, 1378.
- [123] G. Pon, R. D. Willet, B. A. Prince, W. T. Robinson, M. M. Turnbull, *Inorg. Chim. Acta* **1997**, *255*, 325.
- [124] J. T. Maeyer, T. J. Johnson, A. K. Smith, B. D. Borne, R. D. Pike, W. T. Pennington, M. Krawiec, A. L. Rheingold, *Polyhedron*, **2003**, *22*, 419.
- [125] P. C. Healy, J. D. Kildea, B. W. Skelton, A. H. White, *Aust. J. Chem.* **1989**, *42*, 115.
- [126] P. M. Graham, R. D. Pike, M. Sabat R. D. Bailey W. T. Pennington, *Inorg. Chem.* **2000**, *39*, 5121.
- [127] C. Janiak, L. Uehlin, H.-P. Wu, P. Klufers, H. Piotrowski, T. G. Scharmann, *J. Chem. Soc. Dalton Trans.* **1999**, 3121.
- [128] M. A. S. Goher, T. C. W. Mak, *Inorg. Chim. Acta.* **1985**, *101*, L27.

- [129] P. C. Healy, J. D. Kildea, B. W. Skelton, A. H. White, *Aust. J. Chem.* **1989**, *42*, 93.
- [130] P. C. Healy, B. W. Skelton, F. Waters, A. H. White, *Aust. J. Chem.* **1991**, *44*, 1041.
- [131] L. M. Engelhardt, P. C. Healy, J. D. Kildea, B. W. Skelton, A. H. White, *Aust. J. Chem.* **1989**, *42*, 933.
- [132] M. A. S. Goher, T. C. W. Mak, *Polyhedron* **1999**, *17*, 3485.
- [133] R. K. Barman, S. K. Singh, B. K. Dask, *J. Chem. Cryst.* **2002**, *32*, 369.
- [134] C. B. Aakeroy, A. M. Beatty, K. R. Lorimer, *J. Chem. Soc. Dalton Trans.* **2000**, 3869.
- [135] A. Lennartson, K. Salo, M. Hakansson, *Acta Cryst.* **2005**, *E61*, m1261.
- [136] S. Kawata, S. Kitagawa, H. Kurnagai, S. Iwabuchi, M. Katada, *Inorg. Chim. Acta* **1998**, *267*, 143.
- [137] Y. L. Jack, B. R. Cabrera, R.-J. Wang, J. Li, *Inorg. Chem.* **1999**, *38*, 4608.
- [138] J. Y. Lu, B. R. Cabrera, R.-J. Wang, J. Li, *Inorg. Chem. Cryst.* **1998**, *37*, 4480.
- [139] T. Kromp, W. S. Sheldrick, C. Näther, *Z. Anorg. Allg. Chem.* **2003**, *629*, 45.
- [140] N. S. Persky, J. M. Chow, K. A. Poschmann, N. N. Lacuesta, S. L. Stoll, *Inorg. Chem.* **2001**, *40*, 29.
- [141] R. D. Willet, J. R. Jeitler, B. Twamley, *Inorg. Chem* **2001**, *40*, 6502.
- [142] S. R. Batten, J. C. Jeffery, M. D. Ward, *Inorg. Chim. Acta* **1999**, *292*, 231.
- [143] A. J. Blake, N. R. Brooks, N. R. Champness, P. A. Cooke, M. Crew, A. M. Deveson, L. R. Hanton, P. Hubberstey, D. Fenske, M. Schröder, *Cryst. Eng.* **1999**, *2*, 181.
- [144] A. M. Goforth, M. D. Smith, H.-C. zur Loye, *J. Chem. Cryst.* **2003**, *33*, 303.
- [145] C. B. Aakeroy, A. M. Beatty, D. S. Leinen, K. R. Lorimer, *Chem. Commun.* **2000**, 935.
- [146] E. Cariati, X. Bu, P. C. Ford, *Chem. Mater.* , **2000**, *12*, 3385.
- [147] E. Bosch, W. Cordes, *J. Chem. Cryst.* **2003**, *33*, 723.
- [148] D. J. Chesnut, A. Kusnetzow, R. R. Birge, J. Zubieta, *Inorg. Chem.* **1999**, *38*, 2663.
- [149] S. Wang, E. Wang, Y. Hou, Y. Li, M. Yuan, N. Hu, *Inorg. Chim. Acta* **2003**, *349*, 123.
- [150] J. C. Dyason, P. C. Healy, L. M. Engelhardt, C. Pakawatchai, V. A. Patrick, C. L. Raston, A. H. White, *J. Chem. Soc. Dalton Trans.* **1985**, 831.
- [151] L. M. Engelhardt, P. C. Healy, J. D. Kildea, A. H. White, *Aust. J. Chem.*, **1989**, *42*, 107.
- [152] E. Sugahara, M. M. S. Paula, I. Vencato, C. V. Franco, *J. Coord. Chem.*, **1996**, *39*, 59.
- [153] M. R. Churchill, G. Davies, M. A. El-Sayed, J. P. Hutchinson, M. W. Rupic, *Inorg. Chem.*, **1982**, *21*, 995.
- [154] Y. Cui, J. Chen, G. Chen, J. Ren, W. Yu, Y. Qian, *Acta Cryst.*, **2001**, *C57*, 349.
- [155] Y. Moreno, E. Spodine, A. Vega, J.-Y. Saillard, *Inorg. Chim. Acta*, **2003**, *350*, 651.
- [156] J. Y. Lu, B. R. Cabrera, R.-J. Wang, J. Li, *Inorg. Chem.* **1998**, *37*, 4480.

- [157] I. Georgiev, C. L. Barnes, E. Bosch, *J. Supramol. Chem.*, **2001**, *1*, 153.
- [158] A. J. Blake, N. R. Brooks, N. R. Champness, P. A. Cook, A. M. Deveson, D. Fenske, P. Hubberstey, W.-S. Li, M. Schröder, *J. Chem. Soc. Dalton Trans.*, **1999**, 2103.
- [159] G. Li, Z. Shi, X. Liu, Z. Dai, S. Feng, *Inorg. Chem.* **2004**, *43*, 6884.
- [160] J. Strähle, W. Hiller, E. Eitel, D. Oelkrug, *Z. Krist.*, **1980**, *153*, 277.
- [161] D. Adam, B. Herrschaft, H. Hartl, *Z. Naturforsch. Chem. Sci.* **1991**, *46b*, 738.
- [162] D. M. L. Goodgame, P. D. Lickiss, S. J. Rooke, A. J. P. White, D. J. Williams, *Inorg. Chim. Acta*, **2001**, *324*, 218.
- [163] Zannetti, Serra, *Gazz. Chim. Ital.* **1960**, *90*, 328.
- [164] B. K. S. Lundberg, *Acta Cryst.*, **1966**, *21*, 901.
- [165] N.C. Baenziger R. J. Schuttltz, *Inorganic Chemistry*, **1971**, *10*, 661.
- [166] H. Lynton, M. C. Sears, *Can. J. Chem.* **1971**, *49*, 3418.
- [167] L. Fanfani, A. Nunzi, P. F. Zanazzi, *Acta Crystallogr.* **1972**, *28*, 323.
- [168] M. Laing, *Acta Crystallogr.* **1975**, *A31*, 147.
- [169] W. L. Steffen, G. J. Palenik, *Inorg.Chem.* **1977**, *16*, 1119.
- [170] J. F. Le Querler, M. M. Borel, A. Leclaire, *Acta Crystallogr.* **1977**, *33*, 2299.
- [171] A. Z. Amanov, D. A. Iashvili, A. N. Shnulin, N. I. Guseva, A. A. Akhundova, M. A. Porai.
- [172] Koshits, *Proc. Nat. Acad. Sci. Azebaidzhan*, **1984**, *40*, 55.
- [173] A. L. Beauchamp, *Inorganica Chimica Acta* **1984**, *91*, 33.
- [174] E. Bouwman, W. L. Driessen, R. A. G. de Graaff, J. Reedijk, *Acta Cryst.* **1984**, *C40*, 1562.
- [175] A. Mirceva, L. Golic, *Bull. Slovenian Chem. Soc.* **1987**, *34*, 449
- [176] E. Dubler, G. Hanggi, H. Schmalle, *Inorg. Chem.* **1992**, *31*, 3728.
- [177] H. L. Laity, M. R. Taylor, *Acta Cryst.* **1995**, *C51*, 1791.
- [178] C. A. Grapperhaus, T. Tuntulani, J. H. Reibenspies, M. Y. Darensbourg, *Inorg. Chem.* **1998**, *37*, 4052.
- [179] E. M. Cameron, W. E. Louch, T. S. Cameron, O. Knop, *Z. Anorg. Allg. Chem.* **1998**, *624*, 1629.
- [180] J. Qin, N. Su, C. Dai, C. Yang, D. Liu, M. W. Day, B. Wu., *Polyhedron* **1999**, *18*, 3461.
- [181] C. Hu, U. Englert, *Cryst. Eng. Comm.* **2002**, *4*, 20.
- [182] G. W. V. Cave, C. L. Raston, *J. Supramol. Chem.* **2002**, *2*, 317.
- [183] E. Sahin, S. Ide, A. Atac, S. Yurdakul, *J. Mol. Struct.* **2002**, *616*, 253.
- [184] H.-F. Zhu, L. Li, T. Okamura, W. Zhao, W.-Y. Sun, N. Ueyama, *Bull. Chem. Soc. Jpn.* **2003**, *76*, 761.

- [185] U. Siemeling, I. Scheppelmann, B. Neumann, A. Stammler, H.-G. Stammler, J. Frelek, *Chem. Commun.* **2003**, 2236.
- [186] C. Hu, J. Huster, U. Englert, Z. Kristallogr. **2003**, 218, 761.
- [187] C. de Cires-Mejias, S. Tanase, J. Reedijk, F. Gonzalez-Vilchez, R. Vilaplana, A. M. Mills, H. Kooijman, A. L. Spek, *Inorg. Chim. Acta* **2004**, 357, 1494.
- [188] L. Pazderski, E. Szlyk, A. Wojtczak, L. Kozerski, J. Sitkowskib, *Acta Cryst.* **2004**, E60, m1270.
- [189] C. H. Zhou, H. Y. Zhua, Y. Y. Wanga, P. Liua, L. J. Zhoua, D. S. Lia, Q. Z. Shia, *J. Mol. Struct.* **2005**, 779, 61.
- [190] L.-Q. Fan, J.-H. Wu, *Acta Crystallogr.* **2006**, C62, m548.
- [191] H. Pasaoglu, S. Guven, Z. Heren, O. Buyukgungor, *J. Mol. Struct.*, **2006**, 794, 270
- [192] W. L. Steffen, G. J. Palenik, *Acta Crystallogr.* **1976**, B32, 298.
- [193] A. S. Antsyshkina, M. A. Porai-Koshits, B. I. Saidov, N. N. Mal'tseva, N. S. Kedrova, V. N. Ostrikoval, *Russ. J. Inorg. Chem.* **1991**, **36**, 2291
- [194] J. Glerup, P. A. Goodson, D. J. Hodgson, K. Michelsen, U. Rychlewska, H. Weihe, *Bull. Chem. Soc. Ethiop.* **2000**, 14 129.
- [195] Y. Yamamoto, T. Suzuki, S. Kaizaki, *J. Chem. Soc., Dalton Trans.* **2001**, 1566.
- [196] C. Papatriantafyllopoulou, C. P. Raptopoulou, A. Terzis, E. Manessi-Zoupa, S. P. Perlepes, *Z. Naturforsch.* **2006**, B61, 37.
- [197] Corbridge, Cox, *J. Chem. Soc.* **1956**, 594.
- [198] F. W. B. Einstein, B. R. Penfold, *Acta Crystallogr.* **1966**, 20, 924.
- [199] M. Vlasse, T. Rojo, D. Beltran-Porter, *Acta Crystallogr.* **1983**, C39, 560.
- [200] F. Pezet, I. Sasaki, J.-C. Daran, J. Hydrio, H. Ait-Haddou, G. Balavoine, *Eur. J. Inorg. Chem.* **2001**, 2669.
- [201] K.-Y. Ho, W.-Y. Yu, K.-K. Cheung, C.-M. Che, *Dalton Trans.* **1999**, 1581.
- [202] Y. D. M. Champouret, J.-D. Marechal, I. Dadhiwala, J. Fawcett, D. Palmer, K. Singh, G. A. Solan, *Dalton Trans.* **2006**, 2350.
- [203] C.-Y. Su, A. M. Goforth, M. D. Smith, P. J. Pellechia, H.-C. Loye, *J. Am. Chem. Soc.*, **2004**, 126, 3576.
- [204] J. Pickardt, B. Staub *Z. Naturforsch.* **1996**, B51, 947.
- [205] C. Hu, U. Englert, *Cryst. Eng. Comm.* **2001**, 3, 91.
- [206] C. Hu, U. Englert, *Angew. Chem., Int. Ed.* **2005**, 44, 2281.
- [207] Y. Song, Y. Niu, H. Hou, Y. Zhu, *J. Mol. Struct.*, **2004** 689, 69
- [208] L. Hou, D. Li, *Inorg. Chem. Comm.* **2005**, 8, 190.
- [209] N.A. Bell, H.M.M. Shearer, C.B. Spencer, *Acta C*, **1983**, 39, 1182
- [210] B. Luo, B.E. Kucera, W.L. Gladfelter, *Polyhedron*, **2006**, 25, 279.
- [211] D. Das, B.G. Chand, K.K. Sarker, J. Dinda, C. Sinha, *Polyhedron*, **2006**, 25, 2333

- [212] F.A.Mautner, C.Kratky, *Cryst.Res.and Technol*, **1988**, 23,1477.
- [213] F.A. Mautner, H.Krischner, C.Kratky, *Z.Naturforsch.,B*, **1988**,43, 253
- [214] H. Hao, C. Cui, *H.W.Roesky, G. Bai, H.-G.Schmidt, M.Noltemeyer, Chem.Commun* **2001**, 1118.

2. Publications

2.1

Inorg. Chem. 2006, 45, 6508–6515

Inorganic Chemistry
: Article

On the Preparation of Coordination Polymers by Controlled Thermal Decomposition: Synthesis, Crystal Structures, and Thermal Properties of Zinc Halide Pyrazine Coordination Compounds

Gaurav Bhosekar, Inke Jess, and Christian Näther*

Institut für Anorganische Chemie, Universität zu Kiel, Olshausenstrasse 40 (Otto-Hahn-Platz 6-7), D-24098 Kiel, Germany

Received February 21, 2006

The five zinc(II) halide pyrazine coordination compounds poly-bis(μ_2 -pyrazine)-dichloro-zinc(II) (I), poly-(μ_2 -pyrazine-*N,N'*)-dichloro-zinc(II) (II), poly-bis(μ_2 -pyrazine-*N,N'*)-dibromo-zinc(II) (III), catena-(μ_2 -pyrazine-*N,N'*)-dibromo-zinc(II) (IV), and catena-(μ -pyrazine)-diiodo-zinc(II) (V) were prepared by the reaction of ZnX_2 ($X = Cl, Br, I$) with pyrazine in acetonitrile. In the crystal structure of compound I, the zinc atoms are coordinated by two chlorine atoms and two pyrazine ligands within distorted tetrahedra. The zinc atoms are linked by the N-donor ligands into layers. The crystal structure of compound III is very similar to that of compound I. The structure of compound III was originally reported in space group *Ccca* with similar *a* and *b* axes, but it was proved that the correct space group is *I4/mmm*. Ligand-poor compound V is isotopic to compound IV, in which ZnX_2 units ($X = Br, I$) are connected by the pyrazine ligands into chains. It was originally reported in the noncentrosymmetric space group *P2₁*, but we found that the correct space group is *P2₁/m*. If ligand-rich 1:2 compounds I and III are heated in a thermobalance, different mass steps are observed. We have proven that in the first step, ligand-poor compounds II and IV are formed in quantitative yields. On further heating, a second mass step occurs that leads to the formation of two new compounds of composition $(ZnCl_2)_2(\text{pyrazine})$ (VI) and $(ZnBr_2)_2(\text{pyrazine})$ (VII). However, the mass step is not well-resolved, and the new compounds are not phase-pure after the thermal event. If ligand-poor 1:1 compound V is investigated by thermogravimetry, a not-well-resolved single mass step is observed in which new ligand-poor 2:1 compound $(ZnI_2)_2(\text{pyrazine})$ (VIII) is formed. On further heating, all 2:1 compounds lose their remaining ligands and transform into the pure zinc(II) halides.

Introduction

In the past few years, numerous investigations on the synthesis, structures, and properties of new coordination polymers have been reported.^{1–10} The major goal in this area

is the preparation of new coordination compounds with well-defined physical properties. To reach this goal, researchers have to overcome several problems. First of all, strategies for a more-directed design of their crystal structures are needed; second, structure property relationships have to be investigated. However, for the investigations of the properties of compounds, we need large and pure amounts, which in the case of coordination polymers is sometimes difficult to achieve. In practically all cases, such compounds are prepared in a solution in which different compounds are in equilibrium, and therefore, mixtures of different solids are frequently obtained that have to be separated by hand. Moreover, some

* To whom correspondence should be addressed. E-mail: cnaether@ac.uni-kiel.de. Fax: 49 (0)431/880-1520.

- (1) Batten, S. R.; Robson, R. *Angew. Chem.* **1998**, *110*, 1558–1595; *Angew. Chem., Int. Ed.* **1998**, *37*, 1460–1467.
- (2) Robson, R.; Abrahams, B. F.; Batten, S. R.; Grable, R. W.; Hoskins, B. F.; Liu, J. In *Supramolecular Architecture*; American Chemical Society Publications: Washington, DC, 1992; Chapter 19.
- (3) Moulton, B.; Zaworotko, M. J. *Chem. Soc. Rev.* **2001**, *101*, 1629–1658.
- (4) Hagrman, P. J.; Hagrman, D.; Zubieta, J. *Angew. Chem.* **1999**, *111*, 2798–2848; *Angew. Chem., Int. Ed.* **1999**, *38*, 2638–2688.
- (5) Robson, R. In *Comprehensive Supramolecular Chemistry*; Pergamon: New York, 1996; Chapter 22, pp 733–748.
- (6) Blake, A. J.; Champness, N. R.; Hubberstey, P.; Li, W.-S.; Schröder, M. *Coord. Chem. Rev.* **1999**, *183*, 17–33.
- (7) Braga, D.; Maini, L.; Polito, M.; Scaccianoce, L.; Cojazzi, G.; Grepioni, F. *Coord. Chem. Rev.* **2001**, *216*, 783–788.

(8) Muthu, S.; Yip, J. H. K.; Vittal, J. J. *J. Chem. Soc., Dalton Trans.* **2001**, *24*, 3577–3584.

(9) Chen, W.; Yuan, H.; Wang, J.; Liu, Z.; Xu, J.; Yang, M.; Chen, J. *J. Am. Chem. Soc.* **2003**, *125*, 9266–9267.

(10) Wu, C.; Lin, W. *Inorg. Chem.* **2005**, *44*, 1178–1180.

Zinc Halide Pyrazine Coordination Compounds

compounds cannot be prepared in solution or are overlooked, especially if these compounds are thermodynamically metastable. Therefore, alternative routes for the discovery and preparation of pure new or known coordination polymers are really needed.

In our own investigations, we have investigated coordination polymers on the basis of copper(I) halides and different N-donor ligands.^{11–22} For one specific halide atom and one specific ligand, several compounds of a different ratio between the copper halide and the ligand are frequently observed and therefore ligand-rich and ligand-poor compounds can be prepared. We found that most of the ligand-rich coordination polymers can be transformed into ligand-poor coordination polymers on heating before decomposition into the pure copper(I) halides is observed.^{11–22} In most cases, the ligand-poor intermediates are obtained very pure and always in quantitative yields. Only in some minor cases is no ligand-poor intermediate observed at all.¹⁴ We have also found that coordination polymers on the basis of copper(I) pseudohalides react in a similar way^{23–25} and that ligand-poor compounds on the basis of silver(I) halides can also be prepared.²⁶ Especially the copper(I) pseudohalides are of interest, because most of them show luminescence or thermoluminescence properties.²³ To understand such reactions in more detail, we have started systematic investigations on the thermal behavior of these compounds. We found, for example, that in some cases, several ligand-poor intermediates can be obtained and that the reactivity can be influenced by mixed-crystal formation.¹⁵ We have also demonstrated that the product formation depends on the kinetics of all reactions involved, and therefore, different products can be prepared by heating-rate-dependent measurements.¹⁷ During these investigations, we identified different isomers and polymorphic modifications; as one of the major results of the experiments, no simple relationship between the structures of these compounds and their thermal reactivity or thermodynamic stability could be established.^{18–20} Because the dimensionality of the coordination networks increases in the direction of the ligand-poor compounds, we applied

Table 1. Crystal Data and Results of the Structure Refinement for Compounds I, III, and V

	I	III	V
chemical formula	C ₈ H ₈ Cl ₂ N ₄ Zn	C ₈ H ₈ N ₄ Br ₂ Zn	C ₄ H ₃ N ₂ I ₂ Zn
fw	296.46	375.35	399.26
space group	Ccca	I4/mmm	P2 ₁ /m
a (Å)	10.1630(11)	7.1969 (8)	6.3113 (8)
b (Å)	10.6042(15)	7.1969 (8)	9.8980 (13)
c (Å)	10.1858(10)	11.1356(15)	7.4380 (9)
β (deg)			109.871 (14)
V (Å ³)	1097.7(2)	576.77(12)	436.98 (10)
T (°C)	20	20	20
Z	4	2	2
D _{calcd} (g cm ⁻³)	1.794	2.058	3.034
μ (mm ⁻¹)	2.693	9.014	9.798
I (Å)	0.71073	0.71073	0.71073
R ₁ ^a [I > 2σ(I)]	0.0260	0.0228	0.0357
wR ₂ ^a [all data]	0.0725	0.0552	0.0933

$$^a R_1 = \sum ||F_o| - |F_c|| / \sum |F_o|; wR_2 = [\sum [w(F_o^2 - F_c^2)^2] / \sum [w(F_o^2)^2]]^{1/2}.$$

this method to the preparation of coordination polymers that exhibit cooperative magnetic properties.²⁷

However, to investigate if the preparation of coordination polymers can be widely used as a preparative tool or for the discovery of new compounds, we have started systematic investigations of the thermal properties of other coordination compounds. In the beginning, we decided to investigate coordination polymers on the basis of zinc halides and N-donor ligands.²⁸ Only a few of such compounds were reported in the literature, but the analysis of their structures has shown that the topologies of their coordination networks are very often similar to that of the copper(I) coordination polymers.^{29–34} In addition, in contrast to copper(I), in zinc compounds, octahedral coordination can also be found, which increases the structural diversity dramatically. Therefore, for zinc halides, ligand-rich and ligand-poor compounds can be expected, which might show a thermal reactivity similar to that of the copper(I) coordination compounds. Because we are predominantly interested in the thermal reactivity, we decided to first investigate compounds for which at least some coordination compounds were reported. This is the case for the Zn halide coordination polymers with the diazine ligand pyrazine. Altogether, four different compounds were structurally characterized: ligand-rich compound poly-bis-(μ₂-pyrazine-*N,N'*)-dibromo-zinc(II) (III)³² and ligand-poor compounds poly-(μ₂-pyrazine-*N,N'*)-dichloro-zinc(II) (II),³³ catena-(μ₂-pyrazine-*N,N'*)-dibromo-zinc(II) (IV),³² and catena-(μ₂-pyrazine-*N,N'*)-diiodo-zinc(II) (V).³⁴ The crystallographic data reported for compounds III and V highly suggest that the structure determinations were not correctly performed. Therefore, we redetermined these structures in

- (11) Näther, C.; Greve, J.; Jess, I. *Polyhedron* **2001**, *20* (9–10), 1017–1022.
 (12) Näther, C.; Jess, I.; Studzinski, H. *Z. Naturforsch.* **2001**, *56b*, 997–1002.
 (13) Näther, C.; Jess, I. *Monatsh. Chem.* **2001**, *132*, 897–910.
 (14) Näther, C.; Wriedt, M.; Jess, I. *Z. Anorg. Allg. Chem.* **2002**, *628*, 394–400.
 (15) Näther, C.; Greve, J.; Jess, I. *Solid State Sci.* **2002**, *4*(6), 813–820.
 (16) Näther, C.; Jess, I. *Z. Naturforsch.* **2002**, *57b*, 1133–1140.
 (17) Näther, C.; Jess, I. *J. Solid State Chem.* **2002**, *169*, 103–112.
 (18) Näther, C.; Wriedt, M.; Jess, I. *Inorg. Chem.* **2003**, *42*, 2391–2397.
 (19) Näther, C.; Jess, I. *Inorg. Chem.* **2003**, *42*, 2968–2976.
 (20) Näther, C.; Jess, I.; Lehnert, N.; Hinz-Hübner, D. *Solid State Sci.* **2003**, *5*, 1343–1357.
 (21) Näther, C.; Jess, I.; Bolte, M. *Z. Naturforsch.* **2003**, *58b*, 1105–1111.
 (22) Kromp, T.; Sheldrick, W. S.; Näther, C. *Z. Anorg. Allg. Chem.* **2003**, *629*, 45–54.
 (23) Näther, C.; Greve, J.; Jess, I.; Wickleder, C. *Solid State Sci.* **2003**, *5*, 1167–1176.
 (24) Näther, C.; Jess, I.; Kowallik, P. *Z. Anorg. Allg. Chem.* **2003**, *629*, 2144–2155.
 (25) Greve, J.; Näther, C. *Z. Naturforsch.* **2004**, *59b*, 1325–1331.
 (26) Näther, C.; Beck, A. *Z. Naturforsch.* **2004**, *59b*, 992–998.

- (27) Näther, C.; Greve, J. *J. Solid State Chem.* **2003**, *176*, 259–265.
 (28) Bhosekar, G.; Jess, I.; Näther, C. *Z. Naturforsch.* **2006**, *61b*, 721–726.
 (29) Godfrey, S. M.; McAuliffe, C. A.; Pritchard, R. G.; Sheffield, J. M. *Inorg. Chim. Acta* **1999**, *292*, 213–219.
 (30) Bottomley, F.; Ferris, E. C.; White, P. S. *Acta Crystallogr., Sect. C* **1989**, *45*, 816–817.
 (31) Chunhua, Hu; Englert, U. *CrystEngComm* **2001**, *3*, 91–95.
 (32) Bourne, S. A.; Kilkenny, M.; Nassimbeni, L. R. *J. Chem. Soc., Dalton Trans.* **2001**, 1176–1179.
 (33) Staub, B.; Pickardt, J. *Z. Naturforsch.* **1996**, *51b*, 947–952.
 (34) Zhu, Y.; Hou, H.; Niu, Y.; Song, Y. *J. Mol. Struct.* **2004**, *689*, 69–74.

the beginning. In addition, for ZnCl_2 and ZnI_2 , no ligand-rich compounds were reported until now, which is surprising because one would expect a ligand-rich coordination polymer for at least one of these compounds. For zinc chloride, we identified, prepared, and structurally characterized such a ligand-rich coordination polymer. Finally, all compounds were investigated with respect to their thermal properties, which shows that the ligand-rich compounds transform into the ligand-poor coordination polymers and that there are additional ligand-poor samples that were not expected in the beginning. Here, we report on these investigations.

Experimental Section

Synthesis. All compounds were prepared by stirring the reactants in acetonitrile for 2 days. The residues were filtered off and washed with diethyl ether. The purity of these compounds was checked by X-ray powder diffraction (see the Supporting Information).

Synthesis of Poly-bis(μ_2 -pyrazine)-dichloro-zinc(II) (I). Crystalline powder of compound **I** was prepared by the reaction of 0.5 mmol (68.1 mg) ZnCl_2 and 5.0 mmol (400.4 mg) pyrazine in 2.0 mL of acetonitrile. Yield: 90.4% (134.0 mg) on the basis of ZnCl_2 . CHN anal. Calcd for $\text{C}_8\text{H}_8\text{Cl}_2\text{N}_4\text{Zn}$: C, 32.41; H, 2.72; N, 18.90. Found: C, 32.68; H, 2.52; N, 18.57. IR (KBr, cm^{-1}): 3106 (w), 1483 (w), 1415 (s), 1377 (w), 1155 (m), 1118 (m), 1053 (s), 992 (w), 818 (m), 790 (m), 427 (s), 446 (w). Preparation of single crystals: 0.5 mmol (68.09 mg) ZnCl_2 was mixed with 5.0 mmol (400.4 mg) pyrazine in 3.0 mL of acetone. After slow evaporation of the solvent, colorless crystals are obtained within about 1 week.

Synthesis of Poly(μ_2 -pyrazine- N,N')-dichloro-zinc(II) (II). Crystalline powder of compound **II** was prepared by the reaction of 0.5 mmol (68.1 mg) ZnCl_2 and 0.5 mmol (40.0 mg) pyrazine in 2.0 mL of acetonitrile. Yield: 52.6% (56.9 mg). CHN anal. Calcd for $\text{C}_4\text{H}_4\text{Cl}_2\text{N}_2\text{Zn}$: C, 22.20; H, 1.86; N, 12.95. Found: C, 22.32; H, 1.93; N, 13.17. IR (KBr, cm^{-1}): 3114 (w), 1483 (w), 1417 (s), 1168 (m), 1118 (m), 1054 (s), 790 (m), 466 (s), 446.3 (w).

Synthesis of Poly-bis(μ_2 -pyrazine- N,N')-dibromo-zinc(II) (III). Crystalline powder of compound **III** was prepared by the reaction of 1.0 mmol (225.2 mg) ZnBr_2 and 2.0 mmol (160.2 mg) pyrazine in 2.0 mL of acetonitrile. Yield: 88.7% (341.8 mg). CHN anal. Calcd for $\text{C}_8\text{H}_8\text{Br}_2\text{N}_4\text{Zn}$: C, 24.93; H, 2.09; N, 14.54. Found: C, 24.92; H, 2.08; N, 14.13. IR (KBr, cm^{-1}): 3106 (w), 3088 (w), 1963 (w), 1428 (m), 1409 (s), 1375 (m), 1155 (m), 1118 (s), 1053 (s), 992 (m), 817 (s), 463 (s). Preparation of single crystals: 0.1 mmol (22.5 mg) ZnBr_2 was mixed with 1.0 mmol (80.1 mg) pyrazine in 3.0 mL of methanol. After slow evaporation of the solvent, colorless crystals are obtained within about 1 week.

Synthesis of Catena(μ_2 -pyrazine- N,N')-dibromo-zinc(II) (IV). Crystalline powder of compound **IV** was prepared by the reaction of 1.0 mmol (225.2 mg) ZnBr_2 and 1.0 mmol (80.1 mg) pyrazine in 2.0 mL of acetonitrile. Yield: 89.0% (271.7 mg). CHN anal. Calcd for $\text{C}_4\text{H}_4\text{Br}_2\text{N}_2\text{Zn}$: C, 15.74; H, 1.32; N, 9.18. Found: C, 15.89; H, 1.31; N, 9.13. IR (KBr, cm^{-1}): 3124 (m), 3088 (m), 3042 (m), 2999 (w), 2923 (w), 1943 (w), 1880 (w), 1774 (w), 1496 (w), 1427 (s), 1165 (s), 1123 (s), 1112 (m), 1063 (s), 984 (w), 815 (s), 469 (s), 446 (s).

Synthesis of Catena(μ -pyrazine)-diiodo-zinc(II) (V). Crystalline powder of compound **V** was prepared by the reaction of 1.0 mmol (319.2 mg) ZnI_2 and 1.0 mmol (80.1 mg) pyrazine in 2.0 mL of acetonitrile. Yield: 91.9% (366.9 mg). CHN anal. Calcd for $\text{C}_4\text{H}_4\text{I}_2\text{N}_2\text{Zn}$: C, 12.03; H, 1.01; N, 7.02. Found: C, 12.12; H, 0.96; N, 8.29. IR (KBr, cm^{-1}): 3117 (m), 3075 (w), 3036 (m), 1875 (w), 1769 (w), 1492 (w), 1424 (s), 1165 (s), 1121 (s), 1062

(s), 814 (s), 468 (s), 444 (s). Preparation of single crystals: 0.05 mmol (15.95 mg) ZnI_2 was mixed with 0.05 mmol (4.00 mg) pyrazine in 0.3 mL of water. After slow evaporation of the solvent, colorless crystals were obtained within about 2 weeks.

CHN Analysis of the Residues Obtained in the Thermal Decomposition of Compounds I–V. (A) Isolated after first heating step for compound **I** (%). Found: C, 22.22; H, 1.75; N, 12.86. Calcd for compound **I**: C, 22.20; H, 1.86; N, 12.95. (B) Isolated after first heating step for compound **II** (%). Found: C, 13.44; H, 1.38; N, 7.68. Calcd for **II**: C, 13.62; H, 1.14; N, 7.94. (C) Isolated after first heating step for compound **III** (%). Found: C, 15.91; H, 1.32; N, 10.23. Calcd for compound **III**: C, 15.74; H, 1.32; N, 9.18. (D) Isolated after first heating step for compound **IV** (%). Found: C, 8.96; H, 0.79; N, 5.14. Calcd for compound **IV**: C, 9.06; H, 0.76; N, 5.28. (E) Isolated after first heating step for compound **V** (%). Found: C, 5.49; H, 0.35; N, 3.19. Calcd for compound **V**: C, 6.69; H, 0.56; N, 3.90.

Single-Crystal Structure Analysis. All investigations were performed with an imaging plate diffraction system (IPDS-1) from STOE & CIE. The structure solutions were performed with direct methods using SHELXS-97,³⁵ and structure refinements were performed against F^2 using SHELXL-97.³⁶ For all structures, a numerical absorption correction was applied using X-Red³⁷ and X-Shape.³⁸ All non-hydrogen atoms were refined with anisotropic displacement parameters. All hydrogen atoms were positioned with idealized geometry and were refined with fixed isotropic displacement parameters ($U_{\text{eq}}(\text{H}) = 1.2U_{\text{eq}}(\text{C})$) using a riding model with $d\text{C}-\text{H} = 0.95 \text{ \AA}$. Details of the structure determination are given in Table 1 and in the Supporting Information.

Crystallographic data (excluding structure factors) for the structures reported in this paper have been deposited with the Cambridge Crystallographic Data Centre as supplementary publication no. CCDC602639 (**I**), CCDC602640 (**III**), and CCDC602641 (**V**). Copies of the data can be obtained, free of charge, on application to CCDC, 12 Union Road, Cambridge CB2 1EZ, U.K. (fax: 44-(0)1223-336033 or e-mail: deposit@ccdc.ca.ac.uk).

X-ray Powder Diffraction. Powder-diffraction experiments were performed using a STOE STADI P transmission powder diffractometer with $\text{Cu K}\alpha$ radiation ($\lambda = 154.0598 \text{ pm}$) that is equipped with a position-sensitive detector (scan range: $5-45^\circ$) from STOE & CIE.

Differential Thermal Analysis, Thermogravimetry, and Mass Spectroscopy. The heating-rate-dependent DTA-TG measurements were performed in a nitrogen atmosphere (purity: 5.0) in Al_2O_3 crucibles using a STA-409CD instrument from Netzsch. The DTA-TG-MS measurements were performed with the same instrument, which is connected to a quadrupole mass spectrometer from Balzers via Skimmer coupling from Netzsch. The MS measurements were performed in analogue and trend scan mode in Al_2O_3 crucibles in a dynamic nitrogen atmosphere (purity: 5.0) using heating rates of $4^\circ\text{C}/\text{min}$. All measurements were performed with a flow rate of $75 \text{ mL}/\text{min}$ and were corrected for buoyancy and current effects. The instrument was calibrated using standard reference materials.

Elemental Analysis. CHN analysis has been performed using

(35) Sheldrick, G. M. *SHELXS 97, Program for Crystal Structure Solution*; University of Göttingen: Göttingen, Germany, 1997.

(36) Sheldrick, G. M. *SHELXL-97, Program for the Refinement of Crystal Structures*; University of Göttingen: Göttingen, Germany, 1997.

(37) *X-Red, version 1.11: Program for Data Reduction and Absorption Correction*; STOE & CIE GmbH: Darmstadt, Germany, 1998.

(38) *X-Shape, version 1.03: Program for the Crystal Optimization for Numerical Absorption Correction*; STOE & CIE GmbH: Darmstadt, Germany, 1998.

Zinc Halide Pyrazine Coordination Compounds

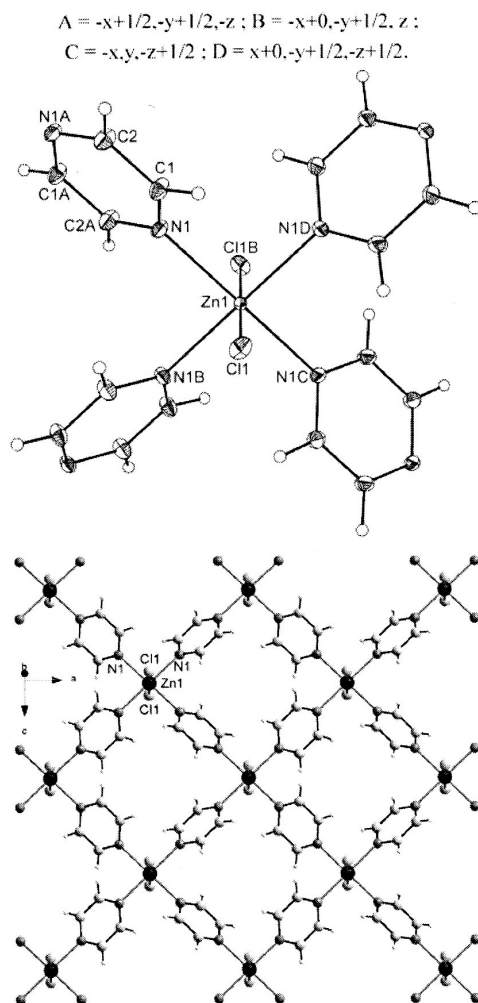


Figure 1. Crystal structure of compound **I** with view of the coordination sphere of the zinc cations with labeling and displacement ellipsoids drawn at the 50% probability level (top) and view of the structure approximately in the direction of the crystallographic *b* axis (bottom). Symmetry codes: $A = -x + 1/2, -y + 1/2, -z$; $B = -x + 0, -y + 1/2, z$; $C = -x, y, -z + 1/2$; $D = x + 0, -y + 1/2, -z + 1/2$.

an EURO EA elemental analyzer, fabricated by EURO VECTOR Instruments and Software.

Results and Discussion

Synthetic Aspects. The formation of all compounds was investigated in solution using ex situ time-dependent X-ray powder diffraction. Compounds **II–V** can be prepared phase-pure by reacting stoichiometric amounts of the reactants in acetonitrile. However, if zinc(II) chloride is reacted with pyrazine in a 1:2 ratio, which should lead to the formation of ligand-rich compound **I**, ligand-poor 1:1 compound **II** is obtained as phase-pure material. Compound **I** can be prepared only if a 5-fold excess of pyrazine is used in the synthesis, which might be the reason that this compound was overlooked in previous reports. However, both ligand-rich compounds are not stable as solids. In solution, ligand-rich

Table 2. Bond Lengths (Å) and Angles (deg) for Compound **I**^a

Zn(1)–N(1D)	2.2053(15)	Zn(1)–N(1)	2.2053(15)
Zn(1)–N(1B)	2.2053(15)	Zn(1)–Cl(1)	2.4143(7)
Zn(1)–N(1C)	2.2053(15)	Zn(1)–Cl(1B)	2.4143(7)
N(1D)–Zn(1)–N(1B)	179.36(6)	N(1C)–Zn(1)–Cl(1)	90.32(3)
N(1D)–Zn(1)–N(1C)	90.16(8)	N(1)–Zn(1)–Cl(1)	90.32(3)
N(1B)–Zn(1)–N(1C)	89.84(8)	N(1D)–Zn(1)–Cl(1B)	90.32(3)
N(1D)–Zn(1)–N(1)	89.84(8)	N(1B)–Zn(1)–Cl(1B)	90.32(3)
N(1B)–Zn(1)–N(1)	90.16(8)	N(1C)–Zn(1)–Cl(1B)	89.68(3)
N(1C)–Zn(1)–N(1)	179.36(6)	N(1)–Zn(1)–Cl(1B)	89.68(3)
N(1D)–Zn(1)–Cl(1)	89.68(3)	Cl(1)–Zn(1)–Cl(1B)	180.0
N(1B)–Zn(1)–Cl(1)	89.68(3)		

^a Symmetry transformations used to generate equivalent atoms: $A = -x + 1/2, -y + 1/2, -z$; $B = -x + 0, -y + 1/2, z$; $C = -x, y, -z + 1/2$; $D = x + 0, -y + 1/2, -z + 1/2$.

compound **I** transforms into ligand-poor 1:1 compound **II** within a few days. If ligand-rich compound **III** is prepared by the reaction of $ZnBr_2$ with pyrazine in acetonitrile, it also transforms into the ligand-poor compound; however, the decomposition is much slower than for the $ZnCl_2$ compound **I**, which shows that the stability of the ligand-rich compounds increases from chlorine to bromine. However, it can also be assumed that the stability of the ligand-poor 1:1 compounds increases from chlorine to iodine, which would explain why no ligand-rich compound with ZnI_2 and pyrazine can be prepared. In our thermal investigations, we proved that there exist additional ligand-poor compounds of composition $(ZnX_2)_2(\text{pyrazine})$ ($X = Cl, Br, I$) (see thermoanalytical investigations). Therefore, we tried to prepare these compounds in solution as well. But, if the zinc(II) halides and pyrazine are mixed in a 2:1 molar ratio, only ligand-poor 1:1 compounds **II**, **IV**, and **V** are obtained, which demonstrates that the 1:1 coordination polymers represent the thermodynamically most stable compounds in this system. This is somewhat surprising, because one can expect that in the ligand-poor 2:1 compounds, a more-condensed coordination network with condensed $(ZnX_2)_n$ substructures ($X = Cl, Br, I$) can be found.

Crystal Structures. Compound **I** crystallizes in orthorhombic space group $Pnma$ with 4 formula units in the unit cell. In the crystal structure, the zinc atoms are each coordinated by two symmetry-related chlorine atoms and four symmetry-equivalent pyrazine ligands within slightly distorted octahedra (Figure 1, top, and Table 2).

The nitrogen atoms are located in the basal plane, whereas the chlorine atoms occupy the apical positions. The zinc atoms are connected by the pyrazine ligands by μ - N,N' coordination into layers that are parallel to the a - b plane (Figure 1, bottom). These layers are stacked in the direction of the crystallographic c axis, with the zinc atoms and pyrazine ligands arranged in separate columns.

The crystal structure of compound **III** was originally reported in orthorhombic space group $Cmmm$ with $a = 10.1904(4)$, $b = 10.1981(6)$, and $c = 11.1516(7)$.³² In this structure, the pyrazine ligands are disordered in two different orientations because of symmetry. The similarity of the a and b axes as well as the disorder of the ligands give strong hints that either the structure will crystallize tetragonal or the cell parameters are wrong, maybe because super structure reflections were overlooked. We redetermined the structure

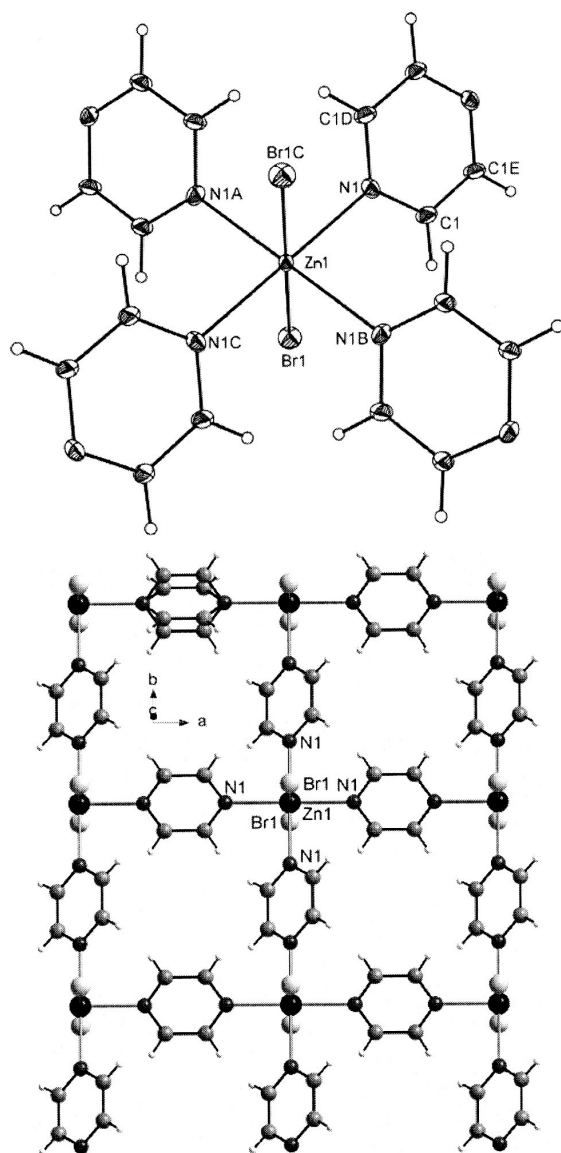


Figure 2. Crystal structure of compound III with view of the coordination sphere of the zinc cations with labeling and displacement ellipsoids drawn at the 70% probability level (top) and view of the structure approximately in the direction of the crystallographic *c* axis (bottom). Symmetry codes: A = $y, -x + 1, -z + 1$; B = $-y + 1, x, z$; C = $-x + 1, -y + 1, -z + 1$; D = $-x + 1, y, -z + 1$; E = $x, -y + 2, z$. For clarity, the disorder of the pyrazine ligand is shown for only one ligand.

and found no hints for super structure reflections, but the structure can easily be refined in the tetragonal space group $I4/mmm$. In this space group, the disorder of the pyrazine ligands is still present. The zinc atoms are located on $4/mmm$ sites, the bromine atom on the $4mm$ position, and the pyrazine ligand on sites with symmetry mmm .

In the crystal structure, the zinc atoms are coordinated by two symmetrically related bromine atoms and four symmetry equivalent pyrazine ligands within a distorted octahedron. (Figure 2, top, and Table 3). The zinc atoms are connected

Table 3. Bond Lengths (Å) and Angles (deg) for Compound III^a

Zn(1)–N(1A)	2.206(3)	Zn(1)–Br(1C)	2.5782(5)
Zn(1)–N(1B)	2.206(3)	Zn(1)–N(1C)	2.206(3)
Zn(1)–N(1)	2.206(3)	Zn(1)–Br(1)	2.5782(5)
N(1A)–Zn(1)–N(1B)	180.0	N(1A)–Zn(1)–Br(1C)	90.0
N(1)–Zn(1)–N(1C)	180.0	N(1B)–Zn(1)–Br(1C)	90.0
N(1A)–Zn(1)–N(1)	90.000(1)	N(1)–Zn(1)–Br(1C)	90.0
N(1B)–Zn(1)–N(1C)	90.000(1)	N(1C)–Zn(1)–Br(1C)	90.0
N(1A)–Zn(1)–Br(1)	90.0	N(1B)–Zn(1)–N(1)	90.0
Br(1)–Zn(1)–Br(1C)	180.0	N(1A)–Zn(1)–N(1C)	90.0
N(1)–Zn(1)–Br(1)	90.0	N(1B)–Zn(1)–Br(1)	90.0
N(1C)–Zn(1)–Br(1)	90.0		

^a Symmetry transformations used to generate equivalent atoms: A = $y, -x + 1, -z + 1$; B = $-y + 1, x, z$; C = $-x + 1, -y + 1, -z + 1$; D = $-x + 1, y, -z + 1$; E = $x, -y + 2, z$.

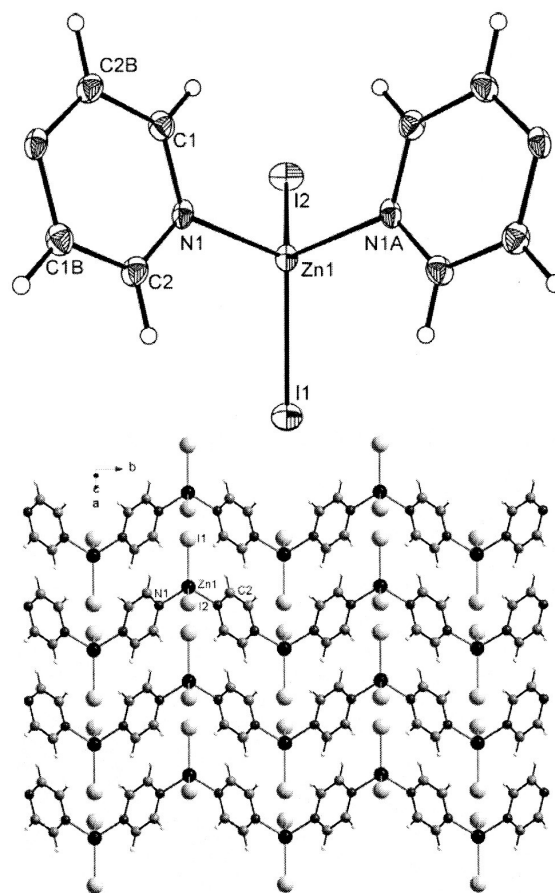


Figure 3. Crystal structure of compound V with view of the coordination sphere of the zinc cations with labeling and displacement ellipsoids drawn at the 50% probability level (top) and view of the structure in the direction of approximately the crystallographic *c* axis (bottom). Symmetry codes: A = $x, -y + 1/2, z$; B = $-x, -y, -z + 1$.

by the pyrazine ligands into chains, which are further joined by ligands into layers that are parallel to the a – b axis (Figure 2, bottom).

Compound V crystallizes in monoclinic space group $P2_1/m$ with 2 formula units in the unit cell and is isotypic to bromine compound IV. This structure was previously reported in noncentrosymmetric space group $P2_1$;³⁴ however, the cell parameters are very similar to those of compound IV, and it

Zinc Halide Pyrazine Coordination Compounds

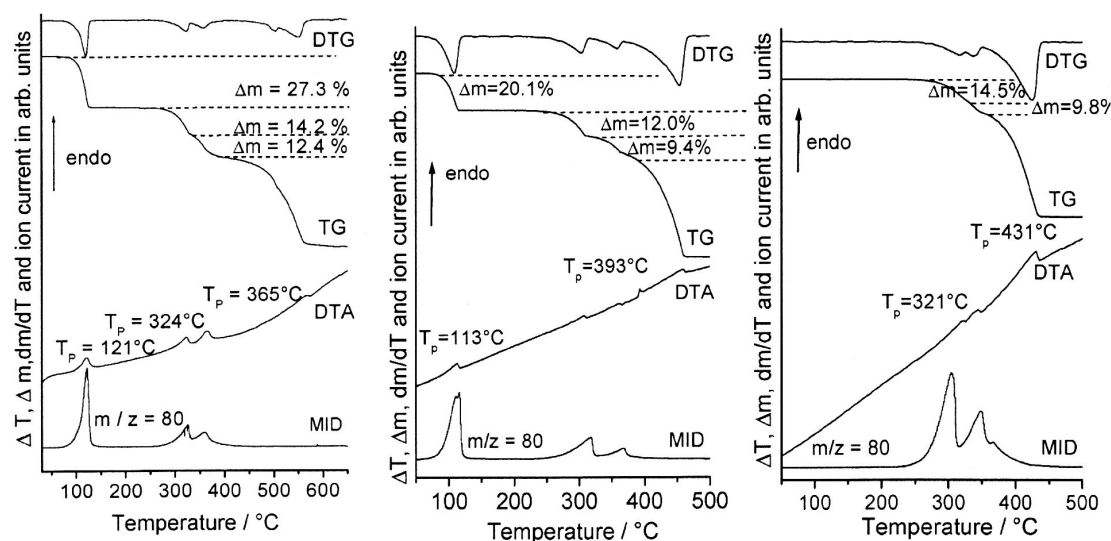


Figure 4. DTA, TG, DTG, and MS trend scan curve for compound **I** (left), **III** (middle), and **V** (right). Heating rate = 4 °C/min; $m/z = 80$ (pyrazine); given are the mass changes (%) and the peak temperatures T_p (°C).

Table 4. Bond Lengths (Å) and Angles (deg) for Compound **V**^a

I(1)–Zn(1)	2.5194(11)	Zn(1)–N(1)	2.082(4)
I(2)–Zn(1)	2.5193(10)	Zn(1)–N(1A)	2.082(4)
N(1)–Zn(1)–N(1A)	94.3(2)	N(1)–Zn(1)–I(1)	110.23(13)
N(1)–Zn(1)–I(2)	109.11(13)	N(1A)–Zn(1)–I(1)	110.23(13)
N(1A)–Zn(1)–I(2)	109.11(13)	I(2)–Zn(1)–I(1)	120.64(3)
C(2)–N(1)–Zn(1)	121.0(3)	C(1)–N(1)–Zn(1)	120.9(4)

^a Symmetry transformations used to generate equivalent atoms: A = $x, -y + 1/2, z$; B = $-x, -y, -z + 1$.

is obvious that the structure was refined in a wrong space group. In the crystal structure, the zinc atoms are each coordinated by two symmetry-related iodine atoms and two symmetry-equivalent pyrazine ligands (Figure 3, top, and Table 4). The zinc atoms as well as the two crystallographically independent iodine atoms are located on a mirror plane, whereas the pyrazine ligand is situated on a center of inversion. The ZnI_2 units are connected by the pyrazine ligands by μ - N,N' coordination into chains that elongate in the direction of the crystallographic b axis (Figure 3, bottom).

Thermoanalytic Investigations. On heating 1:2 compound **I** to 650 °C, four mass steps are observed in the TG curve that are accompanied with endothermic events in the DTA curve (Figure 4, left). From the MS trend scan curve, it is obvious that the ligand ($m/z = 80$) is emitted during only the first three mass steps. The mass loss in the first step of 27.3% is in good agreement with that calculated for the removal of half of the ligands, 27.0%. Therefore, one can assume that during this thermal reaction, ligand-poor compound **II** has been formed. From the DTG curve, it is obvious that the second mass step is not well-resolved, and therefore, the mass loss is difficult to estimate (Figure 4, left). However, the experimental mass loss of this step of about 14.2% is in reasonable agreement with that calculated for the removal of an additional half a ligand ($\Delta m_{\text{theo}}(-1/2 \text{ pyrazine}) = 13.5\%$), which may lead to a new ligand-poor 2:1 compound of composition $(ZnCl_2)_2(\text{pyrazine})$. On further heating, the remaining ligands are emitted; this leads to the

formation of $ZnCl_2$, which vaporizes on further heating (Figure 4, left).

If the ligand-rich 1:2 compound $ZnBr_2(\text{pyrazine})_2$ (**III**) is heated, a similar behavior as for compound **I** is observed (Figure 4, middle). Compared to those in compound **I**, all decomposition temperatures are shifted to higher values. The experimental mass loss observed in the first TG step of 20.1% is in reasonable agreement with that expected for the removal of half of the ligands ($\Delta m_{\text{theo}}(-1 \text{ pyrazine}) = 20.7\%$). As for the thermal decomposition of compound **I**, the second TG step cannot be resolved successfully (Figure 4, middle). However, the estimated mass loss of about 12.0% is in rough agreement with that calculated for the formation of a ligand-poor 2:1 compound ($\Delta m_{\text{theo}}(-1/2 \text{ pyrazine}) = 10.3\%$).

For ZnI_2 , no ligand-rich 1:2 compound can be prepared; therefore, ligand-poor 1:1 compound **V** was investigated. The curves are similar to those obtained for compounds **I** and **III**, starting after the first TG step (Figure 4, right). The experimental mass loss during the first TG step of 14.5% is in rough agreement with that expected for the formation of a ligand-poor 2:1 compound of 10.0%.

From the DTA-TG-MS measurements, there are hints that ligand-rich 2:1 compounds **I** and **III** decompose in the first step into ligand-poor 1:1 compounds **II** and **IV**. To prove these assumptions, we performed additional TG measurements and stopped after the first TG step. Afterward, the residues were investigated by X-ray powder diffraction (Figure 5). Comparing the powder patterns of these residues with those calculated for 1:1 compounds **II** and **IV** from single-crystal data, it is obvious that these phases were formed in the thermal decomposition reaction. In addition, the residues were investigated by elemental analysis, demonstrating that the compositions are in good agreement with those calculated for 1:1 compounds **II** and **IV** (see Experimental Section).

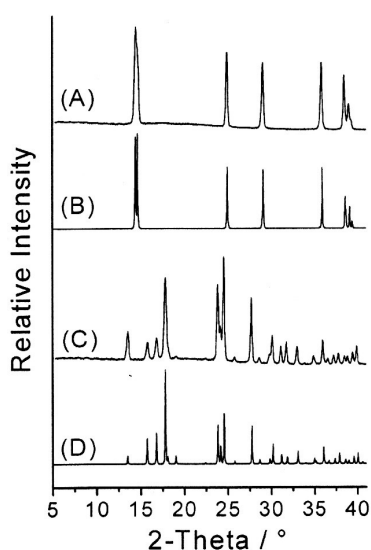


Figure 5. Experimental X-ray powder patterns of the residues obtained during the thermal decomposition of ligand-rich compounds **I** (A) and **III** (C) at 160 °C and calculated patterns for ligand-poorer compounds **II** (B) and **IV** (D).

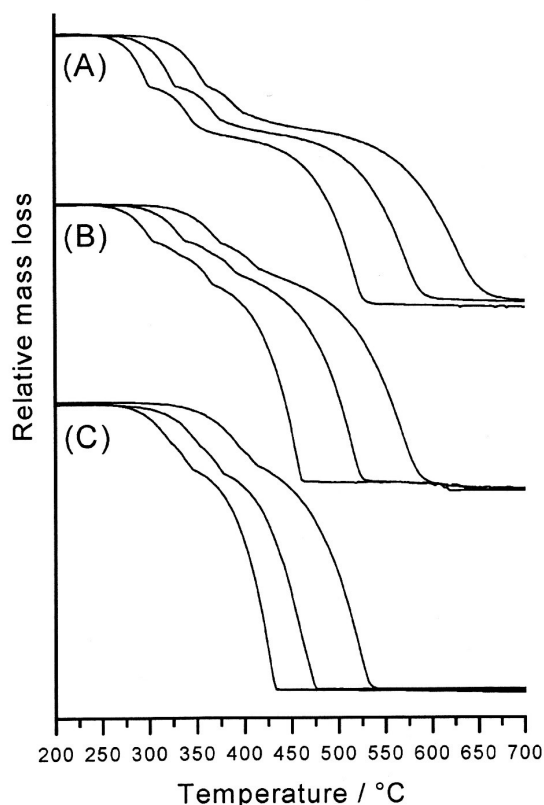


Figure 6. Heating-rate-dependent measurements for ligand-poor compounds **II** (A), **IV** (B), and **V** (C); heating rates = 1, 4, and 16 K/min, from left to right.

From the investigations described above, there are hints for the formation of ligand-poor 2:1 intermediate compounds (Figure 4). But the TG curves are not well-resolved, and

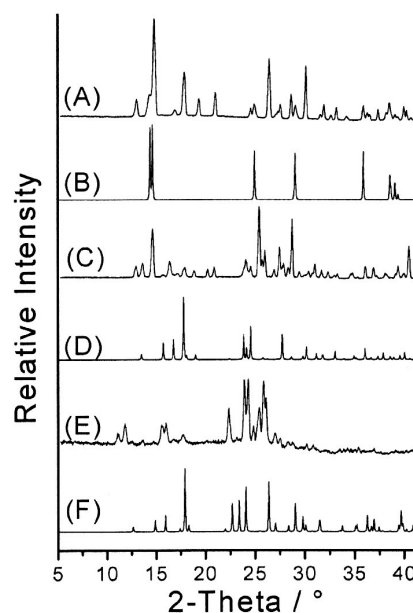


Figure 7. Experimental X-ray powder patterns of the residues obtained after the first TG step during the thermal decomposition of ligand-poor 1:1 compounds at 345 °C for compound **II** (A), at 345 °C for compound **IV** (C), and at 373 °C for compound **IV** (E), together with calculated X-ray powder patterns for compounds **II** (B), **IV** (D), and **V** (F).

therefore, isolation of such intermediates will be difficult. To check whether the resolution can be improved, we performed heating-rate-dependent measurements for ligand-poor 1:1 compounds **II**, **IV**, and **V** with 1, 4, and 16 K/min. (Figure 6). For chlorine compound **II**, it is obvious that the resolution can be significantly improved using lower heating rates (Figure 6A). The same improvement is observed for compound **IV**, whereas the resolution of the TG step during the thermal decomposition of compound **V** cannot be improved (Figure 6B,C).

To prove whether an additional ligand-poor 2:1 intermediate compound has formed during the thermal decomposition reaction of compounds **II**, **IV**, and **V**, we performed additional TG measurements with lower heating rates of 1 K/min that were stopped after the first TG step. The residues obtained in this experiment were investigated by X-ray powder diffraction (Figure 7A–F). The powder pattern of the intermediate of chlorine compound **II** is different from that of the pristine material. A detailed analysis shows there are no reflections of compound **II** or ZnCl_2 , which is the final product of the thermal decomposition reaction (Figure 7A,B). Therefore, one can assume that the intermediate compound obtained is very pure. Elemental analysis of the intermediate yields a composition that is in reasonable agreement with that calculated for a ligand-poor compound of composition $(\text{ZnCl}_2)_2(\text{pyrazine})$ (see Experimental Section). Similar results were obtained for the residues isolated during the thermal decomposition of compounds **IV** (Figure 7C,D) and **V** (Figure 7E,F). The X-ray powder patterns gave evidence that the ligand-poor intermediates are not isotypic (compare Figure 7A with Figure 7C,E). In addition, the

Zinc Halide Pyrazine Coordination Compounds

ligand-poor compound with ZnI_2 cannot be obtained as phase-pure material.

Conclusion

In the present work, we have shown for the first time that even ligand-poor zinc halide coordination polymers can be prepared by controlled thermal decomposition of ligand-rich precursor compounds. Despite the fact that the ligand-poor 1:1 compounds presented in this paper are the thermodynamically most stable compounds in this system and therefore can also be prepared in solution by applying stoichiometric amounts of the reactants, we demonstrated impressively that controlled thermal decomposition can be an alternative tool for the preparation of pure and quantitative amounts of coordination polymers. In any case, we demonstrated that thermal decomposition reactions are suitable for discovering additional ligand-poor phases, independent of whether they can be isolated as pure compounds, which might depend on the actual system investigated. The results of thermal decomposition experiments show that the overall thermal reactions are frequently much more complicated than expected. Therefore, detailed investigations of the thermal

behavior using different methods gave much more insight into the chemical reactivity and mechanisms of the thermal reactions of a given class of compounds. However, the results presented in this paper are only a first report. Similar coordination polymers have to be investigated in the future. From such investigations, we expect a large number of new compounds.

Acknowledgment. We gratefully acknowledge financial support by the State of Schleswig-Holstein and the Deutsche Forschungsgemeinschaft (Project NA 720/1-1). We are very thankful to Professor Dr. Wolfgang Bensch for the use of his facility for experimental equipment.

Supporting Information Available: List with details of the structure determination, atomic coordinates, and isotropic and anisotropic displacement parameters, as well as CIF files and drawings of the two structures. Experimental and calculated X-ray powder patterns as well as IR and Raman spectra of compounds I–V. This material is available free of charge via the Internet at <http://pubs.acs.org>.

IC060298F

Supplemental Material

On the Preparation of Coordination Polymers by Controlled Thermal Decomposition: Synthesis, Crystal Structures and Thermal Properties of Zinc Halide Pyrazine Coordination Polymers

Gaurav Bhosekar, Inke Jeß and Christian Näther*

- Details of the structure determination for compound **I**.
- Details of the structure determination of compound **III**.
- Details of the structure determination of compound **V**.
- Experimental and calculated X-ray powder patterns for compounds **I** to **V**.
- DTA-, TG-, DTG- and MS trend scan curves for compounds **II** to **IV**.
- IR- and Raman spectra of compounds **I** to **V**.

2 Publications

Table 1. Crystal data and structure refinement for dichloro bis(pyrimidine) zinc(II) (I)

Identification code	gb99	
Empirical formula	C ₈ H ₈ Cl ₂ N ₄ Zn	
Formula weight	296.46	
Temperature	200(2) K	
Wavelength	0.71073 Å	
Crystal system	orthorhombic	
Space group	Cc ₂ ca	
Unit cell dimensions	a = 10.1630(11) Å	α = 90°.
	b = 10.6042(15) Å	β = 90°.
	c = 10.1858(10) Å	γ = 90°.
Volume	1097.7(2) Å ³	
Z	4	
Density (calculated)	1.794 Mg/m ³	
Absorption coefficient	2.693 mm ⁻¹	
F(000)	592	
Crystal size	0.07 x 0.09 x 0.12 mm ³	
Theta range for data collection	4.00 to 28.04°.	
Index ranges	-13 ≤ h ≤ 13, -13 ≤ k ≤ 13, -13 ≤ l ≤ 11	
Reflections collected	2840	
Independent reflections	665 [R(int) = 0.0292]	
Completeness to theta = 28.04°	98.8 %	
Refinement method	Full-matrix least-squares on F ²	
Data / restraints / parameters	665 / 0 / 34	
Goodness-of-fit on F ²	1.049	
Final R indices [I > 2σ(I)]	R1 = 0.0260, wR2 = 0.0692	
R indices (all data)	R1 = 0.0311, wR2 = 0.0725	
Extinction coefficient	0.0068(14)	
Largest diff. peak and hole	0.379 and -0.432 e.Å ⁻³	

Remarks:

All non-hydrogen atoms were refined using anisotropic displacement parameters. The hydrogen atoms were positioned with idealized geometry and were refined isotropic ($U_{eq}(H) = 1.2 \cdot U_{eq}(C)$) using a riding model with C-H = 0.95 Å.

2 Publications

Table 2. Atomic coordinates ($\times 10^4$) and equivalent isotropic displacement parameters ($\text{\AA}^2 \times 10^3$)

U(eq) is defined as one third of the trace of the orthogonalized U_{ij} tensor.

	x	y	z	U(eq)
Zn(1)	0	2500	2500	9(1)
Cl(1)	0	4777(1)	2500	18(1)
N(1)	1537(2)	2488(1)	971(2)	13(1)
C(1)	2564(1)	3272(1)	1027(1)	16(1)
C(2)	3520(1)	3285(1)	60(1)	17(1)

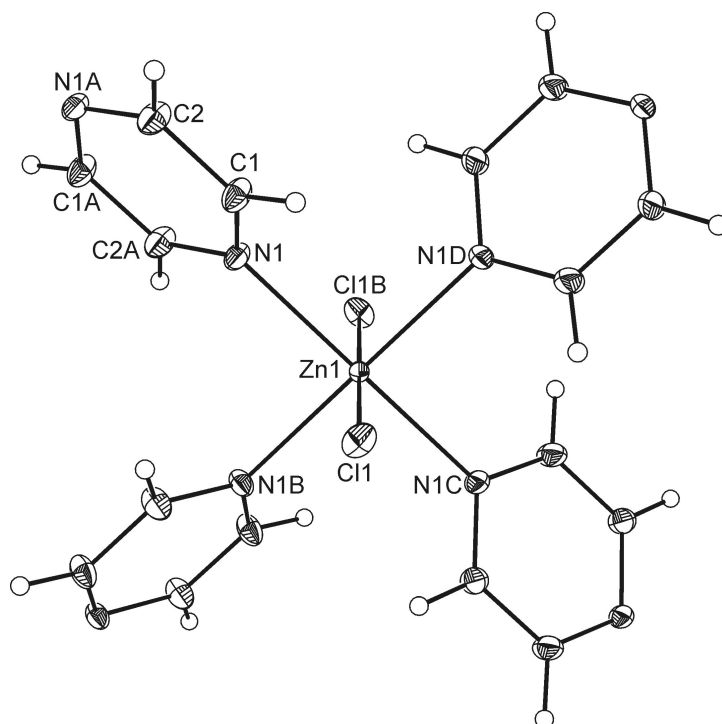


Table 3. Bond lengths [\AA] and angles [$^\circ$]

Zn(1)-N(1D)	2.2053(15)	N(1C)-Zn(1)-N(1)	179.36(6)
Zn(1)-N(1B)	2.2053(15)	N(1D)-Zn(1)-Cl(1)	89.68(3)
Zn(1)-N(1C)	2.2053(15)	N(1B)-Zn(1)-Cl(1)	89.68(3)
Zn(1)-N(1)	2.2053(15)	N(1C)-Zn(1)-Cl(1)	90.32(3)
Zn(1)-Cl(1)	2.4143(7)	N(1)-Zn(1)-Cl(1)	90.32(3)
Zn(1)-Cl(1B)	2.4143(7)	N(1D)-Zn(1)-Cl(1B)	90.32(3)
N(1)-C(2A)	1.3336(18)	N(1B)-Zn(1)-Cl(1B)	90.32(3)
N(1)-C(1)	1.3356(17)	N(1C)-Zn(1)-Cl(1B)	89.68(3)
C(1)-C(2)	1.3835	N(1)-Zn(1)-Cl(1B)	89.68(3)
C(2)-N(1A)	1.3336(18)	Cl(1)-Zn(1)-Cl(1B)	180.0
N(1D)-Zn(1)-N(1B)	179.36(6)	C(2A)-N(1)-C(1)	116.71(12)
N(1D)-Zn(1)-N(1C)	90.16(8)	C(2A)-N(1)-Zn(1)	121.97(10)
N(1B)-Zn(1)-N(1C)	89.84(8)	C(1)-N(1)-Zn(1)	121.32(10)
N(1D)-Zn(1)-N(1)	89.84(8)	N(1)-C(1)-C(2)	121.62(8)
N(1B)-Zn(1)-N(1)	90.16(8)	N(1A)-C(2)-C(1)	121.67(8)

Symmetry transformations used to generate equivalent atoms:

A : $-x+1/2, -y+1/2, -z$ B : $-x+0, -y+1/2, z$ C : $-x, y, -z+1/2$ D : $x+0, -y+1/2, -z+1/2$

2 Publications

Table 4. Anisotropic displacement parameters ($\text{\AA}^2 \times 10^3$). The anisotropic displacement factor exponent takes the form: $-2\pi^2 [h^2 a^{*2} U_{11} + \dots + 2 h k a^* b^* U_{12}]$

	U_{11}	U_{22}	U_{33}	U_{23}	U_{13}	U_{12}
Zn(1)	7(1)	14(1)	7(1)	0	0	0
Cl(1)	19(1)	16(1)	18(1)	0	5(1)	0
N(1)	11(1)	17(1)	11(1)	-3(1)	3(1)	-2(1)
C(1)	16(1)	19(1)	14(1)	-6(1)	3(1)	-5(1)
C(2)	14(1)	20(1)	16(1)	-6(1)	3(1)	-6(1)

Table 5. Hydrogen coordinates ($\times 10^4$) and isotropic displacement parameters ($\text{\AA}^2 \times 10^3$)

	x	y	z	U(eq)
H(1)	2640	3834	1749	19
H(2)	4234	3858	132	20

2 Publications

Table 1. Crystal data and structure refinement for dibromine-bis(pyrazine-N) zinc(II) (III)

Identification code	gb77	
Empirical formula	C ₈ H ₈ Br ₂ N ₂ Zn	
Formula weight	357.35	
Temperature	170(2) K	
Wavelength	0.71073 Å	
Crystal system	tetragonal	
Space group	I4/mmm	
Unit cell dimensions	a = 7.1969(8) Å	α = 90°.
	b = 7.1969(8) Å	β = 90°.
	c = 11.1356(15) Å	γ = 90°.
Volume	576.77(12) Å ³	
Z	2	
Density (calculated)	2.058 Mg/m ³	
Absorption coefficient	9.014 mm ⁻¹	
F(000)	340	
Crystal size	0.07 x 0.09 x 0.11 mm ³	
Theta range for data collection	3.37 to 27.91°.	
Index ranges	-4<=h<=9, -9<=k<=9, -14<=l<=14	
Reflections collected	1231	
Independent reflections	229 [R(int) = 0.0279]	
Completeness to theta = 27.91°	98.3 %	
Refinement method	Full-matrix least-squares on F ²	
Data / restraints / parameters	229 / 0 / 20	
Goodness-of-fit on F ²	1.188	
Final R indices [I>2sigma(I)]	R1 = 0.0228, wR2 = 0.0552	
R indices (all data)	R1 = 0.0231, wR2 = 0.0554	
Extinction coefficient	0.019(3)	
Largest diff. peak and hole	0.809 and -0.712 e.Å ⁻³	

Remarks:

All non-hydrogen atoms were refined using anisotropic displacement parameters. The hydrogen atoms were positioned with idealized geometry and were refined isotropic ($U_{eq}(H) = 1.2 \cdot U_{eq}(C)$) using a riding model with C-H = 0.95 Å for aromatic hydrogen atoms. The complex is located on Position 4/mmm. The pyrazine ligand is disordered around a crystallographic mirror plane. If the structure is refined in space groups where this mirror plane is absent, the disorder remain constant. Therefore, space group I4/mmm was selected. The crystal investigated shows some extremely weak reflections which disturb the systematic extinctions for the I-centering. However, if the structure is refined in a primitive space group practically none of these reflections are observed and the disorder remains the same.

2 Publications

Table 2. Atomic coordinates ($\times 10^4$) and equivalent isotropic displacement parameters ($\text{\AA}^2 \times 10^3$). $U(\text{eq})$ is defined as one third of the trace of the orthogonalized U_{ij} tensor.

	x	y	z	U(eq)
Zn(1)	5000	5000	5000	6(1)
Br(1)	5000	5000	7315(1)	12(1)
N(1)	5000	8066(4)	5000	9(1)
C(1)	3928(4)	9038(4)	5759(2)	11(1)

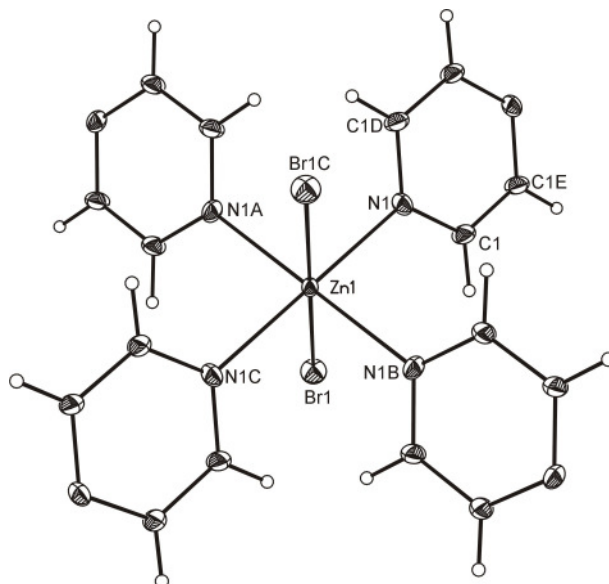


Table 3. Bond lengths [\AA] and angles [$^\circ$].

Zn(1)-N(1A)	2.206(3)	Zn(1)-N(1C)	2.206(3)
Zn(1)-N(1B)	2.206(3)	Zn(1)-Br(1)	2.5782(5)
Zn(1)-N(1)	2.206(3)	Zn(1)-Br(1C)	2.5782(5)
N(1A)-Zn(1)-N(1B)	180.0	N(1)-Zn(1)-Br(1)	90.0
N(1A)-Zn(1)-N(1)	90.000(1)	N(1C)-Zn(1)-Br(1)	90.0
N(1B)-Zn(1)-N(1)	90.0	N(1A)-Zn(1)-Br(1C)	90.0
N(1A)-Zn(1)-N(1C)	90.0	N(1B)-Zn(1)-Br(1C)	90.0
N(1B)-Zn(1)-N(1C)	90.000(1)	N(1)-Zn(1)-Br(1C)	90.0
N(1)-Zn(1)-N(1C)	180.0	N(1C)-Zn(1)-Br(1C)	90.0
N(1A)-Zn(1)-Br(1)	90.0	Br(1)-Zn(1)-Br(1C)	180.0
N(1B)-Zn(1)-Br(1)	90.0	C(1)-C(1E)	1.384(6)
N(1)-C(1D)	1.342(3)	N(1)-C(1)-C(1E)	121.45(16)
N(1)-C(1)	1.342(3)	C(1D)-N(1)-C(1)	117.1(3)

Symmetry transformations used to generate equivalent atoms: A: $y, -x+1, -z+1$ B: $-y+1, x, z$
 C: $-x+1, -y+1, -z+1$ D: $-x+1, y, -z+1$ E: $x, -y+2, z$

2 Publications

Table 4. Anisotropic displacement parameters ($\text{\AA}^2 \times 10^3$). The anisotropic displacement factor exponent takes the form: $-2\pi^2 [h^2 a^{*2} U_{11} + \dots + 2 h k a^* b^* U_{12}]$

	U_{11}	U_{22}	U_{33}	U_{23}	U_{13}	U_{12}
Zn(1)	5(1)	5(1)	10(1)	0	0	0
Br(1)	13(1)	13(1)	10(1)	0	0	0
N(1)	10(1)	5(1)	11(1)	0	0	0
C(1)	12(2)	8(2)	14(1)	0(1)	8(1)	0(1)

Table 5. Hydrogen coordinates ($\times 10^4$) and isotropic displacement parameters ($\text{\AA}^2 \times 10^3$).

	x	y	z	U(eq)
H(1A)	3152	8393	6309	14

2 Publications

Table 1. Crystal data and structure refinement for diiodo(μ -pyrazine) zinc(II) (V).

Identification code	gb24	
Empirical formula	C ₄ H ₄ I ₂ N ₂ Zn	
Formula weight	399.26	
Temperature	170(2) K	
Wavelength	0.71073 Å	
Crystal system	monoclinic	
Space group	P2 ₁ /m	
Unit cell dimensions	a = 6.3113(8) Å	$\alpha = 90^\circ$.
	b = 9.8980(13) Å	$\beta = 109.871(14)^\circ$.
	c = 7.4380(9) Å	$\gamma = 90^\circ$.
Volume	436.98(10) Å ³	
Z	2	
Density (calculated)	3.034 Mg/m ³	
Absorption coefficient	9.798 mm ⁻¹	
F(000)	356	
Crystal size	0.06 x 0.08 x 0.13 mm ³	
Theta range for data collection	2.91 to 29.12°.	
Index ranges	-6 ≤ h ≤ 8, -13 ≤ k ≤ 13, -10 ≤ l ≤ 10	
Reflections collected	3265	
Independent reflections	1226 [R(int) = 0.0746]	
Completeness to theta = 29.12°	98.7 %	
Refinement method	Full-matrix least-squares on F ²	
Data / restraints / parameters	1226 / 0 / 47	
Goodness-of-fit on F ²	1.116	
Final R indices [I > 2σ(I)]	R1 = 0.0357, wR2 = 0.0933	
R indices (all data)	R1 = 0.0416, wR2 = 0.0956	
Extinction coefficient	0.0266(19)	
Largest diff. peak and hole	1.966 and -1.469 e.Å ⁻³	

Remarks:

All non-hydrogen atoms were refined using anisotropic displacement parameters. The hydrogen atoms were positioned with idealized geometry and were refined isotropic ($U_{eq} = -1.2$) using a riding model with C-H = 0.95 Å for aromatic hydrogen atoms. There is one crystallographically independent molecules into the asymmetric unit, located at special positions.

2 Publications

Table 2. Atomic coordinates ($\times 10^4$) and equivalent isotropic displacement parameters ($\text{\AA}^2 \times 10^3$). U(eq) is defined as one third of the trace of the orthogonalized U_{ij} tensor.

	x	y	z	U(eq)
I(1)	7222(1)	2500	7273(1)	20(1)
I(2)	3627(1)	2500	1097(1)	25(1)
Zn(1)	3590(1)	2500	4473(1)	14(1)
N(1)	1489(7)	957(4)	4769(7)	15(1)
C(1)	-411(8)	642(5)	3331(8)	18(1)
C(2)	1907(8)	315(5)	6424(7)	17(1)

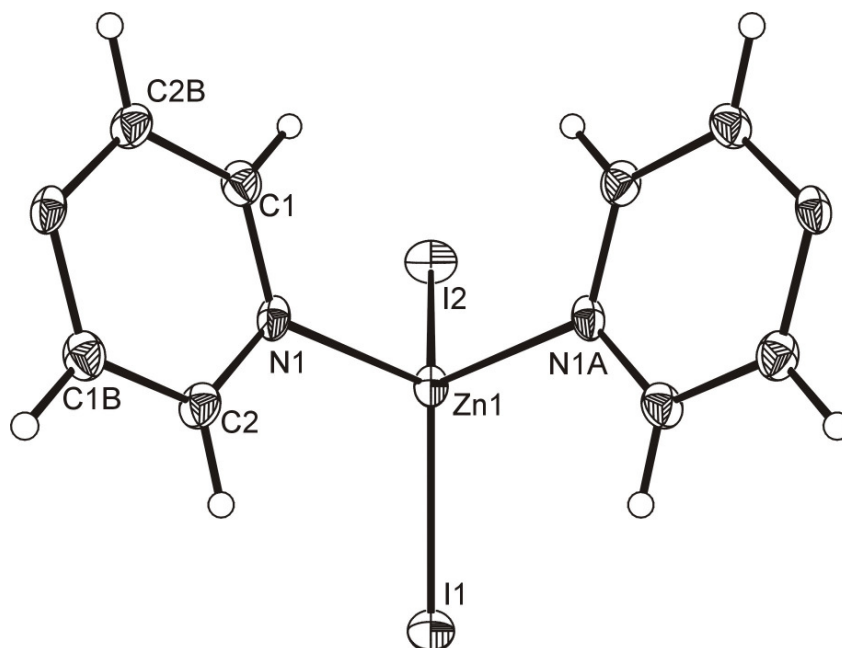


Table 3. Bond lengths [\AA] and angles [$^\circ$].

I(1)-Zn(1)	2.5194(11)	Zn(1)-N(1)	2.082(4)
I(2)-Zn(1)	2.5193(10)	Zn(1)-N(1A)	2.082(4)
N(1)-Zn(1)-N(1A)	94.3(2)	N(1)-Zn(1)-I(1)	110.23(13)
N(1)-Zn(1)-I(2)	109.11(13)	N(1A)-Zn(1)-I(1)	110.23(13)
N(1A)-Zn(1)-I(2)	109.11(13)	I(2)-Zn(1)-I(1)	120.64(3)
N(1)-C(2)	1.330(6)	C(1)-C(2B)	1.393(6)
N(1)-C(1)	1.344(7)	C(2)-C(1B)	1.393(6)
C(2)-N(1)-C(1)	117.9(4)	N(1)-C(1)-C(2B)	121.0(5)
C(2)-N(1)-Zn(1)	121.0(3)	N(1)-C(2)-C(1B)	121.1(5)
C(1)-N(1)-Zn(1)	120.9(4)		

Symmetry transformations used to generate equivalent atoms: A: $x, -y+1/2, z$ B: $-x, -y, -z+1$

2 Publications

Table 4. Anisotropic displacement parameters ($\text{\AA}^2 \times 10^3$). The anisotropic displacement factor exponent takes the form: $-2\pi^2 [h^2 a^{*2} U_{11} + \dots + 2 h k a^* b^* U_{12}]$

	U_{11}	U_{22}	U_{33}	U_{23}	U_{13}	U_{12}
I(1)	11(1)	24(1)	25(1)	0	7(1)	0
I(2)	22(1)	35(1)	20(1)	0	11(1)	0
Zn(1)	11(1)	13(1)	22(1)	0	9(1)	0
N(1)	11(2)	10(2)	26(2)	-1(2)	9(2)	-1(2)
C(1)	16(2)	16(2)	23(2)	3(2)	9(2)	-1(2)
C(2)	14(2)	16(2)	23(2)	0(2)	7(2)	-3(2)

Table 5. Hydrogen coordinates ($\times 10^4$) and isotropic displacement parameters ($\text{\AA}^2 \times 10^3$).

	x	y	z	U(eq)
H(1)	-738	1079	2130	21
H(2)	3249	512	7456	21

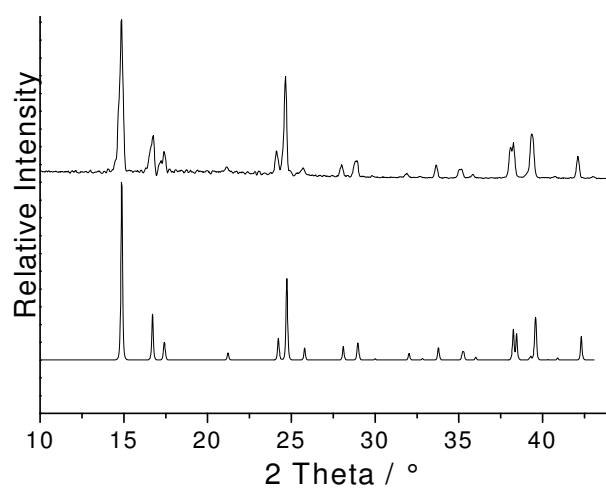
Experimental and calculated X-ray powder patterns for compounds I and V.

Fig. 1. Experimental (top) and calculated (bottom) X-ray powder pattern for compound **I** (Transmission; PSD 5-50°; Cu-K α -radiation).

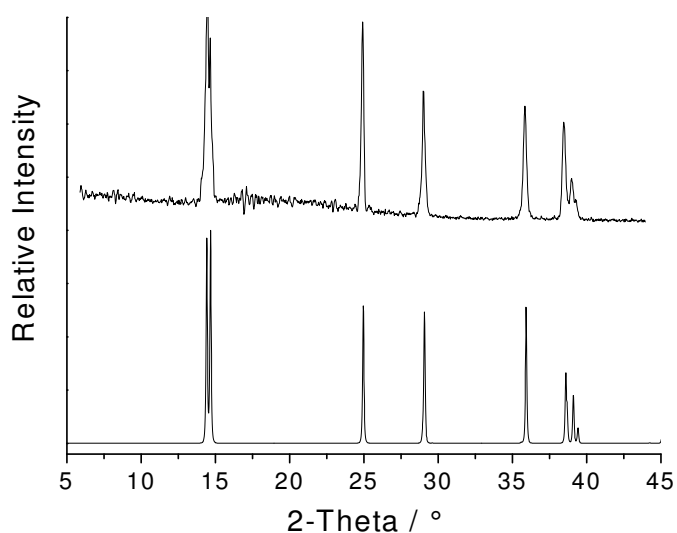


Fig. 2. Experimental (top) and calculated (bottom) X-ray powder pattern for compound **II** (Transmission; PSD 5-45°; Cu-K α -radiation).

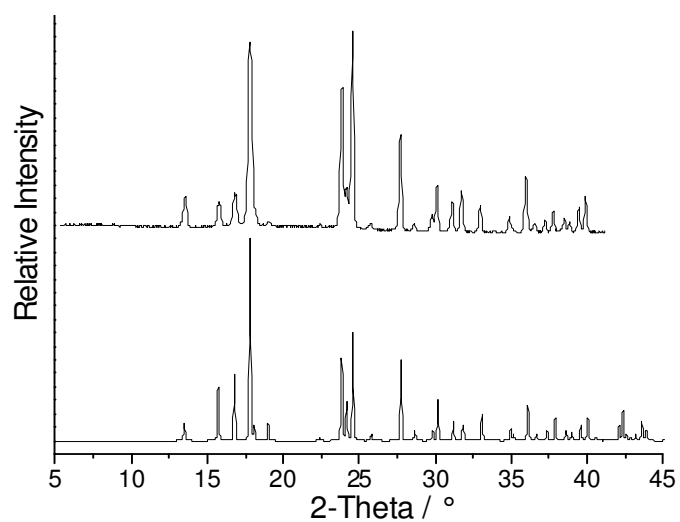


Fig. 3. Experimental (top) and calculated (bottom) X-ray powder pattern for compound **III** (Transmission; PSD 5-50°; Cu-K α -radiation).

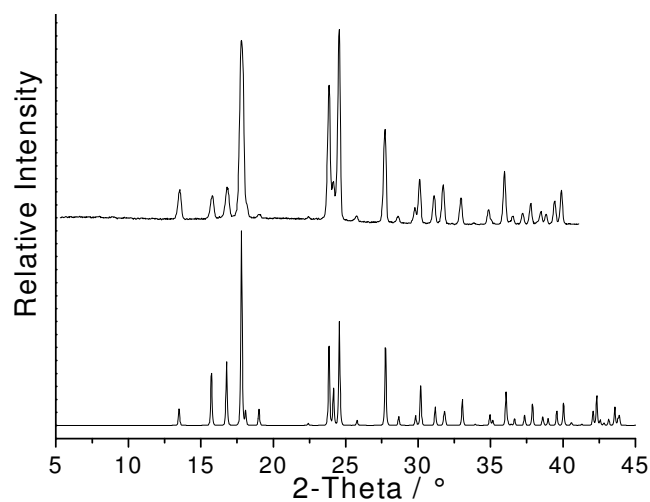


Fig. 4. Experimental (top) and calculated (bottom) X-ray powder pattern for compound **IV** (Transmission; PSD 5-50°; Cu-K α -radiation).

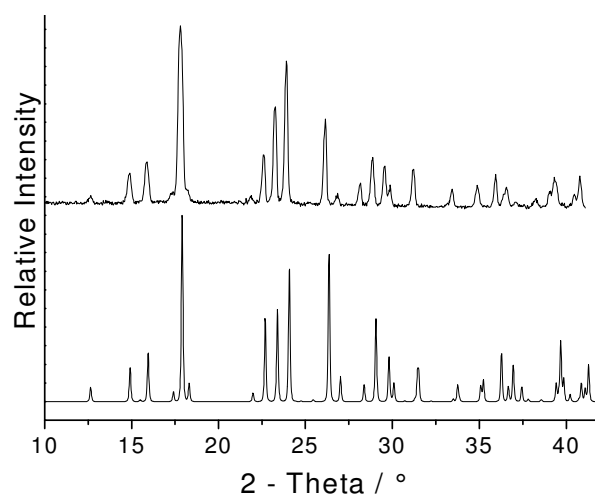


Fig. 5. Experimental (top) and calculated (bottom) X-ray powder pattern for compound **V** (Transmission; PSD 5-50°; Cu-K α -radiation).

DTA-, TG-, DTG- and MS trend scan curves for compounds II and IV.

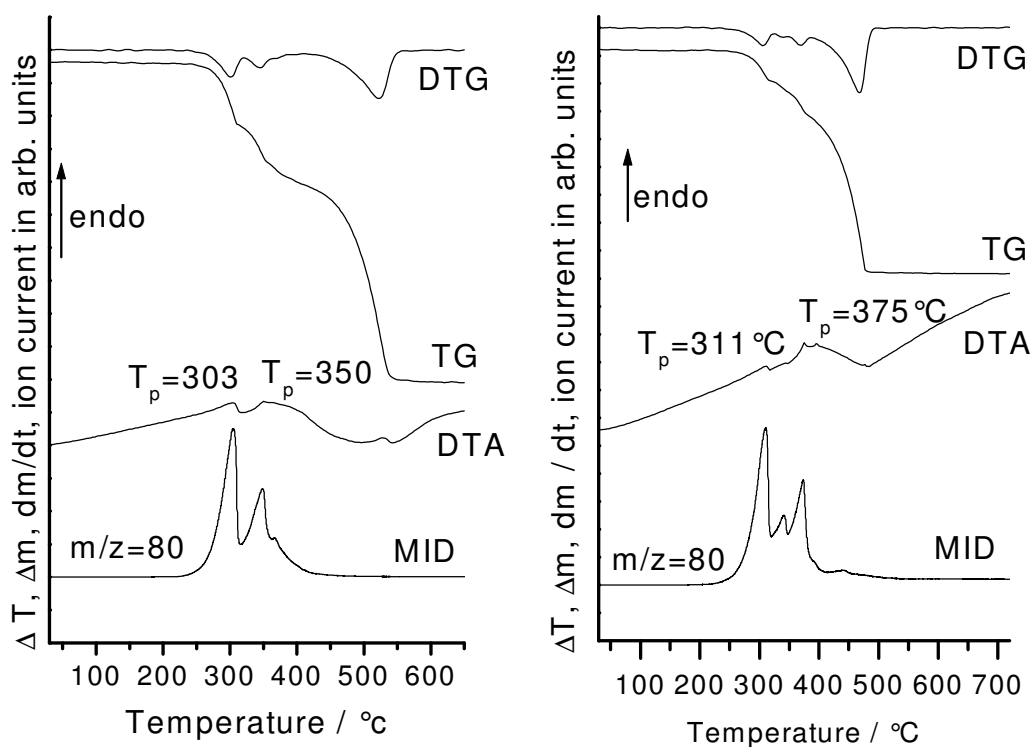
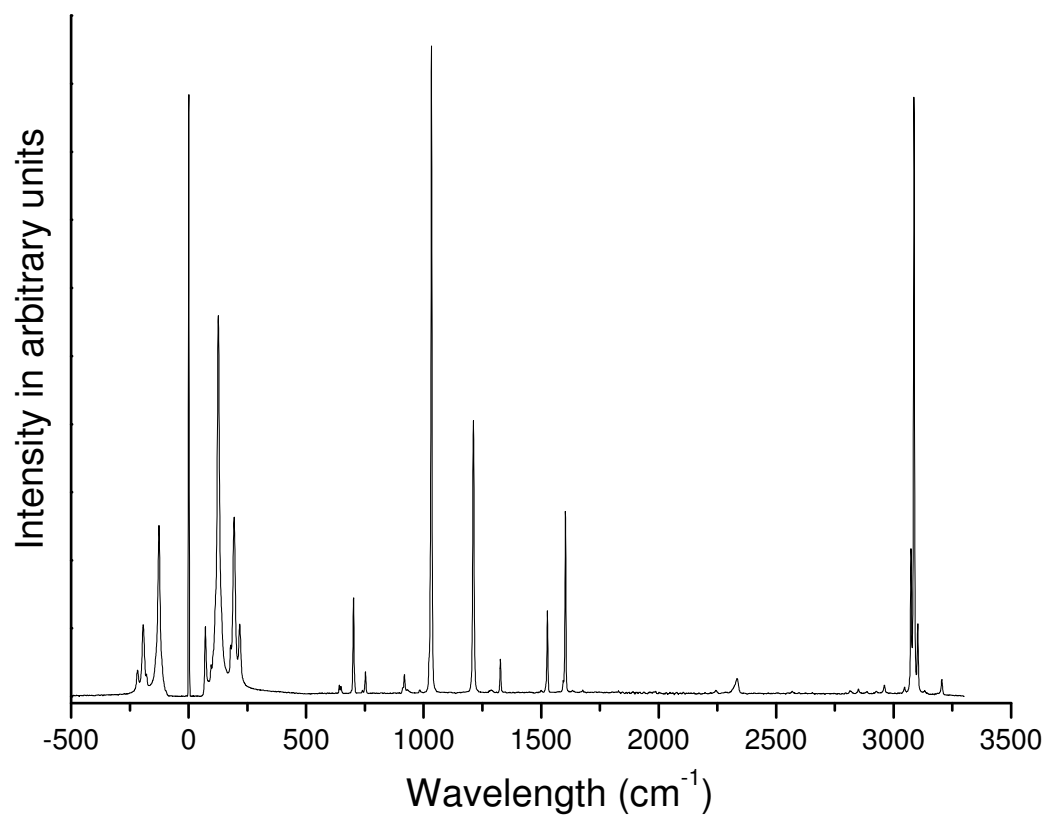
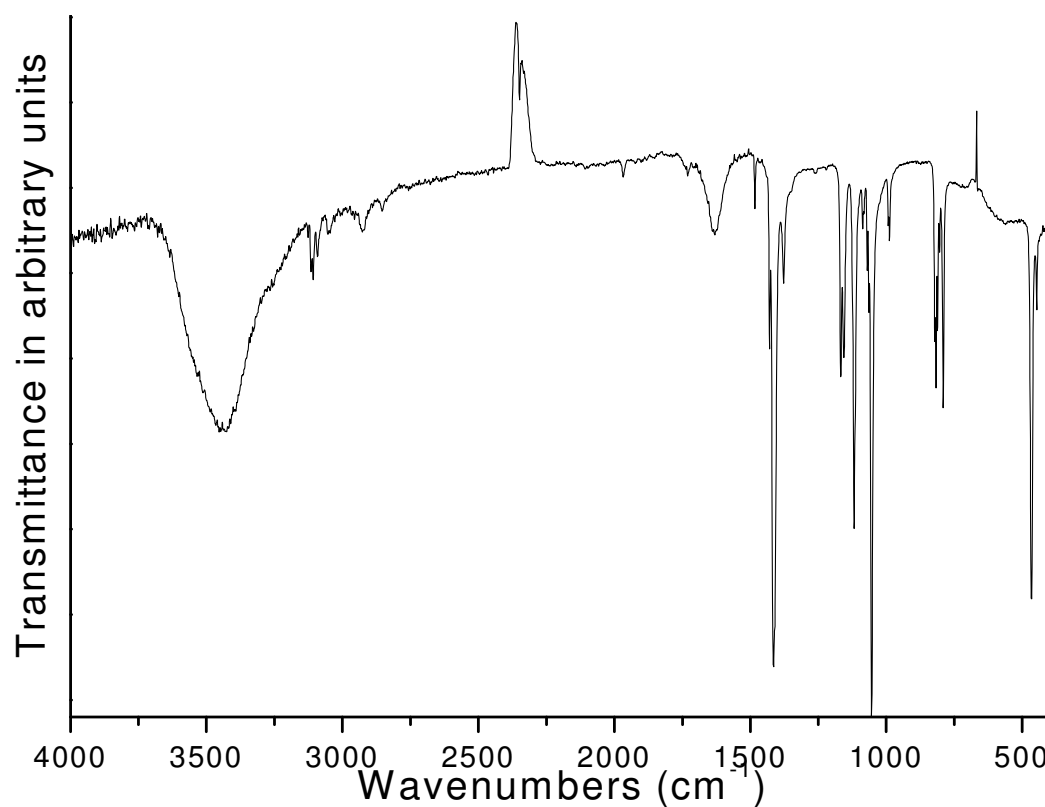
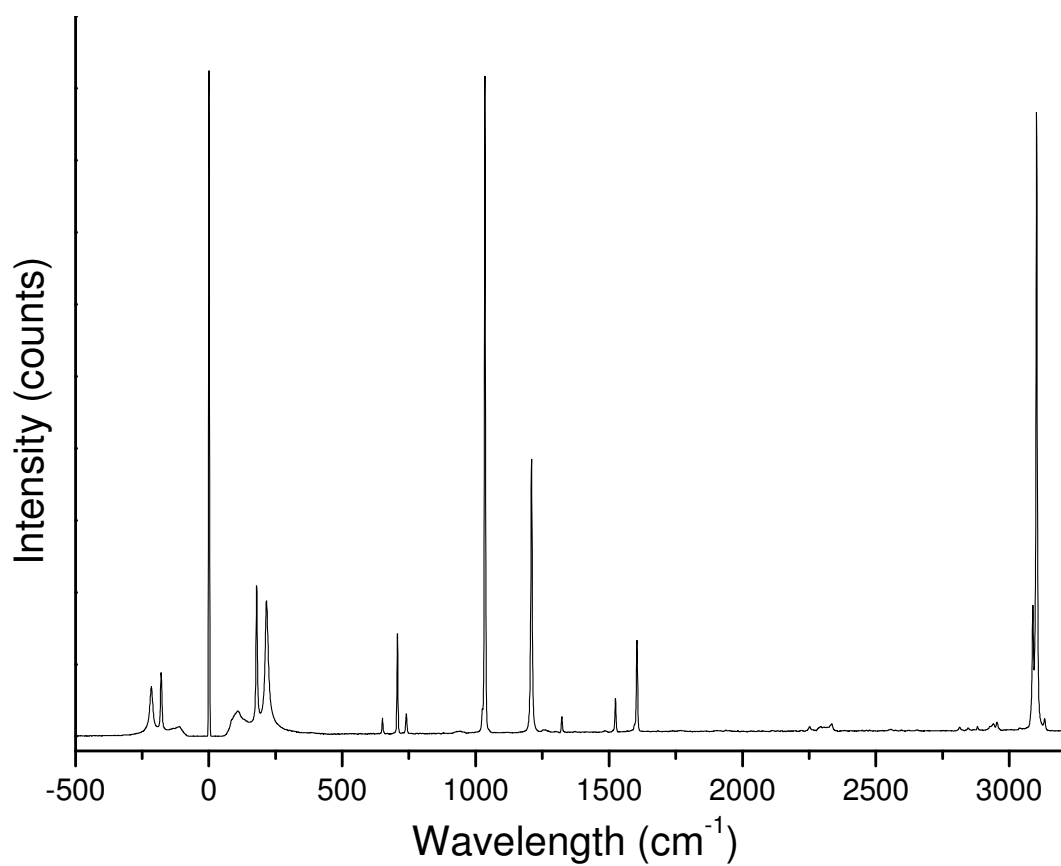
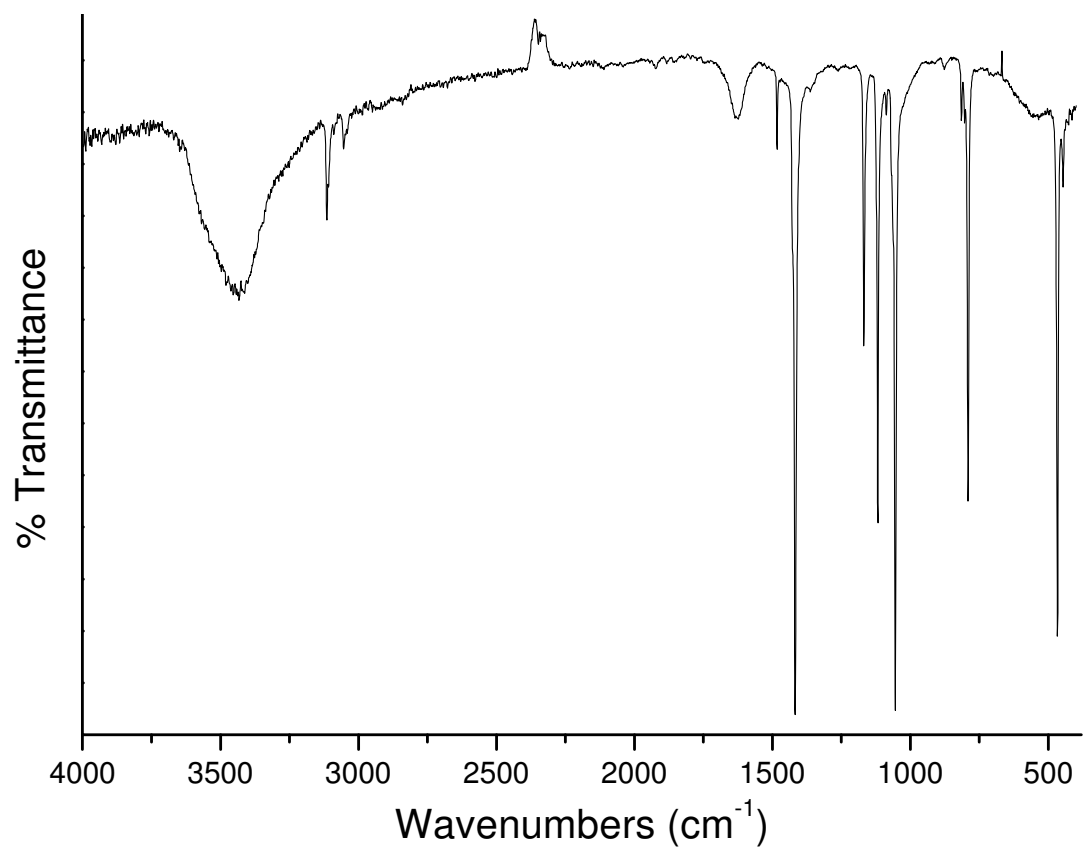


Fig. 6. DTA, TG, DTG and MS trend scan curve for compound **II** (left) **IV** (right) compound (heating rate: 4 °C/min.; $m/z = 80$ (pyrazine)); given are the mass changes in (%) and the peak temperatures T_p in °C).

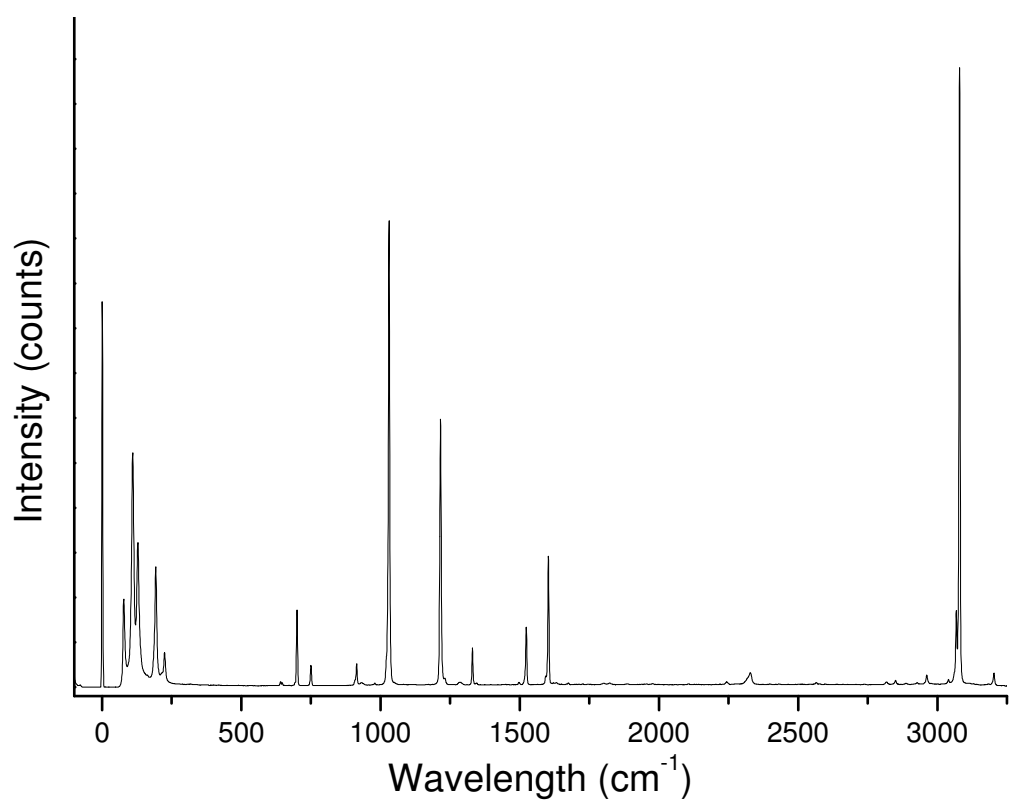
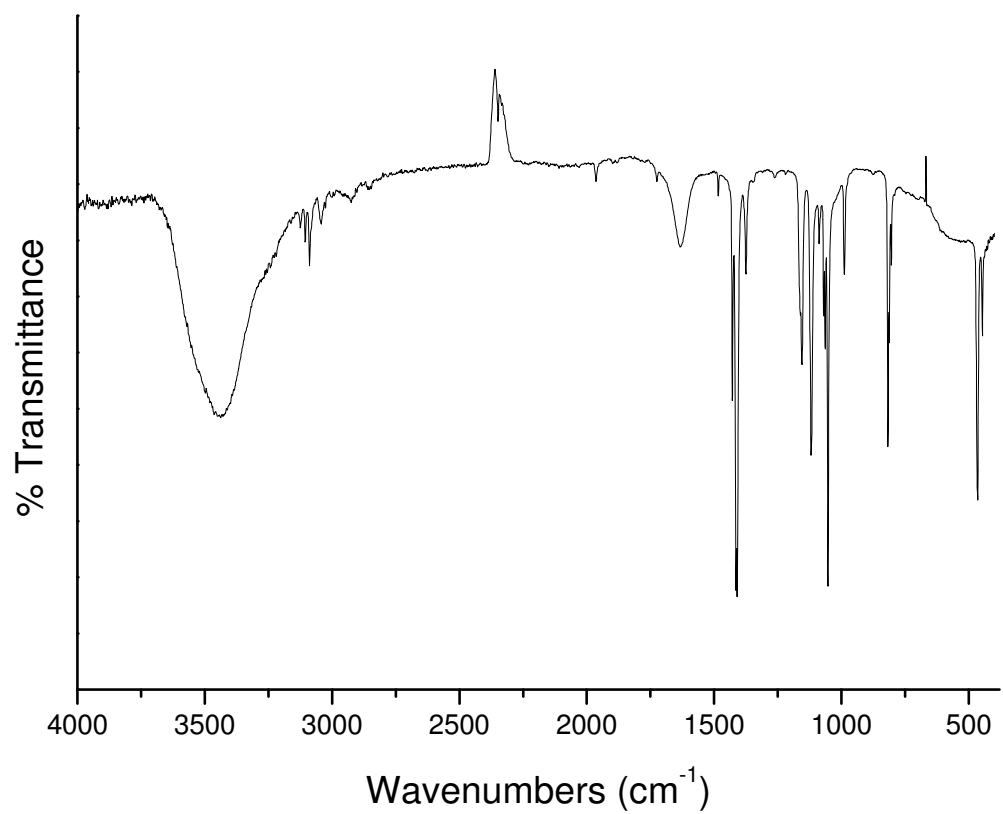
IR- and Raman spectra of compounds I to V.



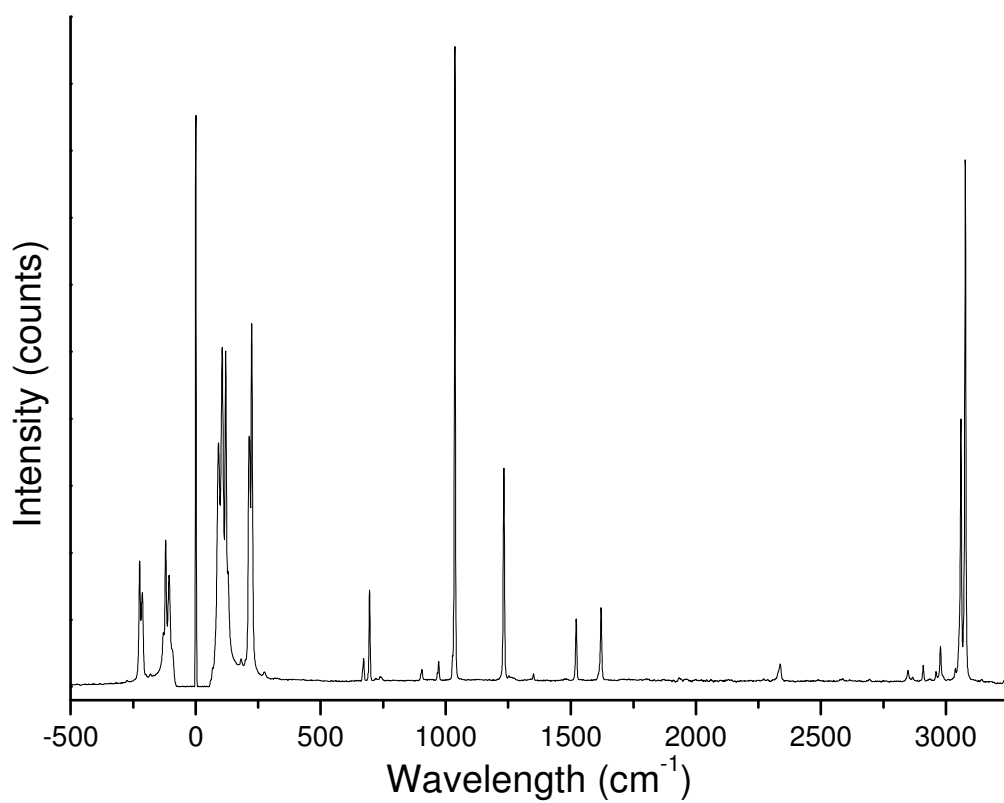
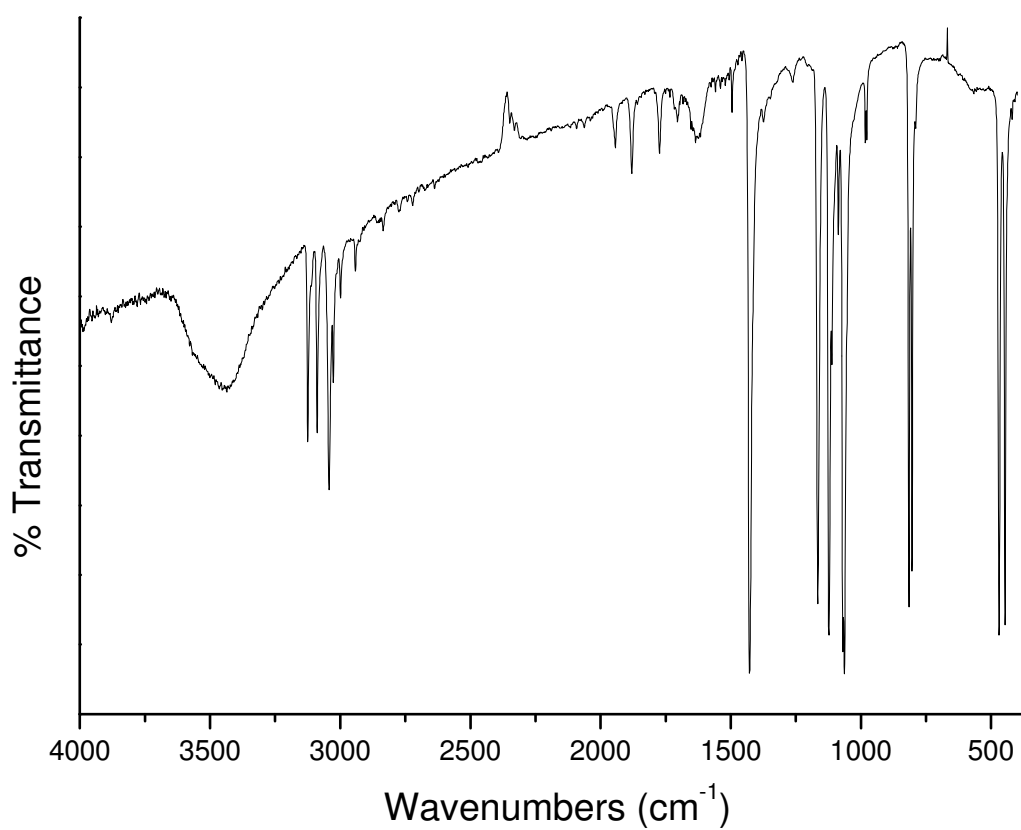
IR- (top) and Raman spectra (bottom) for compound **I**.



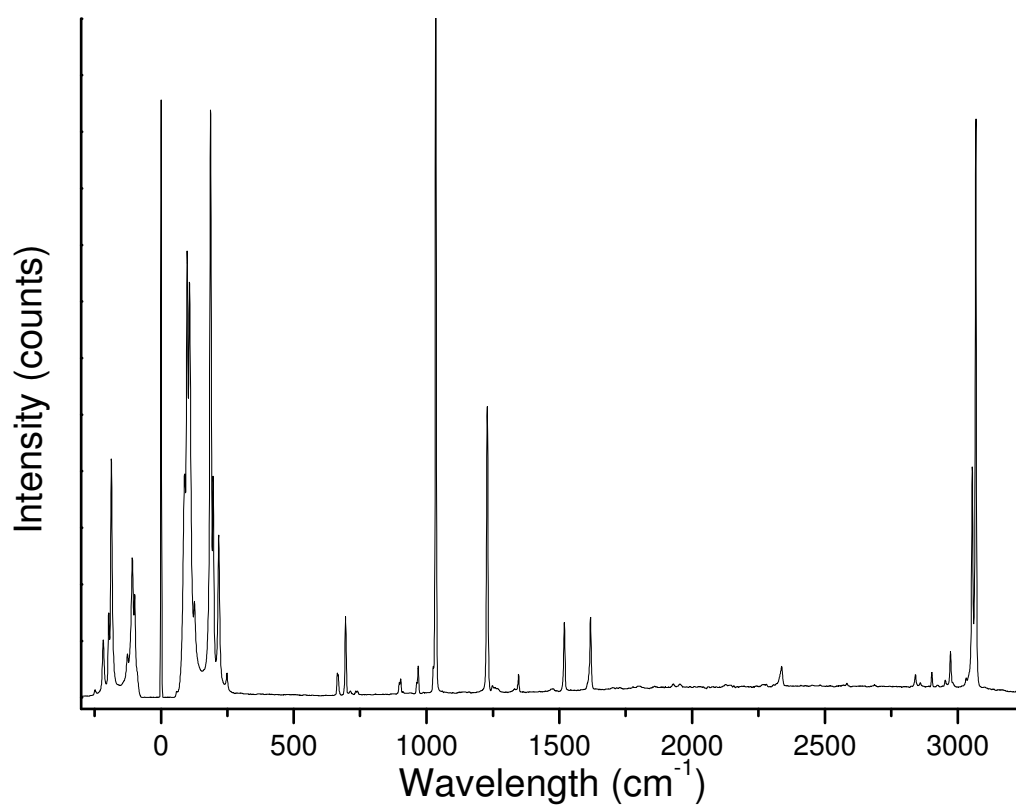
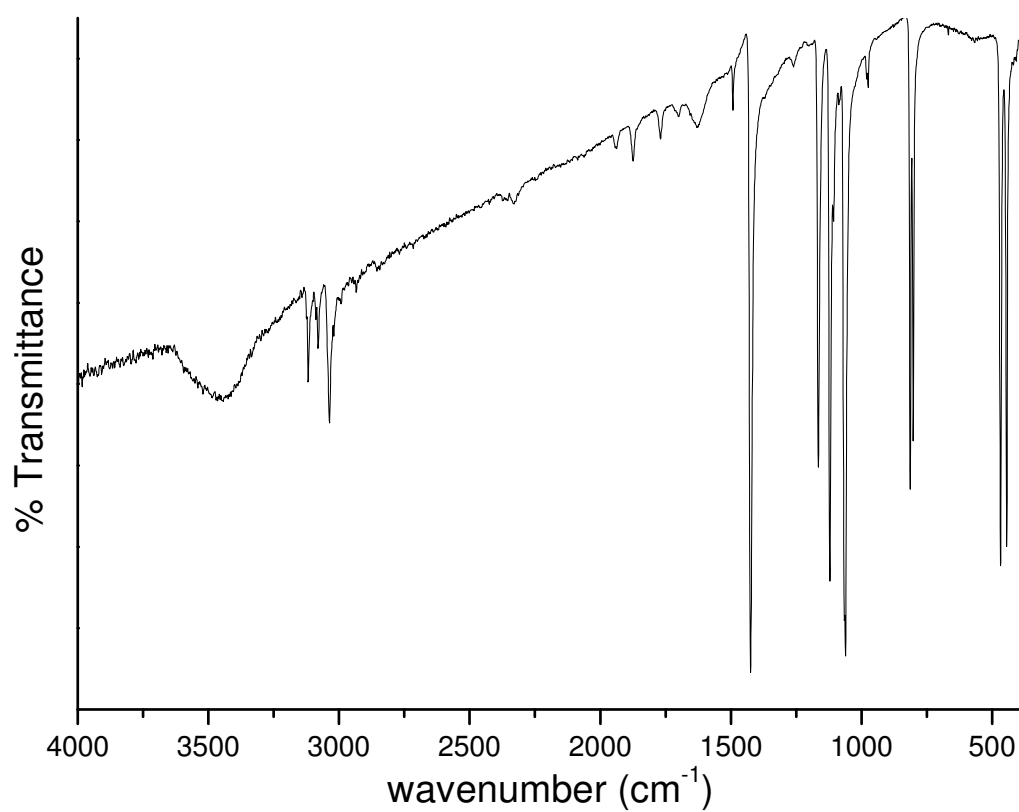
IR- (top) and Raman spectra (bottom) for compound **II**.



IR- (top) and Raman spectra (bottom) for compound **III**.



IR- (top) and Raman spectra (bottom) for compound **IV**.



IR- (top) and Raman spectra (bottom) for compound V

Preparation of Stable and Metastable Coordination Compounds: Insight into the Structural, Thermodynamic, and Kinetic Aspects of the Formation of Coordination Polymers

Christian Näther,* Gaurav Bhosekar, and Inke Jess

Institut für Anorganische Chemie der Christian-Albrechts-Universität zu Kiel, Olshausenstrasse 40, D-24098 Kiel, Germany

Received June 1, 2007

The reaction of ZnI_2 and pyrimidine in acetonitrile results in the formation of the 1:2 compound $ZnI_2(\text{pyrimidine})_2$ (**1**), which consists of discrete tetrahedral building blocks. Slow heating of **1** at 1 °C/min leads to its transformation into the ligand-deficient intermediate 1:1 compound $ZnI_2(\text{pyrimidine})$ (**3**), which upon further heating decomposes into the most ligand-deficient 2:1 compound $(ZnI_2)_2(\text{pyrimidine})$ (**4**). In contrast, the 2:3 compound $(ZnI_2)_2(\text{pyrimidine})_3$ (**2**) is formed as an intermediate by decomposing **1** using a faster heating rate of 8 °C/min. Compound **2** consists of oligomeric units in which each ZnI_2 unit is coordinated by two iodine atoms and one bridging and one terminal pyrimidine ligand. The crystal structure of compound **3** is built up of ZnI_2 units, which are connected by the ligands into chains. For the thermal transformation of **1** into **3** via **2** as the intermediate, a smooth reaction pathway is found in the crystal structure, for which only small translational and rotational changes are needed. The metastable solvated compound $(ZnI_2)(\text{pyrimidine})(\text{acetonitrile})_{0.25}$ (**5**) consisting of $(ZnI_2)_4(\text{pyrimidine})_4$ rings is obtained by quenching the reaction of ZnI_2 and pyrimidine in acetonitrile using an antisolvent. On heating, **5** decomposes into a new polymorphic 1:1 compound **6**, which consists of $(ZnI_2)(\text{pyrimidine})$ chains. On further heating, **6** transforms into a third polymorphic 1:1 compound **7**, which consists of $(ZnI_2)_3(\text{pyrimidine})_3$ rings, and finally into the 1:1 compound **3**. Solvent-mediated conversion experiments reveal that compounds **1–4** are thermodynamically stable, whereas compounds **5–7** are metastable. Time-dependent crystallization experiments unambiguously show that compound **7** is formed by kinetic control and transforms within minutes into compound **6**, which finally transforms into **3**. Compound **3** represents the thermodynamically most stable 1:1 modification, whereas compounds **6** and **7** are metastable. The different compounds obtained by thermal decomposition and by crystallization from solution represent a snapshot of the species in solution and thus provide insight into the formation of coordination compounds.

Introduction

Recently, the preparation of new coordination polymers, inorganic–organic hybrid compounds, or metal–organic frameworks has become of increasing interest.^{1–12} One major goal in this field is the preparation of compounds with desired

physical properties, for which structure–property relationships must be investigated and general strategies for a more directed design of solids must be developed.^{13–19} However, for any characterization or application, pure compounds are

* To whom correspondence should be addressed. E-mail: cnaether@ac.uni-kiel.de. Fax: +49-(0)431-8801520.

- (1) Robin, A. Y.; Fromm, K. M. *Coord. Chem. Rev.* **2006**, *250*, 2127.
- (2) James, S. L. *Chem. Soc. Rev.* **2003**, *5*, 276.
- (3) Hargman, P. J.; Hargman, D.; Zubieta, J. *Angew. Chem.* **1999**, *111*, 2798; *Angew. Chem., Int. Ed. Engl.* **1999**, *38*, 2638.
- (4) Robson, R. *Comprehensive Supramolecular Chemistry*; Pergamon: New York, 1996, Vol. 22, p 733.
- (5) Robson, R.; Abrahams, B. F.; Batten, S. R.; Grable, R. W.; Hoskins, B. F.; Liu, J. *Supramolecular Architecture*; American Chemical Society: Washington, DC, 1992; Chapter 19.
- (6) Moulton, B.; Zaworotko, M. *J. Chem. Soc. Rev.* **2001**, *101*, 1629.

- (7) Blake, A. J.; Champness, N. R.; Hubberstey, P.; Li, W.-S.; Schröder, M. *Coord. Chem. Rev.* **1999**, *183*, 17.
- (8) Braga, D.; Maini, L.; Polito, M.; Scaccianoce, L.; Cozzani, G.; Gregorini, F. *Coord. Chem. Rev.* **2001**, *216*, 783.
- (9) Kitagawa, S.; Uemura, K. *Chem. Soc. Rev.* **2005**, *34*, 109.
- (10) Batten, S. R.; Murray, K. *Coord. Chem. Rev.* **2003**, *246*, 103.
- (11) Khlobystov, A. N.; Blake, A. J.; Champness, N. R.; Lemenovskii, D. A.; Majouga, A. G.; Zyk, N. V.; Schröder, M. *Coord. Chem. Rev.* **2001**, *222*, 155.
- (12) Puddephatt, R. J. *Coord. Chem. Rev.* **2001**, *216*, 313.
- (13) Janiak, C. *J. Chem. Soc., Dalton. Trans.* **2003**, 2781.
- (14) Yaghi, O. M.; Li, H.; Davis, C.; Richardson, D.; Groy, T. L. *Acc. Chem. Res.* **1998**, *31*, 474.
- (15) Chen, C.-T.; Suslik, K. S. *Coord. Chem. Rev.* **1993**, *128*, 293.

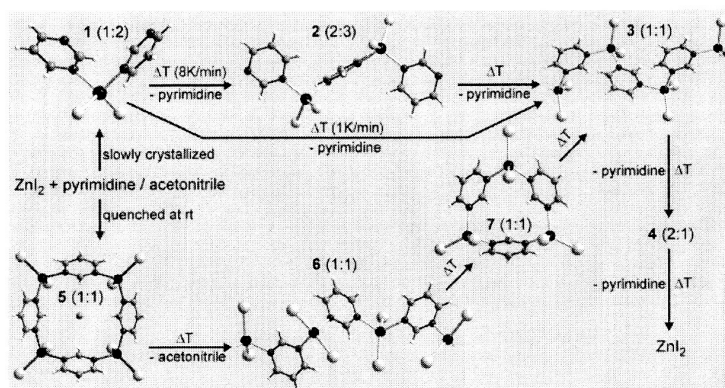


Figure 1. Schematic representation of the thermal decomposition and solution reactions of the different $\text{ZnI}_2(\text{pyrimidine})$ coordination compounds reported in this paper.

required in large amounts, and in most cases, syntheses are performed in solution. In solution, different species are in equilibrium, and product formation will depend on a number of parameters like the nature of the solvent, the ratio of the reactants, the stability of the products, etc. In some reactions, metastable compounds can also form in the beginning of the reaction and will transform into the thermodynamically stable compounds as a function of time. In view of this, a mixture of compounds rather than a single product is obtained, or alternatively metastable intermediates might be overlooked. Therefore, alternative preparation methods and investigations on the formation of such compounds in solution are essential.

In our recent work, we have demonstrated that the thermal decomposition of ligand-rich precursor compounds is a convenient method for the discovery and facile synthesis of novel coordination polymers in phase-pure form.^{20–27} Starting from ligand-rich precursor compounds, several ligand-deficient intermediate compounds can be obtained during the reaction. By this method, the equilibrium is shifted irreversibly into the direction of the ligand-deficient compounds and, therefore, compounds that cannot be normally prepared in solution or that can only be obtained as mixtures can also be obtained. In addition, by this procedure most compounds that exist in solution can be discovered in a single thermal investigation starting from the most ligand-rich compound. Therefore, such investigations can give information on the species present in solution and the formation of coordination compounds. Here we report on a combined study in the solid

state as well as in solution on a simple system based on ZnI_2 coordination compounds with pyrimidine, which can act as a model for more complex reactions. In these investigations, we have prepared seven different stable and metastable species by thermal decomposition and solution reactions (Figure 1), which were structurally characterized by single-crystal structural analysis and investigated for their kinetic and thermodynamic stability. The results of our study provide insight into the complexity of even simple reactions and into the mechanistic aspects of the formation of coordination polymers.

Experimental Section

Compound 1. ZnI_2 (319.18 mg, 1.0 mmol) and pyrimidine (160.16 mg, 2.0 mmol) were stirred in 0.5 mL of acetonitrile for 1 day at room temperature. Afterward, the precipitate was filtered off. CHN analysis (in %). Found: C, 20.02; H, 1.65; N, 11.44. Calcd for $\text{C}_8\text{H}_8\text{I}_2\text{N}_4\text{Zn}$: C, 20.05; H, 1.68; N, 11.69. IR (KBr, cm^{-1}): 3049 (w), 2353 (w), 1648 (w), 1589 (s), 1560 (s), 1470 (s), 1373 (m), 1225 (m), 1174 (m), 1081 (m), 1013 (m), 824 (m), 712 (m), 687 (m), 642 (m). Single crystals were prepared by the reaction of ZnI_2 (79.79 mg, 0.25 mmol) with pyrimidine (120.12 mg, 1.5 mmol) at room temperature in 2.0 mL of acetonitrile. Upon evaporation of the solvent, crystals of **1** grew within 7 days.

Compound 2. ZnI_2 (319.18 mg, 1.0 mmol) and pyrimidine (120.12 mg, 1.5 mmol) were stirred in 0.5 mL of acetonitrile for 1 day at room temperature. Afterward, the precipitate was filtered off. CHN analysis (in %). Found: C, 16.71; H, 1.45; N, 9.69. Calcd for $\text{C}_{12}\text{H}_{12}\text{I}_4\text{N}_6\text{Zn}_2$: C, 16.40; H, 1.38; N, 9.56. IR (KBr, cm^{-1}): 3427 (w), 3091 (w), 3057 (w), 2363 (w), 2344 (m), 1990 (w), 1961 (w), 1916 (w), 1772 (w), 1734 (w), 1717 (w), 1698 (w), 1681 (w), 1653 (w), 1660 (m), 1593 (s), 1560 (s), 1470 (s), 1418 (s), 1367 (m), 1227 (m), 1175 (m), 1082 (s), 1013 (m), 963 (w), 817 (m), 703 (s), 643 (s). Single crystals of the compound were prepared by the reaction of ZnI_2 (159.59 mg, 0.5 mmol) with pyrimidine (40.04 g, 0.5 mmol) in 2.0 mL of acetonitrile. Upon evaporation of the solvent, crystals of **2** grew within 7 days.

Compound 3. ZnI_2 (319.18 mg, 1.0 mmol) and pyrimidine (80.08 mg, 1.0 mmol) were stirred in 0.5 mL of acetonitrile for 1 day at room temperature. Afterward, the precipitate was filtered off. CHN analysis (in %). Found: C, 12.26; H, 0.98; N, 7.10. Calcd for $\text{C}_4\text{H}_4\text{I}_2\text{N}_2\text{Zn}$: C, 12.03; H, 1.01; N, 7.02. IR (KBr, cm^{-1}): 3123 (m), 3069 (w), 3050 (m), 3027 (m), 2377 (w), 1990 (w), 1900 (w),

- (16) Horcajada, P.; Patricia Serre, C.; Vallet-Regi, M.; Sebban, M.; Taulelle, F.; Férey, G. *Angew. Chem., Int. Ed.* **2006**, *45*, 5974.
 (17) Eddaoudi, M.; Kim, J.; Rosi, N.; Vodak, D.; Wachter, J.; O'Keefe, M.; Yaghi, O. M. *Science* **2002**, *295*, 469.
 (18) Rowsell, J. L. C.; Yaghi, O. M. *Microporous Mesoporous Mater.* **2004**, *73*, 3.
 (19) Chae, H. K.; Siberio-Perez, D. Y.; Kim, J.; Go, Y. B.; Eddaoudi, M.; Matzger, A. J.; O'Keefe, M.; Yaghi, O. M. *Nature* **2004**, *427*, 523.
 (20) Näther, C.; Wriedt, M.; Jess, I. *Inorg. Chem.* **2003**, *42*, 2391.
 (21) Näther, C.; Jess, I. *Inorg. Chem.* **2003**, *42*, 2968.
 (22) Näther, C.; Jess, I.; Lehnert, N.; Hinz-Hübner, D. *Solid State Sci.* **2003**, *5*, 1343.
 (23) Näther, C.; Jess, I. *Inorg. Chem.* **2006**, *45*, 7446.
 (24) Näther, C.; Jess, I. *J. Solid State Chem.* **2002**, *169*, 103.
 (25) Näther, C.; Greve, J. *J. Solid State Chem.* **2003**, *176*, 259.
 (26) Näther, C.; Jess, I. *Eur. J. Inorg. Chem.* **2004**, 2868.
 (27) Bhosekar, G.; Jess, I.; Näther, C. *Inorg. Chem.* **2006**, *43*, 6508.

Stable and Metastable Coordination Compounds

Table 1. Selected Crystal Data and Details on the Structure Determinations^a

compd	1	2	3	5	6	7
formula	C ₈ H ₈ I ₂ N ₄ Zn	C ₁₂ H ₁₂ I ₄ N ₆ Zn ₂	C ₄ H ₄ I ₂ N ₂ Zn	C _{4.50} H _{4.75} I ₂ N _{2.25} Zn	C ₄ H ₄ I ₂ N ₂ Zn	C ₄ H ₄ I ₂ N ₂ Zn
MW/(g/mol)	479.35	878.62	399.26	409.53	399.26	399.26
cryst syst	monoclinic	monoclinic	monoclinic	tetragonal	monoclinic	orthorhombic
space group	P2 ₁ /n	C2/c	P2 ₁ /c	P4/m	P2 ₁ /c	Pnma
Z	4	4	4	8	8	12
temp/K	170	293	293	293	220	220
a/Å	8.0546(6)	23.5621(13)	7.5576(5)	17.0267(8)	6.5487(13)	13.4555(7)
b/Å	12.7334(8)	8.0398(5)	13.5380(8)	17.0267(8)	14.427(3)	19.0259(13)
c/Å	12.6152(12)	11.7637(6)	9.6246(8)	7.5579(4)	18.990(4)	11.285(7)
β/deg	92.208(10)	98.010(6)	112.310(8)		90.021(6)	
V/Å ³	1292.89(18)	2206.7(2)	911.02(11)	2191.10(19)	1794.1(6)	2889.0(18)
d _{calc} /(Mg/m ³)	2.463	2.645	2.911	2.483	2.956	2.754
μ/mm	6.650	7.777	9.399	7.820	9.546	8.892
min/max transn	0.3223/0.4166	0.2680/0.3858	0.2129/0.3424	0.2304/0.3772	0.1053/0.4472	0.1037/0.4289
θ _{max} /deg	28.0	28.0	28.0	28.0	28.0	28.0
measd reflns	6375	11059	8716	11244	17487	26815
R _{int}	0.0353	0.0834	0.0707	0.0380	0.0721	0.0738
unique reflns	3085	2572	2130	2584	4326	3576
reflns [F _o > 4σ(F _o)]	2342	2251	1757	2055	3892	3089
param	137	111	84	92	155	128
R1 [F _o > 4σ(F _o)]	0.0321	0.0319	0.0318	0.0383	0.0334	0.0317
wR2 (all data)	0.0769	0.0839	0.0808	0.1024	0.0767	0.0790
GOF	0.969	1.041	1.065	1.060	1.016	1.028
res elec/(e/Å ³)	0.839/-1.163	1.214/-0.973	1.232/-1.345	1.396/-1.064	1.705/-1.217	1.287/-1.718

^a All non-hydrogen atoms were refined using anisotropic displacement parameters. The hydrogen atoms were positioned with idealized geometry and were refined isotropically ($U_{eq} = -1.2$) using a riding model with C-H = 0.95 Å for aromatic hydrogen atoms. The data were corrected using a numerical absorption correction ($T_{min} = 0.3223$; $T_{max} = 0.4166$). U_{eq} is defined as one-third of the trace of the orthogonalized U_{ij} tensor.

1803 (w), 1708 (w), 1606 (s), 1471 (s), 1404 (s), 1223 (m), 1188 (m), 1080 (s), 1035 (m), 818 (m), 694 (s), 671 (s). Single crystals of this compound were prepared by the reaction of ZnI₂ (159.59 mg, 0.5 mmol) with pyrimidine (20.02 mg, 0.25 mmol) in 2 mL of ethanol and 0.3 mL of water. Upon evaporation of the solvent, crystals of **3** grew within 7 days.

Compound 4. ZnI₂ (159.59 mg, 0.5 mmol) and pyrimidine (20.02 mg, 0.25 mmol) were stirred in 1.0 mL of heptane for 1 day at room temperature. Afterward, the precipitate was filtered off. In most cases, the product was not phase-pure and was contaminated with ZnI₂. Therefore, for further characterization by CHN and spectroscopic analysis, compound **4** was prepared by a thermal decomposition reaction. CHN analysis (in %). Found: C, 6.59; H, 0.56; N, 3.97. Calcd for C₄H₄I₄N₂Zn₂: C, 6.69; H, 0.56; N, 3.90. IR (KBr, cm⁻¹): 3105 (w), 3063 (w), 2926 (w), 1606 (s), 1562 (m), 1472 (m), 1410 (s), 1369 (w), 1229 (m), 1179 (m), 1144 (w), 1084 (m), 1032 (m), 815 (w), 695 (s), 673 (s), 645 (w).

Compound 5. ZnI₂ (159.59 mg, 0.5 mmol) and pyrimidine (40.04 mg, 0.5 mmol) were reacted in 2.0 mL of acetonitrile at room temperature. To the clear solution was added 2.0 mL of carbon tetrachloride as a precipitant, and the residue formed was filtered off. CHN analysis (in %). Found: C, 12.73; H, 1.21; N, 7.96. Calcd for C_{4.25}H_{4.75}I₂N_{2.25}Zn: C, 12.56; H, 1.18; N, 7.74. IR (KBr, cm⁻¹): 3102 (m), 3064 (m), 3031 (m), 2920 (w), 2241 (w), 1606 (s), 1568 (m), 1473 (m), 1411 (s), 1368 (w), 1230 (m), 1186 (m), 1151 (w), 1087 (m), 1034 (m), 988 (w), 961 (w), 820 (m), 781 (m), 701 (s), 672 (s). Single crystals of the compound were prepared by the reaction of ZnI₂ (159.59 mg, 0.5 mmol) with pyrimidine (40.04 mg, 0.5 mmol) in 2.0 mL of acetonitrile at room temperature. Upon slow evaporation of the solvent, crystals of **5** grew within 3 days.

Compound 6. ZnI₂ (159.59 mg, 0.5 mmol) and pyrimidine (40.04 mg, 0.5 mmol) were reacted in 0.5 mL of acetonitrile at room temperature. To the clear solution was added 2.0 mL of carbon tetrachloride as a precipitant, and the residue was immediately filtered off. This compound was really difficult to obtain because in some cases compounds **3**, **5**, or **7** was formed. CHN analysis (in %). Found: C, 12.12; H, 1.07; N, 7.01. Calcd for C₄H₄I₂N₂Zn: C,

12.03; H, 1.01; N, 7.02. Single crystals of this compound were prepared by the reaction of ZnI₂ (159.59 mg, 0.5 mmol) with pyrimidine (10.01 mg, 0.125 mmol) in 2.0 mL of acetonitrile and 0.3 mL of water. Upon slow evaporation of the solvent from the clear solution, crystals of **6** grew within 2 days.

Compound 7. ZnI₂ (159.59 mg, 0.5 mmol) and pyrimidine (40.04 mg, 0.5 mmol) were reacted in 0.5 mL of acetonitrile at room temperature. To the clear solution was added 2.0 mL of carbon tetrachloride as a precipitant, and after 1 h, the product was filtered off. CHN analysis (in %). Found: C, 12.21; H, 1.09; N, 7.11. Calcd for C₄H₄I₂N₂Zn: C, 12.03; H, 1.01; N, 7.02. IR (KBr, cm⁻¹): 3107 (m), 3058 (s), 3021 (m), 2923 (w), 2375 (w), 2001 (w), 1812 (w), 1608 (s), 1563 (m), 1472 (s), 1411 (s), 1236 (m), 1189 (s), 1147 (m), 1087 (s), 1035 (m), 817 (m), 702 (s), 671 (s). Single crystals of the compound were prepared by the reaction of ZnI₂ (159.59 mg, 0.5 mmol) with pyrimidine (40.04 mg, 0.5 mmol) in 2.0 mL of acetonitrile. Upon slow evaporation of the solvent, crystals grew within 1 day.

Single-Crystal X-ray Diffraction. All data were measured using an IPDS-1 with Mo K α radiation. Structure solutions were performed with *SHELXS-97*, and structure refinements were done against F^2 using *SHELXL-97*. Numerical absorption corrections were performed with X-RED and X-Shape. The metric parameters of compound **6** with $\beta = 90.021(6)^\circ$ indicate that it crystallizes orthorhombic but it is definitely monoclinic. The crystal investigated for this compound is pseudomerohedral-twinned. Therefore, a twin refinement was performed using the twin matrix $-1\ 0\ 0\ 0\ 1\ 0\ 0\ 0\ 1$, which leads to an BASF parameter of 0.326(1). Details of the structure determinations are given in Table 1.

Crystallographic data have been deposited with the Cambridge Crystallographic Data Centre [CCDC 656322 (**1**), CCDC 656323 (**2**), CCDC 656324 (**3**), CCDC 656325 (**5**), CCDC 656326 (**6**), and CCDC 656327 (**7**)]. These data can be obtained free of charge from the Cambridge Crystallographic Data Centre via www.ccdc.cam.ac.uk/data_request.cif.

Powder X-ray Diffraction (PXRD). PXRD diffraction experiments were performed using a STOE STADI P transmission powder

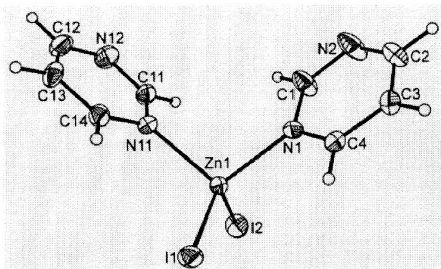


Figure 2. Crystal structure of the ligand-rich 1:2 compound **1** with labeling and displacement ellipsoids drawn at the 50% probability level.

diffractometer with Cu K α radiation ($\lambda = 154.0598$ pm), which is equipped with a position-sensitive detector (scan range: 5–45°) from STOE & CIE.

Thermogravimetry and Differential Thermoanalysis (TG/DTA). The TG/DTA measurements were performed in a nitrogen atmosphere (purity: 5.0) and Al₂O₃ crucibles using a STA-409CD thermobalance from Netzsch. For the mass spectrometry (MS) measurements, the thermobalance was connected to a quadrupole mass spectrometer from Balzers. All measurements were performed with a flow rate of 75 mL/min and were corrected for buoyancy and current effects. The instrument was calibrated using standard reference materials.

Differential Scanning Calorimetry (DSC). DSC investigations were performed with the DSC 204/1/F device from Netzsch. The measurements were performed in aluminum pans with heating rates of 3 °C/min. The instrument was calibrated using standard reference materials.

Elemental Analysis. CHN analysis was performed using a EURO EA elemental analyzer, fabricated by EURO VECTOR Instruments and Software.

Spectroscopy. Fourier transform IR spectra were recorded on a Genesis series FTIR spectrometer, by ATI Mattson, in KBr pellets.

Results and Discussion

The reaction of ZnI₂ with pyrimidine in acetonitrile leads to the ligand-rich 1:2 compound diiodobis(pyrimidine-*N*)-zinc(II) (**1**), which crystallizes in space group $P2_1/n$ with $Z = 4$ and all atoms in general positions. In this structure, the zinc atoms are coordinated by two iodine atoms and two pyrimidine ligands within distorted tetrahedra into discrete complexes (Figure 2 and Table 2).

TG/DTA measurements on **1** with 1 °C/min in a nitrogen atmosphere show four mass steps, which are accompanied by four endothermic events in the DTA curve, and from the DTG curve, it is obvious that all steps are well resolved (Figure 3). The experimental mass loss of 16.7% in the first TG step is in good agreement with that calculated for the removal of one pyrimidine ligand of 16.7%. The experimental mass losses in the second and third TG steps of 8.3 and 8.5%, respectively, indicate the loss of 0.5 mol of the pyrimidine ligands ($\Delta m_{\text{theo}} - 1/2 \text{pyrimidine} = 8.35\%$). The final product after the third step was identified as ZnI₂ by PXRD. On the basis of the above results, it can be inferred that in the first TG step a 1:1 compound of composition ZnI₂-(pyrimidine) (**3**) is formed, whereas the second step leads to the formation of a 2:1 compound of composition (ZnI₂)₂-(pyrimidine) (**4**), which upon further heating decomposes into

8082 Inorganic Chemistry, Vol. 46, No. 19, 2007

Table 2. Bond Lengths [Å] and Angles [deg] for Compounds **1–3**^a

Compound 1			
Zn1–N1	2.070(4)	Zn1–I1	2.5429(7)
Zn1–N11	2.081(4)	Zn1–I2	2.5455(7)
N1–Zn1–I1	106.42(12)	N11–Zn1–I1	106.04(12)
N1–Zn1–I2	109.39(12)	N11–Zn1–I2	106.29(13)
I1–Zn1–I2	123.32(2)	N1–Zn1–N11	103.72(16)
Compound 2			
Zn1–N11	2.072(4)	Zn1–I2	2.5241(6)
Zn1–N1	2.098(3)	Zn1–I1	2.5539(6)
N11–Zn1–N1	101.76(14)	N11–Zn1–I1	104.77(11)
N11–Zn1–I2	111.29(12)	N1–Zn1–I1	106.03(10)
N1–Zn1–I2	110.43(9)	I2–Zn1–I1	120.75(2)
Compound 3			
Zn1–N1	2.109(3)	Zn1–I1	2.5245(6)
Zn1–N2A	2.102(3)	Zn1–I2	2.5263(7)
N2A–Zn1–N1	96.37(14)	N2A–Zn1–I2	108.97(10)
N2A–Zn1–I1	110.07(10)	N1–Zn1–I2	107.03(11)
N1–Zn1–I1	107.18(10)	I1–Zn1–I2	123.69(2)

^a Symmetry codes for **3**: $A = x, -y + 1/2, z - 1/2$.

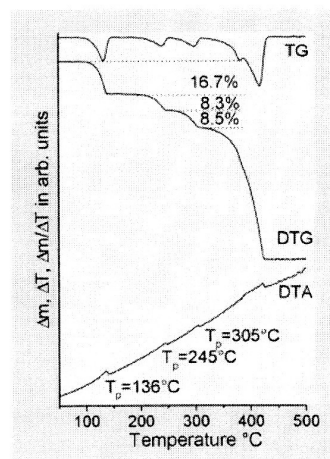


Figure 3. DTG, TG, and DTA curves for compound **1** with 1 °C/min.

ZnI₂, which vaporizes in the last TG step. These conclusions are supported by PXRD and elemental analysis of the residues formed in each of the TG steps (see the Experimental Section).

Single crystals of **3** were grown in solution (see the Experimental Section), and crystal structural analysis shows that this compound crystallizes in space group $P2_1/c$ with $Z = 4$ and all atoms in general positions. In diiodo(μ_2 -pyrimidine-*N,N'*)zinc(II) (**3**), the zinc atoms are coordinated by two iodine atoms and two pyrimidine ligands within distorted tetrahedra (Figure 4). Most bond lengths and angles are comparable to those in compound **1**, but the Zn–N distances are slightly elongated (Table 2). In contrast to **1**, the ZnI₂ units are connected by the pyrimidine ligands via μ -*N,N'* coordination into chains that elongate in the direction of the *a* axis (Figure 8, bottom).

For the ligand-deficient 2:1 compound **4**, no single crystals could be grown and, therefore, this compound was characterized only by PXRD and elemental analysis (see below).

Stable and Metastable Coordination Compounds

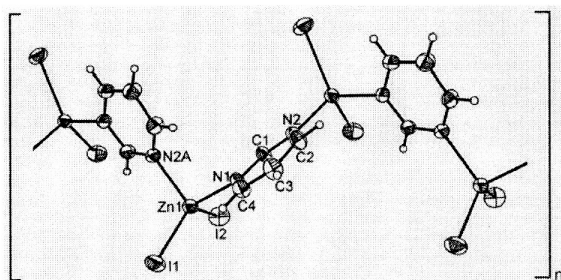


Figure 4. Crystal structure of the 1:1 compound **3** with labeling and displacement ellipsoids drawn at the 50% probability level.

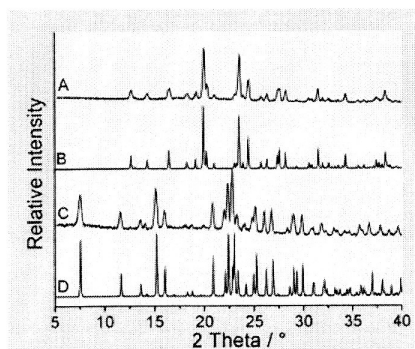


Figure 5. Experimental PXRD patterns of the residue obtained after the first (A) and second (C) TG step in the thermal decomposition reaction of compound **1** and calculated PXRD patterns for the 1:1 compound **3** (B) and the 2:3 compound **2** (D).

However, from the composition of this compound, it can be expected that its structure might consist of a more condensed ZnI substructure like, e.g., ZnI_4N_2 octahedra connected via common corners.

To definitely prove the formation of the 1:1 compound **3** in the beginning of the thermal reaction, an additional TG experiment was performed, and the heating was stopped immediately after the first TG step. The residue thus obtained was investigated by PXRD. The experimental powder pattern of this residue is in good agreement with that calculated for compound **3** from single-crystal data, indicating its formation as an intermediate in very pure form (Figure 5). These findings are further supported by elemental analysis (see the Experimental Section).

From investigations reported previously, it is known that in some cases the product formation depends on the kinetics of all reactions involved and, therefore, can be influenced by heating rate dependent measurements.²⁴ In view of this, the thermal decomposition of the ligand-rich 1:2 compound **1** was investigated using different heating rates. This study revealed that the first mass step is split into two different steps upon faster heating and that the best resolution is obtained with 8 °C/min (Figure 6). The PXRD pattern of the residue formed in the first TG step with 8 °C/min is completely different from that of compounds **1** and **3**, and elemental analysis of this residue is in good agreement with that calculated for a 2:3 compound of composition $(ZnI_2)_2$ -(pyrimidine)₃ (**2**; see the Experimental Section).

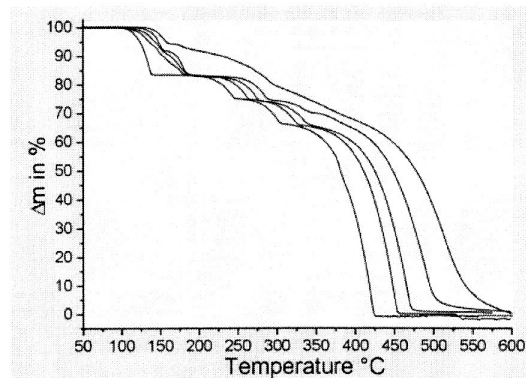


Figure 6. Heating rate dependent TG curves for **1** (from left to right: 1, 2, 4, 8, and 16 °C/min).

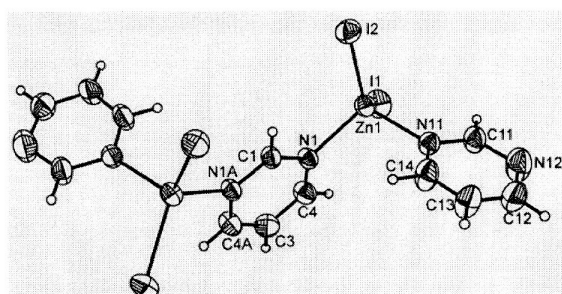


Figure 7. Crystal structure of the 2:3 compound **2** with labeling and displacement ellipsoids drawn at the 50% probability level.

Single crystals of the new compound **2** can also be grown in solution, and structural analysis shows that a 2:3 compound has formed, which crystallizes in space group $C2/c$ with $Z = 4$ and all atoms in general positions. The structure of the 2:3 compound **2** consists of discrete $(ZnI_2)_2$ -(pyrimidine)₃ units, in which each of the two zinc atoms are coordinated by one terminal and one bridging pyrimidine ligand (Figure 7). These units are located on the centers of inversion. Bond lengths and angles of **2** are in good agreement with those of **1** and are comparable to values retrieved from the literature (Table 2). The formation of compound **2** as an intermediate in the thermal reaction of compound **1** was further confirmed by comparing the experimental PXRD pattern of the residue formed in the thermal reaction with that calculated from single-crystal data (Figure 4).

From a structural point of view, compound **2** represents an intermediate for the transformation of the tetrahedral discrete ZnI_2 (pyrimidine)₂ units in compound **1** into the infinite ZnI_2 (pyrimidine) chains in the 1:1 compound **3**. Interestingly, a detailed analysis of the crystal structures of compounds **1**–**3** reveals a smooth reaction pathway for the transformation of **1** into **3** via **2**, which requires only small rotational and translational steps (Figure 8). This clearly indicates that there are some three-dimensional similarities, even if a topotactic reaction pathway is unlikely.

In further experiments, we investigated the reaction of zinc iodide with pyrimidine in acetonitrile as described in the

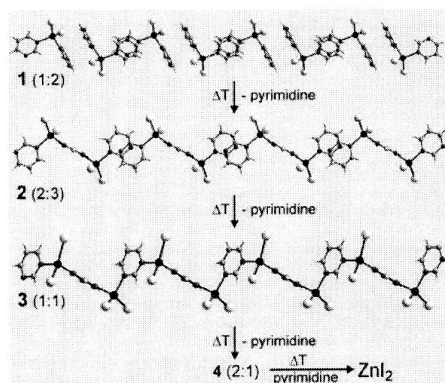


Figure 8. Structural aspects of the thermal decomposition reaction of compound **1** into **3** via **2** as the intermediate.

beginning, but this reaction was quenched by the addition of an antisolvent (see the Experimental Section). Surprisingly, the PXRD pattern of the precipitate does not correspond to those of compounds **1–4**. Elemental analysis shows that the composition corresponds approximately to that of a new 1:1 compound (**5**). Single crystals of this compound can also be grown from solution, by evaporating the solvent at different rates (see below and the Experimental Section). Single-crystal structural analysis of compound **5** shows that the compound has the expected 1:1 composition and in addition contains a small amount of acetonitrile. Compound **5** crystallizes in space group $P4/m$ with eight formula units in the unit cell. The structure consists of $ZnI_2(\text{pyrimidine})$ units, in which the zinc atoms are coordinated by two iodine atoms and two pyrimidine ligands within distorted tetrahedra (Figure 9, top, and Table 3).

These units are connected by the ligands via $\mu\text{-N,N'}$ coordination into $[(ZnI_2)(\text{pyrimidine})_4]$ rings, which are located on a 4-fold axis.

These rings are stacked in the direction of the c axis, forming channels in which additional solvent molecules are located (Figure 8, bottom).

In further investigations, compound **5** was stored under reduced pressure in order to determine whether the solvent can be deintercalated in a topotactic reaction, but no changes were observed. Therefore, TG/DTA–MS measurements were performed, which show four mass steps. The MS measurements confirm that in the first step only acetonitrile is removed, whereas in the second and third steps half of each of the pyrimidine ligands is emitted (Figure 10). The loss of the CH_3CN solvent can be accounted for by the formation of a 1:1 compound, while the loss of the nitrogen donor ligand can be attributed to the formation of the ligand-deficient 2:1 compound **4**.

Surprisingly, the PXRD pattern of the residue formed in the first TG step does not correspond to that calculated for the 1:1 compound **3**, indicating the formation of a new 1:1 compound **6**. In addition, the DSC thermogram exhibits a more complex profile, pointing to the formation of more intermediates (Figure 10). In view of this, the reaction was stopped at different temperatures after the first TG step and

8084 Inorganic Chemistry, Vol. 46, No. 19, 2007

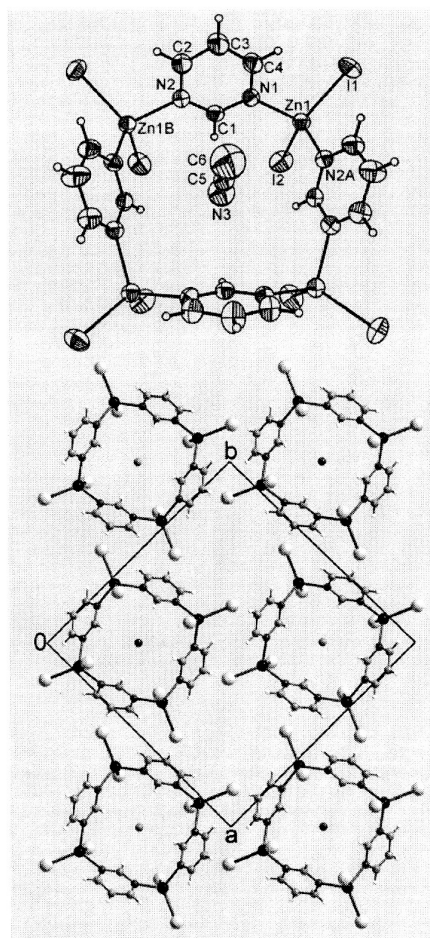


Figure 9. Crystal structure of the 1:1 compound **5** with labeling and displacement ellipsoids drawn at the 50% probability level (top) and with a view along the c axis (bottom).

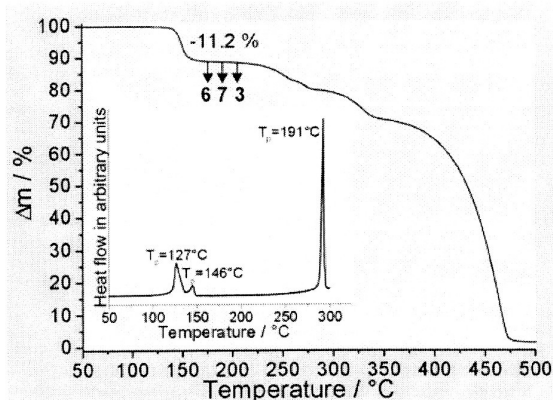


Figure 10. TG curve of compound **5** (the inset shows the DSC curve of this compound).

investigated by PXRD, which shows that, depending on the temperature and where the residues are isolated, three different compounds were obtained. Because the composition of these compounds remains constant, all of them must

Stable and Metastable Coordination Compounds

Table 3. Bond Lengths [Å] and Angles [deg] for Compounds 5–7

Compound 5			
Zn1–N1	2.104(4)	Zn1–I2	2.5217(8)
Zn1–N2A	2.105(4)	Zn1–I1	2.5307(7)
N2–Zn1B	2.105(4)		
N2A–Zn1–I2	108.70(13)	N2A–Zn1–I1	106.20(12)
N1–Zn1–I1	106.20(12)	I2–Zn1–I1	122.79(3)
Compound 6			
Zn1–N1	2.083(5)	Zn2–N2	2.116(5)
Zn1–N12A	2.134(5)	Zn2–N11	2.120(5)
Zn1–I2	2.5005(10)	Zn2–I3	2.5253(9)
Zn1–I1	2.5364(10)	Zn2–I4	2.5660(9)
N12–Zn1B	2.134(5)		
N1–Zn1–N12A	96.8(2)	N2–Zn2–N11	106.57(19)
N1–Zn1–I2	110.06(14)	N2–Zn2–I3	106.25(14)
N12A–Zn1–I2	111.13(15)	N11–Zn2–I3	105.20(14)
N1–Zn1–I1	111.04(15)	N2–Zn2–I4	102.32(14)
N12A–Zn1–I1	105.39(15)	N11–Zn2–I4	99.60(14)
I2–Zn1–I1	119.85(3)	I3–Zn2–I4	134.44(3)
Compound 7			
Zn1–N1	2.102(4)	Zn2–N2A	2.101(4)
Zn1–N11	2.107(4)	Zn2–N2	2.101(4)
Zn1–I2	2.5140(7)	Zn2–I4	2.5013(16)
Zn1–I1	2.5276(5)	Zn2–I3	2.5364(7)
N1–Zn1–N11	95.02(14)	N2A–Zn2–N2	96.24(19)
N1–Zn1–I2	108.54(10)	N2A–Zn2–I4	107.77(10)
N11–Zn1–I2	107.67(10)	N2–Zn2–I4	107.77(10)
N1–Zn1–I1	107.41(9)	N2A–Zn2–I3	107.15(9)
N11–Zn1–I1	106.97(10)	N2–Zn2–I3	107.15(9)
I2–Zn1–I1	126.66(3)	I4–Zn2–I3	126.59(3)

represent different modifications of a 1:1 compound. The product isolated at the highest temperature after the first TG step corresponds to the 1:1 compound **3**, also obtained from the thermal decomposition reaction of compound **1**, and the product formed in the second TG step corresponds to the 2:1 compound **4**.

To investigate this reaction in more detail and to identify the two additional intermediates **6** and **7**, several crystallization experiments were performed. In these experiments, the solvent was removed at different rates and the single crystals formed by this procedure were investigated by PXRD. In the PXRD pattern of some of these batches, additional reflections were observed that correspond to those also observed in the PXRD pattern of the intermediates **6** and **7** observed in the thermal decomposition reaction of compound **5**. From these batches, different single crystals were selected, and by this procedure, the crystal structures of compounds **6** and **7** were determined.

The 1:1 compound **6** formed in the beginning crystallizes in space group $P2_1/c$ with $Z = 8$ and two crystallographically independent ZnI_2 (pyrimidine) units in the asymmetric unit (Figure 11). In the crystal structure, each zinc atom is connected by two iodine atoms and two pyrimidine ligands and the coordination polyhedron can be described as a distorted tetrahedron (Table 3). Bond lengths and angles are in good agreement with those in compound **3**. The ZnI_2 units are connected via the pyrimidine ligands into chains that elongate in the direction of the c axis. Thus, the topology of the 1:1 compound **6** is identical with that of the 1:1 compound **3**, and both compounds represent polymorphic modifications.

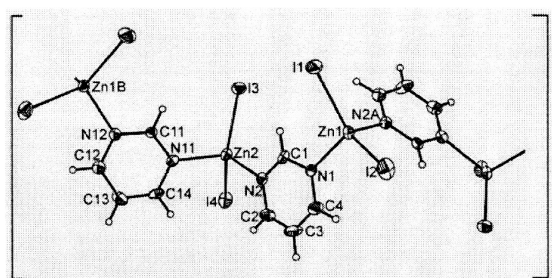


Figure 11. Crystal structure of the 1:1 compound **6** with labeling and displacement ellipsoids drawn at the 50% probability level.

The 1:1 compound **7** crystallizes in space group $Pnma$ with $Z = 12$ and 1.5 crystallographically independent ZnI_2 (pyrimidine) units in the asymmetric unit. The zinc and iodine atoms as well as one ligand are located in general positions, and the second ligand occupies a special position. As in all other compounds, the zinc atoms are tetrahedrally coordinated by the iodine atoms and the pyrimidine ligands. In contrast to compounds **3** and **6**, the ZnI_2 (pyrimidine) units are connected into cyclic $[(ZnI_2(\text{pyrimidine}))_3]$ trimers (Figure 12 and Table 3).

On the basis of the structural results, all intermediates in the thermal decomposition reaction of compound **5** were identified. This shows clearly that compound **5** loses the solvent and transforms into the new 1:1 compound **6**, which undergoes two successive polymorphic phase transitions. It is surprising that the $[(ZnI_2(\text{pyrimidine}))_4]$ tetramers in **5** transform into chains (**6**) that reorganize into $[(ZnI_2(\text{pyrimidine}))_3]$ trimers (**7**) before chains are formed again. It might be more likely that **5** transforms first into **7** before a transformation into chains is observed. However, this can be excluded. Moreover, for a reaction of the tetramers into trimers, no smooth reaction pathway can be found, whereas for the reaction of the tetramers into the chains, only small translational and rotational movements are needed.

In order to determine if compounds **6** and **7** can also be obtained in solution and to prove which of the compounds represents the thermodynamically most stable compounds, crystalline powders formed from different ratios of ZnI_2 and pyrimidine were stirred in acetonitrile for 1 week and afterward identified by PXRD (Table 4). These investigations clearly show that only compounds **1–4** can be obtained by this procedure and, therefore, represent the most stable compounds. Compounds **5–7** cannot be obtained and, thus, must be metastable.

In order to determine if the polymorphic compounds **6** and **7** are formed by kinetic control, several ex situ time-dependent PXRD measurements were performed (Figure 13). These experiments confirm that compound **6** is initially formed but transforms within a few minutes into compound **7**, which finally transforms within about 1 day into compound **3**. Therefore, forms **6** and **7** are thermodynamically metastable, whereas form **3** is stable.

In this context, it is surprising that single crystals of the metastable compounds **5–7** can be grown because one would expect that in solution a transformation into the thermody-

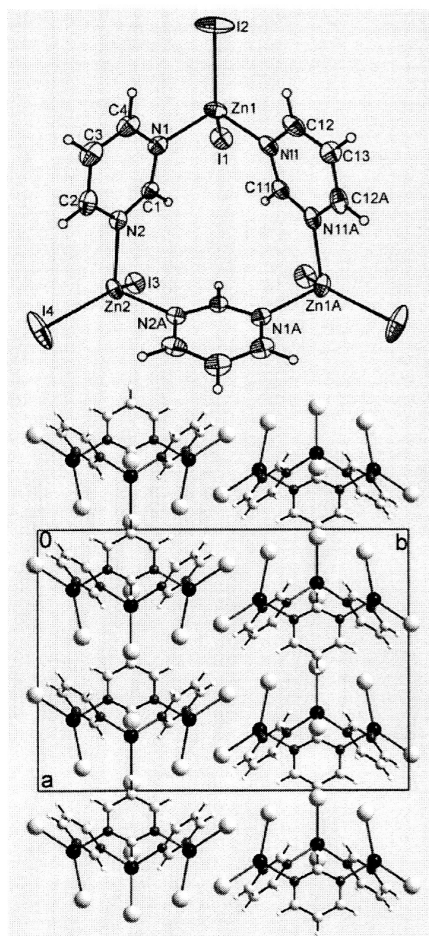


Figure 12. Crystal structure of the 1:1 compound **7** with labeling and displacement ellipsoids drawn at the 50% probability level.

Table 4. Results of the Solvent-Mediated Conversion Experiments If Different Ratios of ZnI_2 Are Reacted with Pyrimidine in Acetonitrile for 1 Week

product	ZnI_2 /ligand					
	1:3	1:2	2:3	1:1	3:2	2:1
	1 (1:2)		2 (2:3)	3 (1:1)	3 (1:1)	4 (2:1)

namically stable compounds will occur before large crystals are formed. However, in the beginning the thermodynamic, metastable compounds will crystallize, but the transformation can be suppressed if the solution is supersaturated and always new crystal nuclei of the metastable compounds will form. This can be reached if the solvent is quickly evaporated. In this case, the metastable nuclei formed in the beginning will grow continuously. However, this process is difficult to control and, therefore, in the present study a large number of crystallization experiments were performed using different ratios of ZnI_2 and pyrimidine, in which the solvent was evaporated at different rates. When sufficient crystals had formed for single-crystal XRD, crystallization was stopped and a part of the crystalline product was investigated by PXRD. In those batches in which reflections of a desired

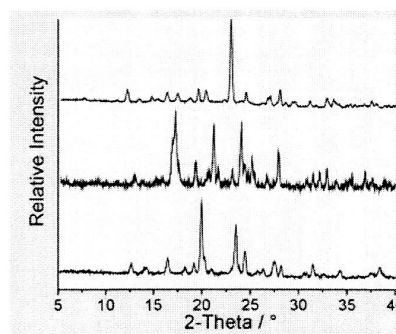


Figure 13. Experimental PXRD pattern of the residue obtained after 5 min (**6**) (top), 30 min (**7**) (middle), and 1 day (**3**) (bottom) if ZnI_2 is reacted with pyrimidine in acetonitrile in a ratio of 1:1 ($Cu\ K\alpha$ radiation).

compound were identified, several crystals of this batch were checked by single-crystal XRD. There is absolutely no doubt that this procedure is difficult to reproduce but as shown in this work is very effective.

Conclusions

In this contribution, we have reported seven new coordination compounds based on ZnI_2 and pyrimidine. We have clearly shown that new stable and metastable coordination compounds can be efficiently discovered and conveniently prepared by thermal decomposition reactions of suitable ligand-rich precursor compounds. In the present case, the seven compounds reported can also be isolated from solution. For the simple reaction of ZnI_2 with pyrimidine completely, different products (**1** and **5**) were obtained under thermodynamic or kinetic control, leading to completely different compounds on thermal decomposition (Figure 1). Six of the seven metastable and stable compounds were characterized by single-crystal XRD and, therefore, provide detailed information of the structural aspects of the thermal decomposition reactions. For some of the decomposition reactions, a smooth reaction pathway was found, which provides clear indications that structural information is transferred from the reactants into the products and thus conserved during the reaction.

The thermoanalytical investigations clearly demonstrate that **3** is the thermodynamically most stable 1:1 compound at higher temperatures and that the order of stability is $7 < 6 < 3$. The time-dependent PXRD experiments show that **3** represents the thermodynamically most stable 1:1 compound at room temperature, that **6** and **7** are metastable, and that the order of thermodynamic stability remains constant. In this context, it must be mentioned that the preparation of the metastable compound **6** is difficult to reproduce. Although this compound could be prepared phase pure in solution and by thermal decomposition in the beginning of our investigations, in later investigations it was noted that several batches were contaminated with other phases. This is not an unusual phenomenon and is well-known for metastable polymorphic modifications. If the experimental environment is contaminated with nuclei of the thermodynamic stable forms, the preparation of the metastable forms

Stable and Metastable Coordination Compounds

is mostly difficult to achieve.^{28,29} To solve this problem, systematic investigations on the control of nucleation are essential.^{30,31}

Our investigations show that different species are in equilibria in solution, with some of them being thermodynamically stable or metastable. The unambiguous characterization of the different compounds shows that several compounds exist in solution and gives insight into the formation of coordination compounds and polymers. The simple system based on zinc(II) coordination compounds with pyrimidine reported herein can act as a model for more

complex reactions, which will proceed via several intermediates. Thus, the present investigations provide more insight into the structural, thermodynamic, and kinetic aspects of the formation of coordination polymers.

Acknowledgment. This work was supported by the State of Schleswig-Holstein and the DFG (Project NA 720/1-1). We thank Prof. Dr. W. Bensch for access to his equipment.

Supporting Information Available: Experimental and calculated PXRD patterns for compounds 1–3 and 5–7, experimental pattern of the residues obtained in the thermal decomposition reaction of compound 5 and calculated pattern for compounds 3, 6, and 7, and details on the structure determination of compounds 1–3 and 5–7. This material is available free of charge via the Internet at <http://pubs.acs.org>.

(28) Dunitz, J. D.; Bernstein, J. *Acc. Chem. Res.* **1995**, *28*, 193.

(29) Bernstein, J.; Henck, J. O. *Mater. Res. Bull.* **1998**, *119*.

(30) Blagden, N.; Davey, R. J.; Liebermann, H. F.; Williams, L.; Payne, R. Rowe, R.; Docherty, R. *J. Chem. Soc., Faraday Trans.* **1998**, *94*, 1041.

(31) Breu, J.; Seidel, W.; Huttner, D.; Kraus, F. *Chem.—Eur. J.* **2002**, *8*, 19.

IC701079X

Supplemental Material

Preparation of stable and metastable coordination compounds: Insight into the structural, thermodynamic and kinetic aspects of the formation of coordination polymers.

Christian Näther, Gaurav Bhosekar and Inke Jeß.

- ❖ Experimental and calculated X-ray powder patterns for compounds **1-3** and **5-7**
- ❖ Experimental pattern of the residues obtained in the thermal decomposition reaction of compound **5** and calculated pattern for compounds **3**, **6** and **7**.
- ❖ Details on the structure determination of compounds **1-3** and **5-7**.

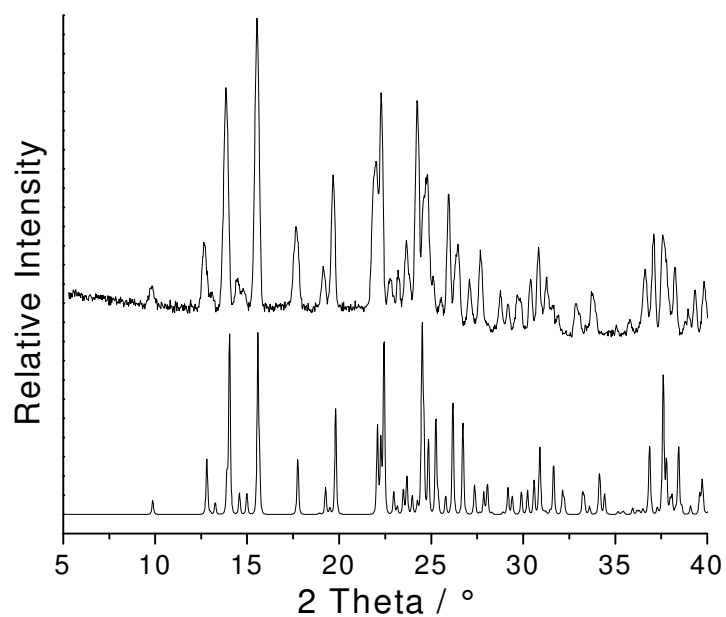


Figure S1: Experimental X-ray powder pattern of compound **1** (top) and X-ray powder pattern of compound **1** calculated from single crystal data (bottom) (CuK α radiation).

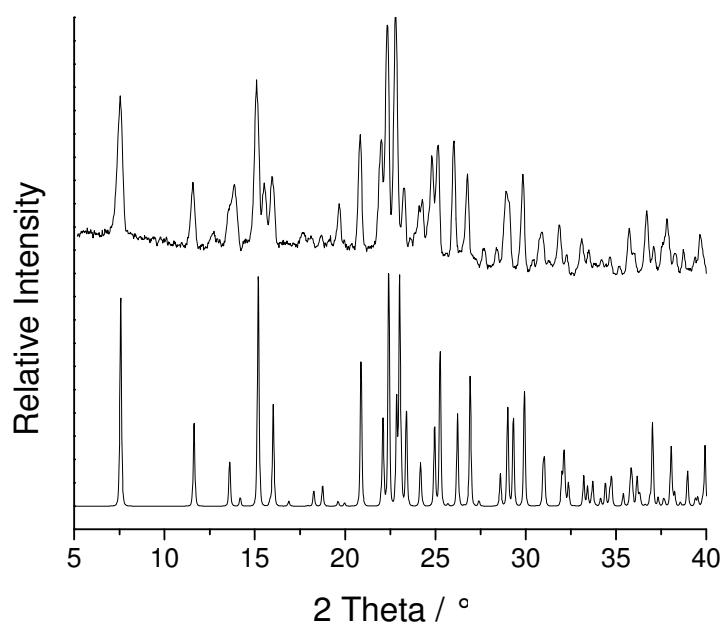


Figure S2: Experimental X-ray powder pattern of compound **2** (top) and X-ray powder pattern of compound **2** calculated from single crystal data (bottom) (CuK α radiation).

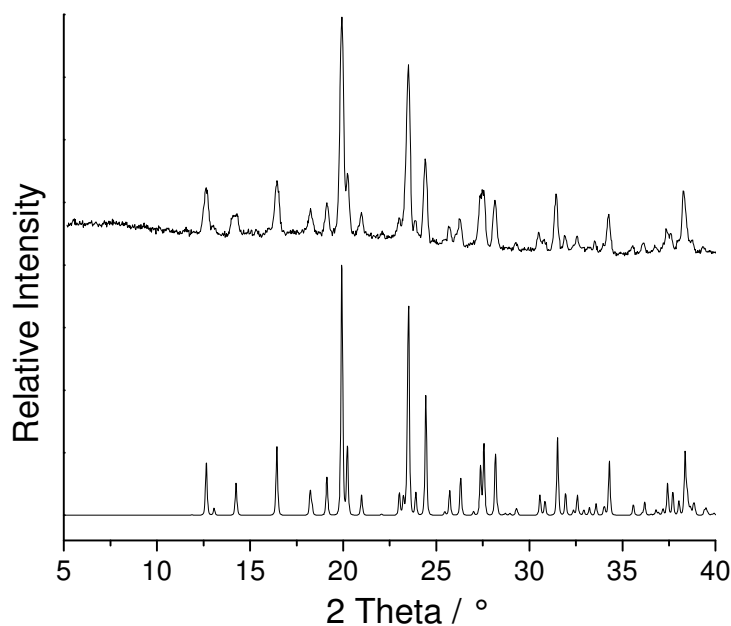


Figure S3: Experimental X-ray powder pattern of compound **3** (top) and X-ray powder pattern of compound **3** calculated from single crystal data (bottom) (CuK α radiation).

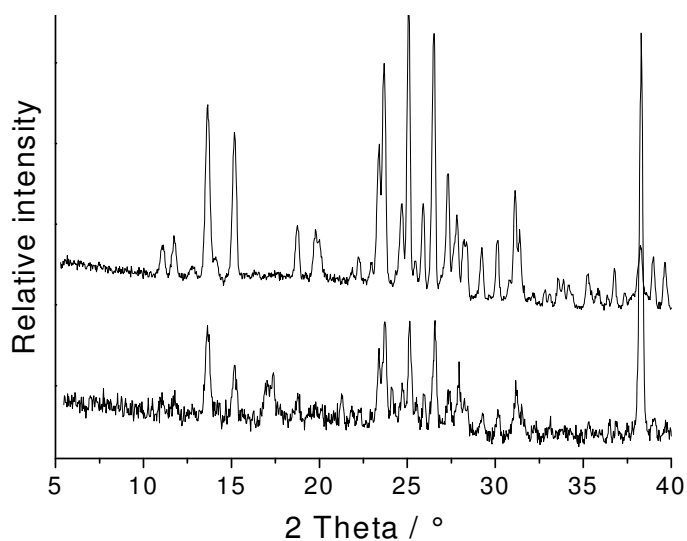


Figure S4: Experimental X-ray powder pattern of the residue obtained after the second TG step obtained in the thermal decomposition reaction of compound **1** that corresponds to the 2:1 compound **4** (top) and experimental pattern of compound **4** which was prepared in solution (bottom) (CuK α radiation). The additional strong peak in the spectra shown in the bottom originated from unreacted ZnI₂, which shows, that compound **4** in most cases can only be prepared pure by thermal decomposition reaction.

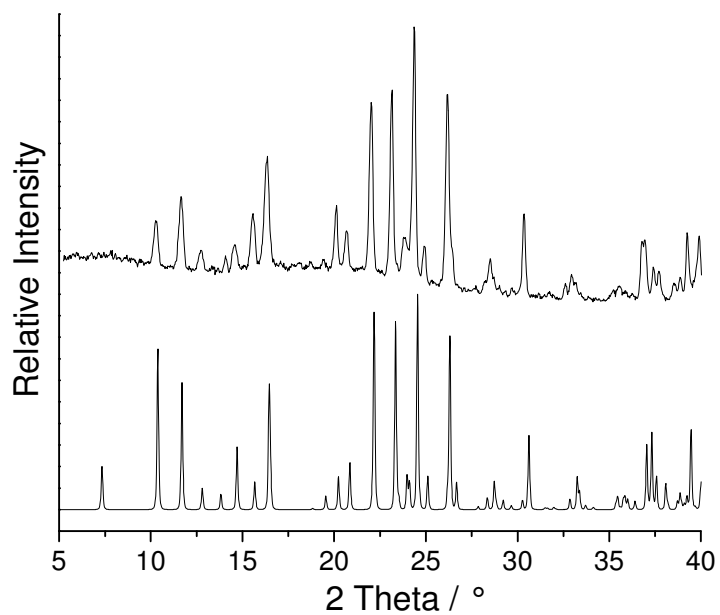


Figure S5: Experimental X-ray powder pattern of compound **5** (top) and X-ray powder pattern of compound **5** calculated from single crystal data (bottom) (CuK α radiation).

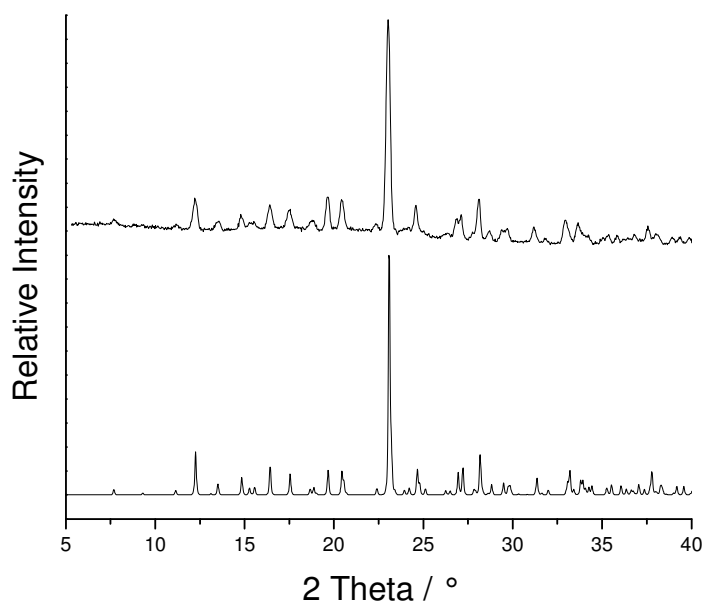


Figure S6: Experimental X-ray powder pattern of compound **6** (top) and X-ray powder pattern of compound **6** calculated from single crystal data (bottom) (CuK α radiation).

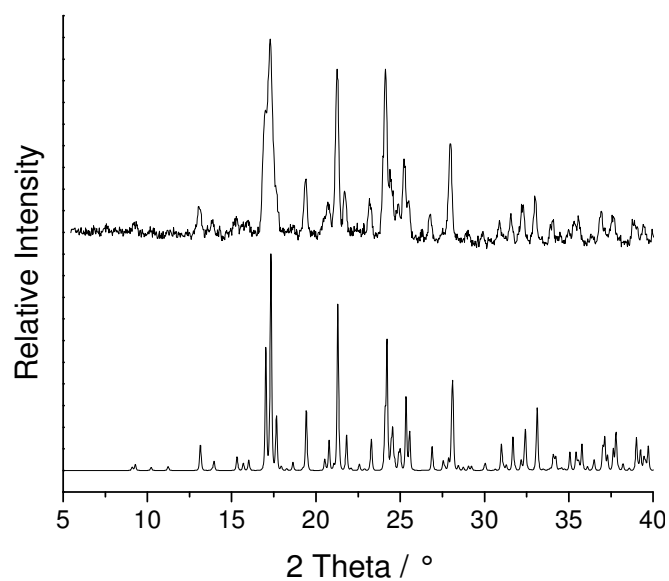


Figure S7: Experimental X-ray powder pattern of compound **7** (top) and X-ray powder pattern of compound **7** calculated from single crystal data (bottom) (CuK α radiation).

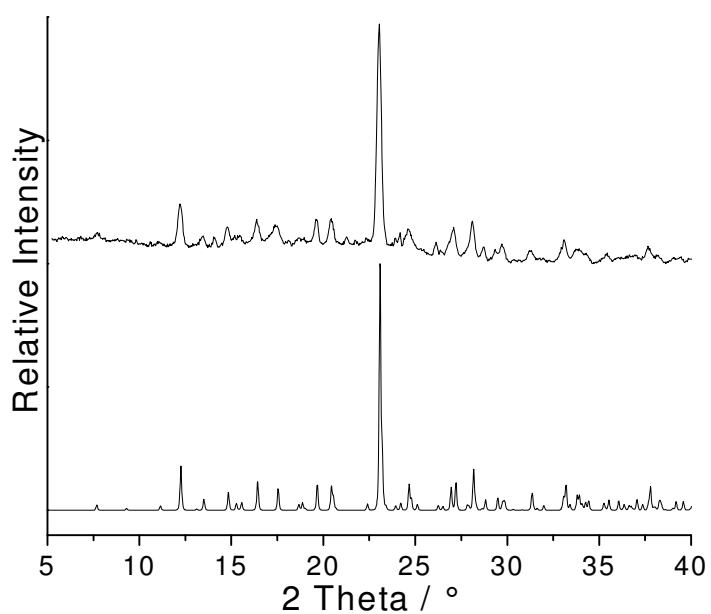


Figure S8: Experimental X-ray powder pattern of the residue obtained after the first TG step at 180°C obtained in the thermal decomposition reaction of compound **5** with 4°C/min (top) and calculated X-ray powder pattern for compound **6** (bottom) (CuK α radiation).

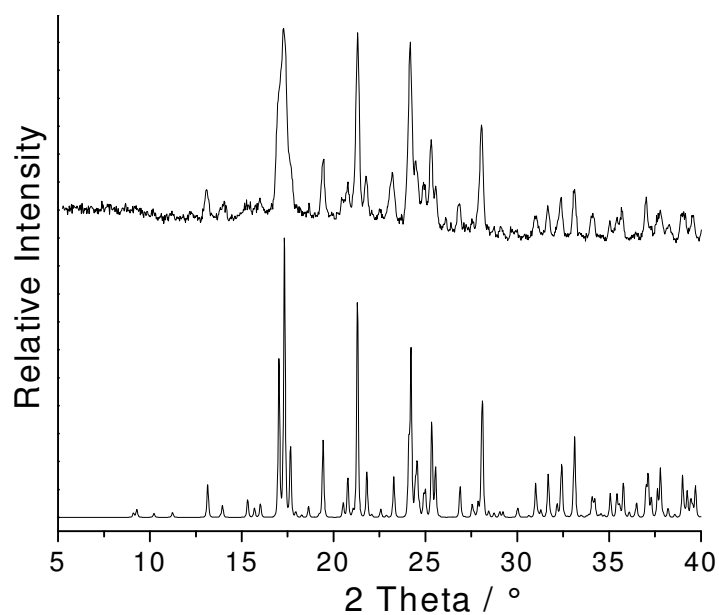


Figure S9: Experimental X-ray powder pattern of the residue obtained after the first TG step at 205°C obtained in the thermal decomposition reaction of compound **5** with 4°C/min (top) and calculated X-ray powder pattern for compound **7** (bottom) (CuK α radiation).

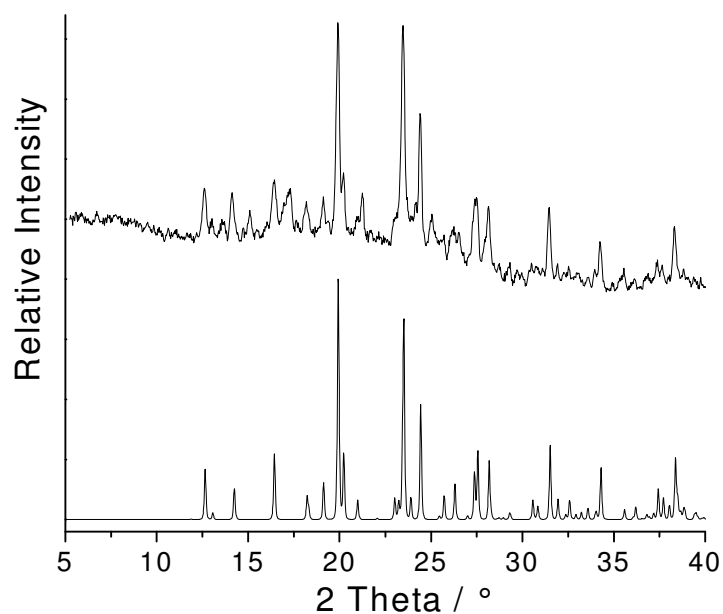


Figure S10: Experimental X-ray powder pattern of the residue obtained after the first TG step at 244°C obtained in the thermal decomposition reaction of compound **5** with 4°C/min (top) and calculated X-ray powder pattern for compound **3** (bottom) (CuK α radiation).

Table S2: Details on the structure determination of compound **1**.Table 1. Crystal data and structure refinement for **1**.

Identification code	blz29	
Empirical formula	C ₈ H ₈ I ₂ N ₄ Zn	
Formula weight	479.35	
Temperature	170(2) K	
Wavelength	0.71073 Å	
Crystal system	monoclinic	
Space group	P2 ₁ /n	
Unit cell dimensions	a = 8.0546(6) Å	α = 90°.
	b = 12.7334(8) Å	β = 92.208(10)°.
	c = 12.6152(12) Å	γ = 90°.
Volume	1292.89(18) Å ³	
Z	4	
Density (calculated)	2.463 Mg/m ³	
Absorption coefficient	6.650 mm ⁻¹	
F(000)	880	
Crystal size	0.07 x 0.1 x 0.14 mm ³	
Theta range for data collection	2.27 to 28.00°	
Index ranges	-10 ≤ h ≤ 10, -16 ≤ k ≤ 15, -14 ≤ l ≤ 16	
Reflections collected	6375	
Independent reflections	3085 [R(int) = 0.0353]	
Completeness to theta = 28.00°	98.6 %	
Refinement method	Full-matrix least-squares on F ²	
Data / restraints / parameters	3085 / 0 / 137	
Goodness-of-fit on F ²	0.969	
Final R indices [I > 2σ(I)]	R1 = 0.0321, wR2 = 0.0709	
R indices (all data)	R1 = 0.0522, wR2 = 0.0769	
Extinction coefficient	0.0035(3)	
Largest diff. peak and hole	0.839 and -1.163 e.Å ⁻³	

Remarks:

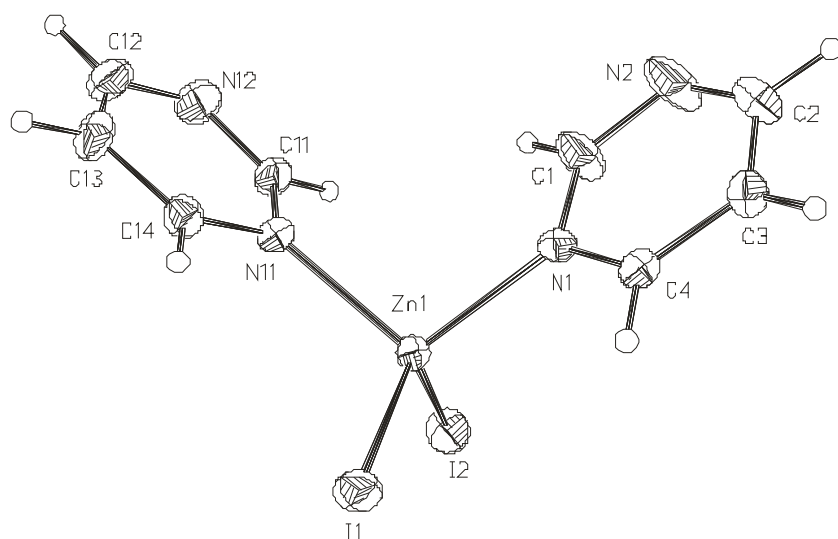
All non-hydrogen atoms were refined using anisotropic displacement parameters. The hydrogen atoms were positioned with idealized geometry and were refined isotropic ($U_{eq} = -1.2$) using a riding model with C-H = 0.95 Å for aromatic hydrogen atoms. The data were corrected using a numerical absorption correction (T_{min} : 0.3223, T_{max} : 0.4166).

2 Publications

Table 2. Atomic coordinates ($\times 10^4$) and equivalent isotropic displacement parameters ($\text{\AA}^2 \times 10^3$)

$U(\text{eq})$ is defined as one third of the trace of the orthogonalized U_{ij} tensor.

	x	y	z	U(eq)
Zn(1)	3137(1)	6146(1)	2391(1)	18(1)
I(1)	5408(1)	7534(1)	2505(1)	25(1)
I(2)	270(1)	6473(1)	1536(1)	30(1)
N(1)	2889(5)	5584(3)	3916(3)	18(1)
C(1)	2103(8)	4682(4)	4076(5)	33(1)
N(2)	1799(8)	4269(4)	5021(4)	41(1)
C(2)	2307(7)	4810(5)	5867(4)	30(1)
C(3)	3153(7)	5748(4)	5789(4)	26(1)
C(4)	3414(7)	6120(4)	4773(4)	23(1)
N(11)	4132(5)	4880(3)	1588(3)	20(1)
C(11)	3167(7)	4074(4)	1253(5)	27(1)
N(12)	3672(7)	3220(4)	769(4)	38(1)
C(12)	5295(9)	3163(5)	579(5)	37(1)
C(13)	6378(7)	3971(5)	857(4)	30(1)
C(14)	5765(7)	4822(4)	1376(4)	23(1)



2 Publications

Table 3. Bond lengths [Å] and angles [°]

Zn(1)-N(1)	2.070(4)	Zn(1)-N(11)	2.081(4)
Zn(1)-I(1)	2.5429(7)	Zn(1)-I(2)	2.5455(7)
N(1)-C(1)	1.330(6)	N(11)-C(11)	1.345(7)
N(1)-C(4)	1.333(7)	N(11)-C(14)	1.355(7)
C(1)-N(2)	1.334(7)	C(11)-N(12)	1.319(7)
N(2)-C(2)	1.322(8)	N(12)-C(12)	1.340(8)
C(2)-C(3)	1.380(8)	C(12)-C(13)	1.385(10)
C(3)-C(4)	1.390(7)	C(13)-C(14)	1.368(7)
N(1)-Zn(1)-I(1)	106.42(12)	N(11)-Zn(1)-I(1)	106.04(12)
N(1)-Zn(1)-I(2)	109.39(12)	N(11)-Zn(1)-I(2)	106.29(13)
I(1)-Zn(1)-I(2)	123.32(2)	N(1)-Zn(1)-N(11)	103.72(16)
C(1)-N(1)-C(4)	117.2(4)	C(11)-N(11)-C(14)	116.7(4)
C(1)-N(1)-Zn(1)	120.2(4)	C(11)-N(11)-Zn(1)	121.0(3)
C(4)-N(1)-Zn(1)	122.5(3)	C(14)-N(11)-Zn(1)	122.2(3)
N(1)-C(1)-N(2)	125.4(6)	N(12)-C(11)-N(11)	126.2(5)
C(2)-N(2)-C(1)	117.1(5)	C(11)-N(12)-C(12)	116.6(5)
N(2)-C(2)-C(3)	122.1(5)	N(12)-C(12)-C(13)	121.5(5)
C(2)-C(3)-C(4)	117.0(5)	C(14)-C(13)-C(12)	118.3(5)
N(1)-C(4)-C(3)	121.2(5)	N(11)-C(14)-C(13)	120.6(5)

Table 4. Anisotropic displacement parameters ($\text{\AA}^2 \times 10^3$). The anisotropic displacement factor exponent takes the form: $-\frac{1}{2} 2\pi^2 [h^2 a^{*2} U_{11} + \dots + 2 h k a^* b^* U_{12}]$

	U_{11}	U_{22}	U_{33}	U_{23}	U_{13}	U_{12}
Zn(1)	18(1)	17(1)	19(1)	1(1)	4(1)	0(1)
I(1)	22(1)	19(1)	33(1)	1(1)	5(1)	-3(1)
I(2)	19(1)	38(1)	34(1)	6(1)	1(1)	6(1)
N(1)	22(2)	14(2)	20(2)	0(2)	2(2)	-1(2)
C(1)	45(4)	30(3)	24(3)	4(2)	3(2)	-17(3)
N(2)	55(4)	37(3)	30(3)	12(2)	-1(2)	-24(2)
C(2)	34(3)	33(3)	24(3)	10(2)	1(2)	-3(2)
C(3)	32(3)	28(3)	19(3)	-1(2)	3(2)	3(2)
C(4)	27(3)	18(2)	24(3)	-1(2)	6(2)	3(2)
N(11)	23(2)	17(2)	22(2)	0(2)	3(2)	3(2)
C(11)	33(3)	17(2)	32(3)	-3(2)	12(2)	-2(2)
N(12)	54(3)	21(2)	40(3)	-7(2)	12(3)	0(2)
C(12)	52(4)	31(3)	27(3)	-1(2)	6(3)	19(3)
C(13)	27(3)	43(3)	19(3)	1(2)	0(2)	18(2)
C(14)	26(3)	27(3)	17(2)	1(2)	1(2)	4(2)

Table 5. Hydrogen coordinates ($\times 10^4$) and isotropic displacement parameters ($\text{\AA}^2 \times 10^3$)

	x	y	z	U(eq)
H(1)	1725	4301	3466	39
H(2)	2082	4545	6551	36
H(3)	3539	6122	6401	31
H(4)	3977	6768	4687	28
H(11)	2014	4125	1377	33
H(12)	5713	2553	245	44
H(13)	7517	3935	691	36
H(14)	6492	5377	1590	28

2 Publications

Table S3: Details on the structure determination of compound **2**.

Table 1. Crystal data and structure refinement for **2**.

Identification code	gb316	
Empirical formula	C ₁₂ H ₁₂ I ₄ N ₆ Zn ₂	
Formula weight	878.62	
Temperature	293(2) K	
Wavelength	0.71073 Å	
Crystal system	monoclinic	
Space group	C2/c	
Unit cell dimensions	a = 23.5621(13) Å	α = 90°.
	b = 8.0398(5) Å	β = 98.010(6)°.
	c = 11.7637(6) Å	γ = 90°.
Volume	2206.7(2) Å ³	
Z	4	
Density (calculated)	2.645 Mg/m ³	
Absorption coefficient	7.777 mm ⁻¹	
F(000)	1592	
Crystal size	0.06 x 0.1 x 0.14 mm ³	
Theta range for data collection	2.68 to 28.03°.	
Index ranges	-31 ≤ h ≤ 30, -10 ≤ k ≤ 10, -14 ≤ l ≤ 15	
Reflections collected	11059	
Independent reflections	2572 [R(int) = 0.0834]	
Completeness to theta = 28.03°	95.9 %	
Refinement method	Full-matrix least-squares on F ²	
Data / restraints / parameters	2572 / 0 / 111	
Goodness-of-fit on F ²	1.041	
Final R indices [I > 2σ(I)]	R1 = 0.0319, wR2 = 0.0810	
R indices (all data)	R1 = 0.0382, wR2 = 0.0839	
Extinction coefficient	0.00245(12)	
Largest diff. peak and hole	1.214 and -0.973 e.Å ⁻³	

Remarks:

All non-hydrogen atoms were refined using anisotropic displacement parameters. The hydrogen atoms were positioned with idealized geometry and were refined isotropic ($U_{eq} = 1.2$) using a riding model with C-H = 0.93 Å for aromatic hydrogen atoms. The data were corrected using a numerical absorption correction (T_{min} : 0.2680, T_{max} : 0.3858).

Table 2. Atomic coordinates ($\times 10^4$) and equivalent isotropic displacement parameters (Å² × 10³)

2 Publications

$U(\text{eq})$ is defined as one third of the trace of the orthogonalized U_{ij} tensor.

	x	y	z	$U(\text{eq})$
Zn(1)	996(1)	4055(1)	6103(1)	24(1)
I(1)	1168(1)	2041(1)	4507(1)	40(1)
I(2)	689(1)	7016(1)	5644(1)	30(1)
N(1)	412(1)	2872(4)	7027(3)	21(1)
C(1)	0	3653(7)	7500	21(1)
C(3)	0	321(8)	7500	33(1)
C(4)	414(2)	1202(5)	7052(4)	27(1)
N(11)	1743(2)	3972(5)	7260(3)	28(1)
C(11)	2257(2)	3885(10)	6907(5)	49(2)
N(12)	2758(2)	3829(11)	7682(5)	73(2)
C(13)	2191(2)	4024(9)	9170(4)	43(1)
C(14)	1736(2)	4041(8)	8375(4)	39(1)
C(12)	2693(2)	3904(8)	8816(5)	45(1)

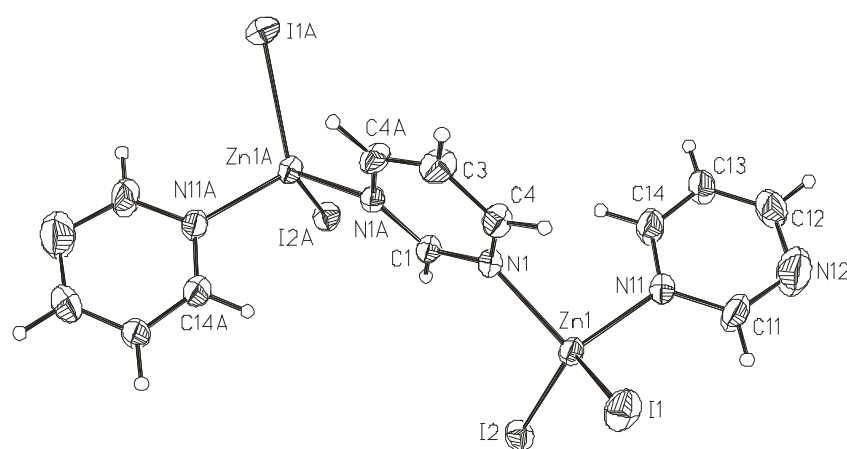


Table 3. Bond lengths [Å] and angles [°]

Zn(1)-N(11)	2.072(4)	Zn(1)-I(2)	2.5241(6)
Zn(1)-N(1)	2.098(3)	Zn(1)-I(1)	2.5539(6)
N(11)-Zn(1)-N(1)	101.76(14)	N(11)-Zn(1)-I(1)	104.77(11)
N(11)-Zn(1)-I(2)	111.29(12)	N(1)-Zn(1)-I(1)	106.03(10)
N(1)-Zn(1)-I(2)	110.43(9)	I(2)-Zn(1)-I(1)	120.75(2)
N(1)-C(1)	1.340(4)	C(3)-C(4A)	1.369(5)
N(1)-C(4)	1.343(6)	C(3)-C(4)	1.369(5)
C(1)-N(1A)	1.340(4)	N(1)-C(1)-N(1A)	124.1(5)
C(1)-N(1)-C(4)	117.4(4)	C(4A)-C(3)-C(4)	117.6(6)
C(1)-N(1)-Zn(1)	124.6(3)	N(1)-C(4)-C(3)	121.7(4)
C(4)-N(1)-Zn(1)	117.6(3)	N(12)-C(12)	1.365(8)
N(11)-C(14)	1.315(6)	C(13)-C(12)	1.312(7)
N(11)-C(11)	1.335(6)	C(13)-C(14)	1.320(6)
C(11)-N(12)	1.387(8)	C(12)-N(12)-C(11)	116.1(5)
C(14)-N(11)-C(11)	116.8(4)	C(12)-C(13)-C(14)	117.0(5)
C(14)-N(11)-Zn(1)	121.7(3)	N(11)-C(14)-C(13)	125.8(4)
C(11)-N(11)-Zn(1)	121.5(3)	C(13)-C(12)-N(12)	122.9(5)
N(11)-C(11)-N(12)	121.5(5)		

Symmetry transformations used to generate equivalent atoms: A: $-x, y, -z+3/2$

Symmetry transformations used to generate equivalent atoms: A: $x, -y+1/2, z-1/2$ B: $x, -y+1/2, z+1/2$

Table 4. Anisotropic displacement parameters ($\text{\AA}^2 \times 10^3$). The anisotropic displacement factor exponent takes the form: $-2\pi^2 [h^2 a^{*2} U_{11} + \dots + 2 h k a^* b^* U_{12}]$

	U_{11}	U_{22}	U_{33}	U_{23}	U_{13}	U_{12}
Zn(1)	20(1)	26(1)	26(1)	0(1)	7(1)	1(1)
I(1)	41(1)	45(1)	36(1)	-14(1)	14(1)	2(1)
I(2)	29(1)	25(1)	36(1)	0(1)	4(1)	3(1)
N(1)	19(2)	22(2)	23(2)	-1(1)	4(1)	-1(1)
C(1)	20(2)	16(3)	28(3)	0	6(2)	0
C(3)	40(3)	19(3)	41(4)	0	13(3)	0
C(4)	28(2)	19(2)	37(2)	-3(2)	11(2)	4(2)
N(11)	22(2)	32(2)	31(2)	0(2)	5(1)	2(1)
C(11)	25(2)	92(5)	32(3)	1(3)	12(2)	-2(3)
N(12)	36(3)	124(6)	61(4)	-3(4)	9(2)	-1(3)
C(13)	26(2)	86(4)	16(2)	-5(2)	-2(2)	10(2)
C(14)	26(2)	63(4)	29(3)	-7(2)	6(2)	3(2)
C(12)	30(2)	64(4)	37(3)	-3(3)	-7(2)	4(2)

Table 5. Hydrogen coordinates ($\times 10^4$) and isotropic displacement parameters ($\text{\AA}^2 \times 10^3$)

	x	y	z	U(eq)
H(1)	0	4810	7500	26
H(3)	0	-836	7500	39
H(4)	704	630	6757	33
H(11)	2280	3861	6125	59
H(13)	2156	4094	9947	52
H(14)	1380	4108	8625	47
H(12)	3019	3869	9361	54

Table S4: Details on the structure determination of compound **3**.

Table 1. Crystal data and structure refinement.

Identification code	gb253	
Empirical formula	C ₄ H ₄ I ₂ N ₂ Zn	
Formula weight	399.26	
Temperature	293(2) K	
Wavelength	0.71073 Å	
Crystal system	monoclinic	
Space group	P2 ₁ /c	
Unit cell dimensions	a = 7.5576(5) Å	α = 90°.
	b = 13.5380(8) Å	β = 112.310(8)°.
	c = 9.6246(8) Å	γ = 90°.
Volume	911.02(11) Å ³	
Z	4	
Density (calculated)	2.911 Mg/m ³	
Absorption coefficient	9.399 mm ⁻¹	
F(000)	712	
Crystal size	0.05 x 0.09 x 0.13 mm ³	
Theta range for data collection	2.74 to 28.07°.	
Index ranges	-9 ≤ h ≤ 9, -17 ≤ k ≤ 17, -12 ≤ l ≤ 12	
Reflections collected	8716	
Independent reflections	2130 [R(int) = 0.0707]	
Completeness to theta = 28.07°	96.7 %	
Refinement method	Full-matrix least-squares on F ²	
Data / restraints / parameters	2130 / 0 / 84	
Goodness-of-fit on F ²	1.065	
Final R indices [I > 2σ(I)]	R1 = 0.0318, wR2 = 0.0774	
R indices (all data)	R1 = 0.0410, wR2 = 0.0808	
Extinction coefficient	0.0345(11)	
Largest diff. peak and hole	1.232 and -1.345 e.Å ⁻³	

Remarks:

All non-hydrogen atoms were refined using anisotropic displacement parameters. The hydrogen atoms were positioned with idealized geometry and were refined isotropic ($U_{eq} = -1.2$) using a riding model with C-H = 0.95 Å for aromatic hydrogen atoms. The data were corrected using a numerical absorption correction (T_{min} : 0.2129, T_{max} : 0.3424).

2 Publications

Table 2. Atomic coordinates ($\times 10^4$) and equivalent isotropic displacement parameters ($\text{\AA}^2 \times 10^3$)
 $U(\text{eq})$ is defined as one third of the trace of the orthogonalized U_{ij} tensor.

	x	y	z	$U(\text{eq})$
Zn(1)	5105(1)	3803(1)	2830(1)	27(1)
I(1)	6596(1)	5415(1)	2524(1)	44(1)
I(2)	1540(1)	3526(1)	1940(1)	44(1)
N(1)	6286(6)	3438(2)	5133(4)	27(1)
C(1)	5581(7)	2692(3)	5678(5)	28(1)
N(2)	6339(5)	2377(2)	7096(4)	26(1)
C(2)	7875(7)	2847(3)	8017(5)	32(1)
C(3)	8644(7)	3649(4)	7575(5)	37(1)
C(4)	7803(7)	3920(3)	6089(5)	31(1)

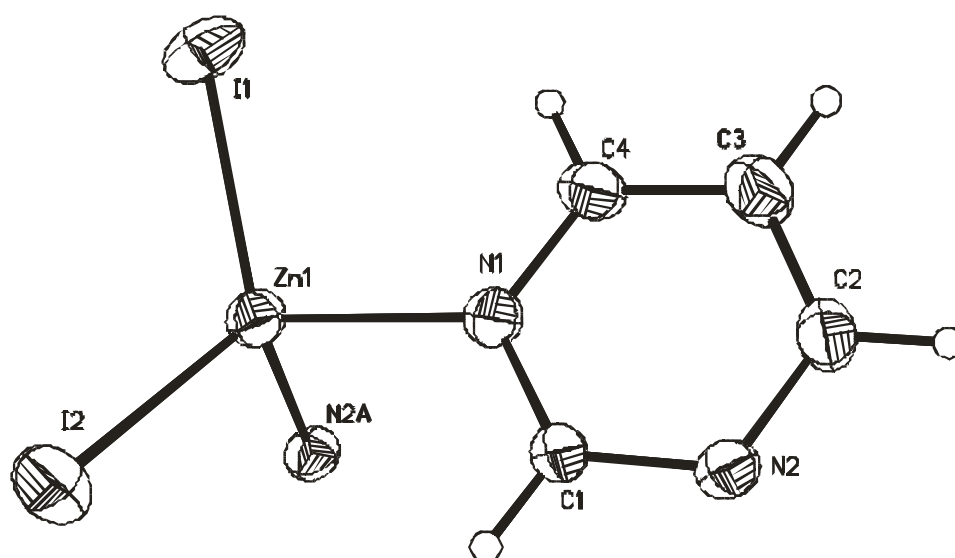


Table 3. Bond lengths [\AA] and angles [$^\circ$]

Zn(1)-N(2A)	2.102(3)	N(2A)-Zn(1)-N(1)	96.37(14)
Zn(1)-N(1)	2.109(3)	N(2A)-Zn(1)-I(1)	110.07(10)
Zn(1)-I(1)	2.5245(6)	N(1)-Zn(1)-I(1)	107.18(10)
Zn(1)-I(2)	2.5263(7)	N(2A)-Zn(1)-I(2)	108.97(10)
N(2)-Zn(1B)	2.102(3)	N(1)-Zn(1)-I(2)	107.03(11)
C(4)-N(1)-Zn(1)	121.3(3)	I(1)-Zn(1)-I(2)	123.69(2)
C(1)-N(2)-Zn(1B)	120.9(3)	C(2)-N(2)-Zn(1B)	121.8(3)

Symmetry transformations used to generate equivalent atoms: A: $x, -y+1/2, z-1/2$ B: $x, -y+1/2, z+1/2$

2 Publications

Table 4. Anisotropic displacement parameters ($\text{\AA}^2 \times 10^3$). The anisotropic displacement factor exponent takes the form: $-2\pi^2 [h^2 a^{*2} U_{11} + \dots + 2 h k a^* b^* U_{12}]$

	U_{11}	U_{22}	U_{33}	U_{23}	U_{13}	U_{12}
Zn(1)	33(1)	23(1)	24(1)	0(1)	11(1)	0(1)
I(1)	49(1)	29(1)	60(1)	10(1)	29(1)	-2(1)
I(2)	33(1)	43(1)	47(1)	-4(1)	6(1)	-5(1)
N(1)	33(2)	26(2)	21(2)	1(1)	10(2)	-4(1)
C(1)	35(2)	25(2)	19(2)	1(2)	5(2)	-6(2)
N(2)	32(2)	22(2)	25(2)	1(1)	11(2)	-3(1)
C(2)	31(3)	38(2)	23(2)	3(2)	6(2)	-5(2)
C(3)	33(3)	42(3)	32(3)	-1(2)	7(2)	-10(2)
C(4)	37(3)	28(2)	28(2)	-3(2)	11(2)	-9(2)

Table 5. Hydrogen coordinates ($\times 10^4$) and isotropic displacement parameters ($\text{\AA}^2 \times 10^3$)

	x	y	z	U(eq)
H(1)	4492	2373	5027	33
H(2)	8454	2625	9001	38
H(3)	9683	3993	8247	44
H(4)	8302	4450	5742	38

2 Publications

Table S5: Details on the structure determination of compound **5**.

Table 1. Crystal data and structure refinement.

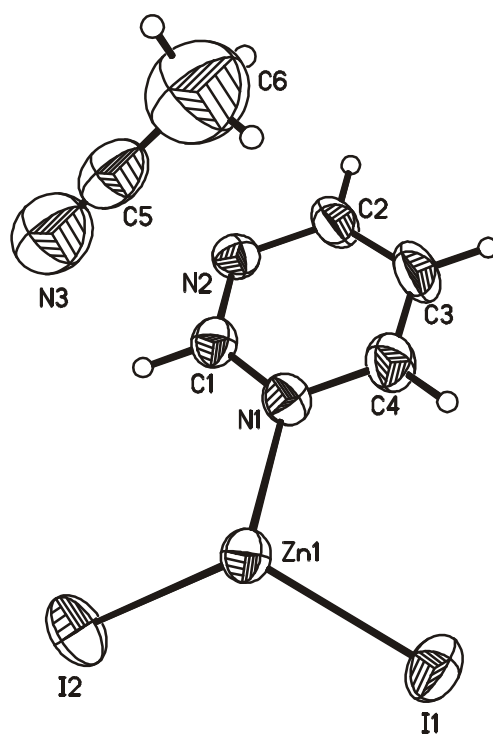
Identification code	gb107	
Empirical formula	$C_{4.50}H_{4.75}I_2N_{2.25}Zn$	
Formula weight	409.53	
Temperature	293(2) K	
Wavelength	0.71073 Å	
Crystal system	tetragonal	
Space group	P4/n	
Unit cell dimensions	a = 17.0267(8) Å	$\alpha = 90^\circ$.
	b = 17.0267(8) Å	$\beta = 90^\circ$.
	c = 7.5579(4) Å	$\gamma = 90^\circ$.
Volume	2191.10(19) Å ³	
Z	8	
Density (calculated)	2.483 Mg/m ³	
Absorption coefficient	7.820 mm ⁻¹	
F(000)	1468	
Crystal size	0.06 x 0.1 x 0.14 mm ³	
Theta range for data collection	2.95 to 28.01°.	
Index ranges	-20 ≤ h ≤ 22, -22 ≤ k ≤ 22, -5 ≤ l ≤ 9	
Reflections collected	11244	
Independent reflections	2584 [R(int) = 0.0380]	
Completeness to theta = 28.01°	97.4 %	
Refinement method	Full-matrix least-squares on F ²	
Data / restraints / parameters	2584 / 0 / 92	
Goodness-of-fit on F ²	1.060	
Final R indices [I > 2σ(I)]	R1 = 0.0383, wR2 = 0.0956	
R indices (all data)	R1 = 0.0520, wR2 = 0.1024	
Extinction coefficient	0.0032(4)	
Largest diff. peak and hole	1.396 and -1.064 e.Å ⁻³	

Remarks:

All non-hydrogen atoms were refined using anisotropic displacement parameters. The hydrogen atoms were positioned with idealized geometry and were refined isotropic ($U_{eq} = 1.2 \cdot U_{eq}(C_{aromatic}) = 1.5 \cdot U_{eq}(C_{methyl})$) using a riding model with C-H = 0.98 Å for methyl and 0.95 Å for aromatic hydrogen atoms. The data were corrected using a numerical absorption correction ($T_{min}: 0.2304, T_{max}: 0.3772$).

Table 2. Atomic coordinates ($\times 10^4$) and equivalent isotropic displacement parameters ($\text{\AA}^2 \times 10^3$).U(eq) is defined as one third of the trace of the orthogonalized U_{ij} tensor.

	x	y	z	U(eq)
Zn(1)	4778(1)	1507(1)	4743(1)	38(1)
I(1)	6068(1)	947(1)	3663(1)	56(1)
I(2)	4452(1)	1654(1)	7981(1)	61(1)
N(1)	3889(3)	849(3)	3498(6)	36(1)
C(1)	3173(3)	783(3)	4171(7)	36(1)
N(2)	2608(2)	346(2)	3506(6)	35(1)
C(2)	2770(3)	-65(4)	2055(8)	45(1)
C(3)	3499(4)	-32(5)	1272(9)	57(2)
C(4)	4048(4)	440(4)	2045(8)	47(1)
N(3)	2500	2500	3390(30)	86(5)
C(5)	2500	2500	1950(30)	59(4)
C(6)	2500	2500	80(50)	129(10)



2 Publications

Table 3. Bond lengths [Å] and angles [°].

Zn(1)-N(1)	2.104(4)	N(2)A-Zn(1)-I(2)	108.70(13)
Zn(1)-N(2)A	2.105(4)	N(1)-Zn(1)-I(1)	106.20(12)
Zn(1)-I(2)	2.5217(8)	N(2)A-Zn(1)-I(1)	106.20(12)
Zn(1)-I(1)	2.5307(7)	I(2)-Zn(1)-I(1)	122.79(3)
N(1)-C(1)	1.326(7)	C(1)-N(1)-C(4)	117.4(5)
N(1)-C(4)	1.328(7)	C(1)-N(1)-Zn(1)	122.3(4)
C(1)-N(2)	1.317(7)	C(4)-N(1)-Zn(1)	120.1(4)
N(2)-C(2)	1.330(7)	N(2)-C(1)-N(1)	125.0(5)
N(2)-Zn(1)B	2.105(4)	C(1)-N(2)-C(2)	117.4(5)
C(2)-C(3)	1.376(8)	C(1)-N(2)-Zn(1)B	122.5(4)
C(3)-C(4)	1.365(9)	C(2)-N(2)-Zn(1)B	119.9(4)
N(3)-C(5)	1.08(2)	N(2)-C(2)-C(3)	121.4(5)
C(5)-C(6)	1.42(4)	C(4)-C(3)-C(2)	117.3(6)
N(1)-Zn(1)-N(2)A	101.76(17)	N(1)-C(4)-C(3)	121.5(5)
N(1)-Zn(1)-I(2)	109.19(12)	N(3)-C(5)-C(6)	180.000(10)

Symmetry transformations used to generate equivalent atoms: A: $-y+1/2, x, z$ B: $y, -x+1/2, z$

Table 4. Anisotropic displacement parameters ($\text{Å}^2 \times 10^3$). The anisotropic displacement factor exponent takes the form: $-2\pi^2 [h^2 a^{*2} U_{11} + \dots + 2 h k a^* b^* U_{12}]$

	U_{11}	U_{22}	U_{33}	U_{23}	U_{13}	U_{12}
Zn(1)	39(1)	37(1)	37(1)	1(1)	3(1)	1(1)
I(1)	48(1)	63(1)	56(1)	8(1)	7(1)	19(1)
I(2)	88(1)	62(1)	34(1)	-1(1)	6(1)	-7(1)
N(1)	40(2)	37(2)	32(2)	2(2)	4(2)	-4(2)
C(1)	38(2)	33(2)	37(3)	0(2)	2(2)	3(2)
N(2)	35(2)	36(2)	33(2)	4(2)	-1(2)	0(2)
C(2)	47(3)	58(3)	30(3)	-9(2)	2(2)	-5(2)
C(3)	56(4)	84(5)	32(3)	-19(3)	12(3)	-12(3)
C(4)	46(3)	56(3)	37(3)	-3(3)	10(2)	-3(2)
N(3)	77(7)	77(7)	105(15)	0	0	0
C(5)	45(4)	45(4)	88(13)	0	0	0
C(6)	120(13)	120(13)	150(30)	0	0	0

Table 5. Hydrogen coordinates ($\times 10^4$) and isotropic displacement parameters ($\text{Å}^2 \times 10^3$).

	x	y	z	U(eq)
H(1)	3061	1068	5191	43
H(2)	2383	-382	1560	54
H(3)	3612	-320	257	69
H(4)	4546	476	1544	56
H(6A)	3026	2577	-343	194
H(6B)	2170	2917	-343	194
H(6C)	2304	2006	-343	194

2 Publications

Table S6: Details on the structure determination of compound **6**.

Table 1. Crystal data and structure refinement.

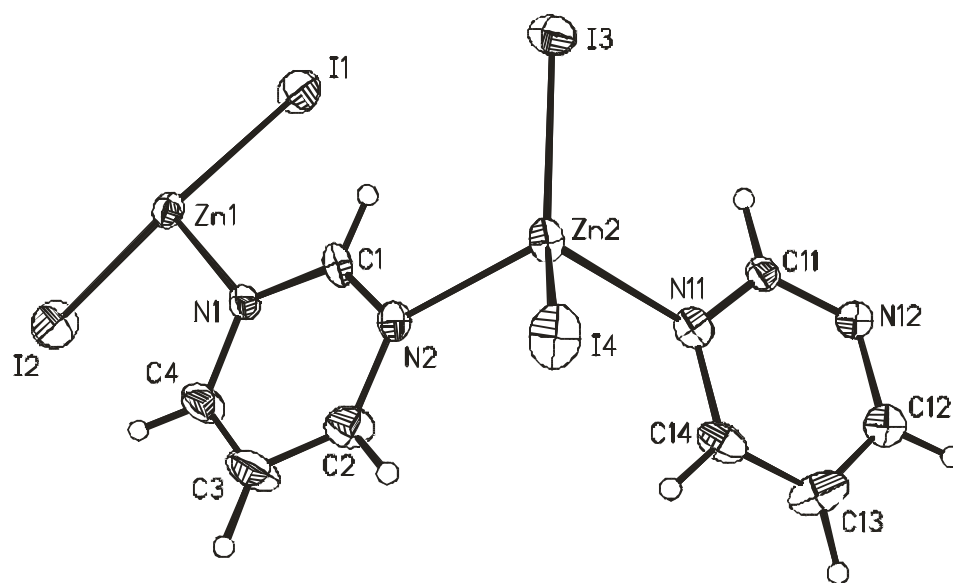
Identification code	gb361	
Empirical formula	C ₈ H ₈ I ₄ N ₄ Zn ₂	
Formula weight	798.52	
Temperature	220(2) K	
Wavelength	0.71073 Å	
Crystal system	orthorhombic	
Space group	P2 ₁ /c	
Unit cell dimensions	a = 6.5462(3) Å	α = 90°.
	b = 14.4316(10) Å	β = 90.021(6)°.
	c = 19.0146(10) Å	γ = 90°.
Volume	1796.35(18) Å ³	
Z	1	
Density (calculated)	2.953 Mg/m ³	
Absorption coefficient	9.534 mm ⁻¹	
F(000)	1424	
Crystal size	0.05 x 0.11 x 0.18 mm ³	
Theta range for data collection	2.57 to 28.03°.	
Index ranges	-8 ≤ h ≤ 8, -19 ≤ k ≤ 19, -25 ≤ l ≤ 25	
Reflections collected	17487	
Independent reflections	4326 [R(int) = 0.0721]	
Completeness to theta = 28.03°	99.6 %	
Refinement method	Full-matrix least-squares on F ²	
Data / restraints / parameters	4326 / 0 / 155	
Goodness-of-fit on F ²	1.015	
Final R indices [I > 2σ(I)]	R1 = 0.0334, wR2 = 0.0744	
R indices (all data)	R1 = 0.0393, wR2 = 0.0767	
Extinction coefficient	0.00223(15)	
Largest diff. peak and hole	1.701 and -1.215 e.Å ⁻³	
Remarks:		

All non-hydrogen atoms were refined using anisotropic displacement parameters. The hydrogen atoms were positioned with idealized geometry and were refined isotropic ($U_{eq} = -1.2$) using a riding model with C-H = 0.94 Å for aromatic hydrogen atoms. This compound is merohedral twinned and therefore a twin refinement was performed. The data were corrected using a numerical absorption correction ($T_{min}: 0.1053, T_{max}: 0.4472$).

Table 2. Atomic coordinates ($\times 10^4$) and equivalent isotropic displacement parameters ($\text{\AA}^2 \times 10^3$)

$U(\text{eq})$ is defined as one third of the trace of the orthogonalized U^{ij} tensor.

	x	y	z	$U(\text{eq})$
Zn(1)	11584(1)	2679(1)	9174(1)	19(1)
Zn(2)	6104(1)	2714(1)	6695(1)	19(1)
I(1)	13561(1)	1499(1)	8455(1)	36(1)
I(2)	13451(1)	3772(1)	9967(1)	40(1)
I(3)	7475(1)	1081(1)	6770(1)	27(1)
I(4)	2518(1)	3421(1)	6606(1)	30(1)
N(1)	9532(7)	3407(3)	8544(3)	17(1)
N(2)	7376(8)	3442(3)	7557(3)	17(1)
C(1)	8764(9)	3033(4)	7961(3)	20(1)
C(2)	6726(10)	4287(5)	7753(4)	26(1)
C(3)	7512(11)	4717(5)	8326(4)	35(2)
C(4)	8893(10)	4253(5)	8720(4)	27(1)
N(11)	7431(8)	3283(3)	5773(3)	18(1)
N(12)	9368(7)	3103(4)	4744(3)	20(1)
C(11)	8650(9)	2801(4)	5356(3)	18(1)
C(12)	8802(9)	3937(4)	4523(4)	24(1)
C(13)	7591(10)	4495(5)	4938(4)	31(2)
C(14)	6949(8)	4149(5)	5556(4)	24(1)



2 Publications

Table 3. Bond lengths [Å] and angles [°].

Zn(1)-N(1)	2.083(5)	N(1)-Zn(1)-N(12A)	96.8(2)
Zn(1)-N(12A)	2.134(5)	N(1)-Zn(1)-I(2)	110.06(14)
Zn(1)-I(2)	2.5005(10)	N(12A)-Zn(1)-I(2)	111.13(15)
Zn(1)-I(1)	2.5364(10)	N(1)-Zn(1)-I(1)	111.04(15)
Zn(2)-N(2)	2.116(5)	N(12A)-Zn(1)-I(1)	105.39(15)
Zn(2)-N(11)	2.120(5)	I(2)-Zn(1)-I(1)	119.85(3)
Zn(2)-I(3)	2.5253(9)	N(2)-Zn(2)-N(11)	106.57(19)
Zn(2)-I(4)	2.5660(9)	N(2)-Zn(2)-I(3)	106.25(14)
N(12)-Zn(1B)	2.134(5)	N(11)-Zn(2)-I(3)	105.20(14)
C(1)-N(1)-Zn(1)	121.1(4)	N(2)-Zn(2)-I(4)	102.32(14)
C(4)-N(1)-Zn(1)	121.3(4)	N(11)-Zn(2)-I(4)	99.60(14)
C(1)-N(2)-Zn(2)	119.7(4)	I(3)-Zn(2)-I(4)	134.44(3)
C(2)-N(2)-Zn(2)	122.7(4)	C(11)-N(11)-Zn(2)	122.6(4)
C(14)-N(11)-Zn(2)	120.9(4)	C(12)-N(12)-Zn(1B)	120.6(4)
C(11)-N(12)-Zn(1B)	120.7(4)		

Symmetry transformations used to generate equivalent atoms: A: $x, -y+1/2, z+1/2$; B: $x, -y+1/2, z-1/2$

Table 4. Anisotropic displacement parameters ($\text{Å}^2 \times 10^3$). The anisotropic displacement factor exponent takes the form: $-2\pi^2 [h^2 a^{*2} U_{11} + \dots + 2 h k a^* b^* U_{12}]$

	U_{11}	U_{22}	U_{33}	U_{23}	U_{13}	U_{12}
Zn(1)	21(1)	22(1)	15(1)	2(1)	-1(1)	-1(1)
Zn(2)	17(1)	25(1)	16(1)	-3(1)	0(1)	2(1)
I(1)	41(1)	32(1)	35(1)	4(1)	16(1)	13(1)
I(2)	48(1)	39(1)	33(1)	-1(1)	-15(1)	-18(1)
I(3)	29(1)	21(1)	32(1)	-2(1)	2(1)	0(1)
I(4)	14(1)	46(1)	29(1)	1(1)	0(1)	1(1)
N(1)	21(2)	17(2)	14(2)	-2(2)	-3(2)	1(2)
N(2)	15(2)	22(2)	15(2)	-1(2)	-2(2)	0(2)
C(1)	20(2)	26(3)	14(3)	-6(3)	1(2)	-1(2)
C(2)	21(3)	23(3)	32(4)	0(3)	-6(3)	6(2)
C(3)	44(3)	23(3)	38(4)	-12(3)	-13(4)	14(3)
C(4)	32(3)	21(3)	27(4)	-8(3)	-9(3)	0(3)
N(11)	12(2)	22(2)	21(3)	-3(2)	1(2)	1(2)
C(11)	21(3)	16(3)	17(3)	-3(2)	-4(2)	1(2)
C(13)	18(2)	28(3)	45(4)	14(3)	11(3)	7(3)
C(14)	17(3)	22(3)	34(4)	-7(3)	4(2)	7(2)

Table 5. Hydrogen coordinates ($\times 10^4$) and isotropic displacement parameters ($\text{Å}^2 \times 10^3$)

	x	y	z	U(eq)
H(1)	9232	2442	7828	24
H(2)	5706	4585	7488	31
H(3)	7109	5322	8445	42
H(4)	9415	4534	9129	32
H(11)	9035	2203	5502	22
H(12)	9232	4148	4080	29
H(13)	7228	5096	4794	37
H(14)	6136	4522	5849	29

2 Publications

Table S7: Details on the structure determination of compound **7**.

Table 1. Crystal data and structure refinement.

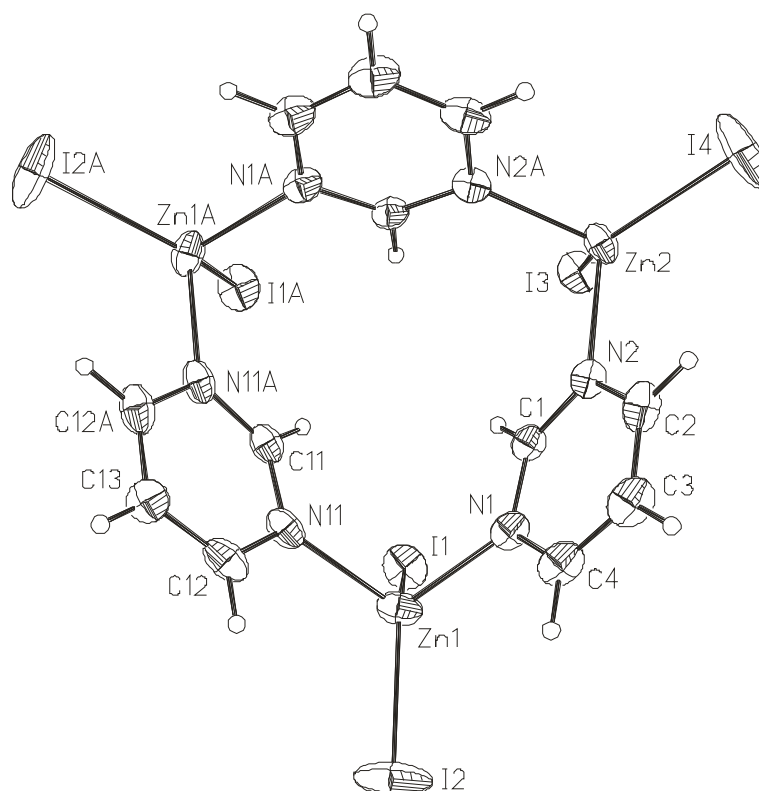
Identification code	gb328	
Empirical formula	$C_{12}H_{12}I_6N_6Zn_3$	
Formula weight	399.26	
Temperature	220(2) K	
Wavelength	0.71073 Å	
Crystal system	orthorhombic	
Space group	Pnma	
Unit cell dimensions	$a = 13.4555(7)$ Å	$\alpha = 90^\circ$.
	$b = 19.0259(13)$ Å	$\beta = 90^\circ$.
	$c = 11.285(7)$ Å	$\gamma = 90^\circ$.
Volume	$2889.0(18)$ Å ³	
Z	12	
Density (calculated)	2.754 Mg/m ³	
Absorption coefficient	8.892 mm ⁻¹	
F(000)	2136	
Crystal size	$0.05 \times 0.1 \times 0.19$ mm ³	
Theta range for data collection	2.36 to 28.03° .	
Index ranges	$-17 \leq h \leq 17$, $-25 \leq k \leq 24$, $-14 \leq l \leq 14$	
Reflections collected	26815	
Independent reflections	3576 [R(int) = 0.0738]	
Completeness to theta = 28.03°	99.4 %	
Refinement method	Full-matrix least-squares on F ²	
Data / restraints / parameters	3576 / 0 / 128	
Goodness-of-fit on F ²	1.028	
Final R indices [I > 2σ(I)]	R1 = 0.0317, wR2 = 0.0759	
R indices (all data)	R1 = 0.0388, wR2 = 0.0790	
Extinction coefficient	0.00113(9)	
Largest diff. peak and hole	1.287 and -1.718 e.Å ⁻³	

Remarks:

All non-hydrogen atoms were refined using anisotropic displacement parameters. The hydrogen atoms were positioned with idealized geometry and were refined isotropic ($U_{eq} = -1.2$) using a riding model with C-H = 0.94 Å for aromatic hydrogen atoms. The data were corrected using a numerical absorption correction (T_{min} : 0.1037, T_{max} : 0.4289).

Table 2. Atomic coordinates ($\times 10^4$) and equivalent isotropic displacement parameters ($\text{\AA}^2 \times 10^3$)
U(eq) is defined as one third of the trace of the orthogonalized U_{ij} tensor.

	x	y	z	U(eq)
Zn(1)	2700(1)	5952(1)	5483(1)	30(1)
I(1)	866(1)	6197(1)	5737(1)	39(1)
I(2)	3652(1)	4931(1)	6327(1)	59(1)
Zn(2)	2072(1)	7500	1037(1)	26(1)
I(3)	291(1)	7500	1775(1)	33(1)
I(4)	2628(1)	7500	-1079(1)	67(1)
N(1)	3022(2)	6027(2)	3665(4)	27(1)
C(1)	2571(3)	6509(2)	3011(4)	23(1)
N(2)	2814(2)	6678(2)	1909(3)	24(1)
C(2)	3553(3)	6306(3)	1397(4)	32(1)
C(3)	4029(3)	5780(3)	1994(5)	36(1)
C(4)	3745(3)	5654(3)	3145(5)	33(1)
C(11)	3038(4)	7500	5758(5)	26(1)
N(11)	3462(2)	6878(2)	5952(3)	27(1)
C(12)	4372(3)	6881(3)	6453(4)	34(1)
C(13)	4836(5)	7500	6728(6)	34(1)



2 Publications

Table 3. Bond lengths [Å] and angles [°]

Zn(1)-N(1)	2.102(4)	N(1)-Zn(1)-N(11)	95.02(14)
Zn(1)-N(11)	2.107(4)	N(1)-Zn(1)-I(2)	108.54(10)
Zn(1)-I(2)	2.5140(7)	N(11)-Zn(1)-I(2)	107.67(10)
Zn(1)-I(1)	2.5276(5)	N(1)-Zn(1)-I(1)	107.41(9)
Zn(2)-N(2A)	2.101(4)	N(11)-Zn(1)-I(1)	106.97(10)
Zn(2)-N(2)	2.101(4)	I(2)-Zn(1)-I(1)	126.66(3)
Zn(2)-I(4)	2.5013(16)	N(2A)-Zn(2)-N(2)	96.24(19)
Zn(2)-I(3)	2.5364(7)	N(2A)-Zn(2)-I(4)	107.77(10)
C(1)-N(1)-Zn(1)	119.8(3)	N(2)-Zn(2)-I(4)	107.77(10)
C(4)-N(1)-Zn(1)	122.7(3)	N(2A)-Zn(2)-I(3)	107.15(9)
C(1)-N(2)-Zn(2)	120.2(3)	N(2)-Zn(2)-I(3)	107.15(9)
C(2)-N(2)-Zn(2)	122.6(3)	I(4)-Zn(2)-I(3)	126.59(3)
C(11)-N(11)-Zn(1)	119.6(3)	C(12)-N(11)-Zn(1)	123.3(3)

Symmetry transformations used to generate equivalent atoms: A: x,-y+3/2,z

Table 4. Anisotropic displacement parameters ($\text{\AA}^2 \times 10^3$). The anisotropic displacement factor exponent takes the form: $-2\pi^2 [h^2 a^{*2} U_{11} + \dots + 2 h k a^* b^* U_{12}]$

	U_{11}	U_{22}	U_{33}	U_{23}	U_{13}	U_{12}
Zn(1)	20(1)	34(1)	37(1)	12(1)	-1(1)	3(1)
I(1)	19(1)	53(1)	44(1)	1(1)	1(1)	4(1)
I(2)	24(1)	55(1)	98(1)	49(1)	0(1)	4(1)
Zn(2)	19(1)	40(1)	18(1)	0	2(1)	0
I(3)	19(1)	45(1)	35(1)	0	5(1)	0
I(4)	39(1)	143(1)	19(1)	0	8(1)	0
N(1)	21(1)	26(2)	35(2)	-2(2)	-1(1)	2(1)
C(1)	20(2)	23(2)	28(2)	-3(2)	2(1)	4(1)
N(2)	18(1)	27(2)	27(2)	-3(2)	2(1)	-1(1)
C(2)	21(2)	39(3)	36(2)	-12(2)	6(2)	0(2)
C(3)	22(2)	37(3)	48(3)	-7(2)	5(2)	9(2)
C(4)	22(2)	31(2)	48(3)	-4(2)	-2(2)	6(2)
C(11)	20(2)	36(3)	21(3)	0	-2(2)	0
N(11)	19(1)	41(2)	22(2)	4(2)	-1(1)	2(1)
C(12)	24(2)	49(3)	28(2)	6(2)	-3(2)	7(2)

Table 5. Hydrogen coordinates ($\times 10^4$) and isotropic displacement parameters ($\text{\AA}^2 \times 10^3$)

	x	y	z	U(eq)
H(1)	2034	6750	3356	28
H(2)	3743	6411	615	38
H(3)	4533	5513	1631	43
H(4)	4064	5297	3577	40
H(11)	2386	7500	5460	31
H(12)	4692	6452	6614	40
H(13)	5462	7500	7099	41

Synthesis, Crystal Structures and Thermal Properties of New ZnBr₂(pyrimidine) Coordination Compounds

Christian Näther,^{*[a]} Gaurav Bhosekar,^[a] and Inke Jeß^[a]

Keywords: Coordination compounds / Synthesis / Crystal structure / Thermal reactivity

Four new bromidozinc(II) coordination compounds with pyrimidine as a ligand were prepared, either in solution or by thermal decomposition reactions, and the thermal reactivity and thermodynamic stability of these compounds were investigated. These results are compared with those for the corresponding ZnI₂(pyrimidine) compounds. The ligand-rich 1:2 compound dibromidobis(pyrimidine-*N*)zinc(II) (**I**) crystallizes in the monoclinic space group *P2₁/n*. In this structure the zinc atoms are coordinated by two bromido ligands and two pyrimidine ligands within distorted tetrahedra. On heating, compound **I** is transformed into the ligand-deficient 2:3 intermediate bis(dibromido)bis(pyrimidine-*N*)(μ₂-pyrimidine-*N,N'*)dizinc(II) (**II**), which crystallizes in the monoclinic space group *C2/c*. The crystal structure consists of two ZnBr₂(pyrimidine) subunits, which are connected by an additional pyrimidine ligand through μ-*N,N'* coordination. Thermal de-

composition of compound **II** leads to the formation of the ligand-deficient 1:1 compound dibromido(μ₂-pyrimidine-*N,N'*)zinc(II) (**III**), which crystallizes in the orthorhombic space group *Pmma*. In compound **III**, the zinc atoms are coordinated by four bromine atoms and two pyrimidine ligands within distorted octahedra. The ZnBr₂ units are connected through common edges into chains, which are linked by the pyrimidine ligands into layers. On heating, compound **III** is transformed into the ligand-deficient 2:1 compound (ZnBr₂)₂-(pyrimidine) (**IV**), which decomposes to give ZnBr₂. Solvent-mediated conversion experiments in solution show that not all of the compounds can be prepared by treating ZnBr₂ and pyrimidine in the molar ratio given by the formula of the final product.

(© Wiley-VCH Verlag GmbH & Co. KGaA, 69451 Weinheim, Germany, 2007)

Introduction

Investigations on coordination polymers, inorganic–organic hybrid compounds and metal–organic frameworks are attracting increasing interest^[1] because of the potential applications of these systems as electric, magnetic, optical or porous materials.^[2] Most of these compounds are normally prepared in solution, where different stable and metastable species exist in equilibrium. In view of this, mixtures of compounds are often obtained during the synthesis, and some specific target compounds cannot be prepared at all. Recently we have demonstrated that thermal decomposition of ligand-rich precursor materials is a suitable alternative method for the convenient synthesis of new coordination compounds.^[3] In this method, ligand-rich precursors are heated, leading to ligand-deficient coordination compounds by stepwise liberation of the ligands. One advantage of this method is that the equilibrium is shifted irreversibly in the direction of the ligand-deficient coordination compounds, and thus new compounds which are metastable or unstable

in solution can be discovered and prepared as phase-pure solids.

Recently we have reported on new iodidozinc(II) coordination compounds with pyrimidine as a ligand.^[4] Altogether, seven different compounds were obtained, including three polymorphic modifications (Figure 1). The ligand-rich 1:2 compound **1** decomposes in several steps, in which ligand-deficient compounds **2**, **3** and **4** [2:3 (**2**), 1:1 (**3**) and 2:1 (**4**)] are formed as intermediates. Detailed analysis of the crystal structures of these compounds clearly indicates a strong correlation between the crystal structures of the reactants and the products for the first two thermal reactions. Slight changes in the reaction conditions lead to the formation of a further 1:1 compound of composition [ZnI₂(pyrimidine)]₄(acetonitrile)_{0.25} (**5**). On heating, compound **5** loses acetonitrile and decomposes to give a new 1:1 polymorphic modification **6**. Compound **6** undergoes a polymorphic phase transition to yield the new compound **7**, which is finally transformed into the 1:1 compound **3**. Solvent-mediated conversion experiments clearly show that compound **3** represents the thermodynamically most stable form at room temperature, whereas **5**, **6** and **7** are metastable. Our results clearly show that different stable and metastable species are in equilibrium and that product formation in such thermal decomposition reactions depends on the actual structure of the ligand-rich precursor compound.

[a] Institut für Anorganische Chemie, Universität zu Kiel, Olshausenstr. 40 (Otto-Hahn-Platz 6–7), 24098 Kiel
Fax: +49-431-880-1520
E-mail: cnaether@ac.uni-kiel.de

Supporting information for this article is available on WWW under <http://www.eurjic.org> or from the author.

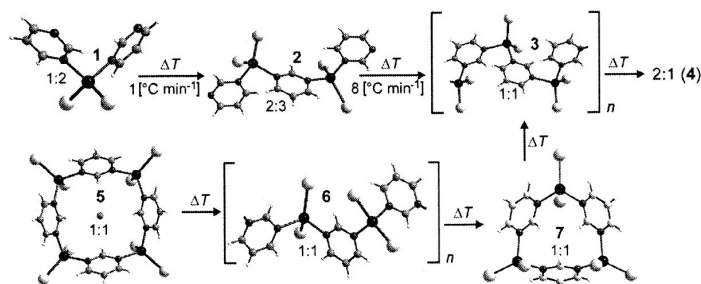


Figure 1. Schematic presentation of the thermal reactions of $\text{ZnI}_2(\text{pyrimidine})$ coordination compounds.^[4]

In order to gain more insight into such reactions, we have investigated the corresponding compounds with ZnBr_2 and pyrimidine. Here we report on the results of these investigations.

Results and Discussion

Crystal Structures

The ligand-rich 1:2 compound **I** crystallizes in the monoclinic space group $P2_1/n$ with four formula units in the unit cell and all atoms in general positions. The crystal structure of **I** is isomorphous to $\text{ZnI}_2(\text{pyrimidine})_2$.^[4] In the crystal structure, there are discrete complexes, in which the zinc atoms are coordinated by two bromine atoms and two nitrogen atoms of the pyrimidine ligands within distorted tetrahedra (Figure 2: top and Table 1). The pyrimidine ligands of adjacent complexes are stacked in the direction of the crystallographic a axis, which indicates π - π interactions (Figure 2: bottom).

The ligand-deficient 2:3 intermediate **II** crystallizes in the monoclinic space group $C2/c$ with eight formula units in the unit cell. This compound is isomorphous to $(\text{ZnI}_2)_2(\text{pyrimidine})_3$.^[4] In the crystal structure discrete $[(\text{ZnBr}_2)_2(\text{pyrimidine})_3]$ units are found, which are located in special positions (Figure 3: top). Each zinc atom is coordinated by two bromine atoms and two nitrogen atoms, one on a terminal and one on a bridging pyrimidine ligand (Figure 3: top and Table 1). The zinc atoms are bridged by a pyrimidine ligand with μ - N,N' coordination. The terminal pyrimidine rings are stacked in the direction of the crystallographic b axis, indicating π - π interactions (Figure 3: bottom).

The ligand-deficient 1:1 compound **III** crystallizes in the orthorhombic space group $Pmma$ with two formula units in the unit cell. The zinc and the bromine atoms as well as the pyrimidine ligands are located on crystallographic mirror planes. This compound is not isomorphous to the corresponding iodido analogue $\text{ZnI}_2(\text{pyrimidine})$.^[4] In this structure the zinc atoms are coordinated by four bromine atoms and two nitrogen atoms of pyrimidine ligands within slightly distorted octahedra (Figure 4: top and Table 1). The zinc atoms are connected by the pyrimidine ligands into zig-zag chains, which elongate in the direction of the crystallo-

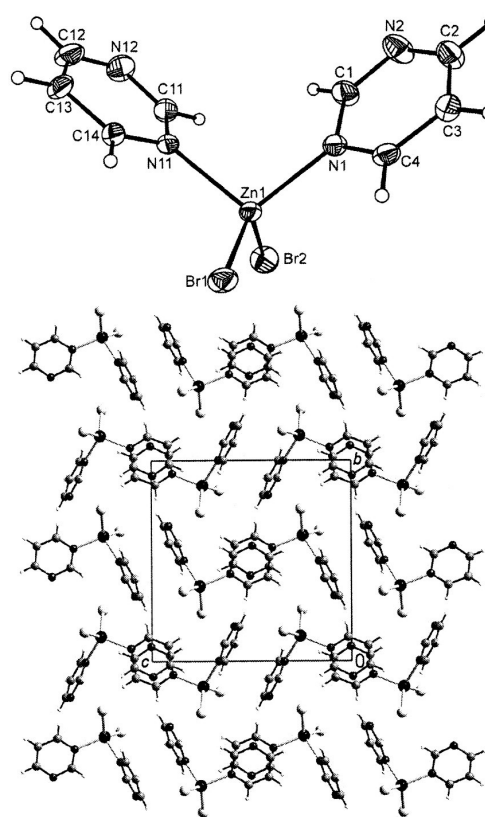


Figure 2. Crystal structure of compound **I** with a view of the coordination sphere of the zinc cations with labelling and displacement ellipsoids drawn at the 50% probability level (top) and a view of the crystal structure in the direction of the crystallographic a axis (bottom).

graphic a axis (Figure 4: middle). The zinc octahedra are additionally connected through common Br edges into corrugated layers, which are located in the ab plane (Figure 4: bottom).

Table 1. Bond lengths [\AA] and angles [$^\circ$] for compounds I, II and III.^[a]

Compound I			
Zn1–N1	2.063(3)	Zn1–N11	2.081(3)
Zn1–Br2	2.3489(6)	Zn1–Br1	2.3500(5)
N1–Zn1–Br2	110.55(9)	N11–Zn1–Br2	105.50(9)
N1–Zn1–Br1	106.94(9)	N1–Zn1–N11	102.79(11)
Br2–Zn1–Br1	124.12(2)	N11–Zn1–Br1	104.78(8)
Compound II			
Zn1–N11	2.070(4)	Zn1–Br2	2.3333(8)
Zn1–N1	2.091(4)	Zn1–Br1	2.3523(8)
N11–Zn1–N1	101.21(16)	N11–Zn1–Br1	104.80(12)
N11–Zn1–Br2	110.28(13)	N1–Zn1–Br1	105.97(11)
N1–Zn1–Br2	110.37(11)	Br2–Zn1–Br1	122.10(3)
Compound III			
Zn1–N1	2.178(3)	Zn1–Br1	2.6287(3)
Zn1–N1B	2.178(3)	Zn1–Br1D	2.6287(3)
Zn1–Br1B	2.6287(3)	Zn1–Br1C	2.6287(3)
Br1–Zn1E	2.6287(3)	Br1–Zn1–Br1D	89.056(12)
N1–Zn1–N1B	180.00(17)	N1–Zn1–Br1C	89.93(6)
N1–Zn1–Br1B	90.07(6)	N1B–Zn1–Br1C	90.07(6)
N1B–Zn1–Br1B	89.93(6)	Br1B–Zn1–Br1C	89.056(12)
N1–Zn1–Br1	89.93(6)	Br1–Zn1–Br1C	90.944(12)
N1B–Zn1–Br1	90.07(6)	Br1D–Zn1–Br1C	180.0
Br1B–Zn1–Br1	180.0	C1–N1–Zn1	122.3(3)
N1–Zn1–Br1D	90.07(6)	C2–N1–Zn1	120.8(3)
N1B–Zn1–Br1D	89.93(6)	Br1B–Zn1–Br1D	90.944(12)

[a] Symmetry transformations used to generate equivalent atoms: A: $-x + 3/2, -y, z$; B: $-x + 1, -y, -z$; C: $x, y - 1, z$; D: $-x + 1, -y + 1, -z$.

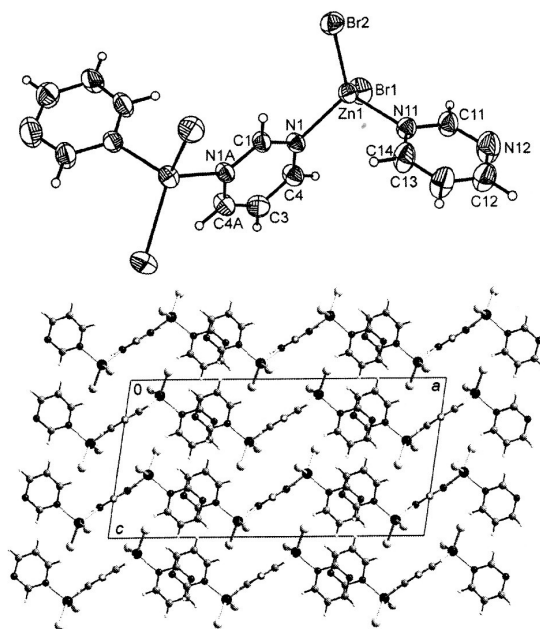


Figure 3. Crystal structure of compound II with a view of the coordination sphere of the zinc cations with labelling and displacement ellipsoids drawn at the 50% probability level (top; symmetry codes: A = $-x, y, -z + 3/2$) and a view of the crystal structure in the direction of the crystallographic b axis (bottom).

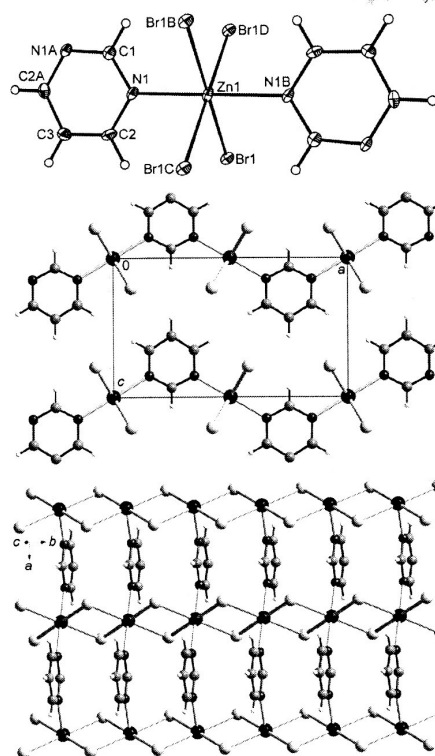


Figure 4. Crystal structure of compound III with a view of the coordination sphere of the zinc cations with labelling and displacement ellipsoids drawn at the 50% probability level (top; symmetry codes: A: $-x + 1, -y, -z$; B: $x, y - 1, z$; C: $-x + 1, -y + 1, -z$) and a view of the structure in the direction of the crystallographic b axis (bottom).

Thermoanalytical Investigations

Five mass steps are observed for compound 1 on heating, of which the first four steps are accompanied by endothermic events in the DTA curve (Figure 5). From the MS trend scan curve it is evident that only pyrimidine ligands ($m/z = 80$) are liberated in the first four steps and the DTG curve shows that not all of the steps are well resolved. The experimental mass loss in each of the first four TG steps is in good agreement with that calculated for the removal of half of the pyrimidine ligands in each step ($\Delta m_{\text{theo}} -1/2$ pyrimidine = -10.4%) (Figure 5). Thus, it can be inferred that in these steps a ligand-deficient 2:3, 1:1 and 2:1 compound is formed, which finally decomposes to give ZnBr_2 , which vaporizes on further heating.

In order to determine the nature of the thermal decomposition products, additional thermogravimetric measurements were performed in which the heating was stopped after each step. The residues thus obtained were investigated by X-ray powder diffraction (Figure 6) and elemental analysis; the results are presented in the Experimental Section.

FULL PAPER

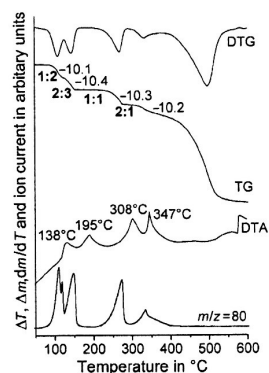


Figure 5. DTA, TG, DTG and MS trend scan curves for compound I [heating rate: 4 °Cmin⁻¹; $m/z = 80$ (pyrimidine)]; given are the mass changes [%] and the peak temperatures T_p [°C].

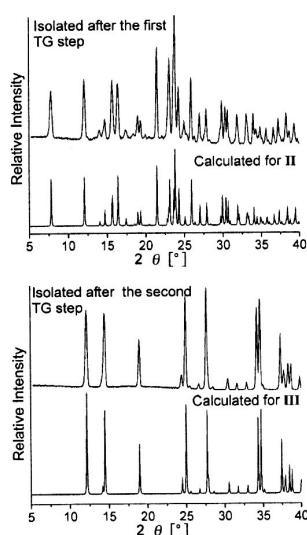


Figure 6. Experimental X-ray powder diffraction pattern of the residue obtained after the first (top) and second (bottom) TG step in the thermal decomposition of the ligand-rich 1:2 compound I, accompanied by the calculated X-ray powder diffraction patterns for compounds II and III.

The experimental X-ray powder diffraction patterns of the residues formed in the first and second TG steps are in excellent agreement with those calculated for compounds II and III, clearly indicating that in the first TG step the ligand-deficient 2:3 intermediate II is formed, and then it is transformed into the ligand-deficient 1:1 compound III on further heating (Figure 5 and Figure 6). In addition, the results of an elemental analysis of the residues agrees with the expected results for a 2:3 and 1:1 compound (Experimental Section). These results show that both compounds are obtained as phase-pure solids even though the first TG step is not well resolved. It is interesting to note that the powder pattern of the residue formed in the third step matches well

with that of the pattern of a solid obtained by stirring a crystalline suspension of ZnBr₂ and pyrimidine in *n*-hexane for several days. This result indicates that the ligand-deficient compound IV can also be prepared in solution.

The elemental analysis of the residue formed in the third TG step corresponds to a new compound of 2:1 stoichiometry of composition (ZnBr₂)₂(pyrimidine) (IV). As expected, the experimental X-ray powder diffraction pattern of this compound is completely different from that calculated for compounds II and III and for ZnBr₂ (Figure 7).

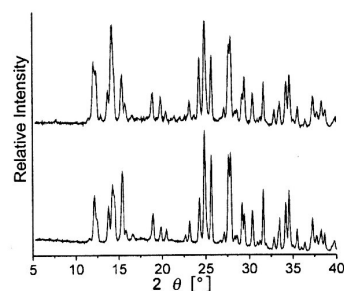


Figure 7. Experimental X-ray powder diffraction pattern of the residue obtained after the third TG step during the thermal decomposition of the ligand-rich 1:2 compound I (top) and the experimental X-ray powder diffraction pattern for compound IV obtained from solution (bottom).

Investigations on the Stability of the Compounds in Solution and in the Solid State

The stability of compounds I, II and III as solids was investigated by time-dependent X-ray powder diffraction. These investigations show that compounds II and III are stable over several days, whereas the ligand-rich 1:2 compound I decomposes even at room temperature within a few days to give compound III.

The stability of these compounds was further investigated in solution by solvent-mediated conversion experiments. In these experiments the metal salt and ligand are mixed in different stoichiometric ratios by using acetonitrile as a solvent. These crystalline suspensions were stirred for a week in order to obtain the thermodynamically most stable form. Afterwards the products were investigated by X-ray powder diffraction (Table 2). These experiments clearly showed that all compounds are stable and can also be prepared in solution. However, it is to be noted that not all of these compounds can be prepared simply by mixing the reactants stoichiometrically as given by the formula. Thus, the reaction of ZnBr₂ and pyrimidine in 2:3 mol ratio results in the formation of the 1:1 compound III, whereas

Table 2. Result of the crystallization experiments in different solvents as a function of the molar ratio between metal and ligand (pyrimidine).

ZnBr ₂ /Ligand	1:4	1:3	1:2	2:3	1:1	2:1
Compound	I (1:2)	II (2:3)	III (1:1)	IV (2:1)		

the reaction in a 1:2 mol ratio leads to the formation of the 2:3 compound **II** (Table 2). This indicates that for the preparation of the ligand-rich compounds, an excess of the ligand must always be used. The ligand-deficient compound **IV** is difficult to prepare, because in many cases it is contaminated with compound **III** or ZnBr_2 (Table 2).

Comparison of $\text{ZnX}_2(\text{pyrimidine})$ Coordination Compounds (X = Cl, I)

As mentioned earlier, for the corresponding coordination compounds with ZnI_2 a variety of compounds and polymorphic modifications were found.^[4] The different polymorphic modifications were detected when the pseudopolymorphic 1:1 compound $[\text{ZnI}_2(\text{pyrimidine})]_4(\text{acetonitrile})_{0.25}$ was decomposed, which was prepared by fast precipitation under kinetic control from a solution of ZnI_2 and pyrimidine in acetonitrile by adding an antisolvent in which the compound is insoluble. In view of this observation, several attempts were made to prepare the corresponding acetonitrile solvate of the bromide compound. However, this always resulted in the formation of the ligand-deficient 1:1 compound **III**. From ZnI_2 and pyrimidine, two metastable polymorphic modifications of the 1:1 compound could also be prepared by performing the crystallization under kinetic control.^[4] Similar attempts to prepare such forms of the bromide compound by nucleation-controlled crystallization^[5] did not result in any polymorphic modifications. It must also be noted that the reaction of ZnCl_2 with pyrimidine leads only to one compound of composition $\text{ZnCl}_2(\text{pyrimidine})$,^[6] which shows that the number of possible compounds in the $\text{ZnX}_2(\text{pyrimidine})$ [X = I, Br, Cl] system decreases from iodine to chlorine.

Differences between the ZnI_2 and ZnBr_2 coordination compounds are also found in the thermal reactivity of the ligand-rich 1:2 compounds, which are isotypic. On slow heating $\text{ZnI}_2(\text{pyrimidine})_2$ (**1**) is transformed directly into the ligand-deficient 1:1 compound $\text{ZnI}_2(\text{pyrimidine})$ (**3**), without the formation of the ligand-deficient 2:3 intermediate **2**. Compound **2** can only be obtained by thermal decomposition if fast heating rates are used, which shows that kinetics plays an important role in product formation. In contrast, thermal decomposition of $\text{ZnBr}_2(\text{pyrimidine})_2$ (**I**)

leads directly to the formation of the 2:3 compound $(\text{ZnBr}_2)_2(\text{pyrimidine})_3$, regardless of the actual heating rate.

In this context, it must be mentioned that for the decomposition reaction of the discrete units in $\text{ZnI}_2(\text{pyrimidine})_2$ (**1**), via the oligomeric units in $(\text{ZnI}_2)_2(\text{pyrimidine})_3$ (**2**), to the chains in $\text{ZnI}_2(\text{pyrimidine})$ (**3**), a smooth reaction pathway can be found (Figure 8: left).^[4] In contrast, only for the reaction of $\text{ZnBr}_2(\text{pyrimidine})_2$ (**I**) to give $(\text{ZnBr}_2)_2(\text{pyrimidine})_3$ (**II**) a smooth reaction pathway is found, whereas for the transformation of the 2:3 intermediate **II** into the ligand-deficient 1:1 compound **III**, large translational and rotational changes are needed and thus no smooth reaction pathway can be expected (Figure 8: right).

Conclusions

In this contribution we have presented four new coordination compounds based on ZnBr_2 and pyrimidine, which can be prepared by thermal decomposition from the ligand-rich compound $\text{ZnBr}_2(\text{pyrimidine})$. These compounds can also be prepared in solution; however, the ligand-rich compounds are only accessible if an excess of ligand is used. The reaction of ZnBr_2 and pyrimidine in a ratio given by the formula of the final compound does not lead to compounds **I** and **II**. This phenomenon is frequently observed in the preparation of such compounds, and therefore new compounds can be easily overlooked if the synthesis is performed only in solution. In contrast, by thermal decomposition of the ligand-rich compounds, all ligand-deficient compounds can be detected in a single measurement. A comparison of the thermal properties of these bromido complexes with those of the corresponding iodidozinc(II) and chloridozinc(II) coordination compounds reveals several differences, which include the influence of the actual heating rate on product formation, the mechanism of such reactions and the possibility of the preparation of thermodynamically metastable compounds and different polymorphic modifications.

Experimental Section

Synthesis of Compound I: ZnBr_2 (112.59 mg, 0.5 mmol) and pyrimidine (240.24 mg, 3.0 mmol) were mixed in acetonitrile (0.5 mL).

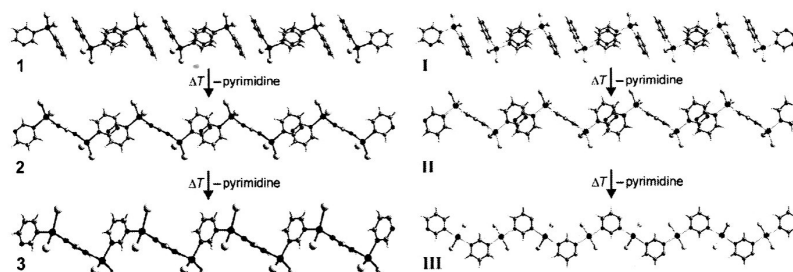


Figure 8. Structural relationships between the crystal structures of the $\text{ZnI}_2(\text{pyrimidine})$ (left) and $\text{ZnBr}_2(\text{pyrimidine})$ coordination polymers.

FULL PAPER

Afterwards, diethyl ether (1.0 mL) was added to the clear solution for precipitation. Yield: 133.6 mg (69.36%) based on ZnBr_2 . $\text{C}_8\text{H}_8\text{Br}_2\text{N}_4\text{Zn}$ (385.37): calcd. C 24.93, H 2.09, N 14.54; found C 25.02, H 2.18, N 14.63. IR (KBr): $\tilde{\nu}$ = 1591 (s), 1561 (m), 1471 (m), 1406 (s), 1369 (w), 1237 (w), 1174 (m), 1082 (m), 1016 (m), 817 (w), 705 (m), 688 (m), 643 (m) cm^{-1} . Single crystals were prepared by the reaction of ZnBr_2 (56.29 mg, 0.25 mmol) and pyrimidine (120.12 mg, 1.5 mmol) in acetonitrile (0.5 mL). Slow evaporation of the solvent from the clear solution yields colourless crystals in about a week.

Synthesis of Compound II: ZnBr_2 (112.59 mg, 0.5 mmol) and pyrimidine (80.08 mg, 1.0 mmol) were mixed in acetonitrile (0.5 mL). Afterwards, diethyl ether (1.0 mL) was added to the clear solution for precipitation. Yield: 161.9 mg (93.77%) based on ZnBr_2 . $\text{C}_{12}\text{H}_{12}\text{Br}_4\text{N}_6\text{Zn}_2$ (690.66): calcd. C 20.87, H 1.75, N 12.17; found C 21.00, H 1.72, N 12.14. IR (KBr): $\tilde{\nu}$ = 3121 (w), 3095 (w), 3064 (m), 1594 (s), 1560 (s), 1472 (s), 1409 (s), 1228 (w), 1173 (m), 1081 (s), 1017 (m), 814 (m), 705 (s), 644 (m) cm^{-1} . Single crystals were prepared by the reaction of ZnBr_2 (112.59 mg, 0.5 mmol) and pyrimidine (80.08 mg, 1.0 mmol) in a mixture of acetonitrile (2.0 mL) and water (0.3 mL). Slow evaporation of the solvent yielded colourless crystals in about 4 d.

Synthesis of Compound III: ZnBr_2 (112.59 mg, 0.5 mmol) and pyrimidine (40.04 mg, 0.5 mmol) were mixed in acetonitrile (0.5 mL). Afterwards diethyl ether (1.0 mL) was added for precipitation. Yield: 129.3 mg (84.71%). $\text{C}_4\text{H}_4\text{Br}_2\text{N}_2\text{Zn}$ (305.28): calcd. C 15.74, H 1.32, N 9.18; found C 15.87, H 1.29, N 9.09. IR (KBr): $\tilde{\nu}$ = 3121 (w), 3075 (w), 1595 (s), 1569 (m), 1465 (s), 1402 (s), 1356 (w), 1220 (m), 1180 (m), 1145 (w), 1081 (s), 1028 (m), 933 (w), 801 (m), 688 (s), 661 (s) cm^{-1} . Single crystals were prepared by the reaction of ZnBr_2 (22.51 mg, 0.1 mmol) and pyrimidine (8.08 mg, 0.1 mmol) in water (0.3 mL). Slow evaporation of the solvent yielded colourless crystals in about one week.

Synthesis of Compound IV: This compound was difficult to obtain in solution, because in most cases it was contaminated with compound III. From several reactions with different stoichiometric ratios of ZnBr_2 and pyrimidine, we obtained only one batch which was phase-pure. Its X-ray powder diffraction pattern is shown in Figure 7. However, the pure compound can be prepared in quanti-

tative yield by thermal decomposition of compound I, II or III. $\text{C}_4\text{H}_4\text{Br}_2\text{N}_2\text{Zn}$ (530.46): calcd. C 9.06, H 0.76, N 5.28; found C 9.13, H 0.81, N 5.35. IR (KBr): $\tilde{\nu}$ = 3106 (w), 3082 (w), 1684 (w), 1596 (s), 1569 (m), 1465 (s), 1403 (s), 1220 (m), 1180 (s), 1082 (s), 1028 (s), 801 (m), 689 (s), 660 (s) cm^{-1} .

Elemental Analysis of the Residues Obtained in the Thermal Decomposition of Compound I

(A) Isolated after the first heating step (compound II) $\text{C}_{12}\text{H}_{12}\text{Br}_4\text{N}_6\text{Zn}_2$ (690.66): calcd. C 20.87, H 1.75, N 12.17; found C 20.94, H 1.69, N 12.20. (B) Isolated after the second heating step (compound III) $\text{C}_4\text{H}_4\text{N}_2\text{Br}_2\text{Zn}$ (305.28): calcd. C 15.74, H 1.32, N 9.18; found C 15.86, H 1.28, N 9.08. (C) Isolated after the third heating step (compound IV) $\text{C}_4\text{H}_4\text{Br}_2\text{N}_2\text{Zn}$ (530.46): calcd. C 9.06, H 0.76, N 5.28; found C 8.48, H 1.47, N 4.98.

Single Crystal Structure Analysis: All investigations were performed with an Imaging Plate Diffraction System (IPDS-1) from STOE & CIE. Structure solutions were performed with direct methods by using SHELXS-97,^[7] and structure refinements were performed against F^2 with SHELXL-97.^[7] For all structures a numerical absorption correction was applied by using X-Red^[8] and X-Shape.^[8] All non-hydrogen atoms were refined with anisotropic displacement parameters. All hydrogen atoms were positioned with idealized geometry and were refined with fixed isotropic displacement parameters [$U_{\text{eq}}(\text{H}) = 1.2 \cdot U_{\text{eq}}(\text{C})$] by using a riding model with $d_{\text{C-H}} = 0.95 \text{ \AA}$. Details of the structural determination are given in Table 3 and in the Supporting Information.

CCDC-651854 (I), -651855 (II) and -651856 (III) contain the supplementary crystallographic data for this paper. These data can be obtained free of charge from The Cambridge Crystallographic Data Centre via www.ccdc.cam.ac.uk/data_request/cif.

X-ray Powder Diffraction: X-ray powder diffraction experiments were performed by using a STOE STADI P transmission powder diffractometer with $\text{Cu-K}\alpha$ -radiation ($\lambda = 154.0598 \text{ pm}$), which is equipped with a position-sensitive detector (scan range: 5° – 45°) from STOE & CIE.

Differential Thermal Analysis, Thermogravimetry and Mass Spectrometry: The heating-rate-dependent DTA-TG measurements were performed under a nitrogen atmosphere (purity: 5.0) with

Table 3. Crystal data and results of the structural refinement for compounds I, II and III.

Compound	I	II	III
Chemical formula	$\text{C}_8\text{H}_8\text{Br}_2\text{N}_4\text{Zn}$	$\text{C}_{12}\text{H}_{12}\text{Br}_4\text{N}_6\text{Zn}_2$	$\text{C}_4\text{H}_4\text{N}_2\text{Br}_2\text{Zn}$
Formula weight	385.37	690.66	305.28
Crystal system	monoclinic	monoclinic	orthorhombic
Space group	$P2_1/n$	$C2/c$	$Pnma$
a [Å]	7.6087(6)	22.8319(19)	12.2327(14)
b [Å]	12.4580(8)	7.7361(5)	3.7481(3)
c [Å]	12.5606(10)	11.4845(9)	7.2659(6)
β [°]	91.854 (10)°	98.656(10)	–
Volume [Å ³]	1189.99 (15)	2005.4(3)	333.14(5)
Z	4	8	2
Calculated density [g cm ⁻³]	2.151	2.288	3.043
μ [mm ⁻¹]	8.751	10.369	15.578
2θ range [°]	2.30 to 28.03	2.78 to 28.03	2.80 to 28.04
Measured reflections	11267	9201	3127
Unique reflections	2778	2394	478
Observed reflections [$I > 2\sigma(I)$]	2341	1809	441
R_1 ^[a] [$I > 2\sigma(I)$]	0.0360	0.0413	0.0268
wR_2 ^[b] [all data]	0.0968	0.1168	0.0697
GOF	1.026	1.024	1.100
Residual electron density [e Å ⁻³]	0.778/–0.918	0.908/–0.759	1.106/–1.128

[a] $R_1 = \sum ||F_o| - |F_c|| / \sum |F_o|$. [b] $wR_2 = \{\sum [w(F_o^2 - F_c^2)^2] / \sum [w(F_o^2)^2]\}^{1/2}$.

Al₂O₃ crucibles in a STA-409CD instrument from Netzsch. The DTA-TG-MS measurements were performed with the same instrument, which is connected to a quadrupole mass spectrometer from Balzers by a Skimmer coupling from Netzsch. The MS measurements were performed in analog and trend scan mode in Al₂O₃ crucibles in a dynamic nitrogen atmosphere (purity: 5.0) by using heating rates of 4 °C min⁻¹. All measurements were performed with a flow rate of 75 mL min⁻¹ and were corrected for buoyancy and current effects. The instrument was calibrated by using standard reference materials.

Elemental Analysis: CHN analysis has been performed with a EURO EA Elemental Analyzer, fabricated by EURO VECTOR Instruments and Software.

Supporting Information (see footnote on the first page of this article): Tables with bond lengths and angles and details of the structure determinations. Experimental and calculated X-ray powder diffraction patterns for compounds I–III. IR and Raman spectra of compounds I–III.

Acknowledgments

We gratefully acknowledge the financial support by the State of Schleswig-Holstein and the Deutsche Forschungsgemeinschaft (Projekt No.: NA 720/1–1). We thank Professor Dr. Wolfgang Bensch for the facility to use his experimental equipment.

- [1] a) A. Y. Robin, K. M. Fromm, *Coord. Chem. Rev.* **2006**, *250*, 2127–2157; b) P. J. Hagrman, D. Hagrman, J. Zubieta, *Angew. Chem. Int. Ed.* **1999**, *38*, 2638–2684; c) S. L. James, *Chem. Soc. Rev.* **2003**, *5*, 276–288; d) R. Robson in *Comprehensive Supramolecular Chemistry*, Pergamon, New York, **1996**, ch. 22, p. 733; e) R. Robson, B. F. Abrahams, S. R. Batten, R. W. Grable, B. F. Hoskins, J. Liu in *Supramolecular Architecture*, ACS publications, Washington DC, **1992**, ch. 19; f) S. R. Batten, R. Robson, *Angew. Chem.* **1998**, *110*, 1558–1595; *Angew. Chem. Int. Ed. Engl.* **1998**, *37*, 1460–1494; g) P. J. Hagrman, D. Hagrman, J. Zubieta, *Angew. Chem.* **1999**, *111*, 2798–2848; *Angew. Chem. Int. Ed.* **1999**, *38*, 2638–2684; h) A. J. Blake, N. R. Champness, P. Hubberstey, W.-S. Li, M. A. Withersby, M. Schröder, *Coord. Chem. Rev.* **1999**, *183*, 117–138; i) D. Braga, L. Maini, M. Polito, L. Scaccianoce, G. Cozzani, F. Gregioni, *Coord. Chem. Rev.* **2001**, *216*–217; j) M. Kosal, J. Chou, S. Wilson, K. Suslick, *Nat. Mater.* **2002**, *1*, 118–121; k) O. M. Yaghi, H. Li, C. Davis, D. Richardson, T. L. Groy, *Acc. Chem. Res.* **1998**, *31*, 474–484.
- [2] a) S. Kitagawa, K. Uemura, *Chem. Soc. Rev.* **2005**, *34*, 109–119; b) P. Horcajada, C. Serre, M. Vallet-Regi, M. Sebban, F. Taulelle, G. Férey, *Angew. Chem. Int. Ed.* **2006**, *45*, 5974–5978; c) B. Paul, C. Näther, B. Walfort, K. M. Fromm, B. Zimmermann, H. Lang, C. Janiak, *Cryst. Eng. Commun.* **2005**, *7*, 309–319; d) M. Eddaoudi, J. Kim, N. Rosi, D. Vodak, J. Wachter, M. O’Keefe, O. M. Yaghi, *Science* **2002**, *295*, 469–472; e) J. L. C. Rowsell, O. M. Yaghi, *Microporous Mesoporous Mater.* **2004**, *73*, 3–14; f) H. K. Chae, D. Y. Siberio-Perez, J. Kim, Y. B. Go, M. Eddaoudi, A. J. Matzger, M. O’Keefe, O. M. Yaghi, *Nature* **2004**, *427*, 523–527; g) S. Noro, S. Kitagawa, M. Kondo, K. Seki, *Angew. Chem. Int. Ed.* **2000**, *39*, 2081–2084; h) M. Latroche, S. Surblé, C. Serre, C. Mellot-Draznieks, P. L. Llewellyn, J.-H. Lee, J.-S. Chang, S. H. Jung, G. Férey, *Angew. Chem. Int. Ed.* **2006**, *45*, 8227–8231; i) S. R. Batten, K. Murray, *Coord. Chem. Rev.* **2003**, *246*, 103–130; j) B. Moulton, J. Lu, R. Hajndl, S. Hariharan, M. J. Zaworotko, *Angew. Chem. Int. Ed.* **2002**, *41*, 2821–2824; k) L.-X. Dai, *Angew. Chem. Int. Ed.* **2004**, *43*, 5726–5729; l) C. Janiak, *Dalton Trans.* **2003**, 2781–2804.
- [3] a) G. Bhosekar, I. Jeß, C. Näther, *Inorg. Chem.* **2006**, *43*, 6508–6515; b) C. Näther, I. Jeß, *Inorg. Chem.* **2006**, *45*, 7446–7454; c) C. Näther, I. Jeß, *Inorg. Chem.* **2003**, *42*, 2968–2976; d) C. Näther, I. Jeß, N. Lehnert, D. Hinz-Hübner, *Solid State Sci.* **2003**, *5*, 1343–1357; e) C. Näther, I. Jeß, *J. Solid State Chem.* **2002**, *169*, 103–112; f) C. Näther, J. Greve, *J. Solid State Chem.* **2003**, *176*, 259–265; g) C. Näther, I. Jeß, *Eur. J. Inorg. Chem.* **2004**, 2868–2876; h) C. Näther, M. Wriedt, I. Jeß, *Inorg. Chem.* **2003**, *42*, 2391–2397.
- [4] C. Näther, G. Bhosekar, I. Jeß, *Inorg. Chem.* **2007**, in press.
- [5] J. Breu, W. Seidl, D. Huttner, F. Kraus, *Chem. Eur. J.* **2002**, *8*, 4454–4460.
- [6] J. Pickardt, B. Staub, *Z. Naturforsch.* **1996**, *51b*, 947–951.
- [7] G. M. Sheldrick, *SHELXS-97 and SHELXL-97*, University of Göttingen, Germany, **1997**.
- [8] *X-Shape, Version 1.03 and X-Red, Version 1.11*, STOE & CIE GmbH, Darmstadt, Germany, **1998**.

Received: July 4, 2007

Published Online: October 11, 2007

Supplemental material

Synthesis, Crystal Structures and Properties of New $\text{ZnBr}_2(\text{Pyrimidine})$ Coordination Compounds

Christian Näther*, Gaurav Bhosekar and Inke Jeß

- Details of the structure determination for compound **I**.
- Details of the structure determination of compound **II**.
- Details of the structure determination of compound **III**.
- Experimental and calculated X-ray powder patterns for compounds **I** to **III**.
- IR- and Raman spectra of compounds **I** to **III**.

2 Publications

Table 1. Crystal data and structure refinement for dibromo-bis(pyrimidine-N) zinc(II) (Compound I).

Identification code	blz17	
Empirical formula	C ₈ H ₈ Br ₂ N ₄ Zn	
Formula weight	385.37	
Temperature	170(2) K	
Wavelength	0.71073 Å	
Crystal system	monoclinic	
Space group	<i>P</i> 2 ₁ / <i>n</i>	
Unit cell dimensions	<i>a</i> = 7.6087(6) Å	$\alpha = 90^\circ$.
	<i>b</i> = 12.4580(8) Å	$\beta = 91.854(10)^\circ$.
	<i>c</i> = 12.5606(10) Å	$\gamma = 90^\circ$.
Volume	1189.99(15) Å ³	
<i>Z</i>	4	
Density (calculated)	2.151 Mg/m ³	
Absorption coefficient	8.751 mm ⁻¹	
F(000)	736	
Crystal size	0.05 x 0.08 x 0.14 mm ³	
Theta range for data collection	2.30 to 28.03°.	
Index ranges	-10 ≤ <i>h</i> ≤ 10, -16 ≤ <i>k</i> ≤ 16, -16 ≤ <i>l</i> ≤ 16	
Reflections collected	11267	
Independent reflections	2778 [R(int) = 0.0590]	
Completeness to theta = 28.03°	96.5 %	
Refinement method	Full-matrix least-squares on F ²	
Data / restraints / parameters	2778 / 0 / 137	
Goodness-of-fit on F ²	1.026	
Final R indices [I > 2σ(I)]	R1 = 0.0360, wR2 = 0.0921	
R indices (all data)	R1 = 0.0442, wR2 = 0.0968	
Extinction coefficient	0.0096(9)	
Largest diff. peak and hole	0.778 and -0.918 e.Å ⁻³	

Remarks:

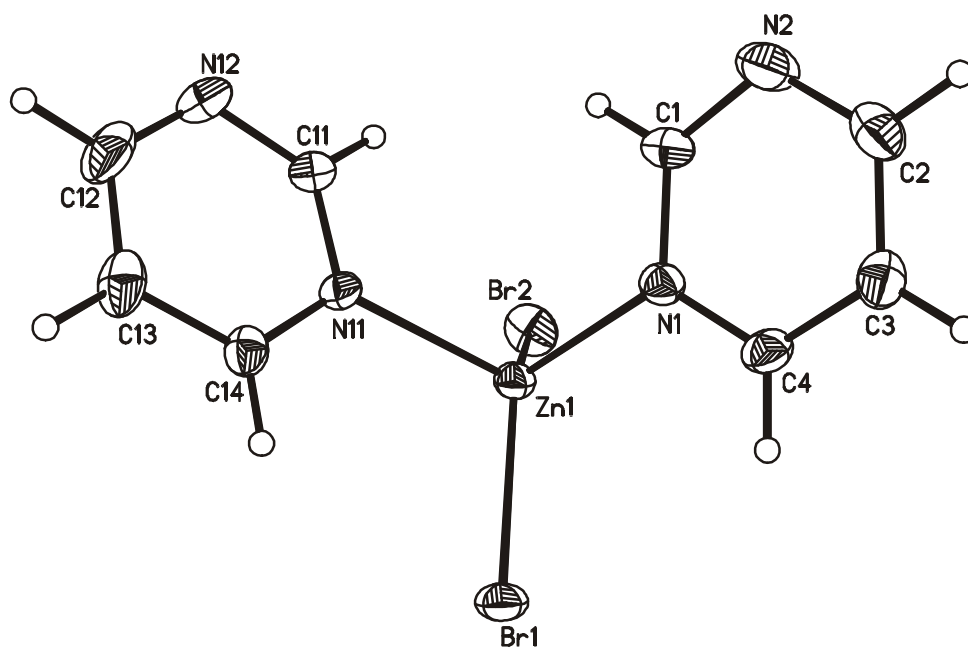
All non-hydrogen atoms were refined using anisotropic displacement parameters. The hydrogen atoms were positioned with idealized geometry and were refined isotropic ($U_{eq} = -1.2 U_{eq}(C)$) using a riding model with C-H = 0.95 Å for aromatic hydrogen atoms. There is one crystallographically independent molecule in the asymmetric unit, which is located in a general position.

2 Publications

Table 2. Atomic coordinates ($\times 10^4$) and equivalent isotropic displacement parameters ($\text{\AA}^2 \times 10^3$)

$U(\text{eq})$ is defined as one third of the trace of the orthogonalized U^{ij} tensor.

	x	y	z	$U(\text{eq})$
Zn(1)	3100(1)	6258(1)	2427(1)	19(1)
Br(1)	5293(1)	7586(1)	2526(1)	26(1)
Br(2)	319(1)	6501(1)	1595(1)	32(1)
N(1)	2855(4)	5658(2)	3945(3)	20(1)
C(1)	2087(5)	4705(3)	4104(3)	27(1)
N(2)	1821(5)	4257(3)	5047(3)	34(1)
C(2)	2347(6)	4823(3)	5904(3)	31(1)
C(3)	3149(5)	5809(3)	5824(3)	27(1)
C(4)	3370(5)	6210(3)	4817(3)	23(1)
N(11)	4240(4)	4986(2)	1628(2)	20(1)
C(11)	3290(6)	4128(3)	1336(3)	28(1)
N(12)	3878(5)	3262(3)	854(3)	37(1)
C(12)	5571(7)	3261(3)	632(4)	37(1)
C(13)	6665(5)	4121(3)	866(3)	30(1)
C(14)	5938(5)	4988(3)	1377(3)	22(1)



2 Publications

Table 3. Bond lengths [Å] and angles [°]

Zn(1)-N(1)	2.063(3)	Zn(1)-N(11)	2.081(3)
Zn(1)-Br(2)	2.3489(6)	Zn(1)-Br(1)	2.3500(5)
N(1)-C(1)	1.340(4)	N(11)-C(11)	1.335(5)
N(1)-C(4)	1.341(5)	N(11)-C(14)	1.340(5)
C(1)-N(2)	1.331(5)	C(11)-N(12)	1.322(5)
N(2)-C(2)	1.337(6)	N(12)-C(12)	1.326(6)
C(2)-C(3)	1.377(5)	C(12)-C(13)	1.383(7)
C(3)-C(4)	1.376(5)	C(13)-C(14)	1.382(5)
N(1)-Zn(1)-Br(2)	110.55(9)	N(11)-Zn(1)-Br(2)	105.50(9)
N(1)-Zn(1)-Br(1)	106.94(9)	C(11)-N(11)-C(14)	117.1(3)
Br(2)-Zn(1)-Br(1)	124.12(2)	C(11)-N(11)-Zn(1)	120.8(3)
C(1)-N(1)-C(4)	116.7(3)	C(14)-N(11)-Zn(1)	122.1(2)
C(1)-N(1)-Zn(1)	120.8(3)	N(12)-C(11)-N(11)	126.2(4)
C(4)-N(1)-Zn(1)	122.4(2)	C(11)-N(12)-C(12)	116.3(4)
N(2)-C(1)-N(1)	125.7(4)	N(12)-C(12)-C(13)	122.5(3)
C(1)-N(2)-C(2)	116.4(3)	C(14)-C(13)-C(12)	117.2(4)
N(2)-C(2)-C(3)	122.3(4)	N(11)-C(14)-C(13)	120.7(3)
C(4)-C(3)-C(2)	117.2(4)	N(1)-Zn(1)-N(11)	102.79(11)
N(1)-C(4)-C(3)	121.6(3)	N(11)-Zn(1)-Br(1)	104.78(8)

Table 4. Anisotropic displacement parameters ($\text{Å}^2 \times 10^3$). The anisotropic displacement factor exponent takes the form: $-2\pi^2 [h^2 a^{*2} U_{11} + \dots + 2 h k a^* b^* U_{12}]$

	U_{11}	U_{22}	U_{33}	U_{23}	U_{13}	U_{12}
Zn(1)	20(1)	15(1)	23(1)	1(1)	4(1)	0(1)
Br(1)	24(1)	15(1)	38(1)	0(1)	6(1)	-3(1)
Br(2)	22(1)	37(1)	38(1)	5(1)	0(1)	4(1)
N(1)	21(1)	17(1)	23(2)	2(1)	3(1)	1(1)
C(1)	33(2)	20(2)	28(2)	2(1)	4(2)	-7(1)
N(2)	42(2)	30(2)	30(2)	7(1)	0(2)	-12(1)
C(2)	34(2)	33(2)	26(2)	7(2)	6(2)	0(2)
C(3)	31(2)	27(2)	23(2)	-2(1)	2(2)	5(2)
C(4)	27(2)	15(1)	27(2)	-1(1)	1(2)	1(1)
N(11)	28(2)	13(1)	21(2)	0(1)	4(1)	0(1)
C(11)	36(2)	18(2)	31(2)	-1(1)	10(2)	-3(1)
N(12)	52(2)	17(1)	42(2)	-6(1)	10(2)	-3(1)
C(12)	55(3)	22(2)	35(2)	-2(2)	4(2)	15(2)
C(13)	31(2)	31(2)	28(2)	2(2)	2(2)	17(2)
C(14)	25(2)	22(2)	19(2)	1(1)	2(1)	5(1)

Table 5. Hydrogen coordinates ($\times 10^4$) and isotropic displacement parameters ($\text{Å}^2 \times 10^3$)

	x	y	z	U(eq)
H(1)	1698	4316	3490	32
H(2)	2161	4534	6591	37
H(3)	3534	6197	6440	32
H(4)	3901	6894	4737	28
H(11)	2076	4141	1490	34
H(12)	6048	2646	300	45
H(13)	7867	4115	683	36
H(14)	6650	5594	1552	26

2 Publications

Table 1. Crystal data and structure refinement for dibromo-bis(pyrimidine-N)-(μ₂-pyrimidine-N,N') zinc(II) (Compound II).

Identification code	gb246	
Empirical formula	C ₆ H ₆ Br ₂ N ₃ Zn	
Formula weight	345.33	
Temperature	293(2) K	
Wavelength	0.71073 Å	
Crystal system	monoclinic	
Space group	C2/c	
Unit cell dimensions	a = 22.8319(19) Å	α = 90°.
	b = 7.7361(5) Å	β = 98.656(10)°.
	c = 11.4845(9) Å	γ = 90°.
Volume	2005.4(3) Å ³	
Z	8	
Density (calculated)	2.288 Mg/m ³	
Absorption coefficient	10.369 mm ⁻¹	
F(000)	1304	
Crystal size	0.07 x 0.10 x 0.14 mm ³	
Theta range for data collection	2.78 to 28.03°.	
Index ranges	-30 ≤ h ≤ 30, -10 ≤ k ≤ 10, -15 ≤ l ≤ 15	
Reflections collected	9201	
Independent reflections	2394 [R(int) = 0.0869]	
Completeness to theta = 28.03°	98.3 %	
Refinement method	Full-matrix least-squares on F ²	
Data / restraints / parameters	2394 / 0 / 111	
Goodness-of-fit on F ²	1.024	
Final R indices [I > 2σ(I)]	R1 = 0.0413, wR2 = 0.1071	
R indices (all data)	R1 = 0.0596, wR2 = 0.1168	
Extinction coefficient	0.0036(4)	
Largest diff. peak and hole	0.908 and -0.759 e.Å ⁻³	

Remarks:

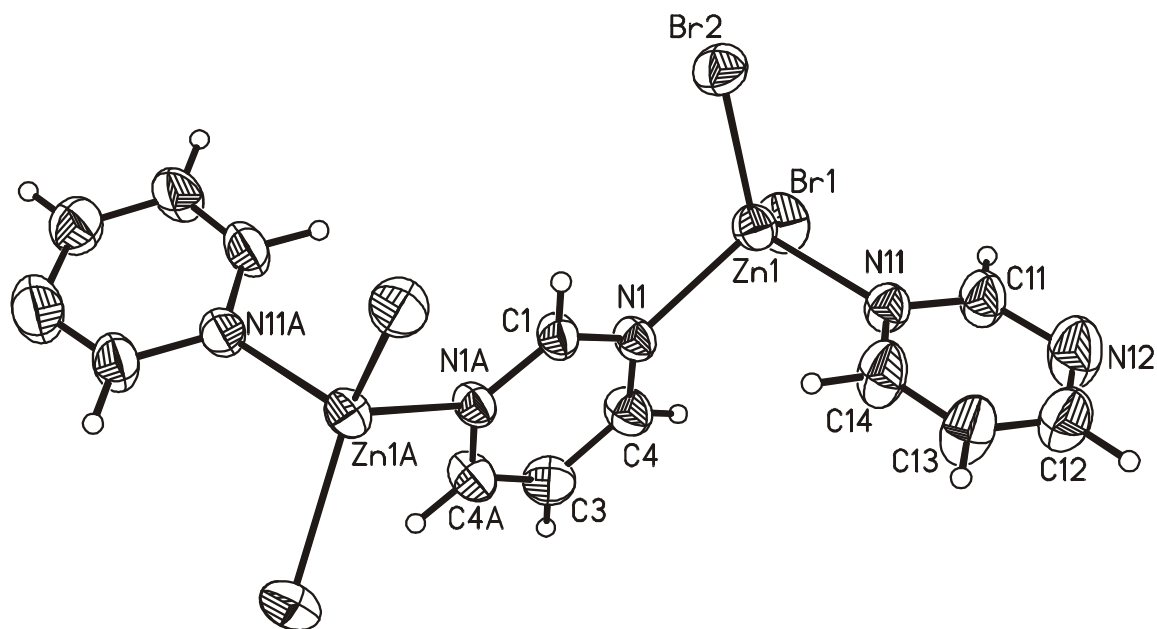
All non-hydrogen atoms were refined using anisotropic displacement parameters. The hydrogen atoms were positioned with idealized geometry and were refined isotropic ($U_{eq} = -1.2 U_{eq}(C)$) using a riding model with C-H = 0.95 Å for aromatic hydrogen atoms. There is one crystallographically independent molecule in the asymmetric unit, which is located in a special position.

2 Publications

Table 2. Atomic coordinates ($\times 10^4$) and equivalent isotropic displacement parameters ($\text{\AA}^2 \times 10^3$).

$U(\text{eq})$ is defined as one third of the trace of the orthogonalized U^{ij} tensor.

	x	y	z	$U(\text{eq})$
Zn(1)	988(1)	3984(1)	6012(1)	34(1)
Br(1)	1147(1)	2053(1)	4508(1)	53(1)
Br(2)	693(1)	6839(1)	5620(1)	45(1)
N(1)	402(2)	2740(5)	6970(3)	32(1)
N(11)	1766(2)	3913(6)	7199(3)	36(1)
C(12)	2749(3)	3904(9)	8816(5)	54(2)
C(1)	0	3545(10)	7500	33(1)
C(3)	0	95(10)	7500	44(2)
C(4)	402(2)	1020(7)	6978(4)	41(1)
C(11)	2294(2)	3689(9)	6867(5)	46(1)
N(12)	2810(2)	3667(9)	7657(5)	67(2)
C(13)	2228(2)	4162(10)	9169(4)	54(2)
C(14)	1761(2)	4118(9)	8346(5)	50(2)



2 Publications

Table 3. Bond lengths [Å] and angles [°]

Zn(1)-N(11)	2.070(4)	N(11)-Zn(1)-Br(1)	104.80(12)
Zn(1)-N(1)	2.091(4)	N(1)-Zn(1)-Br(1)	105.97(11)
Zn(1)-Br(2)	2.3333(8)	Br(2)-Zn(1)-Br(1)	122.10(3)
Zn(1)-Br(1)	2.3523(8)	C(1)-N(1)-C(4)	117.7(5)
N(1)-C(1)	1.330(5)	C(1)-N(1)-Zn(1)	124.5(4)
N(1)-C(4)	1.331(7)	C(4)-N(1)-Zn(1)	117.7(3)
N(11)-C(14)	1.329(6)	C(14)-N(11)-C(11)	116.3(4)
N(11)-C(11)	1.330(6)	C(14)-N(11)-Zn(1)	121.0(3)
C(12)-C(13)	1.327(8)	C(11)-N(11)-Zn(1)	122.6(3)
C(12)-N(12)	1.371(8)	C(13)-C(12)-N(12)	123.0(5)
C(1)-N(1)#1	1.330(5)	N(1)#1-C(1)-N(1)	124.2(7)
C(3)-C(4)	1.371(7)	C(4)-C(3)-C(4)#1	117.1(7)
C(3)-C(4)#1	1.371(7)	N(1)-C(4)-C(3)	121.7(5)
C(11)-N(12)	1.375(8)	N(11)-C(11)-N(12)	122.4(5)
C(13)-C(14)	1.316(8)	C(12)-N(12)-C(11)	115.9(5)
N(11)-Zn(1)-N(1)	101.21(16)	C(14)-C(13)-C(12)	116.3(5)
N(11)-Zn(1)-Br(2)	110.28(13)	C(13)-C(14)-N(11)	126.0(5)
N(1)-Zn(1)-Br(2)	110.37(11)		

Symmetry transformations used to generate equivalent atoms: A: -x,y,-z+3/2

Table 4. Anisotropic displacement parameters ($\text{\AA}^2 \times 10^3$). The anisotropic displacement factor exponent takes the form: $-2\pi^2 [h^2 a^{*2} U_{11} + \dots + 2 h k a^* b^* U_{12}]$

	U_{11}	U_{22}	U_{33}	U_{23}	U_{13}	U_{12}
Zn(1)	34(1)	38(1)	33(1)	0(1)	11(1)	2(1)
Br(1)	59(1)	61(1)	44(1)	-17(1)	19(1)	0(1)
Br(2)	45(1)	36(1)	53(1)	2(1)	5(1)	4(1)
N(1)	32(2)	31(2)	34(2)	-1(2)	13(2)	1(2)
N(11)	32(2)	40(3)	35(2)	-2(2)	7(2)	3(2)
C(12)	42(3)	69(5)	48(3)	-4(3)	0(2)	2(3)
C(1)	29(3)	30(4)	41(3)	0	11(3)	0
C(3)	49(4)	28(4)	53(4)	0	8(3)	0
C(4)	43(3)	36(3)	46(3)	0(2)	18(2)	3(2)
C(11)	34(2)	66(4)	40(3)	0(2)	11(2)	1(2)
N(12)	44(3)	92(5)	65(3)	-6(3)	15(2)	4(3)
C(13)	42(3)	94(5)	26(2)	-15(2)	4(2)	9(3)
C(14)	35(2)	76(5)	42(3)	-12(3)	12(2)	9(3)

Table 11. Hydrogen coordinates ($\times 10^4$) and isotropic displacement parameters ($\text{\AA}^2 \times 10^3$)

	x	y	z	U(eq)
H(12)	3087	3882	9379	65
H(1)	0	4747	7500	39
H(3)	0	-1107	7500	52
H(4)	683	430	6621	49
H(11)	2315	3541	6071	56
H(13)	2196	4363	9956	65
H(14)	1393	4241	8590	60

2 Publications

Table 1. Crystal data and structure refinement for (μ_2 -dibromo-(μ_2 -pyrimidine-N,N') zinc(II) (Compound **III**)

Identification code	gb112a
Empirical formula	C ₄ H ₄ Br ₂ N ₂ Zn
Formula weight	305.28
Temperature	220(2) K
Wavelength	0.71073 Å
Crystal system	orthorhombic
Space group	Pmma
Unit cell dimensions	a = 12.2327(14) Å $\alpha = 90^\circ$. b = 3.7481(3) Å $\beta = 90^\circ$. c = 7.2659(6) Å $\gamma = 90^\circ$.
Volume	333.14(5) Å ³
Z	2
Density (calculated)	3.043 Mg/m ³
Absorption coefficient	15.578 mm ⁻¹
F(000)	284
Crystal size	0.07 x 0.1 x 0.12 mm ³
Theta range for data collection	2.80 to 28.04°.
Index ranges	-16 ≤ h ≤ 16, -4 ≤ k ≤ 4, -9 ≤ l ≤ 9
Reflections collected	3127
Independent reflections	478 [R(int) = 0.0471]
Completeness to theta = 28.04°	99.4 %
Refinement method	Full-matrix least-squares on F ²
Data / restraints / parameters	478 / 0 / 32
Goodness-of-fit on F ²	1.100
Final R indices [I > 2σ(I)]	R1 = 0.0268, wR2 = 0.0688
R indices (all data)	R1 = 0.0288, wR2 = 0.0697
Extinction coefficient	0.038(4)
Largest diff. peak and hole	1.106 and -1.128 e.Å ⁻³

Remarks:

All non-hydrogen atoms were refined using anisotropic displacement parameters. The hydrogen atoms were positioned with idealized geometry and were refined isotropic ($U_{eq} = -1.2 U_{eq}(C)$) using a riding model with C-H = 0.95 Å for aromatic hydrogen atoms. There is one crystallographically independent molecule in the asymmetric unit, which is located in a special positions.

2 Publications

Table 2. Atomic coordinates ($\times 10^4$) and equivalent isotropic displacement parameters ($\text{\AA}^2 \times 10^3$).

U(eq) is defined as one third of the trace of the orthogonalized U_{ij} tensor.

	x	y	z	U(eq)
Zn(1)	5000	0	0	14(1)
Br(1)	4238(1)	5000	2189(1)	14(1)
N(1)	6534(3)	0	1521(5)	14(1)
C(1)	7500	0	683(7)	14(1)
C(2)	6540(3)	0	3365(6)	18(1)
C(3)	7500	0	4354(7)	18(1)

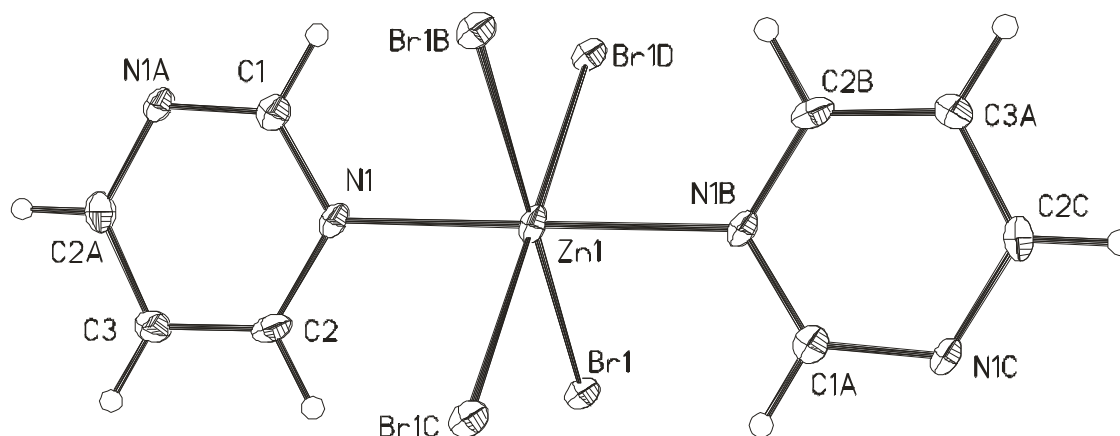


Table 3. Bond lengths [\AA] and angles [$^\circ$].

Zn(1)-N(1)	2.178(3)	Zn(1)-Br(1)	2.6287(3)
Zn(1)-N(1B)	2.178(3)	Zn(1)-Br(1D)	2.6287(3)
Zn(1)-Br(1B)	2.6287(3)	Zn(1)-Br(1C)	2.6287(3)
Br(1)-Zn(1E)	2.6287(3)	Br(1)-Zn(1)-Br(1D)	89.056(12)
N(1)-Zn(1)-N(1B)	180.00(17)	N(1)-Zn(1)-Br(1C)	89.93(6)
N(1)-Zn(1)-Br(1B)	90.07(6)	N(1B)-Zn(1)-Br(1C)	90.07(6)
N(1B)-Zn(1)-Br(1B)	89.93(6)	Br(1B)-Zn(1)-Br(1C)	89.056(12)
N(1)-Zn(1)-Br(1)	89.93(6)	Br(1)-Zn(1)-Br(1C)	90.944(12)
N(1B)-Zn(1)-Br(1)	90.07(6)	Br(1D)-Zn(1)-Br(1C)	180.0
Br(1B)-Zn(1)-Br(1)	180.0	Zn(1)-Br(1)-Zn(1E)	90.944(12)
N(1)-Zn(1)-Br(1D)	90.07(6)	C(1)-N(1)-Zn(1)	122.3(3)
N(1B)-Zn(1)-Br(1D)	89.93(6)	C(2)-N(1)-Zn(1)	120.8(3)
Br(1B)-Zn(1)-Br(1D)	90.944(12)		

Symmetry transformations used to generate equivalent atoms: A: $-x+3/2, -y, z$; B: $-x+1, -y, -z$; C: $x, y-1, z$; D: $-x+1, -y+1, -z$; E: $x, y+1, z$

2 Publications

Table 4. Anisotropic displacement parameters ($\text{\AA}^2 \times 10^3$). The anisotropic displacement factor exponent takes the form: $-2\pi^2 [h^2 a^{*2} U_{11} + \dots + 2 h k a^* b^* U_{12}]$

	U_{11}	U_{22}	U_{33}	U_{23}	U_{13}	U_{12}
Zn(1)	7(1)	17(1)	18(1)	0	-2(1)	0
Br(1)	11(1)	14(1)	16(1)	0	3(1)	0
N(1)	7(1)	21(2)	16(2)	0	0(1)	0
C(1)	13(2)	15(3)	16(2)	0	0	0
C(2)	12(2)	25(2)	16(2)	0	6(1)	0
C(3)	15(3)	27(3)	11(2)	0	0	0

Table 5. Hydrogen coordinates ($\times 10^4$) and isotropic displacement parameters ($\text{\AA}^2 \times 10^3$).

	x	y	z	U(eq)
H(1)	7500	0	-624	17
H(2)	5864	0	4007	21
H(3)	7500	0	5662	21

Experimental and calculated X-ray powder patterns for compounds **I**, **II** and **III**.

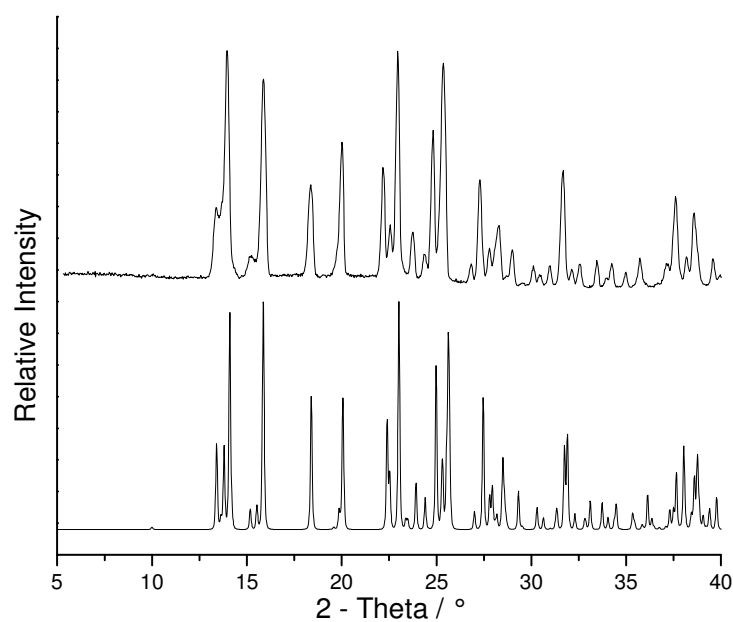


Fig. S1. Experimental (top) and calculated (bottom) X-ray powder pattern for compound **I** (Transmission geometry; Cu-K α -radiation).

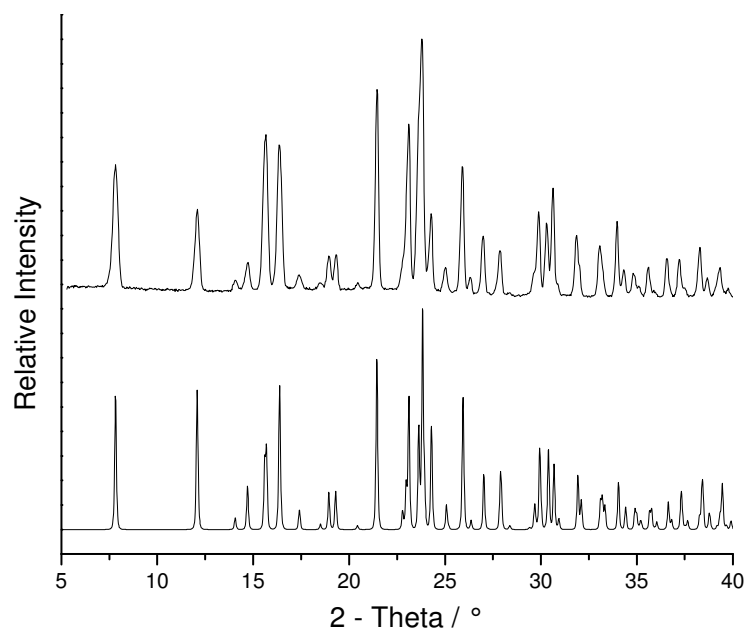


Fig. S2. Experimental (top) and calculated (bottom) X-ray powder pattern for compound **II** (Transmission geometry, Cu-K α -radiation).

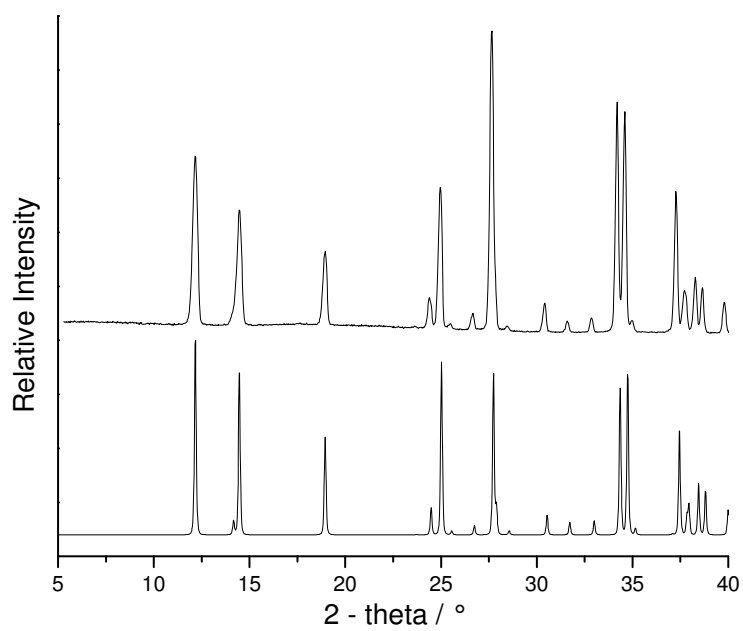


Fig. S3. Experimental (top) and calculated (bottom) X-ray powder pattern for compound **III** (Transmission geometry; Cu-K α -radiation).

IR- and Raman spectra of compounds **I**, **II**, **III** and **IV**.

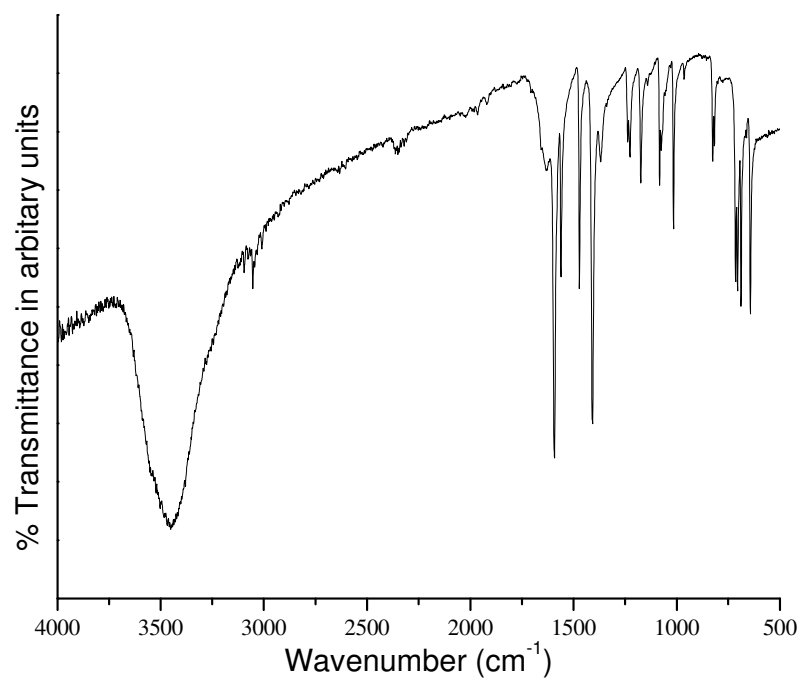


Fig. S4. IR spectra for compound **I**.

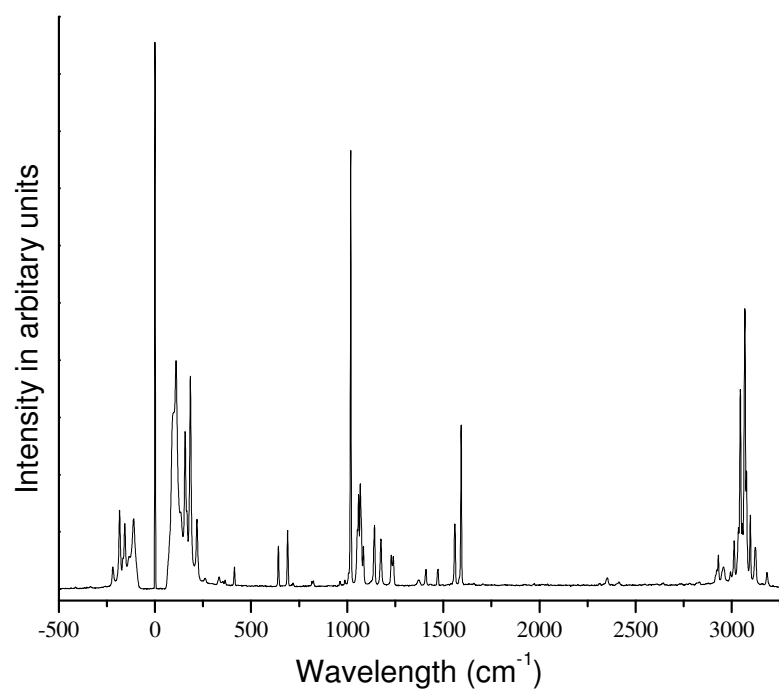


Fig. S5. Raman spectra for compound **I**.

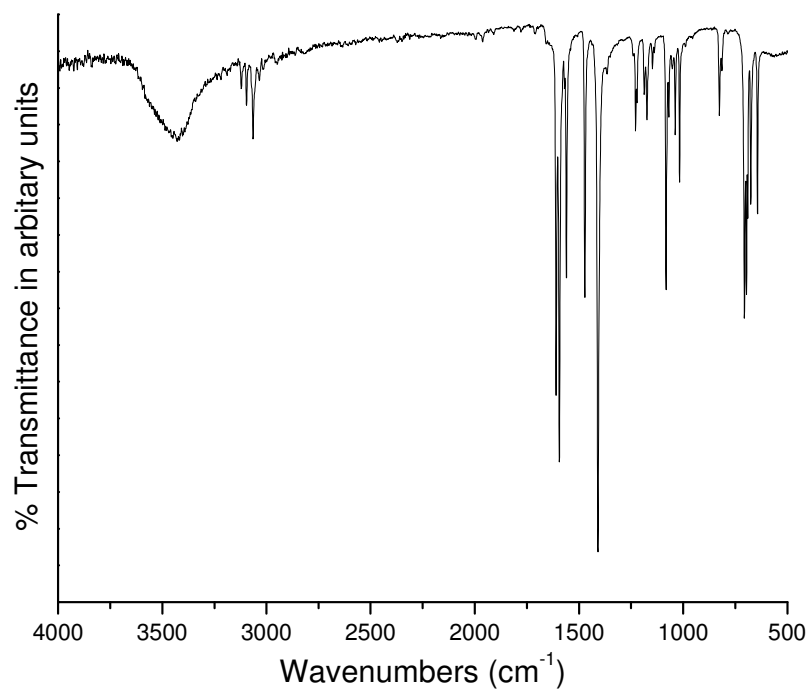


Fig. S6. IR spectra for compound **II**.

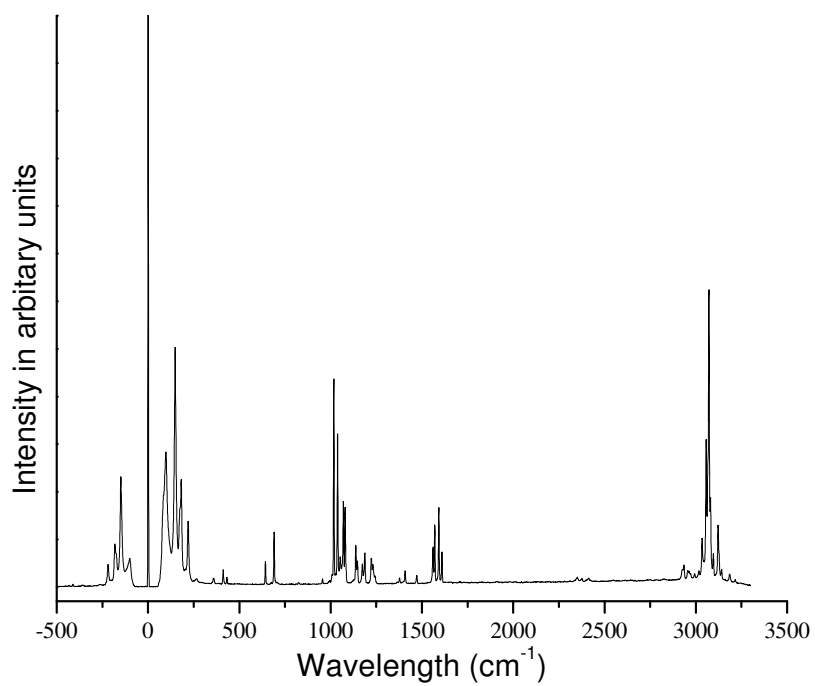


Fig. S7. Raman spectra for compound **II**.

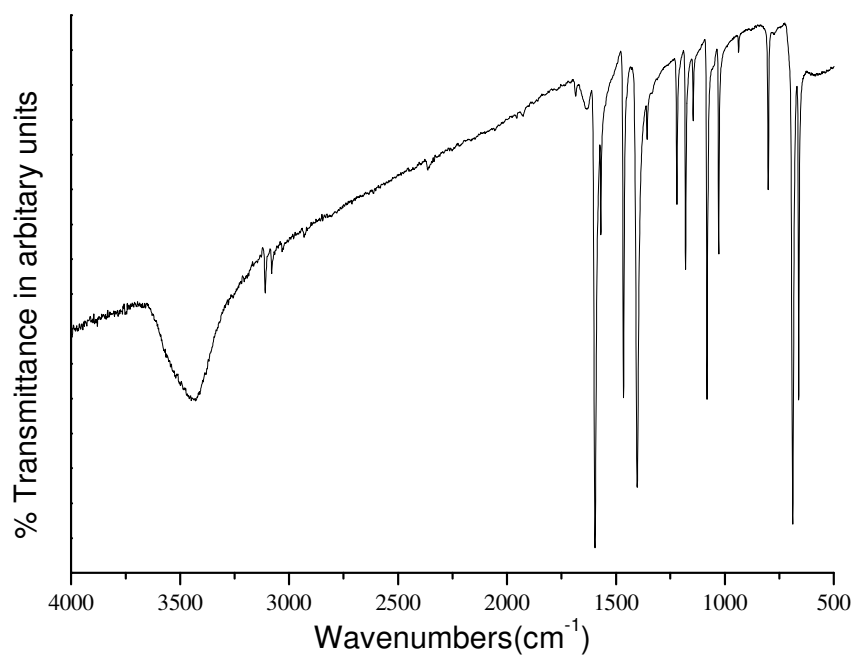


Fig. S8. IR spectra for compound **III**.

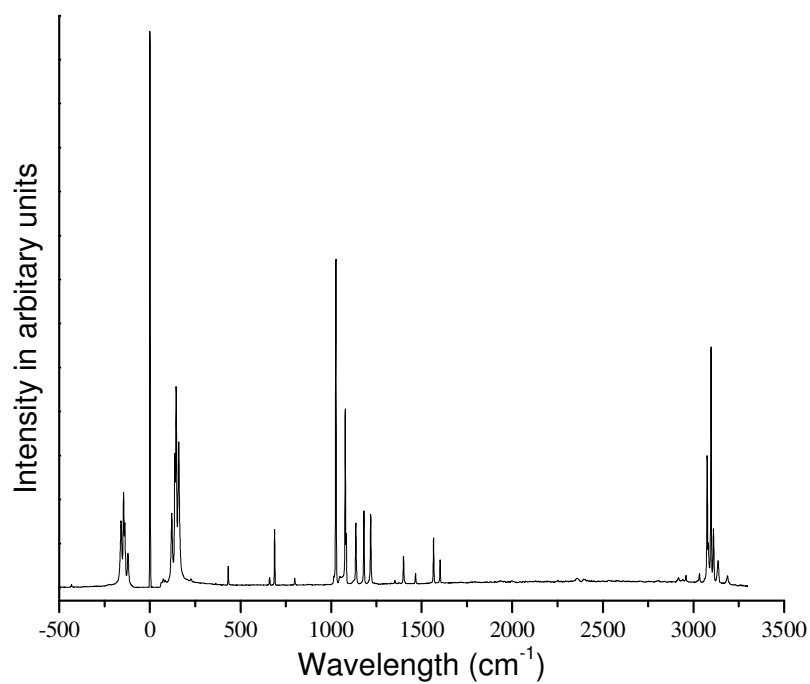


Fig. S9. Raman spectra for compound **III**.

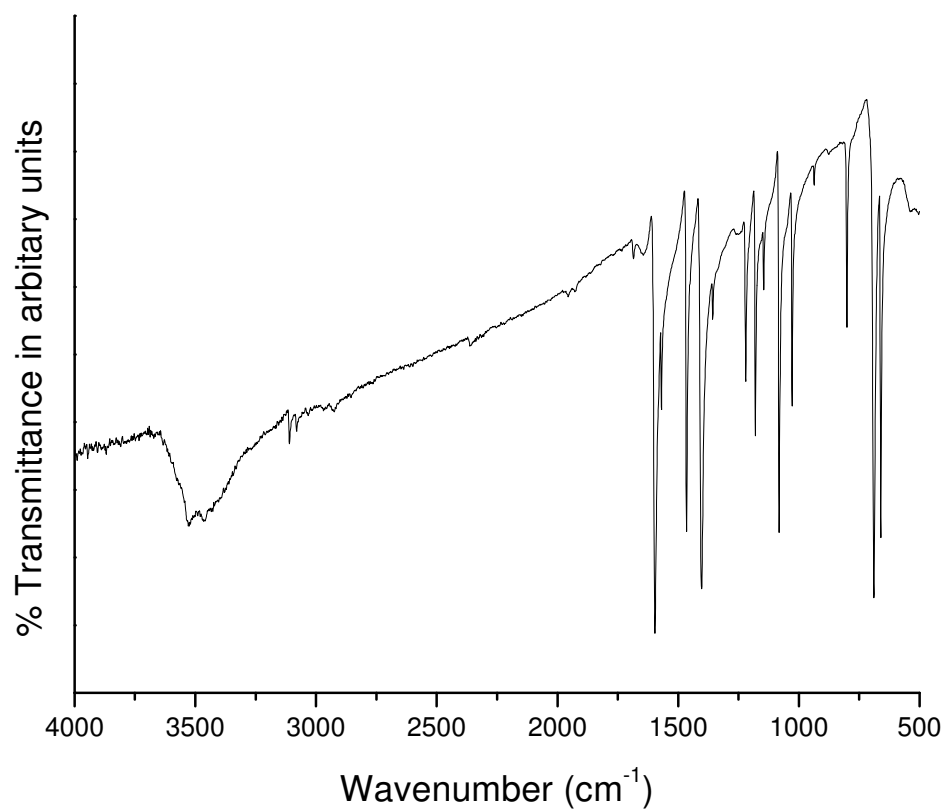


Fig. S10. IR spectra for compound **IV**.

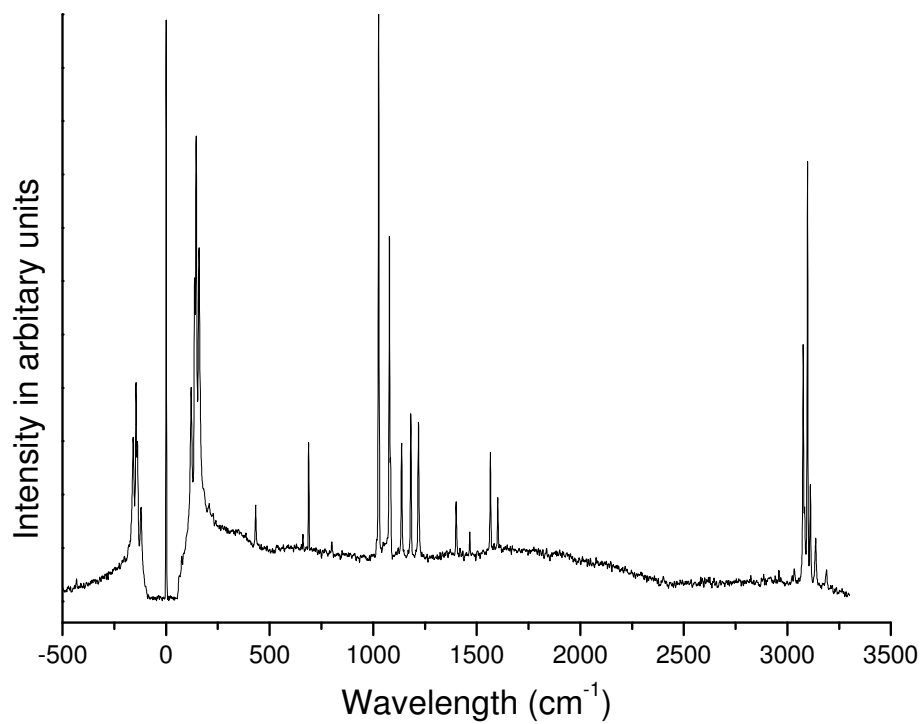


Fig. S11. Raman spectra for compound **IV**.

Acta Crystallographica Section E
Structure Reports
Online

ISSN 1600-5368

Gaurav Bhosekar, Inke Jess and
Christian Näther*

Institut für Anorganische Chemie, Christian-
Albrechts-Universität Kiel, Olshausenstrasse 40,
D-24098 Kiel, Germany

Correspondence e-mail:
cnaether@ac.uni-kiel.de

Key indicators

Single-crystal X-ray study
 $T = 170$ K
Mean $\sigma(\text{C}-\text{C}) = 0.009$ Å
 R factor = 0.038
 wR factor = 0.090
Data-to-parameter ratio = 20.7

For details of how these key indicators were
automatically derived from the article, see
<http://journals.iucr.org/e>.

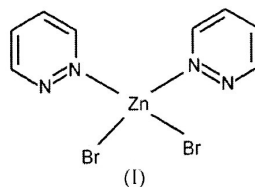
Dibromobis(pyridazine- κN)zinc(II)

In the crystal structure of the title compound, $[\text{ZnBr}_2(\text{C}_4\text{H}_4\text{N}_2)_2]$, each Zn atom is coordinated by two Br atoms and two pyridazine ligands within a distorted tetrahedron to form a discrete complex.

Received 5 July 2006
Accepted 12 July 2006

Comment

Recently, we have become interested in the synthesis, structures and thermal properties of coordination compounds based on zinc(II) halides and N -donor ligands because we have found that such ligand-rich coordination compounds can be transformed into new ligand-poor compounds (Bhosekar *et al.*, 2006*a,b,c*). In further investigations, we have prepared such compounds using pyridazine as ligand. For the corresponding compound with zinc(II) chloride, we have found three different modifications of dichlorobis(pyridazine)-zinc(II), which consist of tetrahedral discrete complexes in which the zinc atom is coordinated by two pyridazine ligands and two chlorine atoms. On heating, these compounds transform into a ligand-poor compound. In a continuation of this work, we have investigated the reaction of zinc(II) bromide with pyridazine. In contrast to the chloro compound, we have found no signs of further modifications and also no sign of a ligand-poor compound. Here we report the structure of this compound, (I).



In the crystal structure of (I), all atoms are in general positions. The Zn^{II} atom is coordinated by two Br atoms and two N atoms of two pyridazine ligands in a distorted tetrahedral geometry (Fig. 1 and Table 1). The Zn—Br and Zn—N bond lengths are comparable to those in related structures retrieved from the Cambridge Structural Database (*Conquest* Version 1.8 of 2006; Allen, 2002).

Experimental

ZnBr_2 and pyridazine were obtained from Alfa Aesar, and acetonitrile was obtained from Fluka. Large amounts of crystalline powder can be prepared if a suspension of 1 mmol of ZnBr_2 and 1 mmol of pyridazine is stirred in 1 ml of acetonitrile for 2 d. Single crystals of (I) are obtained if 0.25 mmol (56.3 mg) ZnBr_2 is dissolved in 1.5 mmol (120.12 mg) pyridazine.

© 2006 International Union of Crystallography
All rights reserved

Acta Cryst. (2006). E62, m1859–m1860

doi:10.1107/S1600536806026997

Bhosekar *et al.* • $[\text{ZnBr}_2(\text{C}_4\text{H}_4\text{N}_2)_2]$ m1859

metal-organic papers

Crystal data

[ZnBr₂(C₄H₄N₂)₂]
M_r = 385.37
 Orthorhombic, *P*2₁2₁2₁
a = 8.8914 (5) Å
b = 9.7191 (7) Å
c = 13.8189 (8) Å
V = 1194.18 (13) Å³

Z = 4
D_x = 2.143 Mg m⁻³
 Mo *K*α radiation
 μ = 8.72 mm⁻¹
T = 170 (2) K
 Block, colourless
 0.10 × 0.08 × 0.06 mm

Data collection

Stoe IPDS-1 diffractometer
 φ scans
 Absorption correction: numerical
 (*X-SHAPE*; Stoe & Cie, 1998)
*T*_{min} = 0.447, *T*_{max} = 0.601

6650 measured reflections
 2833 independent reflections
 2354 reflections with *I* > 2σ(*I*)
*R*_{int} = 0.049
 θ _{max} = 28.0°

Refinement

Refinement on *F*²
R [*F*² > 2σ(*F*²)] = 0.038
wR [*F*²] = 0.090
S = 1.02
 2833 reflections
 137 parameters
 H-atom parameters constrained
 $w = 1/[\sigma^2(F_o^2) + (0.0547P)^2]$
 where $P = (F_o^2 + 2F_c^2)/3$

(Δ/σ)_{max} = 0.001
 $\Delta\rho$ _{max} = 0.81 e Å⁻³
 $\Delta\rho$ _{min} = -0.84 e Å⁻³
 Extinction correction: *SHELXL97*
 Extinction coefficient: 0.0071 (7)
 Absolute structure: Flack (1983),
 1163 Friedel pairs
 Flack parameter: 0.02 (2)

Table 1

Selected geometric parameters (Å, °).

Zn1—Br1	2.3735 (8)	Zn1—N1	2.041 (5)
Zn1—Br2	2.3541 (8)	Zn1—N11	2.056 (5)
N1—Zn1—N11	106.30 (19)	N1—Zn1—Br1	107.76 (13)
N1—Zn1—Br2	109.38 (13)	N11—Zn1—Br1	104.50 (13)
N11—Zn1—Br2	111.56 (13)	Br2—Zn1—Br1	116.75 (3)

H atoms were placed in calculated positions, with C—H = 0.95 Å, and refined in riding mode, with *U*_{iso}(H) = 1.2*U*_{eq}(C).

Data collection: *IPDS* (Stoe & Cie, 1998b); cell refinement: *IPDS*; data reduction: *IPDS*; program(s) used to solve structure: *SHELXS97* (Sheldrick, 1997); program(s) used to refine structure: *SHELXL97* (Sheldrick, 1997); molecular graphics: *SHELXTL*

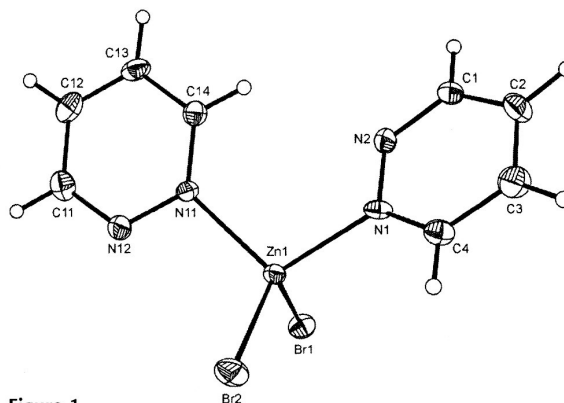


Figure 1

The molecular structure of (I) with 50% probability displacement ellipsoids (arbitrary spheres for H atoms).

(Bruker, 1998); software used to prepare material for publication: *SHELXTL*.

This work is supported by the state of Schleswig-Holstein and the Deutsche Forschungsgemeinschaft (project No. NA 720/1-1). We are very grateful to Professor Dr Wolfgang Bensch for the opportunity to use his experimental equipment.

References

- Allen, F. H. (2002). *Acta Cryst.* **B58**, 380–388.
 Bhosekar, G., Jess, I. & Näther, C. (2006a). *Acta Cryst.* **E62**, m1315–m1316.
 Bhosekar, G., Jess, I. & Näther, C. (2006b). *Z. Naturforsch. Teil B*, **61**, 721–726.
 Bhosekar, G., Jess, I. & Näther, C. (2006c). *Inorg. Chem.* In the press.
 Bruker (1998). *SHELXTL*. Version 5.1. Bruker AXS Inc., Madison, Wisconsin, USA.
 Flack, H. D. (1983). *Acta Cryst.* **A39**, 876–881.
 Sheldrick, G. M. (1997). *SHELXS97* and *SHELXL97*. University of Göttingen, Germany.
 Stoe & Cie (1998). *X-SHAPE* (Version 1.03) and *IPDS* (Version 2.89). Stoe & Cie, Darmstadt, Germany.

Supplemental material

Table 1. Crystal data and structure refinement for dibromo bis(pyridazine-N) znic(II)

Identification code	blz23	
Empirical formula	C ₈ H ₈ Br ₂ N ₄ Zn	
Formula weight	385.37	
Temperature	170(2) K	
Wavelength	0.71073 Å	
Crystal system	orthorhombic	
Space group	P2 ₁ 2 ₁ 2 ₁	
Unit cell dimensions	a = 8.8914(5) Å	α = 90°.
	b = 9.7191(7) Å	β = 90°.
	c = 13.8189(8) Å	γ = 90°.
Volume	1194.18(13) Å ³	
Z	4	
Density (calculated)	2.143 Mg/m ³	
Absorption coefficient	8.721 mm ⁻¹	
F(000)	736	
Crystal size	0.06 x 0.09 x 0.12 mm ³	
Theta range for data collection	2.56 to 28.02°.	
Index ranges	-9 ≤ h ≤ 11, -12 ≤ k ≤ 11, -18 ≤ l ≤ 18	
Reflections collected	6650	
Independent reflections	2833 [R(int) = 0.0487]	
Completeness to theta = 28.02°	99.6 %	
Refinement method	Full-matrix least-squares on F ²	
Data / restraints / parameters	2833 / 0 / 137	
Goodness-of-fit on F ²	1.020	
Final R indices [I > 2σ(I)]	R1 = 0.0382, wR2 = 0.0809	
R indices (all data)	R1 = 0.0549, wR2 = 0.0896	
Absolute structure parameter	0.02(2)	
Extinction coefficient	0.0071(7)	
Largest diff. peak and hole	0.810 and -0.842 e.Å ⁻³	

Remarks:

All non-hydrogen atoms were refined using anisotropic displacement parameters. The hydrogen atoms were positioned with idealized geometry and were refined isotropic ($U_{eq} = -1.2$) using a riding model with C-H = 0.95 Å for aromatic hydrogen atoms. There is one crystallographically independent molecules into the asymmetric unit, located at a general positions.

2 Publications

Table 2. Atomic coordinates ($\times 10^4$) and equivalent isotropic displacement parameters ($\text{\AA}^2 \times 10^3$). $U(\text{eq})$ is defined as one third of the trace of the orthogonalized U^{ij} tensor.

	x	y	z	$U(\text{eq})$
Br(1)	7393(1)	2265(1)	8304(1)	21(1)
Br(2)	7599(1)	593(1)	5642(1)	23(1)
N(1)	4290(5)	2132(5)	6666(3)	16(1)
N(2)	3590(6)	3307(5)	6944(4)	20(1)
C(1)	2105(7)	3304(6)	6950(4)	23(1)
C(2)	1226(7)	2184(7)	6715(5)	26(1)
C(3)	1953(8)	994(7)	6458(5)	26(2)
C(4)	3513(7)	1021(6)	6442(4)	20(1)
N(11)	7073(5)	4236(5)	6188(3)	15(1)
N(12)	8551(6)	4371(5)	6060(3)	20(1)
C(11)	9098(7)	5607(7)	5840(4)	23(1)
C(12)	8208(8)	6767(6)	5751(4)	23(1)
C(13)	6697(8)	6607(6)	5873(4)	22(1)
C(14)	6166(7)	5311(6)	6090(4)	18(1)

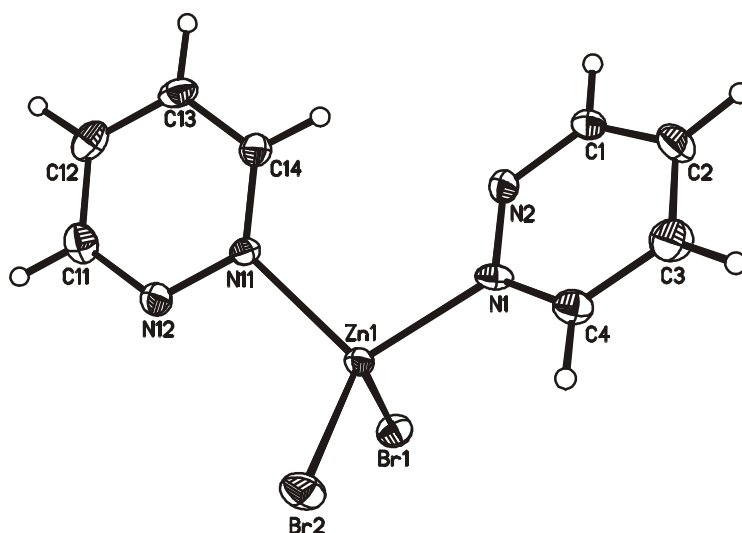


Table 3. Bond lengths [\AA] and angles [$^\circ$]

Zn(1)-N(1)	2.041(5)	N(1)-Zn(1)-Br(1)	107.76(13)
Zn(1)-N(11)	2.056(5)	N(11)-Zn(1)-Br(1)	104.50(13)
Zn(1)-Br(2)	2.3541(8)	Br(2)-Zn(1)-Br(1)	116.75(3)
Zn(1)-Br(1)	2.3735(8)	C(4)-N(1)-N(2)	121.1(5)
N(1)-C(4)	1.319(8)	C(4)-N(1)-Zn(1)	125.7(4)
N(1)-N(2)	1.356(7)	N(2)-N(1)-Zn(1)	113.3(4)
N(2)-C(1)	1.321(9)	C(1)-N(2)-N(1)	117.3(5)
C(1)-C(2)	1.378(9)	N(2)-C(1)-C(2)	124.6(6)
C(2)-C(3)	1.372(9)	C(3)-C(2)-C(1)	117.3(6)
C(3)-C(4)	1.387(9)	C(2)-C(3)-C(4)	117.4(6)
N(11)-C(14)	1.327(8)	N(1)-C(4)-C(3)	122.4(6)
N(11)-N(12)	1.332(7)	C(14)-N(11)-N(12)	120.6(5)
N(12)-C(11)	1.331(8)	C(14)-N(11)-Zn(1)	128.9(4)
C(11)-C(12)	1.383(9)	N(12)-N(11)-Zn(1)	110.1(4)
C(12)-C(13)	1.363(9)	C(11)-N(12)-N(11)	118.6(5)
C(13)-C(14)	1.378(9)	N(12)-C(11)-C(12)	123.2(6)
N(1)-Zn(1)-N(11)	106.30(19)	C(13)-C(12)-C(11)	117.4(6)
N(1)-Zn(1)-Br(2)	109.38(13)	C(12)-C(13)-C(14)	118.0(6)
N(11)-Zn(1)-Br(2)	111.56(13)	N(11)-C(14)-C(13)	122.2(6)

2 Publications

Table 4. Anisotropic displacement parameters ($\text{\AA}^2 \times 10^3$). The anisotropic displacement factor exponent takes the form: $-2\pi^2 [h^2 a^{*2} U_{11} + \dots + 2 h k a^* b^* U_{12}]$

	U_{11}	U_{22}	U_{33}	U_{23}	U_{13}	U_{12}
Zn(1)	13(1)	12(1)	20(1)	0(1)	0(1)	1(1)
Br(1)	23(1)	20(1)	19(1)	0(1)	-3(1)	0(1)
Br(2)	24(1)	19(1)	27(1)	-7(1)	2(1)	5(1)
N(1)	16(2)	15(2)	17(2)	0(2)	-5(2)	5(2)
N(2)	16(3)	15(2)	30(3)	2(2)	3(2)	-2(2)
C(1)	17(3)	15(3)	35(3)	3(2)	4(2)	5(2)
C(2)	14(3)	34(3)	30(3)	6(3)	-3(2)	2(3)
C(3)	25(3)	18(3)	35(4)	-5(2)	-5(3)	-3(3)
C(4)	19(3)	19(3)	20(3)	-1(2)	-3(2)	2(3)
N(11)	16(2)	14(2)	15(2)	2(2)	1(2)	2(2)
N(12)	17(2)	16(2)	26(2)	1(2)	2(2)	-1(2)
C(11)	21(3)	23(3)	25(3)	-5(3)	4(2)	-3(3)
C(12)	33(4)	16(3)	19(3)	-1(2)	0(3)	-5(3)
C(13)	29(3)	15(3)	21(3)	2(2)	1(3)	7(3)
C(14)	19(3)	20(3)	16(2)	1(2)	2(2)	2(2)

Table 5. Hydrogen coordinates ($\times 10^4$) and isotropic displacement parameters ($\text{\AA}^2 \times 10^3$)

	x	y	z	U(eq)
H(1)	1607	4131	7128	27
H(2)	159	2235	6730	31
H(3)	1410	183	6298	31
H(4)	4040	209	6264	23
H(11)	10150	5696	5739	28
H(12)	8633	7641	5611	27
H(13)	6031	7365	5809	26
H(14)	5114	5183	6173	22

Acta Crystallographica Section E
Structure Reports
 Online

ISSN 1600-5368

**Gaurav Bhosekar, Inke Jess and
 Christian Näther***

Institut für Anorganische Chemie, Christian-
 Albrechts-Universität Kiel, Olshausenstrasse 40,
 D-24098 Kiel, Germany

Correspondence e-mail:
 cnaether@ac.uni-kiel.de

Key indicators

Single-crystal X-ray study
 $T = 170$ K
 Mean $\sigma(\text{C}-\text{C}) = 0.007$ Å
 R factor = 0.028
 wR factor = 0.065
 Data-to-parameter ratio = 22.4

For details of how these key indicators were
 automatically derived from the article, see
<http://journals.iucr.org/e>.

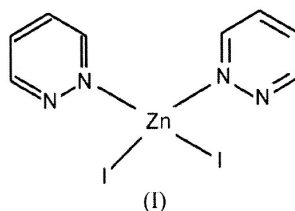
Diiodobis(pyridazine- κN)zinc(II)

In the crystal structure of the molecular title compound, $[\text{ZnI}_2(\text{C}_4\text{H}_4\text{N}_2)_2]$, the Zn atom is coordinated by two I atoms and two pyridazine ligands, resulting in a slightly distorted ZnN_2I_2 tetrahedral geometry.

Received 31 July 2006
 Accepted 1 August 2006

Comment

We are interested in the synthesis, structures and thermal properties of coordination compounds containing zinc(II) cations, halide ions and N -donor ligands (Bhosekar *et al.*, 2006*a,b,c*). For a particular zinc(II) halide and a specific N -donor ligand, frequently several compounds of different stoichiometry are found, which differ in the ratio between the inorganic and organic components. We have found that most of the ligand-rich compounds can be transformed into ligand-poor compounds on heating. Starting from these findings, we have initiated systematic investigations on the structures and properties of zinc(II) halide coordination polymers. We report here the synthesis and structure of the molecular title compound, (I).



In the asymmetric unit of (I), all atoms are in general positions. The Zn atom is coordinated by two I atoms and two N atoms of two pyridazine ligands in a slightly distorted tetrahedral geometry (Fig. 1). The discrete complex molecules are stacked in the a -axis direction (Fig. 2). It should be noted that the title compound is not isotypic with the previously reported dibromobis(pyridazine- κN)zinc(II) compound, which crystallizes in the orthorhombic space group $P2_12_12_1$ (Bhosekar *et al.*, 2006*d*).

Concerning the thermal properties of (I), we have not found any evidence of the formation of a ligand-poor intermediate. On heating, the compound loses all its organic ligands in one step and transforms directly into zinc(II) iodide.

Experimental

A crystalline powder of (I) can be prepared if a suspension of 1 mmol (319.18 mg) of zinc(II) iodide and 1.0 mmol (80 mg) of pyridazine in 1 ml of acetonitrile is stirred for 2 d. Single crystals of (I) were

metal-organic papers

obtained by dissolving 0.1 mmol (31.9 mg) of zinc(II) iodide and 0.1 mmol (8.0 mg) of pyridazine in 1.0 ml of ethanol. After slow evaporation of the solvent, colourless crystals formed. The homogeneity of the product was confirmed by X-ray powder diffraction.

Crystal data

[ZnI₂(C₄H₄N₂)₂]
M_r = 479.35
 Monoclinic, *P*2₁/*n*
a = 7.9702 (5) Å
b = 12.9720 (7) Å
c = 12.5449 (9) Å
 β = 95.928 (8)°
V = 1290.07 (14) Å³

Z = 4
D_x = 2.468 Mg m⁻³
 Mo *K*α radiation
 μ = 6.67 mm⁻¹
T = 170 (2) K
 Block, colourless
 0.09 × 0.08 × 0.07 mm

Data collection

Stoe IPDS-1 diffractometer
 φ scans
 Absorption correction: numerical
 (*X-SHAPE*; Stoe & Cie, 1998)
T_{min} = 0.561, *T_{max}* = 0.632

8867 measured reflections
 3063 independent reflections
 2402 reflections with *I* > 2σ(*I*)
R_{int} = 0.042
 θ_{\max} = 28.0°

Refinement

Refinement on *F*²
R [*F*² > 2σ(*F*²)] = 0.028
wR (*F*²) = 0.065
S = 0.99
 3063 reflections
 137 parameters
 H-atom parameters constrained

$w = 1/[\sigma^2(F_o^2) + (0.036P)^2]$
 where $P = (F_o^2 + 2F_c^2)/3$
 (Δ/σ)_{max} = 0.001
 $\Delta\rho_{\max} = 0.84 \text{ e } \text{Å}^{-3}$
 $\Delta\rho_{\min} = -0.88 \text{ e } \text{Å}^{-3}$
 Extinction correction: *SHELXL97*
 Extinction coefficient: 0.0020 (2)

Table 1

Selected bond lengths (Å).

Zn1–N11	2.058 (4)	Zn1–I2	2.5463 (6)
Zn1–N1	2.065 (3)	Zn1–I1	2.5712 (6)

The H atoms were positioned with idealized geometry (C–H = 0.95 Å) and refined as riding, with *U*_{iso}(H) = 1.2*U*_{eq}(C).

Data collection: *IPDS* (Stoe & Cie, 1998); cell refinement: *IPDS*; data reduction: *IPDS*; program(s) used to solve structure: *SHELXS97* (Sheldrick, 1997); program(s) used to refine structure: *SHELXL97* (Sheldrick, 1997); molecular graphics: *XP* in *SHELXTL* (Bruker, 1998); software used to prepare material for publication: *CIFTAB* in *SHELXTL*.

This work is supported by the state of Schleswig–Holstein and the Deutsche Forschungsgemeinschaft (project No. NA 720/1–1). We are very grateful to Professor Dr. Wolfgang Bensch for the use of his experimental equipment.

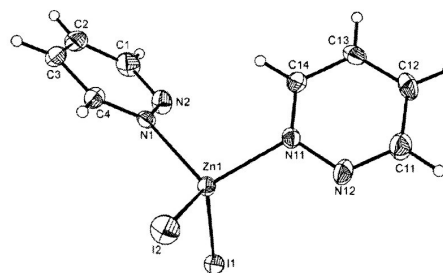


Figure 1
 The molecular structure of (I), showing displacement ellipsoids drawn at the 50% probability level (arbitrary spheres for the H atoms).

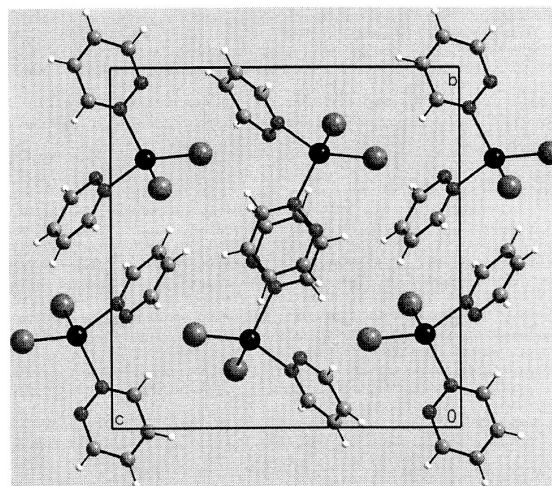


Figure 2
 Packing of (I), viewed along the *a* axis.

References

- Bhosekar, G., Jess, I. & Näther, C. (2006a). *Acta Cryst.* **E62**, m1315–m1316.
 Bhosekar, G., Jess, I. & Näther, C. (2006b). *Z. Naturforsch. Teil B*, **61**, 721–726.
 Bhosekar, G., Jess, I. & Näther, C. (2006c). *Inorg. Chem.* **43**, 6508–6515.
 Bhosekar, G., Jess, I. & Näther, C. (2006d). *Acta Cryst.* **E62**, m1859–m1860.
 Bruker (1998). *SHELXTL*. Bruker AXS Inc., Madison, Wisconsin, USA.
 Sheldrick, G. M. (1997). *SHELXS97* and *SHELXL97*. University of Göttingen, Germany.
 Stoe & Cie (1998). *X-SHAPE* (Version 1.03) and *IPDS* (Version 2.89). Stoe & Cie, Darmstadt, Germany.

Supplemental material

Table 1. Crystal data and structure refinement for diiodo-bis(pyridazin N) zinc (II).

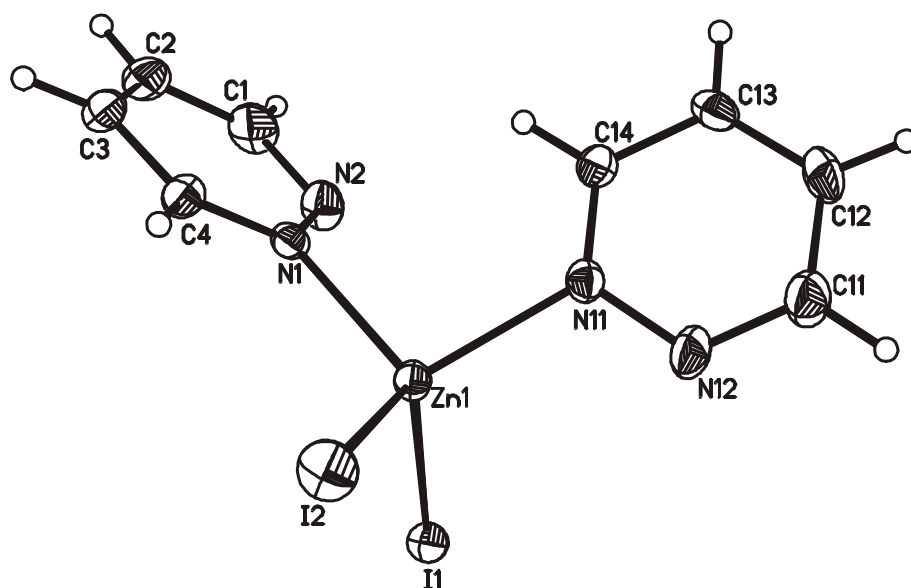
Identification code	gbb35	
Empirical formula	$C_8H_8 I_2 N_4 Zn_1$	
Formula weight	598.89	
Temperature	170(2) K	
Wavelength	0.71073 Å	
Crystal system	monoclinic	
Space group	$P2_1/n$	
Unit cell dimensions	$a = 7.9702(5)$ Å	$\alpha = 90^\circ$.
	$b = 12.9720(7)$ Å	$\beta = 95.928(8)^\circ$.
	$c = 12.5449(9)$ Å	$\gamma = 90^\circ$.
Volume	1290.07(14) Å ³	
Z	4	
Density (calculated)	3.083 Mg/m ³	
Absorption coefficient	9.956 mm ⁻¹	
F(000)	1068	
Crystal size	0.06 x 0.09 x 0.12 mm ³	
Theta range for data collection	2.26 to 27.99°.	
Index ranges	$-9 \leq h \leq 10, -17 \leq k \leq 12, -16 \leq l \leq 16$	
Reflections collected	8867	
Independent reflections	3063 [R(int) = 0.0416]	
Completeness to theta = 27.99°	98.0 %	
Refinement method	Full-matrix least-squares on F ²	
Data / restraints / parameters	3063 / 0 / 137	
Goodness-of-fit on F ²	0.988	
Final R indices [I > 2σ(I)]	R1 = 0.0278, wR2 = 0.0606	
R indices (all data)	R1 = 0.0441, wR2 = 0.0653	
Extinction coefficient	0.0020(2)	
Largest diff. peak and hole	0.838 and -0.877 e.Å ⁻³	

Remarks:

All non-hydrogen atoms were refined using anisotropic displacement parameters. The hydrogen atoms were positioned with idealized geometry and were refined isotropic ($U_{eq} = -1.2$) using a riding model with C-H = 0.95 Å for aromatic hydrogen atoms. There is one crystallographically independent molecules into the asymmetric unit, located at a general positions.

Table 2. Atomic coordinates ($\times 10^4$) and equivalent isotropic displacement parameters ($\text{\AA}^2 \times 10^3$)U(eq) is defined as one third of the trace of the orthogonalized U_{ij} tensor.

	x	y	z	U(eq)
Zn(1)	2926(1)	2429(1)	6009(1)	17(1)
I(1)	5220(1)	2575(1)	7601(1)	20(1)
I(2)	162(1)	1615(1)	6429(1)	29(1)
N(1)	3859(5)	1567(3)	4818(3)	18(1)
N(2)	5372(5)	1907(3)	4575(3)	25(1)
C(1)	6102(7)	1380(4)	3850(4)	32(1)
C(2)	5431(7)	495(4)	3351(4)	30(1)
C(3)	3906(7)	149(4)	3616(3)	27(1)
C(4)	3131(6)	735(3)	4367(3)	21(1)
N(11)	2721(5)	3854(3)	5289(3)	19(1)
N(12)	2094(6)	4580(3)	5899(3)	28(1)
C(11)	2031(7)	5542(4)	5537(4)	32(1)
C(12)	2581(6)	5841(4)	4553(4)	28(1)
C(13)	3222(6)	5089(4)	3958(3)	23(1)
C(14)	3259(6)	4083(3)	4361(3)	20(1)



2 Publications

Table 3. Bond lengths [Å] and angles [°].

Zn(1)-N(1)	2.065(3)	Zn(1)-N(11)	2.058(4)
Zn(1)-I(2)	2.5463(6)	Zn(1)-I(1)	2.5712(6)
N(1)-C(4)	1.324(6)	N(11)-C(14)	1.315(5)
N(1)-N(2)	1.348(5)	N(11)-N(12)	1.342(5)
N(2)-C(1)	1.319(6)	N(12)-C(11)	1.327(6)
C(1)-C(2)	1.388(7)	C(11)-C(12)	1.407(7)
C(2)-C(3)	1.369(8)	C(12)-C(13)	1.360(7)
C(3)-C(4)	1.402(6)	C(13)-C(14)	1.399(6)
N(1)-Zn(1)-I(2)	108.02(11)	N(11)-Zn(1)-N(1)	100.76(14)
N(1)-Zn(1)-I(1)	108.75(10)	N(11)-Zn(1)-I(2)	115.61(11)
I(2)-Zn(1)-I(1)	115.53(2)	C(14)-N(11)-N(12)	121.4(4)
C(4)-N(1)-N(2)	122.2(4)	C(14)-N(11)-Zn(1)	124.9(3)
C(4)-N(1)-Zn(1)	125.1(3)	N(12)-N(11)-Zn(1)	113.4(3)
N(2)-N(1)-Zn(1)	112.6(3)	C(11)-N(12)-N(11)	117.9(4)
C(1)-N(2)-N(1)	117.1(4)	N(12)-C(11)-C(12)	123.7(4)
N(2)-C(1)-C(2)	124.2(5)	C(13)-C(12)-C(11)	116.9(4)
C(3)-C(2)-C(1)	118.2(4)	C(12)-C(13)-C(14)	117.8(4)
C(2)-C(3)-C(4)	116.7(4)	N(11)-C(14)-C(13)	122.2(4)
N(1)-C(4)-C(3)	121.7(4)	N(11)-Zn(1)-I(1)	107.00(10)

Table 4. Anisotropic displacement parameters ($\text{\AA}^2 \times 10^3$). The anisotropic displacement factor exponent takes the form: $-2\pi^2 [h^2 a^{*2} U_{11} + \dots + 2 h k a^* b^* U_{12}]$

	U_{11}	U_{22}	U_{33}	U_{23}	U_{13}	U_{12}
Zn(1)	18(1)	15(1)	19(1)	0(1)	5(1)	0(1)
I(1)	20(1)	21(1)	20(1)	0(1)	2(1)	-1(1)
I(2)	21(1)	33(1)	36(1)	1(1)	10(1)	-7(1)
N(1)	20(2)	17(2)	16(1)	3(1)	3(1)	4(1)
N(2)	22(2)	22(2)	32(2)	1(2)	11(2)	-4(2)
C(1)	34(3)	32(3)	34(2)	5(2)	21(2)	-1(2)
C(2)	41(3)	30(3)	22(2)	-2(2)	11(2)	9(2)
C(3)	37(3)	22(2)	20(2)	-4(2)	-2(2)	5(2)
C(4)	20(2)	21(2)	20(2)	-2(2)	-3(2)	4(2)
N(11)	20(2)	15(2)	21(2)	-1(1)	1(1)	-1(1)
N(12)	34(2)	20(2)	32(2)	-3(2)	12(2)	7(2)
C(11)	38(3)	24(2)	37(3)	1(2)	16(2)	5(2)
C(12)	32(3)	15(2)	36(2)	5(2)	1(2)	-4(2)
C(13)	26(3)	23(2)	19(2)	5(2)	-4(2)	-5(2)
C(14)	22(2)	18(2)	20(2)	-2(2)	1(2)	-2(2)

Table 5. Hydrogen coordinates ($\times 10^4$) and isotropic displacement parameters ($\text{\AA}^2 \times 10^3$)

	x	y	z	U(eq)
H(1)	7154	1623	3658	39
H(2)	6014	140	2840	37
H(3)	3398	-458	3307	32
H(4)	2056	531	4556	25
H(11)	1589	6058	5967	38
H(12)	2508	6536	4315	33
H(13)	3632	5242	3292	28
H(14)	3688	3546	3950	24

Structures and Properties of Three Polymorphic Modifications based on Tetrahedral Building Blocks of Dichlorobis(pyridazine-N) Zinc(II)

Gaurav Bhosekar,[†] Inke Jess,[†] Zdenek Havlas,[‡] and Christian Näther^{*†}

Institut für Anorganische Chemie, Universität zu Kiel, Olshausenstrasse 40 (Otto-Hahn-Platz 6-7), D-24098-Kiel, Germany, and Institut of Organic Chemistry and Biochemistry, Academy of Sciences of the Czech Republic, Flemingovo no. 2, 16610 Prague 6, Czech Republic

Received December 6, 2006; Revised Manuscript Received July 4, 2007

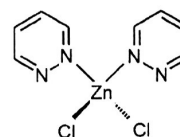
ABSTRACT: Reaction of zinc(II) chloride with pyridazine under different conditions leads to the formation of three polymorphic modifications of dichlorobis(pyridazine-N) zinc(II). Forms **I** and **II** crystallize monoclinic in space group *Cc* (**I**) and *P2₁/c* (**II**), respectively, whereas form **III** crystallizes orthorhombic in space group *Pna2₁*. In all three forms, the zinc atoms are surrounded by two chloro atoms and two pyridazine ligands within distorted tetrahedra, and the orientations of the pyridazine rings within these tetrahedra are different. In the crystal structure, the tetrahedral building blocks are packed differently and are connected by intermolecular C–H···Cl and C–H···N interactions. Crystallization experiments clearly show that form **I** represents the thermodynamically most stable form at room temperature, whereas forms **II** and **III** are metastable. Theoretical calculations show that in form **II** the most stable molecular structure is found, whereas the molecular structure in form **III** is less stable by only 8 kJ/mol. Differential thermoanalysis and thermogravimetry measurements reveal that all forms decompose into a new ligand-deficient compound [ZnCl₂(pyridazine)], which can also be prepared in solution. Form **I** can be transformed into form **II**, which is more stable at higher temperatures as evidenced by differential scanning calorimetry (DSC) measurements. On some of the DSC measurements, form **I** decomposes without further transformation into form **II**. Both forms **I** and **II** behave enantiotropic. The DSC thermogram of form **III** gave no indication of a polymorphic transformation.

Introduction

Recently, investigations on coordination compounds and polymers, inorganic–organic hybrid compounds, or metal organic frameworks have become of increasing interest.^{1–3} One major goal in this area is the preparation of compounds with desired physical properties.^{4–6} Several aspects will have to be taken into consideration to achieve this goal, which include understanding of the structure–property relationships and development of synthetic methodologies for a more directed design of the structures of these solids, in order to influence their physical properties in a desired way.^{5–21} For the design strategies, a specific knowledge of the intermolecular interactions in crystals and their interplay is important. In this context, one has to be aware of the phenomenon of polymorphism or isomerism, which is frequently found in such compounds.^{22–34} If polymorphism or isomerism is detected, in addition to the structural aspects, the thermodynamic stability, as well as the interconversion behavior, should be investigated. It is also desirable to find suitable conditions for the preparation of each form as a phase pure compound.

In our ongoing investigations on the synthesis, structures, and properties of new coordination polymers, we have started systematic investigations of their thermal behavior because we have demonstrated that new ligand-deficient coordination polymers can be conveniently prepared by thermal decomposition of suitable ligand-rich precursor compounds.^{30–38} During these investigations, we obtained several isomers or polymorphic modifications of the precursor compounds, which were characterized for their thermodynamic stability, thermal properties, and transition behavior.^{30–38} For coordination compounds based

Scheme 1



on zinc(II) chloride and pyridazine as the N-donor ligand, we have obtained three different polymorphic modifications of dichlorobis(pyridazine-N) zinc(II) (Scheme 1), all of which transform into a new ligand-deficient compound on heating. The polymorphism of these simple coordination compounds is based predominantly on a different packing of the tetrahedral building blocks within the solid. Here we report the results of these investigations.

Experimental Section

General Remarks. Zinc(II) chloride and pyridazine were purchased from Alfa Aesar. The purity of all compounds was investigated by X-ray powder diffraction.

Preparation of Form I of [ZnCl₂(pyridazine)₂]. Form **I** was prepared by the reaction of zinc(II) chloride (1.0 mmol, 136.28 mg) with pyridazine (2.0 mmol, 160.18 mg) in 0.5 mL of acetonitrile. The mixture was stirred for a day at room temperature, and the residue was filtered off and washed with diethyl ether. Yield = 76.0%. IR data: 402(s), 395(m), 383(w), 327(s), 302(s), 219(m), 208(w), 163(m), 147(m). Raman data: 3143(w), 3062(s), 3022(w), 1575(m), 1292(m), 1237(w), 1206(m), 1146(s), 1070(m), 1004(w), 969(m), 681(w), 640(w), 302(w), 144(w), 99(s).

Single crystals of form **I** were obtained by dissolving zinc(II) chloride (0.25 mmol, 34 mg) and pyridazine (1.5 mmol, 120.12 mg) in 1.0 mL of acetonitrile. On slow evaporation of the solvent, single crystals of form **I** grow within a week.

Preparation of Form II of [ZnCl₂(pyridazine)₂]. Form **II** was prepared by dissolving zinc chloride (1.0 mmol, 136.28 mg) and pyridazine (4.0 mmol, 320.32 mg) in 2.0 mL of acetonitrile. To the

* To whom correspondence should be addressed. Fax: +49 (0)431/880-1520. E-mail: cnaether@ac.uni-kiel.de.

[†] Universität zu Kiel.

[‡] Academy of Sciences of the Czech Republic.

Table 1. Selected Crystal Data and Results of the Structure Refinement for Forms I, II, and III

form	I	II	III
formula	C ₈ H ₈ N ₄ ZnCl ₂	C ₈ H ₈ N ₄ ZnCl ₂	C ₈ H ₈ N ₄ ZnCl ₂
MW/g·mol ⁻¹	296.45	296.45	296.45
crystal color	colorless	colorless	colorless
crystal size/mm ⁻¹	0.07 × 0.10 × 0.13	0.08 × 0.14 × 0.22	0.06 × 0.10 × 0.14
crystal system	monoclinic	monoclinic	orthorhombic
space group	Cc	P2 ₁ /c	Pna2 ₁
a/Å	14.0339 (1)	8.0254 (5)	25.4704 (1)
b/Å	9.2082 (5)	16.9729(2)	7.5932(4)
c/Å	8.9873 (7)	8.5260(6)	11.7460(9)
β/°	100.579(9)	95.619(8)	
V/Å ³	1141.7 (2)	1155.8 (2)	2271.7 (2)
temp/K	170	170	220
Z	4	4	8
D _{calc} /g·cm ⁻³	1.725	1.704	1.734
F(000)	592	592	1184
2θ range/°	2.66–28.00	2.40–27.97	2.36–26.92
h/k/l ranges	–18/18 –11/12 –11/11	–10/10 –22/21 –10/11	–30/30 –9/9 –14/14
μ(MoKα)/mm ⁻¹	2.59	2.56	2.60
absorption corr	numerical	numerical	numerical
min/max transm	0.626/0.734	0.366/0.813	0.630/0.757
measured refln	5399	6630	15632
R _{int}	0.0265	0.0348	0.0333
independent refl.	2547	2692	4685
refln with I > 2σ(I)	2346	2345	4177
parameters	137	137	272
Flack-x parameter	–0.004(11)		0.06(1)
wR ₂ [all data]	0.0595	0.0994	0.0638
R ₁ [I > 2σ(I)]	0.0246	0.0333	0.0257
GOF	0.992	0.797	0.968
residual electron density/e·Å ⁻³	0.292/–0.467	0.742/ –0.862	0.332/–0.461

clear solution 2.0 mL of ether was added as precipitant. The crystalline suspension was stirred for 1 h at room temperature and filtered off. Yield = 79.1% based on ZnCl₂. IR data: 401(m), 393(m), 376(m), 333(m), 309(m), 214(w), 204(w), 179(w), 159(m), 133(m). Raman data: 3143(w), 3062(s), 3027(w), 1565(m), 1297(w), 1202(m), 1166(w), 1065(m), 979(s), 670(w), 645(w), 382(w), 302(m), 210(w), 160(s), 109(m), 88(m).

Single crystals of form **II** were prepared using the same procedure as for single crystals of form **I**. On slow evaporation of the solvent single crystals of form **II** grow within 4 days.

Preparation of Form III of [ZnCl₂(pyridazine)₂]. Form **III** was prepared by dissolving zinc chloride (1.0 mmol, 136.28 mg) and pyridazine (4.0 mmol, 320.32 mg) in 2.0 mL of acetonitrile. To this mixture 2.0 mL of ether was added as precipitant. The crystalline suspension was filtered off immediately. Yield = 63.0% based on ZnCl₂. IR data: 396(s), 308(m), 213(w), 202(w), 167(w), 159(w), 146(m), 188(m). Raman data: 3145(m), 3063(s), 3028(w), 1573(m), 1296(w), 1203(m), 1163(w), 1075(m), 1050(m), 973(m), 680(m), 645(m), 373(w), 297(m), 204(w), 145(m), 96(s).

Single crystals of form **III** were obtained by dissolving zinc(II) chloride (0.5 mmol, 68.14 mg) and pyridazine (1.0 mmol, 80.08 mg) in 2.0 mL of acetonitrile. On slow evaporation of the solvent single crystals of form **III** grow within 2 days.

Single Crystal Structure Analysis. All data were measured using an Imaging Plate Diffraction system (IPDS-1) from STOE & CIE. The structure solutions were performed with direct methods using SHELXS-97,³⁹ and structure refinements were performed against F² using SHELXL-97.³⁹ For all structures, a numerical absorption correction was applied. All nonhydrogen atoms were refined with anisotropic displacement parameters. All hydrogen atoms were positioned with idealized geometry and were refined with fixed isotropic displacement parameters ($U_{eq}(H) = 1.2U_{eq}(C)$) using a riding model with $d_{C-H} = 0.95$ Å. The absolute structures of forms **I** and **III** were determined and are in agreement with the selected setting.

Crystallographic data have been deposited with the Cambridge Crystallographic Data Centre quoting the deposition number CCDC 666927 for form **I**, CCDC 666928 for form **II**, and CCDC 666929 for form **III**. Copies may be obtained free of charge on application to the Director, CCDC, 12 Union Road, Cambridge CB2 1E2, UK (fax: Int. Code +(44)01223/3 36–033, e-mail: deposit@chemcryst.cam.ac.uk).

X-ray Powder Diffraction. Powder diffraction experiments were performed using a STOE STADI P transmission powder diffractometer with CuKα-radiation ($\lambda = 154.0598$ p.m.), which is equipped with a position sensitive detector (scan range: 5° to 45°) from STOE & CIE.

Differential Thermoanalysis and Thermogravimetry (DTA-TG). DTA-TG measurements were performed in Al₂O₃ crucibles using a STA-409CD thermo balance from Netzsch. Several measurements under nitrogen atmosphere (purity 5.0) with a heating rate of 4 °C/min were performed.

Differential Scanning Calorimetry. DSC investigations were performed with the DSC 204/1/F device from Netzsch. The measurements were performed in Al pans with heating rates of 3 °C/min. The instrument was calibrated using standard reference materials.

Spectroscopy. FT-IR spectra were recorded on a Genesis Series FTIR spectrometer, manufactured by ATI Mattson in KBr pellets. Raman spectra were collected using FT-Raman-Modul FRA 106 manufactured by Bruker using laser radiation (1064 nm) in the range of –500 to 3300 cm⁻¹.

Quantum Mechanical Calculations. All calculations were performed using the Turbomole Program, Version 5.8. The calculations were performed at the RI-MP2 level,^{40,41} using the polarized triple-zeta basis set TZVP. The molecular geometry was optimized starting from the crystal structure geometries of different forms, without or with restrictions.

Results and Discussion

Crystal Structures. Reaction of zinc(II) chloride with pyridazine under different conditions leads to three polymorphic modifications of ZnCl₂(pyridazine)₂ (see Experimental Section). Form **I** crystallizes in the monoclinic, noncentrosymmetric space group Cc, form **II** crystallizes in the monoclinic space group P2₁/c, and form **III** crystallizes in the orthorhombic, noncentrosymmetric space group Pna2₁ (Table 1). Forms **I** and **II** crystallize with one crystallographically independent formula unit in the asymmetric unit, while in the structure of form **III** two crystallographically independent formula units are found (Figure 1). The zinc atoms are coordinated to two chlorine atoms

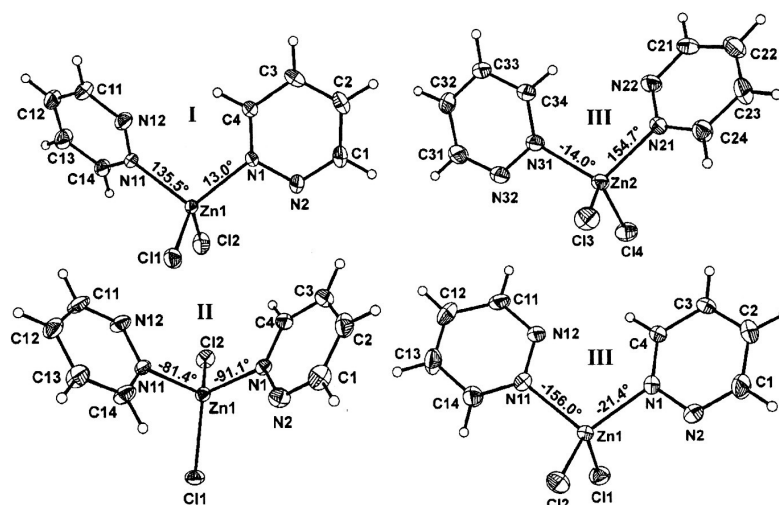


Figure 1. Molecular structures of forms **I**, **II**, and **III** with labelling, displacement ellipsoids drawn at the 50% probability level, and C–N–Zn–N torsion angles ($^{\circ}$) around the Zn–N bonds. Please note: Form **III** crystallizes with two crystallographically independent molecules in the asymmetric unit.

Table 2. Bond Lengths (\AA) and Angles ($^{\circ}$) for Forms **I, **II**, and **III****

form	I	II	III (1)	III (2)
Zn(1)–N(1)	2.049(2)	2.046(2)	2.049(3)	2.065(3)
Zn(1)–N(11)	2.056(2)	2.065(2)	2.058(3)	2.053(3)
Zn(1)–Cl(1)	2.2240(8)	2.2211(6)	2.2282(7)	2.2236(7)
Zn(1)–Cl(2)	2.2180(7)	2.2092(6)	2.2188(7)	2.2181(7)
N(1)–Zn(1)–N(11)	105.87(9)	98.43(7)	107.71(11)	106.20(10)
N(1)–Zn(1)–Cl(1)	110.21(7)	113.04(5)	108.56(7)	104.70(8)
N(11)–Zn(1)–Cl(1)	107.68(7)	103.53(5)	106.55(7)	108.76(8)
N(1)–Zn(1)–Cl(2)	110.81(7)	107.68(5)	111.31(7)	106.58(7)
N(11)–Zn(1)–Cl(2)	104.66(7)	112.89(5)	103.33(7)	111.02(7)
Cl(2)–Zn(1)–Cl(1)	116.85(3)	119.32(2)	118.68(3)	118.69(3)

and two pyridazine ligands within tetrahedra in all forms, which are differently distorted in the three modifications (Figure 1 and Table 2). It must be noted that the distortion increases in the direction **III** < **I** < **II**.

Differences in all three modifications are also found for the orientation of the pyridazine ligands, which are differently rotated around the Zn–N bond (Figure 1). This is obvious if the molecular structures are fitted onto each other (Figure 2). However, it can be assumed that the distortion of the bond angles will influence the energies of all three forms much larger than the rotation of the pyridazine rings. However, because of the large differences in the rotation of the ligands the title compound shows conformational polymorphism.

Differences are also observed in the packing of the tetrahedral building blocks in all three forms (Figures 3–5). In form **I**, two complexes form dimeric units, which are stacked into columns that are oriented in the direction of the crystallographic *c*-axis (Figure 3). Between these columns, short distances are found between the hydrogen atoms of the ligands and the chlorine atoms, which are indicative of weak C–H \cdots Cl interactions.⁴² In form **I** altogether five such interactions are found in which the C \cdots Cl distance is in maximum 3.7 \AA (Table 3 and Figure 3). In addition, one intramolecular C–H \cdots N contact between the two different six-membered rings within one complex is found (Table 3 and figure 3). One of the chlorine atoms (Cl2) in the columns is always directed along the *a*-axis, which is probably responsible for the polar structure of this modification (Figure 3).

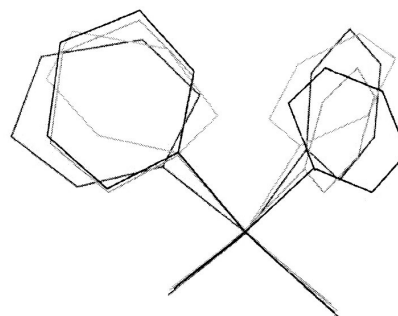


Figure 2. Molecular structures of forms **I**, **II**, and **III** fitted onto each other (form **I** = blue; form **II** = red; form **IIIA** = black; form **IIIB** = green).

In the crystal structure of form **II** a different packing of the tetrahedral building blocks is found. One pyridazine ring of each [ZnCl₂(pyridazine)₂] complex is stacked into columns, which are oriented in the direction of the crystallographic *c*-axis (Figure 4). Within these columns two neighboring pyridazine ligands are rotated relative to each other by 30 $^{\circ}$ along the stacking axis, and the dihedral angle between their molecular planes amounts to 29.8 $^{\circ}$. As in form **I** intermolecular C–H \cdots Cl interactions are found, but in contrast to form **I** only one such interaction is found up to 3.7 \AA ,⁴² (Table 3 and Figure 4). In addition to these interactions, two C–H \cdots N contacts are found between N12 and H4 and between C11–H11 and N2, which are indicative of a very weak interaction (Table 3 and Figure 4).

The crystal structure of form **III** is very similar to that of form **II**. Each of the two pyridazine rings of both crystallographically independent complexes are stacked into columns which elongate in the direction of the *b*-axis (Figure 5). Within these columns, two neighboring pyridazine rings are slightly shifted relative to each other, and the dihedral angles in both independent complexes amount to 9.0 and 10.4 $^{\circ}$. The pyridazine rings within these columns are connected into dimers by weak C–H \cdots N interactions (Table 3 and Figure 5). Additionally, intermolecular C–H \cdots Cl interactions are found, but in contrast

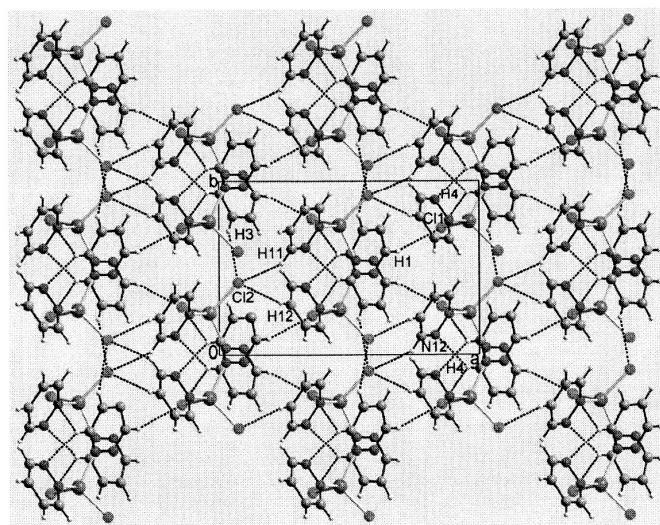


Figure 3. Crystal structure of form I with view along the *c*-axis. Intermolecular C–H···Cl and C–H···N interactions are shown as dashed lines.

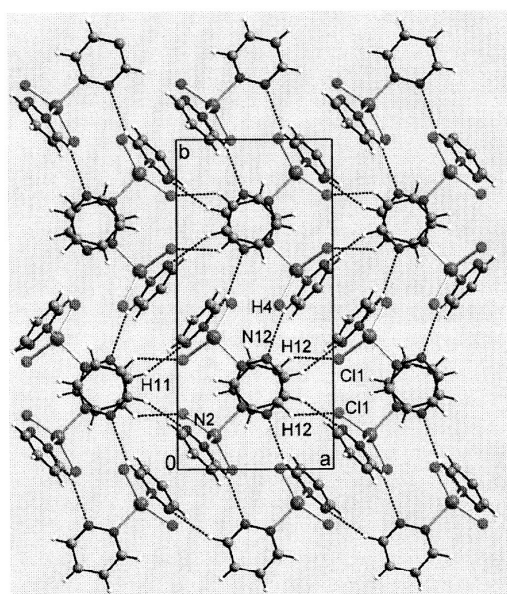


Figure 4. Crystal structure of form II with view along the *c*-axis. Intermolecular C–H···Cl and C–H···N interactions are shown as dashed lines.

to form **I** and **II** altogether six such interactions are observed,⁴² (Table 3 and Figure 5).

Crystallization Experiments. The initial aim of our investigation was to determine if compounds of different stoichiometry can be prepared in solution as a function of the molar ratios of zinc(II) chloride and pyridazine. Accordingly, zinc(II) chloride and pyridazine were mixed in different stoichiometric ratios in constant amounts of acetonitrile so that crystalline powders are formed. These suspensions were stirred for a week so that the thermodynamically most stable compounds are formed. Afterwards the products were identified by X-ray powder diffraction and elemental analysis. These investigations

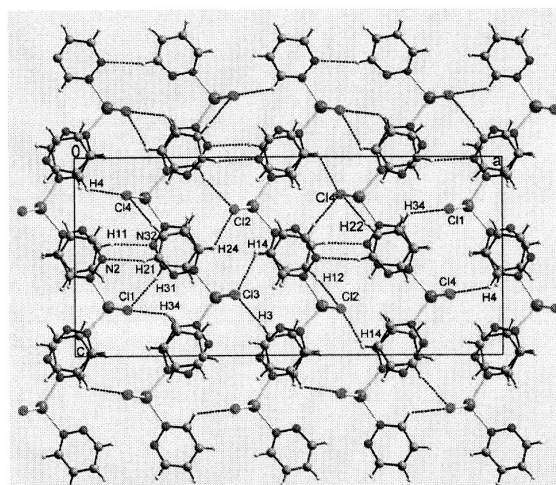


Figure 5. Crystal structure of form III with view along the *b*-axis. Intermolecular C–H···Cl and C–H···N interactions are shown as dashed lines.

clearly show that under these conditions two different compounds, namely, the 1:2 compound (Form **I**) and one ligand-deficient 1:1 compound, are obtained (Table 4). Our attempts to prepare single crystals of the 1:1 compound suitable for structure determination were not successful. Hence this compound was characterized by X-ray powder diffraction.

Time-dependent X-ray powder measurements were performed to determine if forms **I**, **II**, and **III** are formed in solution as function of the reaction time. In this experiment, zinc(II) chloride and pyridazine were mixed in 1:4 ratio in 2.0 mL of acetonitrile to obtain a clear solution. Afterwards the compound was precipitated with diethylether, and the solid product thus formed was investigated by powder diffraction. A comparison of the powder pattern of the products obtained at various time intervals (Figure 6) clearly shows that modification **III** is formed immediately, which transforms within about 1 h into form **II**.

Dichlorobis(pyridazine-N) Zinc(II) Building Blocks

Table 3. Intermolecular C–H...Cl and C–H...N Interactions (Å, °) for Forms I, II, and III^a

D–H...A–Zn	H...A	D...A	D–H...A	H...Cl–Zn
Form I				
C1–H1...C11–Zn1	2.78	3.604	145.2	112.55
C3–H3...C12–Zn1	2.83	3.521	129.4	126.26
C4–H4...C11–Zn1	2.86	3.597	135.2	91.21
C11–H11...C12–Zn1	2.94	3.672	130.3	149.06
C12–H12...C12–Zn1	2.78	3.646	151.9	102.47
C4–H4...N12	2.53	3.291	136.7	
Form II				
C4–H4...N12	2.71	3.396	129.3	
C11–H11...N2	2.73	3.591	150.9	
C12–H12...C11–Zn1	2.73	3.465	134.4	149.99
Form III				
C4–H4...C14–Zn2	2.89	3.588	132.4	86.83
C12–H12...C12–Zn1	2.90	3.663	139.3	105.25
C14–H14...C13–Zn1	2.92	3.606	131.1	130.39
C24–H24...C12–Zn1	2.87	3.578	132.6	132.28
C31–H31...C11–Zn1	2.76	3.684	166.8	126.34
C34–H34...C11–Zn1	2.90	3.550	127.6	87.56
C11–H11...N32	2.52	3.362	148.9	
C21–H21...N2	2.65	3.421	139.4	

^a Only C–H...Cl interactions are considered in which the C...Cl distance is in maximum 3.7 Å and the C–H...Cl angle is larger than 125°.

Table 4. Compounds Obtained from Acetonitrile as a Function of the Molar Ratio of Zinc(II) Chloride and Pyridazine

CuCl/pyridazine product	1:6	1:4	1:2	1:1	2:1
		1:2 (form I)			1:1

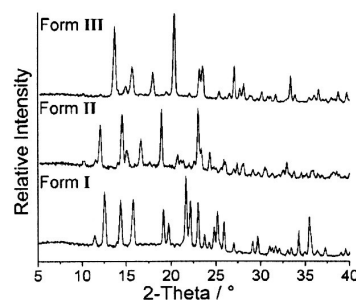
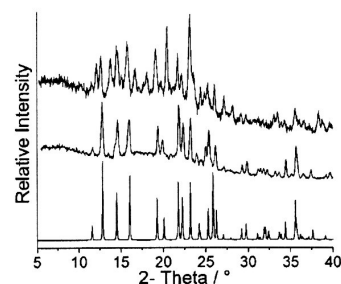
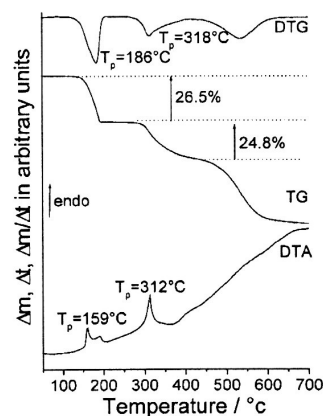
After a day, form II disappeared and only form I is obtained. Thus, this experiment shows that the order of thermodynamic stability at room temperature should be form III < form II < form I.

Afterwards a mixture of forms I, II, and III was stirred in acetonitrile for one week, and the residue thus obtained was investigated by X-ray powder diffraction, in order to determine which of the forms represent the thermodynamically most stable modification at room-temperature. It was observed that forms II and III transform into form I, clearly showing that form I is the most stable modification at room temperature (Figure 7).

Differential Thermoanalysis and Thermogravimetry (DTA-TG). Simultaneous differential thermoanalysis and thermogravimetry were performed (Figure 8) to determine the thermal properties of all the three modifications. The TG-DTA thermograms of the ligand-rich modifications exhibit three mass steps. The first two of which are accompanied by endothermic events in the DTA curve (Figure 8). The DTG curve shows that the first step is well resolved, whereas in the second and third steps a smooth decrease of the sample mass is observed (Figure 8). The experimental mass losses of 26.5 and 24.8% in the first and second steps, respectively, are in close agreement with that calculated for the removal of one pyridazine ligand in each step ($\Delta m_{\text{theo}}(-1 \text{ pyridazine}) = 27.0\%$). The observed mass loss corresponds to the formation of a ligand-deficient 1:1 compound of composition $\text{ZnCl}_2(\text{pyridazine})$ in the first step and zinc(II) chloride in the second step. The product after the second step was identified as ZnCl_2 by X-ray diffraction, and hence, the last TG step can be attributed to the vaporization of zinc(II) chloride.

Afterwards, a second TG experiment was performed in which, the heating was stopped after the first step, and the residue thus formed was investigated by X-ray powder diffraction. The identical nature of this pattern with that of the pattern of the

Crystal Growth & Design, Vol. xxx, No. xx, XXXX E

**Figure 6.** Time-dependent X-ray powder patterns of the residues formed by precipitation measured after 1 min (top), 1 h (middle), and 2 days (bottom).**Figure 7.** X-ray powder pattern of a mixture of forms I, II, and III (top), powder pattern of the residue which was obtained after stirring this mixture for one week in acetonitrile (middle) and the theoretical pattern for form I calculated from single crystal data (bottom).**Figure 8.** DTA, TG, and DTG curves for form I as a representative (DTG = differentiated thermogravimetric curve; T_p = peak temperature).

1:1 compound obtained from solution (Figure 9) unambiguously shows that the ligand-deficient 1:1 compound is formed as an intermediate during thermal decomposition.

Differential Scanning Calorimetry (DSC). The first thermal event in the DTA curve of form I is very broad and split into two different peaks, indicating that the overall decomposition process is much more complex or that this reaction can be due to a polymorphic transformation just before decomposition, which is not successfully resolved using DTA measurements. Hence, all three forms were investigated using DSC to gain

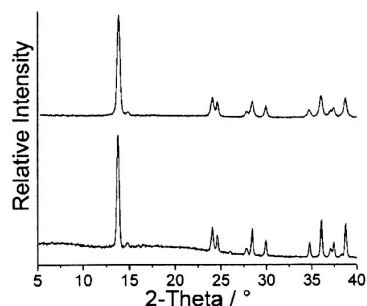


Figure 9. Experimental X-ray powder pattern of the residue obtained after first TG step (bottom) and powder pattern of the ligand-deficient 1:1 compound obtained in solution (top).

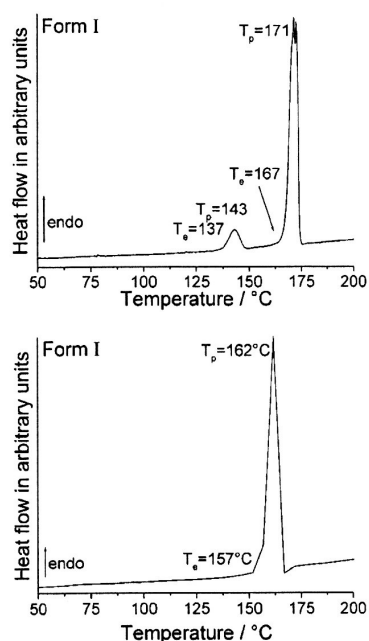


Figure 10. Typical DSC curves for form I. With polymorphic transformation before decomposition (top) and without transformation (bottom).

more insight into the decomposition process. The DSC thermograms of forms **II** and **III** exhibit a single endothermic event, while form **I** exhibits a complex behavior in that different DSC curves are observed (Figure 10). In some of these curves two different endothermic events are observed. The powder pattern of the residue formed after the second DSC step for form **I** corresponds to the ligand-deficient 1:1 compound (see above). Interestingly, the powder pattern of the residue obtained by stopping the DSC measurement, after the first endothermic signal matches that of form **II**, assignable to a polymorphic transformation. This observation shows that form **II** is thermodynamically more stable than form **I** at higher temperatures. Since this transition is endothermic, it can be inferred that both forms behave enantiotropic. However, it is also likely that the real transition temperatures are much lower than that observed in the solid. The energy of the polymorphic transformation of **I** to **II** is about 2.3 kJ/mol, and the heat of decomposition of form **II** is about 25 kJ/mol (Table 5).

Table 5. Results of the DSC Measurements on Forms I, II, and III^a

	Form I	Form II	Form III
$T_{p1}/^{\circ}\text{C}$	143		
$T_{e1}/^{\circ}\text{C}$	137–138		
$\Delta H_1/\text{kJ/mol}$	2.34–2.36 (2.35)		
$T_{p2}/^{\circ}\text{C}$	162	176–177	172–175
$T_{e2}/^{\circ}\text{C}$	157–158	169	168–169
$\Delta H_2/\text{kJ/mol}$	28.4–28.8 (28.6)	24.8–25.4 (25.1)	23.4–25.9 (24.7)

^a T_p = peak temperature, T_e = extrapolated onset temperature, ΔH = heat flow, index 1 = polymorphic transition, index 2 = decomposition in the case of no further polymorphic transformation.

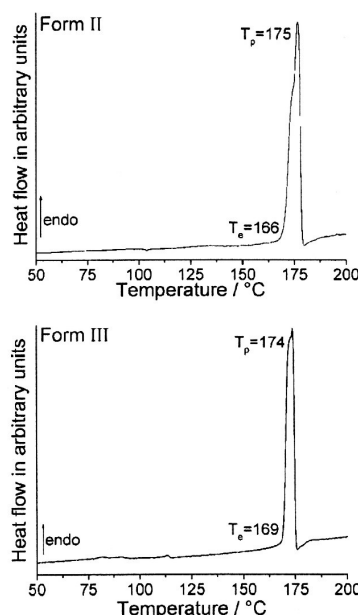


Figure 11. DSC curves for form **II** (top) and form **III** (bottom).

We have also observed that in some DSC experiments, form **I** exhibits a single strong endothermic peak corresponding to the decomposition, and the transformation into form **II** is suppressed. Because in this temperature range form **I** is metastable, the decomposition temperature is shifted to lower values. The heat of decomposition of form **I** of about 29 kJ/mol is much larger than that of form **II**, because form **I** is the most stable form at room temperature (Table 5).

The single endothermic event observed for forms **II** and **III** corresponds to their decomposition into the ligand-deficient 1:1 compound. Since form **II** is more stable than form **I** in this temperature range, it decomposes at higher temperatures (Figure 11 and Table 5). However, the heat of decomposition is much smaller than that of form **I** because form **II** is less stable than form **I** at room temperature. A comparison of the DSC behavior of forms **II** and **III** does not show any significant differences in the decomposition temperatures and the heat of decomposition (Table 5). In addition, the DSC results did not reveal any indications of a transformation of forms **I** or **II** into form **III** or vice versa. In view of this, no definite conclusion can be made on the relative stability of form **III** and if this form behaves monotropic or enantiotropic to form **I** and form **II**.

Quantum Mechanical Calculations. To show which of the four molecular structures of the three forms is close to the energy minimum structure and what the energy differences are, R1-MP2/VTZP calculations have been performed. In the beginning

full geometry optimizations starting from all four experimental structures were done, to ensure that no local minima were overlooked. According to our calculations there is only one stable structure, whatever experimental structure is taken as the starting point. There are no other conformers which looked possible from inspection of the crystal structures. In the experimental structure there is some disagreement especially in the experimental Cl–Zn–Cl angle, which was predicted too large compared to all experimental structures. To examine how much energy is needed to bring the orientation of the pyridazine rings into the experimental position, a restricted optimization, fixing the N–N–Zn–N torsions, was run. The calculations show that this kind of distortion costs only a small amount of energy, between 10 to 19 kcal/mol in the order **II** < **I** = **IIIa** < **IIIb** (**IIIa** and **IIIb** refers to the two crystallographically independent molecules). Fixing the torsions did not reduce the large Cl–Zn–Cl angle.

In further calculations the angles in the tetrahedron around Zn, as well as the torsion angles of the pyridazine rings, were fixed in the respective experimental values. Only the distances and the internal degrees of freedom in pyridazine rings were optimized, so that the structure can relax. Surprisingly, these distortions of the optimal geometry of isolated molecule cost rather small amount of energy, even if the Cl–Zn–Cl bond angles were changed by more than 10 degrees. It shows that the potential energy surface is quite soft, and the molecule can undergo quite large displacements without much of energy; the environment can disturb the geometry substantially, and one can expect large amplitude vibrations in the molecule. The energy cost is 23 and 26 kJ/mol for **IIIa** and **IIIb**, 25 kJ/mol for **I** and 18 kJ/mol for **II**, compared to the energy of the stable structure of the isolated molecule. Therefore, the relative difference between the structures is less than 8 kJ/mol. The structure in form **II** looks always the most stable and that in **IIIb** the less stable. To distort the tetrahedron from optimal to crystal structure, while keeping the pyridazine rings torsions fixed in the experimental values, cost only between 7 to 10 kJ/mol. From the most restricted optimization calculations, it resulted that the bond distances relaxed to the values close to the experimental ones, Zn–Cl being predicted within 1 p.m., and the Zn–N distance remains longer than in the crystal structure, in average by 4 p.m. This bond distance is very sensitive to the rotation of the pyridazine ring and to the geometry environment around central Zn atom and can differ up to 10 p.m. (always longer than the experimental one), depending on the actual structure.

However, according to the results of our calculations one can assume that the stability of form **I** can be traced back predominantly to the crystal packing energy, which overcompensate the internal energy of the molecular structure in this form. However, on higher temperatures form **II** should be the thermodynamically most stable form in agreement with our calculations.

Conclusions

In the present contribution, three different polymorphic modifications of $[\text{ZnCl}_2(\text{pyridazine})_2]$ are presented. The structures of all modifications differ in the distortion of the coordination polyhedron, the orientation of the ligands, and in the packing of these tetrahedral building blocks. The different rotations of the ligands might create a different pattern of weak intermolecular interactions and, therefore, can be responsible to some extent for this polymorphism as was reported previously.⁴² The order of thermodynamic stability at roomtempera-

ture was determined to be form **III** < form **II** < form **I**. Further, form **I** represents the thermodynamically most stable form at room temperature, whereas form **II** is more stable at higher temperatures and both forms should behave enantiotropic. The energy temperature relation of form **III** compared to **I** and **II** could not be determined. Since form **III** exhibits the highest density of all three forms, it is possible that this form is the thermodynamically most stable form at lower temperatures. But in this case the energy need for the decomposition of form **III** into the ligand-deficient 1:1 compound should be the highest, which is not observed in the DSC measurements. Our theoretical calculations reveal that the molecular structure in form **II** is very close to the energy minimum structure, but only small energy differences are found between all three forms.

Form **I** can easily be prepared if the reaction is performed under thermodynamic control, whereas under kinetic control in the beginning form **III** is obtained, which transforms within minutes into form **II** and in the end into the thermodynamically most stable form **I**.

All the polymorphic modifications can be thermally decomposed to the ligand-deficient 1:1 compound, clearly indicating that thermal reaction of ligand-rich precursor compounds is a suitable method for the convenient synthesis of ligand-deficient coordination compounds or coordination polymers.

The present work shows that investigations on the thermodynamic aspects of such polymorphs to determine their relative stability is sometimes difficult to achieve and not always is such information fully accessible. But in any case they are always needed because the crystal structures of polymorphic modifications in most cases are very complicated, and a definite conclusion on the stability of different polymorphic modifications cannot be drawn based on structural data alone. In addition, the stability of a given modification depends on the actual temperature, and in most cases structural data are determined at one temperature. The identification of more number of intermolecular C–H...Cl and C–H...N interactions in form **I** than in form **II** can probably explain why form **I** is more stable at room temperature than form **II**. In this context, the investigations of the thermodynamic aspects of polymorphic modifications by simple methods such as crystallization experiments and thermoanalytical methods are very useful to determine the relative stability in addition to the structural results.

Acknowledgment. We gratefully acknowledge the financial support by the State of Schleswig-Holstein and the Deutsche Forschungsgemeinschaft (Project No.: NA 720/1-1). We thank Professor Dr. Wolfgang Bensch for the facility to use his experimental equipment.

Supporting Information Available: Details of the structure determination of forms **I–III**; experimental X-ray powder pattern of forms **I–III** and the theoretical patterns calculated from single crystal data; IR and Raman spectra for forms **I–III**. This material is available free of charge via the Internet at <http://pubs.acs.org>.

References

- (1) Hagrman, P. J.; Hagrman, D.; Zubieta, J. *Angew. Chem., Int. Ed.* **1999**, *38*, 2638.
- (2) James, S. L. *Chem. Soc. Rev.* **2003**, *5*, 276.
- (3) Robin, A. Y.; Fromm, K. M. *Coord. Chem. Rev.* **2006**, *250*, 2127.
- (4) Janiak, C. *J. Chem. Soc. Dalton. Trans* **2003**, 2781.
- (5) Yaghi, O. M.; Li, H.; Davis, C.; Richardson, D.; Groy, T. L. *Acc. Chem. Res.* **1998**, *31*, 474.
- (6) Chen, C. T.; Suslik, K. S. *Coord. Chem. Rev.* **1993**, *128*, 293.
- (7) Robson, R.; Abrahams, B. F.; Batten, S. R.; Grable, R. W.; Hoskins, B. F.; Liu, J. In *Supramolecular Architecture*, ACS Publications: Washington, DC, 1992; Chapter 19.

- (8) Robson, R. In *Comprehensive Supramolecular Chemistry*; Pergamon: New York, 1996; Chapter 22, p 733.
- (9) Zaworotko, M. J. *Chem. Soc. Rev.* **1994**, 23, 283.
- (10) Lu, J. Y. *Coord. Chem. Rev.* **2003**, 246, 327.
- (11) Zaworotko, M. *Angew. Chem., Int. Ed.* **1998**, 37, 1211.
- (12) Batten, S. R.; Robson, R. *Angew. Chem., Int. Ed.* **1998**, 37, 1460.
- (13) Brammer, L. *Chem. Soc. Rev.* **2004**, 8, 476.
- (14) Braga, D.; Maini, L.; Polito, M.; Scaccianoce, L.; Cojazzi, G.; Grepioni, F. *Coord. Chem. Rev.* **2001**, 216, 225.
- (15) Zhou, Y.; Hong, M.; Wu, X. *Chem. Commun.* **2006**, 135.
- (16) Zheng, S. L.; Tong, M. L.; Chen, X. M. *Coord. Chem. Rev.* **2003**, 246–185.
- (17) Erxleben, A. *Coord. Chem. Rev.* **2003**, 246, 203.
- (18) Khlobystov, A. N.; Blake, A. J.; Champness, N. R.; Lemenovskii, D. A.; Majouga, A. G.; Zyk, N. V.; Schroder, M. *Coord. Chem. Rev.* **2001**, 222, 155.
- (19) Puddephatt, R. J. *Coord. Chem. Rev.* **2001**, 216, 313.
- (20) Zhang, H.; Wang, X.; Zhang, K.; Teo, B. K. *Coord. Chem. Rev.* **1999**, 183, 157.
- (21) Desiraju, G. R. *Crystal Engineering - The Design of Organic Solids. Material Science Monographs*; Elsevier: Amsterdam, 1989; Vol. 54 and literature cited therein.
- (22) Moulton, B.; Zaworotko, M. J. *Chem. Rev.* **2001**, 101, 1629.
- (23) Barnett, A. S.; Blake, A. J.; Champness, N. R. *Chem. Commun.* **2002**, 1640.
- (24) Blake, A. J.; Brooks, N. R.; Champness, N. R.; Crew, M.; Deveson, A.; Fenske, D.; Gregory, D. H.; Hanton, L. R.; Hubberstey, P.; Schröder, M. *Chem. Commun.* **2001**, 1432.
- (25) Barnett, S. A.; Blake, A. J.; Champness, N. R.; Wilson, C. *Chem. Commun.* **2002**, 1640.
- (26) Hennigar, T. L.; MacQuarrie, D. C.; Losier, P.; Rogers, R. D.; Zaworotko, M. J. *Angew. Chem., Int. Ed.* **2003**, 36, 972.
- (27) Braga, D.; Grepioni, F. *Chem. Soc. Rev.* **2000**, 29, 229.
- (28) Braga, D.; Polito, M.; DAddario, D.; Grepioni, F. *Cryst. Growth Des.* **2004**, 4, 1109.
- (29) Smyth, D. R.; Vincent, B. R.; Tiekink, E. R. T. *Cryst. Growth Des.* **2001**, 1, 113.
- (30) Näther, C.; Wriedt, M.; Jess, I. *Inorg. Chem.* **2003**, 42, 2391.
- (31) Näther, C.; Jess, I. *Inorg. Chem.* **2003**, 42, 2968.
- (32) Näther, C.; Jess, I.; Lehnert, N.; Hinz-Hubner, D. *Solid State Sci.* **2003**, 5, 1343.
- (33) Bhosekar, G.; Jess, I.; Näther, C. *Z. Naturforsch.* **2006**, 61b, 721.
- (34) Näther, C.; Jess, I. *Inorg. Chem.* **2006**, 45, 7446.
- (35) Näther, C.; Jess, I. *J. Solid State Chem.* **2002**, 169, 103.
- (36) Näther, C.; Greve, J. *J. Solid State Chem.*, **2003**, 176, 259.
- (37) Näther, C.; Jess, I. *Eur. J. Inorg. Chem.*, **2004**, 2868.
- (38) Bhosekar, G.; Jess, I.; Näther, C. *Inorg. Chem.* **2006**, 43, 6508.
- (39) Sheldrick, G. M. SHELXS 97 and SHELXL-97, Programs for the solution and refinement of Crystal Structures, University of Göttingen, Germany, 1997.
- (40) Weigend, F.; Haser, M. *Theor. Chem. Acc.* **1997**, 97, 331.
- (41) Schafer, A.; Horn, H.; Ahlrichs, R. *J. Chem. Phys.* **1992**, 97, 2571.
- (42) Roay, S.; Banerjee, R.; Nangia, A.; Kruger, G. *J. Chem. Eur. J.* **2006**, 12, 3777.

CG060889G

Supplemental Material

Structures and Properties of Three Polymorphic Modifications based on Tetrahedral Building Blocks of Dichloro-bis(pyridazine-N) zinc(II)

Gaurav Bhosekar, Inke Jeß and Christian Näther*

Details of the structure determination of form **I**

Details of the structure determination of form **II**

Details of the structure determination of form **III**

Experimental X-ray powder pattern of form **I** and theoretical pattern calculated from single crystal data

Experimental X-ray powder pattern of form **II** and theoretical pattern calculated from single crystal data

Experimental X-ray powder pattern of form **III** and theoretical pattern calculated from single crystal data

IR (top) and Raman (bottom) spectra for form **I**

IR (top) and Raman (bottom) spectra for form **II**

IR (top) and Raman (bottom) spectra for form **III**

Table 1. Crystal data and structure refinement for form I

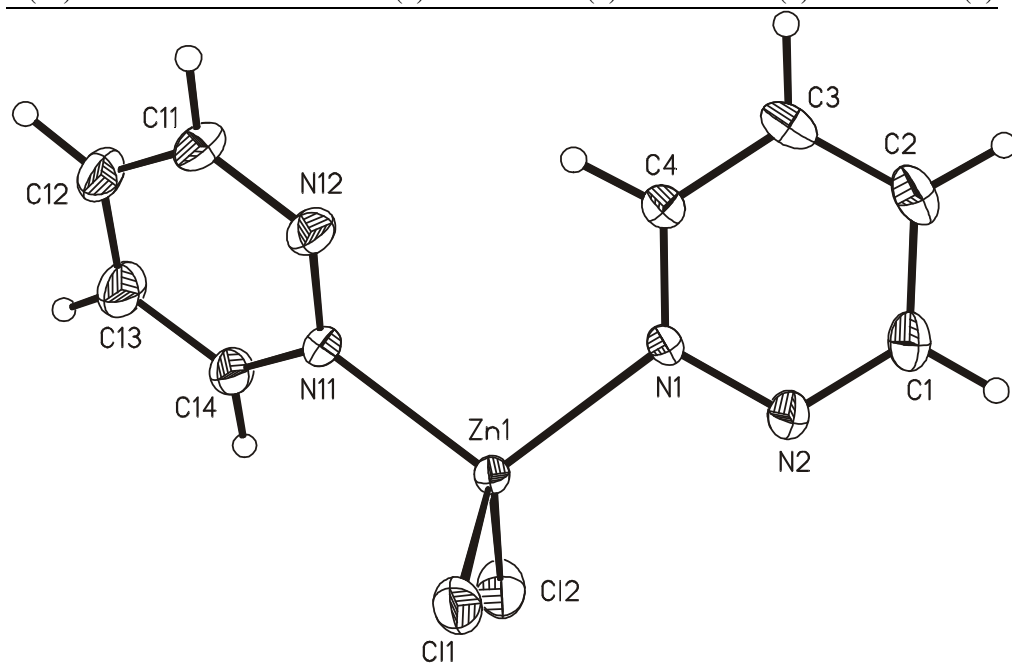
Identification code	blz11	
Empirical formula	$C_8H_8Cl_2N_4Zn$	
Formula weight	296.45	
Temperature	170(2) K	
Wavelength	0.71073 Å	
Crystal system	monoclinic	
Space group	Cc	
Unit cell dimensions	a = 14.0339(12) Å	$\alpha = 90^\circ$.
	b = 9.2082(5) Å	$\beta = 100.579(9)^\circ$.
	c = 8.9873(7) Å	$\gamma = 90^\circ$.
Volume	1141.66(15) Å ³	
Z	4	
Density (calculated)	1.725 Mg/m ³	
Absorption coefficient	2.590 mm ⁻¹	
F(000)	592	
Crystal size	0.07 x 0.1 x 0.13 mm ³	
Theta range for data collection	2.66 to 28.00°.	
Index ranges	-18 ≤ h ≤ 18, -11 ≤ k ≤ 12, -11 ≤ l ≤ 11	
Reflections collected	5399	
Independent reflections	2547 [R(int) = 0.0267]	
Completeness to theta = 28.00°	96.7 %	
Refinement method	Full-matrix least-squares on F ²	
Data / restraints / parameters	2547 / 2 / 137	
Goodness-of-fit on F ²	0.992	
Final R indices [I > 2σ(I)]	R1 = 0.0246, wR2 = 0.0583	
R indices (all data)	R1 = 0.0283, wR2 = 0.0595	
Absolute structure parameter	-0.004(11)	
Extinction coefficient	0.0100(6)	
Largest diff. peak and hole	0.292 and -0.467 e.Å ⁻³	

Remarks:

All non-hydrogen atoms were refined using anisotropic displacement parameters. The hydrogen atoms were positioned with idealized geometry and were refined isotropic ($U_{eq} = -1.2$) using a riding model with C-H = 0.95 Å for aromatic hydrogen atoms. There is one crystallographically independent molecules into the asymmetric unit, located in a general position.

Table 2. Atomic coordinates ($\times 10^4$) and equivalent isotropic displacement parameters ($\text{\AA}^2 \times 10^3$)U(eq) is defined as one third of the trace of the orthogonalized U^{ij} tensor.

	x	y	z	U(eq)
Zn(1)	4616(1)	7397(1)	3407(1)	17(1)
Cl(1)	3562(1)	7760(1)	1270(1)	25(1)
Cl(2)	5727(1)	9103(1)	4080(1)	33(1)
N(1)	5250(2)	5395(2)	3377(3)	18(1)
N(2)	5935(2)	5366(3)	2509(3)	28(1)
C(1)	6388(2)	4114(3)	2387(4)	30(1)
C(2)	6205(2)	2847(3)	3135(4)	29(1)
C(3)	5520(2)	2904(3)	4020(4)	30(1)
C(4)	5041(2)	4226(3)	4102(4)	21(1)
N(11)	3849(2)	7332(2)	5148(3)	19(1)
N(12)	3304(2)	6135(2)	5175(3)	24(1)
C(11)	2768(2)	6051(3)	6241(4)	27(1)
C(12)	2728(2)	7125(4)	7322(4)	30(1)
C(13)	3293(2)	8325(3)	7260(4)	31(1)
C(14)	3854(2)	8387(3)	6143(4)	24(1)

Table 3. Bond lengths [\AA] and angles [$^\circ$].

Zn(1)-N(1)	2.049(2)	N(1)-Zn(1)-Cl(2)	110.81(7)
Zn(1)-N(11)	2.056(2)	N(11)-Zn(1)-Cl(2)	104.66(7)
Zn(1)-Cl(2)	2.2180(7)	N(1)-Zn(1)-Cl(1)	110.21(7)
Zn(1)-Cl(1)	2.2240(8)	N(11)-Zn(1)-Cl(1)	107.68(7)
N(1)-Zn(1)-N(11)	105.87(9)	Cl(2)-Zn(1)-Cl(1)	116.85(3)
C(14)-N(11)-Zn(1)	123.74(19)	C(4)-N(1)-Zn(1)	126.25(19)
N(12)-N(11)-Zn(1)	114.61(18)	N(2)-N(1)-Zn(1)	112.59(17)

Table 4. Anisotropic displacement parameters ($\text{\AA}^2 \times 10^3$). The anisotropic displacement factor exponent takes the form: $-2\pi^2 [h^2 a^{*2} U_{11} + \dots + 2 h k a^* b^* U_{12}]$

	U_{11}	U_{22}	U_{33}	U_{23}	U_{13}	U_{12}
Zn(1)	19(1)	12(1)	22(1)	0(1)	10(1)	1(1)
Cl(1)	29(1)	26(1)	22(1)	-1(1)	7(1)	8(1)
Cl(2)	27(1)	21(1)	54(1)	-9(1)	17(1)	-8(1)
N(1)	18(1)	13(1)	23(1)	1(1)	8(1)	3(1)
N(2)	29(1)	22(1)	38(2)	2(1)	20(1)	4(1)
C(1)	26(1)	30(2)	39(2)	-1(1)	16(1)	8(1)
C(2)	30(2)	22(1)	34(2)	-3(1)	5(1)	10(1)
C(3)	38(2)	15(1)	38(2)	3(1)	9(1)	3(1)
C(4)	24(1)	16(1)	26(2)	0(1)	10(1)	1(1)
N(11)	20(1)	19(1)	19(1)	2(1)	10(1)	2(1)
N(12)	25(1)	21(1)	30(2)	-1(1)	13(1)	-4(1)
C(11)	22(1)	29(2)	31(2)	4(1)	12(1)	-4(1)
C(12)	29(2)	39(2)	26(2)	6(1)	14(1)	6(1)
C(13)	37(2)	31(2)	28(2)	-6(1)	16(1)	0(1)
C(14)	31(2)	20(1)	25(2)	-4(1)	12(1)	0(1)

Table 5. Hydrogen coordinates ($\times 10^4$) and isotropic displacement parameters ($\text{\AA}^2 \times 10^3$).

	x	y	z	U(eq)
H(1)	6862	4083	1756	36
H(2)	6547	1975	3028	35
H(3)	5370	2076	4564	36
H(4)	4550	4284	4700	25
H(11)	2385	5204	6271	32
H(12)	2329	7028	8063	36
H(13)	3301	9097	7964	37
H(14)	4254	9212	6092	29

Table 2. Crystal data and structure refinement for form II

Identification code	gb175a	
Empirical formula	$C_8H_8Cl_2N_4Zn$	
Formula weight	296.45	
Temperature	170(2) K	
Wavelength	0.71073 Å	
Crystal system	monoclinic	
Space group	$P2_1/C$	
Unit cell dimensions	$a = 8.0254(5)$ Å	$\alpha = 90^\circ$.
	$b = 16.9729(16)$ Å	$\beta = 5.619(8)^\circ$.
	$c = 8.5260(6)$ Å	$\gamma = 90^\circ$.
Volume	1155.78(15) Å ³	
Z	4	
Density (calculated)	1.704 Mg/m ³	
Absorption coefficient	2.558 mm ⁻¹	
F(000)	592	
Crystal size	0.08 x 0.14 x 0.22 mm ³	
Theta range for data collection	2.40 to 27.97°.	
Index ranges	-10 ≤ h ≤ 10, -22 ≤ k ≤ 21, -10 ≤ l ≤ 11	
Reflections collected	6630	
Independent reflections	2692 [R(int) = 0.0348]	
Completeness to theta = 27.97°	96.5 %	
Refinement method	Full-matrix least-squares on F ²	
Data / restraints / parameters	2692 / 0 / 137	
Goodness-of-fit on F ²	0.797	
Final R indices [I > 2σ(I)]	R1 = 0.0333, wR2 = 0.0932	
R indices (all data)	R1 = 0.0396, wR2 = 0.0994	
Extinction coefficient	0.023(3)	
Largest diff. peak and hole	0.742 and -0.862 e.Å ⁻³	

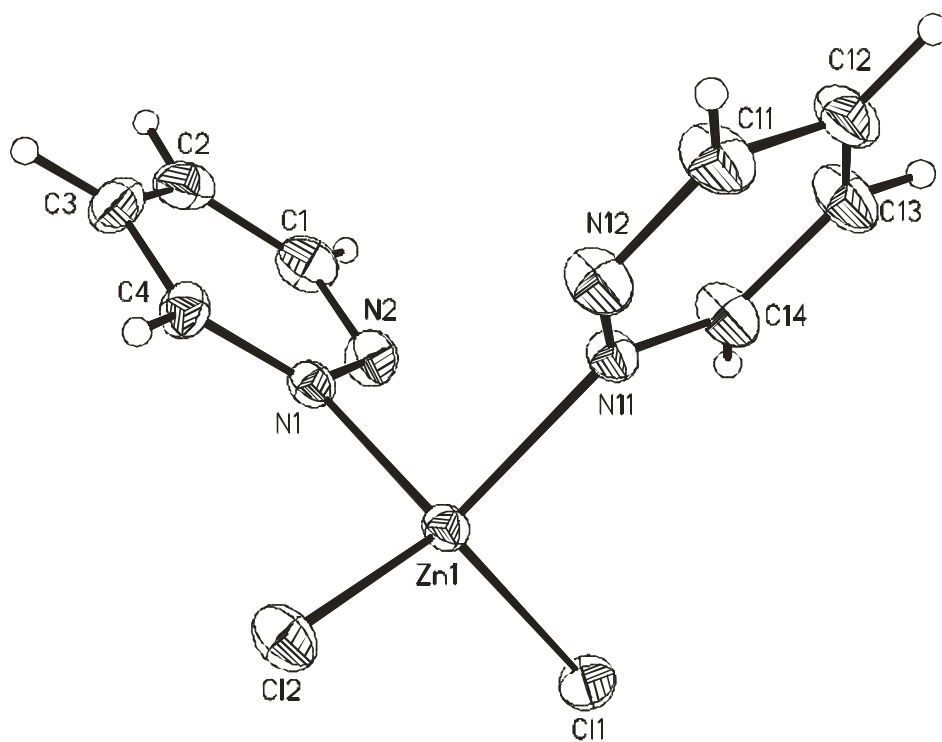
Remarks:

All non-hydrogen atoms were refined using anisotropic displacement parameters. The hydrogen atoms were positioned with idealized geometry and were refined isotropic ($U_{eq} = -1.2$) using a riding model with C-H = 0.95 Å for aromatic hydrogen atoms. There is one crystallographically independent molecules into the asymmetric unit which is located in a general position.

2 Publications

Table 2. Atomic coordinates ($\times 10^4$) and equivalent isotropic displacement parameters ($\text{\AA}^2 \times 10^3$). $U(\text{eq})$ is defined as one third of the trace of the orthogonalized U^{ij} tensor.

	x	y	z	$U(\text{eq})$
Zn(1)	7656(1)	6019(1)	7148(1)	17(1)
Cl(1)	9644(1)	6691(1)	8569(1)	26(1)
Cl(2)	6542(1)	4975(1)	8189(1)	26(1)
N(1)	8320(2)	5702(1)	4979(2)	17(1)
N(2)	9423(3)	6189(1)	4389(2)	25(1)
C(1)	9740(3)	6072(2)	2915(3)	30(1)
C(2)	8998(3)	5483(2)	1945(3)	29(1)
C(3)	7881(3)	4994(2)	2570(3)	28(1)
C(4)	7580(3)	5127(1)	4122(3)	22(1)
N(11)	5905(2)	6870(1)	6432(2)	18(1)
N(12)	4282(2)	6668(1)	6298(3)	27(1)
C(11)	3168(3)	7219(2)	5840(3)	31(1)
C(12)	3586(3)	7990(2)	5508(3)	29(1)
C(13)	5243(3)	8187(2)	5625(3)	30(1)
C(14)	6382(3)	7595(1)	6104(3)	27(1)



2 Publications

Table 3. Bond lengths [Å] and angles [°]

Zn(1)-N(1)	2.0462(19)	N(1)-Zn(1)-N(11)	98.43(7)
Zn(1)-N(11)	2.0654(17)	N(1)-Zn(1)-Cl(2)	107.68(5)
Zn(1)-Cl(2)	2.2092(6)	N(11)-Zn(1)-Cl(2)	112.89(5)
Zn(1)-Cl(1)	2.2211(6)	N(1)-Zn(1)-Cl(1)	113.04(5)
Cl(2)-Zn(1)-Cl(1)	119.32(2)	N(11)-Zn(1)-Cl(1)	103.53(5)
C(4)-N(1)-Zn(1)	123.40(16)	C(14)-N(11)-Zn(1)	120.61(15)
N(2)-N(1)-Zn(1)	114.57(14)	N(12)-N(11)-Zn(1)	118.24(14)

Table 4. Anisotropic displacement parameters ($\text{\AA}^2 \times 10^3$). The anisotropic displacement factor exponent takes the form: $-2\pi^2 [h^2 a^{*2} U_{11} + \dots + 2 h k a^* b^* U_{12}]$

	U_{11}	U_{22}	U_{33}	U_{23}	U_{13}	U_{12}
Zn(1)	15(1)	15(1)	19(1)	1(1)	0(1)	1(1)
Cl(1)	21(1)	26(1)	29(1)	-4(1)	-7(1)	-2(1)
Cl(2)	26(1)	22(1)	31(1)	8(1)	5(1)	-3(1)
N(1)	15(1)	17(1)	20(1)	2(1)	1(1)	1(1)
N(2)	27(1)	21(1)	27(1)	3(1)	4(1)	-7(1)
C(1)	30(1)	32(1)	28(1)	8(1)	8(1)	-1(1)
C(2)	29(1)	37(1)	21(1)	1(1)	2(1)	12(1)
C(3)	26(1)	31(1)	25(1)	-9(1)	-2(1)	3(1)
C(4)	20(1)	20(1)	26(1)	-3(1)	1(1)	-2(1)
N(11)	13(1)	17(1)	23(1)	1(1)	-1(1)	0(1)
N(12)	16(1)	23(1)	40(1)	4(1)	-3(1)	-4(1)
C(11)	13(1)	29(1)	49(2)	3(1)	-6(1)	-2(1)
C(12)	20(1)	25(1)	40(1)	3(1)	-5(1)	6(1)
C(13)	24(1)	19(1)	46(2)	9(1)	-1(1)	0(1)
C(14)	16(1)	21(1)	42(1)	7(1)	-1(1)	-3(1)

Table 5. Hydrogen coordinates ($\times 10^4$) and isotropic displacement parameters ($\text{\AA}^2 \times 10^3$)

	x	y	z	U(eq)
H(1)	10523	6411	2490	35
H(2)	9258	5424	889	35
H(3)	7334	4582	1967	34
H(4)	6816	4793	4587	27
H(11)	2017	7077	5733	37
H(12)	2744	8369	5208	35
H(13)	5602	8703	5390	36
H(14)	7544	7715	6199	32

Table 3. Crystal data and structure refinement for form III

Identification code	gb379	
Empirical formula	C ₈ H ₈ Cl ₂ N ₄ Zn	
Formula weight	296.45	
Temperature	220(2) K	
Wavelength	0.71073 Å	
Crystal system	orthorhombic	
Space group	Pna2 ₁	
Unit cell dimensions	a = 25.4704(13) Å	α = 90°.
	b = 7.5932(4) Å	β = 90°.
	c = 11.7460(9) Å	γ = 90°.
Volume	2271.7(2) Å ³	
Z	8	
Density (calculated)	1.734 Mg/m ³	
Absorption coefficient	2.603 mm ⁻¹	
F(000)	1184	
Crystal size	0.06 x 0.10 x 0.14 mm ³	
Theta range for data collection	2.36 to 26.92°.	
Index ranges	-30 ≤ h ≤ 30, -9 ≤ k ≤ 9, -14 ≤ l ≤ 14	
Reflections collected	15632	
Independent reflections	4685 [R(int) = 0.0333]	
Completeness to theta = 26.92°	96.4 %	
Refinement method	Full-matrix least-squares on F ²	
Data / restraints / parameters	4685 / 1 / 272	
Goodness-of-fit on F ²	0.968	
Final R indices [I > 2σ(I)]	R1 = 0.0257, wR2 = 0.0615	
R indices (all data)	R1 = 0.0311, wR2 = 0.0638	
Absolute structure parameter	0.060(10)	
Extinction coefficient	0.0011(3)	
Largest diff. peak and hole	0.332 and -0.461 e.Å ⁻³	

Remarks:

All non-hydrogen atoms were refined using anisotropic displacement parameters. The hydrogen atoms were positioned with idealized geometry and were refined isotropic ($U_{eq} = -1.2$) using a riding model with C-H = 0.95 Å for aromatic hydrogen atoms. There are two crystallographically independent molecules into the asymmetric unit which is located in a general position.

2 Publications

Table 2. Atomic coordinates ($\times 10^4$) and equivalent isotropic displacement parameters ($\text{\AA}^2 \times 10^3$)

$U(\text{eq})$ is defined as one third of the trace of the orthogonalized U^{ij} tensor.

	x	y	z	$U(\text{eq})$
Zn(1)	-800(1)	2485(1)	2489(1)	20(1)
Cl(1)	-1247(1)	4995(1)	2656(1)	28(1)
Cl(2)	-1232(1)	-43(1)	2636(1)	29(1)
N(1)	-367(1)	2582(3)	1020(2)	23(1)
N(2)	-654(1)	2104(4)	100(2)	32(1)
C(1)	-418(2)	2151(5)	-902(3)	36(1)
C(2)	98(2)	2682(4)	-1068(3)	34(1)
C(3)	379(1)	3164(5)	-134(3)	28(1)
C(4)	126(1)	3102(4)	917(2)	24(1)
N(11)	-284(1)	2402(3)	3836(3)	23(1)
N(12)	188(1)	3120(4)	3641(2)	30(1)
C(11)	538(1)	3123(5)	4480(3)	33(1)
C(12)	431(2)	2440(4)	5562(3)	35(1)
C(13)	-50(1)	1749(4)	5746(3)	35(1)
C(14)	-408(2)	1761(5)	4844(3)	30(1)
Zn(2)	1676(1)	2926(1)	2037(1)	21(1)
Cl(3)	1215(1)	446(1)	1924(1)	33(1)
Cl(4)	1256(1)	5476(1)	1899(1)	30(1)
N(21)	2190(1)	2814(3)	678(2)	23(1)
N(22)	2665(1)	3473(4)	889(2)	32(1)
C(21)	3014(1)	3473(5)	47(3)	36(1)
C(22)	2906(2)	2852(4)	-1029(3)	35(1)
C(23)	2417(2)	2195(4)	-1241(3)	36(1)
C(24)	2061(2)	2213(4)	-344(3)	30(1)
N(31)	2131(1)	2844(3)	3478(2)	24(1)
N(32)	1857(1)	3284(4)	4418(2)	34(1)
C(31)	2111(2)	3271(5)	5404(3)	39(1)
C(32)	2632(2)	2827(5)	5525(3)	35(1)
C(33)	2905(1)	2357(4)	4575(3)	32(1)
C(34)	2631(1)	2408(4)	3552(3)	28(1)

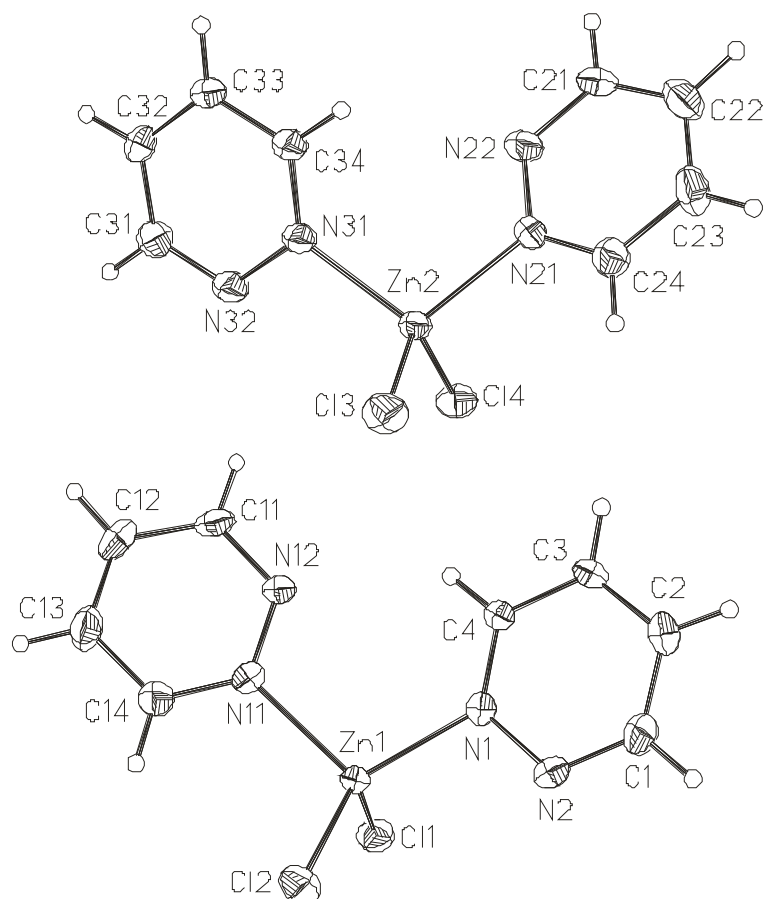


Table 3. Bond lengths [Å] and angles [°]

Zn(1)-N(1)	2.049(3)	Zn(2)-N(31)	2.053(3)
Zn(1)-N(11)	2.058(3)	Zn(2)-N(21)	2.065(3)
Zn(1)-Cl(2)	2.2188(7)	Zn(2)-Cl(4)	2.2181(7)
Zn(1)-Cl(1)	2.2282(7)	Zn(2)-Cl(3)	2.2236(7)
N(1)-Zn(1)-N(11)	107.71(11)	N(31)-Zn(2)-N(21)	106.20(10)
N(1)-Zn(1)-Cl(2)	111.31(7)	N(31)-Zn(2)-Cl(4)	111.02(7)
N(11)-Zn(1)-Cl(2)	103.33(7)	N(21)-Zn(2)-Cl(4)	106.58(7)
N(1)-Zn(1)-Cl(1)	108.56(7)	N(31)-Zn(2)-Cl(3)	108.76(8)
N(11)-Zn(1)-Cl(1)	106.55(7)	N(21)-Zn(2)-Cl(3)	104.70(8)
Cl(2)-Zn(1)-Cl(1)	118.68(3)	Cl(4)-Zn(2)-Cl(3)	118.69(3)
C(4)-N(1)-Zn(1)	126.8(2)	C(24)-N(21)-Zn(2)	123.9(3)
N(2)-N(1)-Zn(1)	111.9(2)	N(22)-N(21)-Zn(2)	114.6(2)
C(14)-N(11)-Zn(1)	123.2(3)	C(34)-N(31)-Zn(2)	127.4(2)
N(12)-N(11)-Zn(1)	115.5(2)	N(32)-N(31)-Zn(2)	112.1(2)

2 Publications

Table 4. Anisotropic displacement parameters ($\text{\AA}^2 \times 10^3$). The anisotropic displacement factor exponent takes the form: $-2\pi^2 [h^2 a^{*2} U_{11} + \dots + 2 h k a^* b^* U_{12}]$

	U_{11}	U_{22}	U_{33}	U_{23}	U_{13}	U_{12}
Zn(1)	15(1)	27(1)	18(1)	3(1)	0(1)	-1(1)
Cl(1)	24(1)	28(1)	33(1)	4(1)	-1(1)	3(1)
Cl(2)	28(1)	27(1)	33(1)	1(1)	4(1)	-6(1)
N(1)	22(2)	31(1)	17(1)	2(1)	0(1)	-1(1)
N(2)	21(2)	51(2)	23(1)	-1(1)	-4(1)	-6(1)
C(1)	36(2)	54(2)	19(2)	-5(1)	-4(1)	-12(2)
C(2)	35(2)	49(2)	19(2)	1(1)	4(2)	-1(1)
C(3)	17(2)	40(2)	26(2)	6(1)	4(1)	-5(1)
C(4)	18(2)	37(2)	18(2)	0(1)	1(1)	-3(1)
N(11)	20(2)	27(1)	23(2)	2(1)	-4(1)	1(1)
N(12)	17(1)	50(2)	22(1)	3(1)	-1(1)	-4(1)
C(11)	16(2)	53(2)	31(2)	-3(1)	-5(1)	-3(1)
C(12)	37(2)	41(2)	27(2)	-1(1)	-15(2)	4(1)
C(13)	44(2)	41(2)	21(2)	4(1)	-6(1)	-8(2)
C(14)	28(2)	37(2)	26(2)	1(1)	-1(1)	-7(1)
Zn(2)	16(1)	26(1)	20(1)	-2(1)	0(1)	-2(1)
Cl(3)	30(1)	27(1)	40(1)	1(1)	-3(1)	-9(1)
Cl(4)	26(1)	25(1)	38(1)	-1(1)	-1(1)	2(1)
N(21)	20(2)	29(2)	19(1)	0(1)	2(1)	-2(1)
N(22)	19(2)	50(2)	28(1)	-2(1)	1(1)	-6(1)
C(21)	15(2)	56(2)	36(2)	6(2)	3(1)	-1(1)
C(22)	33(2)	40(2)	33(2)	5(1)	13(2)	6(1)
C(23)	44(2)	42(2)	21(2)	-4(1)	7(1)	-4(2)
C(24)	29(2)	37(2)	24(2)	-4(1)	1(1)	-5(1)
N(31)	18(2)	31(2)	22(2)	-3(1)	1(1)	2(1)
N(32)	21(2)	56(2)	25(1)	-3(1)	3(1)	6(1)
C(31)	30(2)	66(2)	21(2)	-4(2)	5(1)	10(2)
C(32)	29(2)	56(2)	18(2)	3(1)	-7(1)	-1(2)
C(33)	18(2)	51(2)	27(2)	4(1)	-1(1)	3(1)
C(34)	20(2)	39(2)	24(2)	-1(1)	2(1)	6(1)

Table 5. Hydrogen coordinates ($\times 10^4$) and isotropic displacement parameters ($\text{\AA}^2 \times 10^3$)

	x	y	z	U(eq)
H(3)	-612	1802	-1544	44
H(2)	248	2708	-1799	41
H(1)	731	3525	-195	33
H(4)	311	3441	1573	29
H(11)	872	3604	4341	40
H(12)	685	2463	6142	42
H(13)	-141	1274	6458	42
H(14)	-747	1300	4959	36
H(21)	3352	3921	193	43
H(22)	3163	2880	-1603	42
H(23)	2325	1750	-1960	43
H(24)	1719	1786	-465	36
H(31)	1922	3583	6062	47
H(32)	2794	2848	6243	41
H(33)	3260	2017	4609	38
H(34)	2811	2117	2879	33

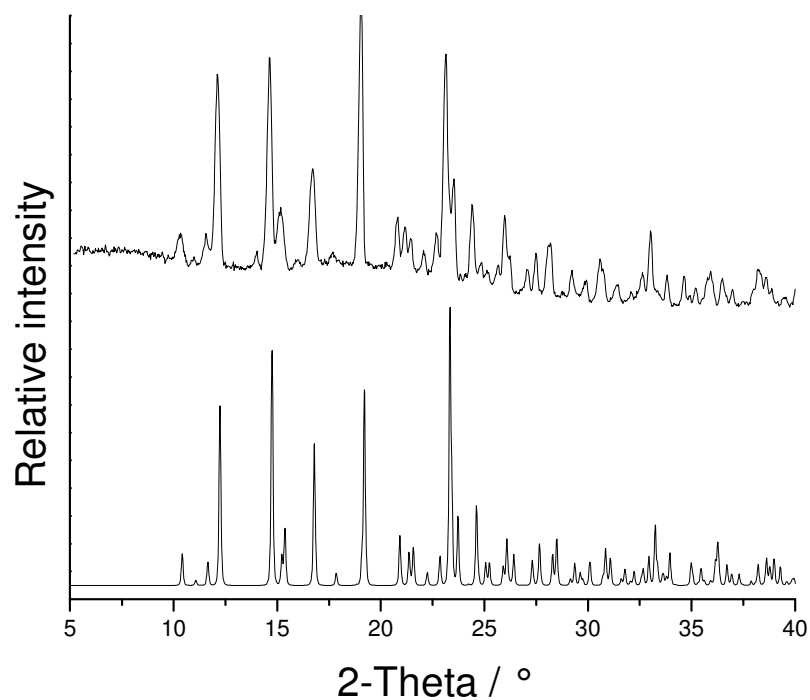


Fig. 1: Experimental X-ray powder pattern of form **I** (top) and theoretical pattern calculated from single crystal data (bottom).

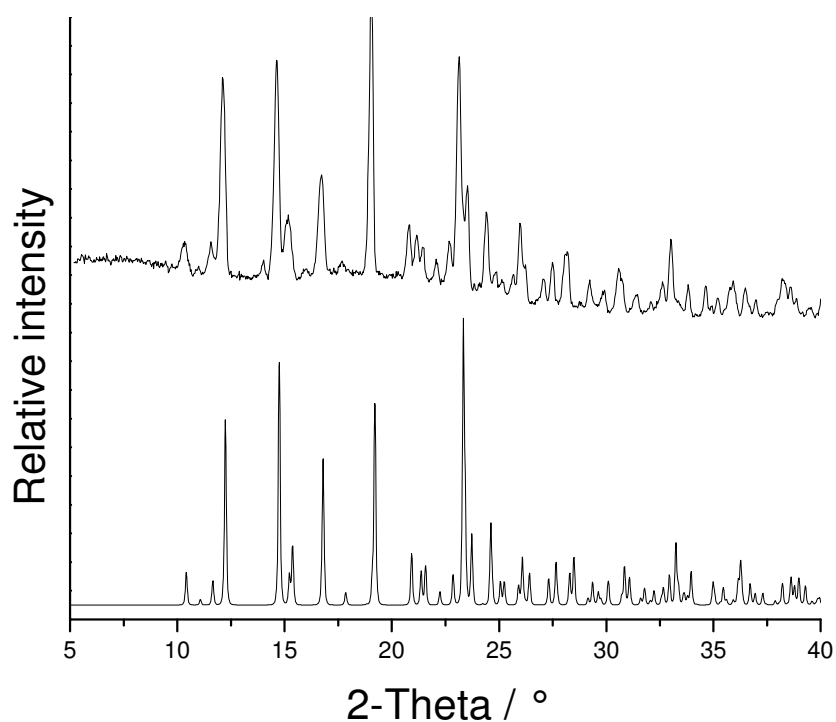


Fig. 2: Experimental X-ray powder pattern of form **II** (top) and theoretical pattern calculated from single crystal data (bottom).

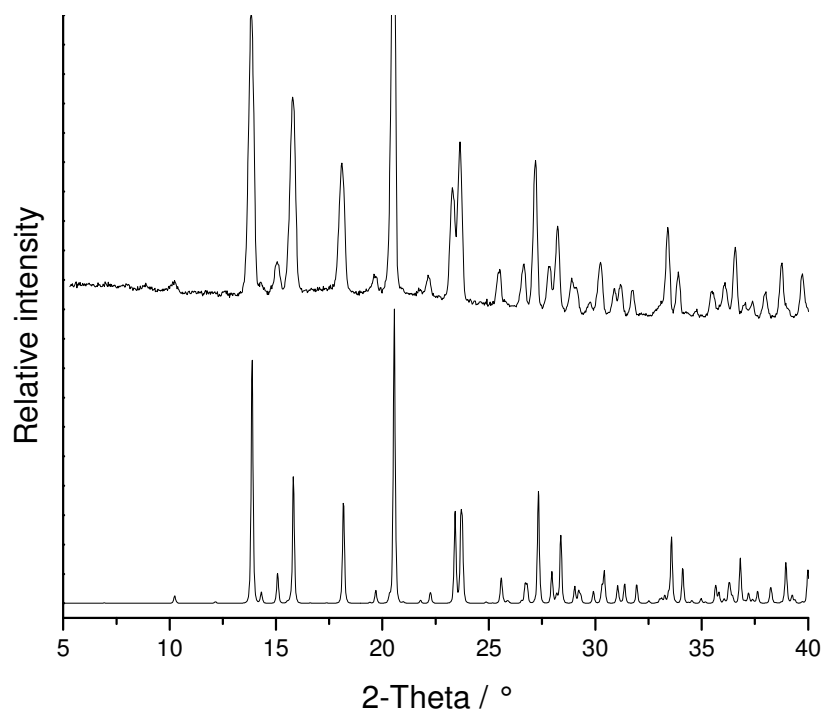


Fig. 3: Experimental X-ray powder pattern of form **III** (top) and theoretical pattern calculated from single crystal data (bottom).

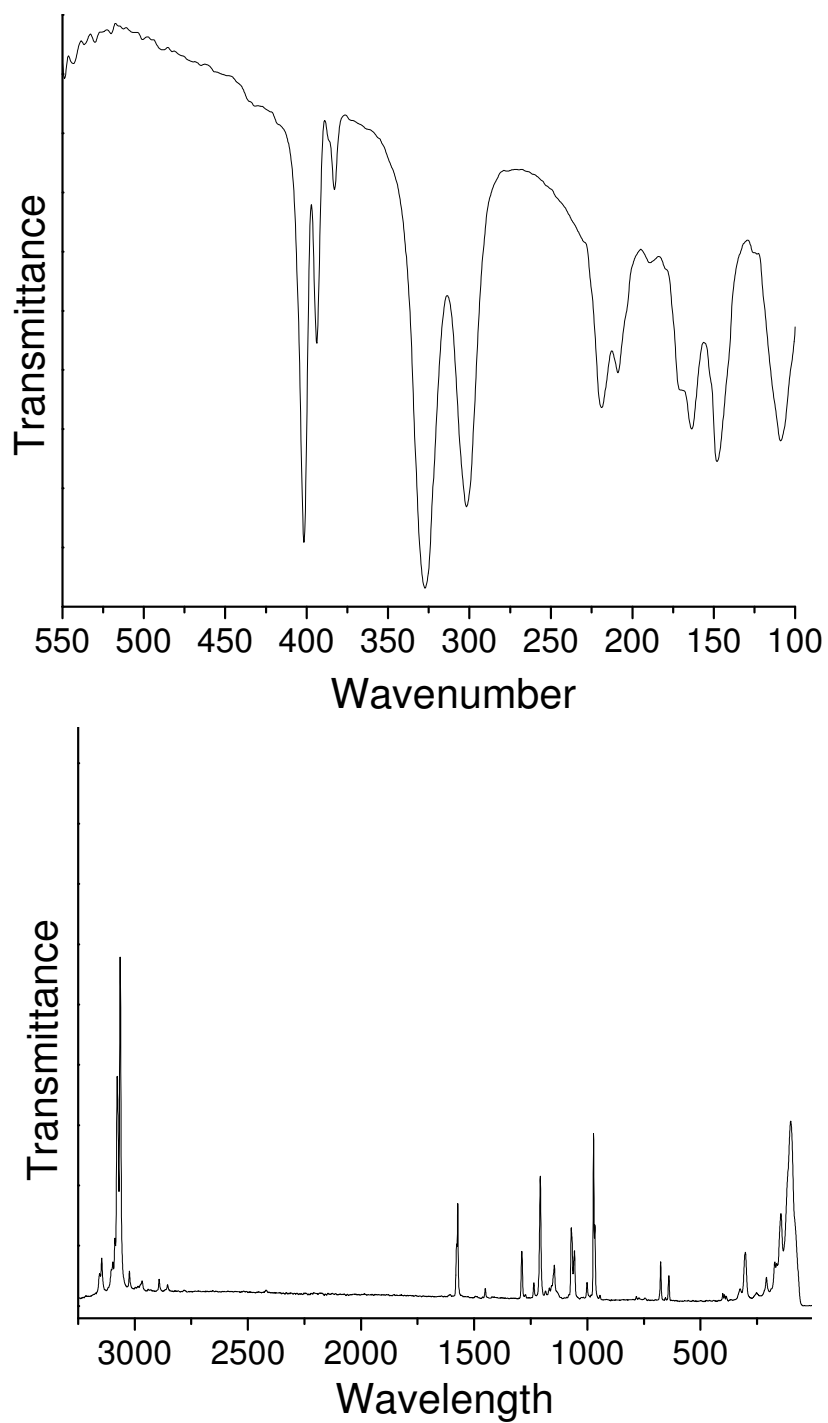


Figure 4:IR (top) and Raman (bottom) spectra for form I

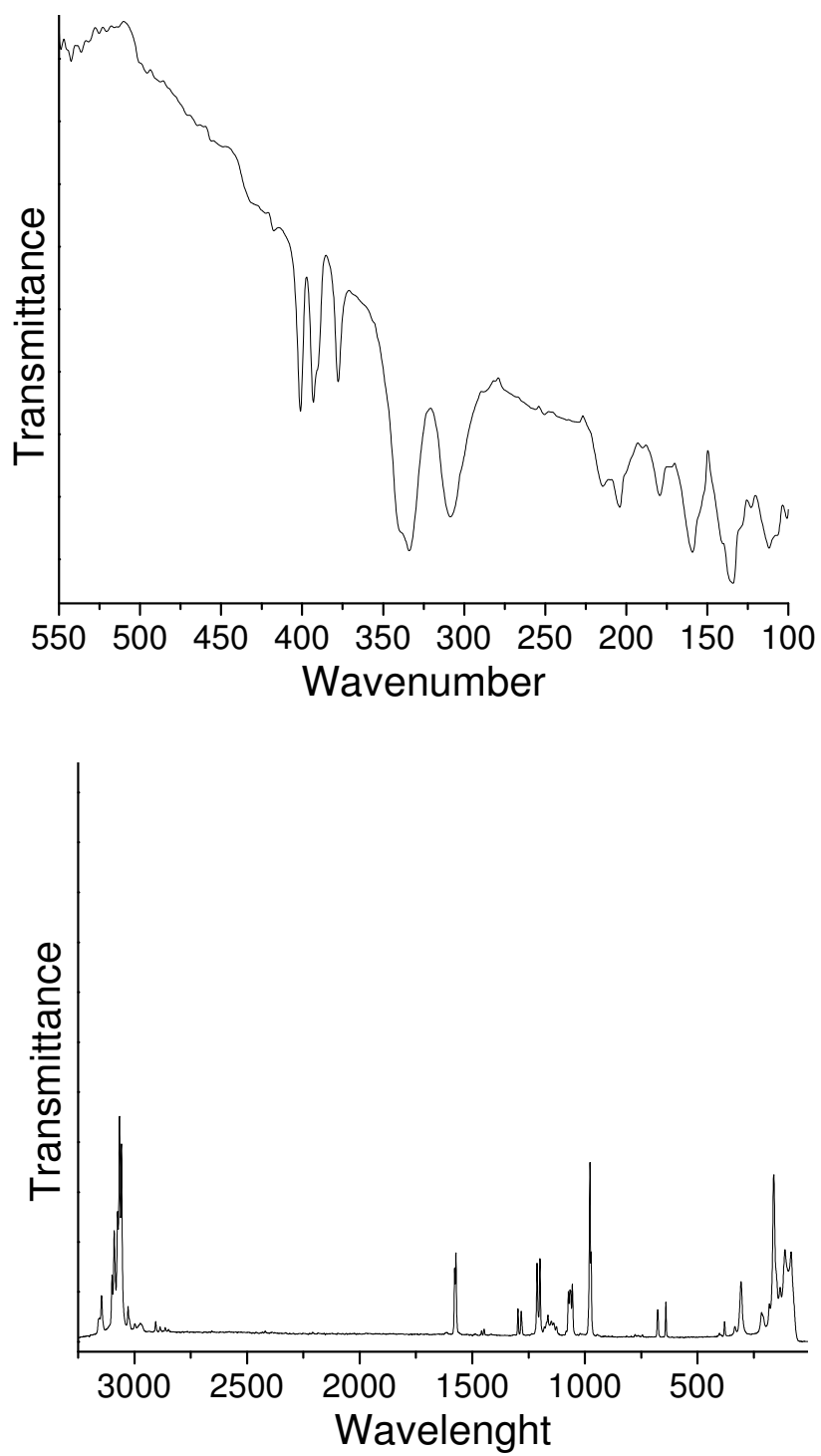


Figure 5: IR (top) and Raman (bottom) spectra for form **II**

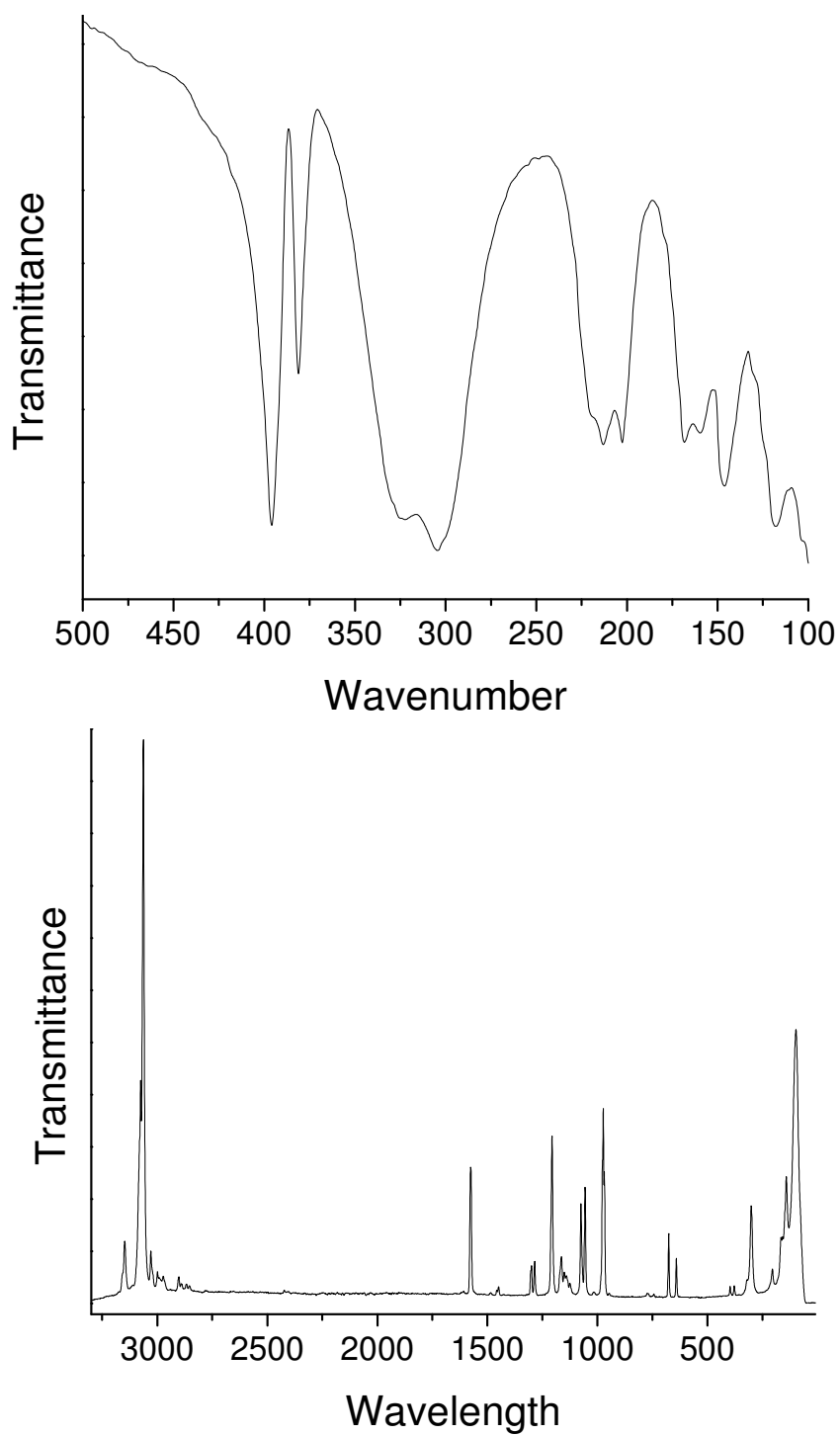


Figure 6: IR (top) and Raman (bottom) spectra for form **III**

Two Polymorphic Modifications of Dibromo-bis(acetonitrile-N)-zinc(II)

Gaurav Bhosekar, Inke Jeß, and Christian Näther

Institut für Anorganische Chemie der Christian-Albrechts-Universität zu Kiel, Olshausenstraße 40, D-24098 Kiel, Germany

Reprint requests to PD Dr. Christian Näther. E-mail: cnaether@ac.uni-kiel.de

Z. Naturforsch. **61b**, 721 – 726 (2006); received February 2, 2006

Dedicated to Professor Wolfgang Jeitschko on the occasion of his 70th birthday

Two polymorphic modifications of dibromo-bis(acetonitrile-N)-zinc(II) have been characterized by single crystal structure analysis and X-ray powder measurements. Form **I** crystallizes in the orthorhombic space group *Pnma* with $a = 13.101(2)$, $b = 10.210(1)$, $c = 6.8078(7)$ Å and $Z = 4$. The structure is composed of discrete molecular complexes in which each zinc cation is coordinated by two bromide anions and two acetonitrile ligands within distorted tetrahedra. Form **II** crystallizes in the orthorhombic space group *Cmcm* with $a = 8.0734(8)$, $b = 11.012(1)$, $c = 10.204(1)$ Å and $Z = 4$. In this compound also discrete complexes are found and the coordination of the zinc atoms is identical to that of form **I**. Two bromide atoms and two acetonitrile ligands coordinate to the zinc cations within distorted tetrahedra. The packing of the discrete molecular complexes in form **II** is completely different from that in form **I**. Form **I** was originally prepared in the presence of 2-chloropyrazine but can also be synthesized phase pure by crystallization from acetonitrile alone. In contrast, form **II** was only obtained in the presence of 2-chloropyrazine if the crystallization is performed under kinetic control but it immediately transforms into form **I**. Crystallization experiments reveal that form **I** is the thermodynamically most stable form between -40 °C and the boiling point of acetonitrile of 80 °C, whereas form **II** is metastable. On storing, the thermodynamically stable form **I** at room temperature decomposes into zinc(II) bromide within a few hours, but in a saturated acetonitrile atmosphere it is stable over a long period. On heating form **I** all ligands are liberated in one step leading to zinc bromide.

Key words: Polymorphism, Coordination Compounds, Zinc Bromide, Crystal Structures

Introduction

For several years we have been interested in the synthesis, crystal structures and properties of inorganic-organic coordination polymers based on copper(I) halides or pseudo halides CuX and nitrogen donor ligands. For a certain copper(I) halide or pseudohalide and a specific nitrogen donor ligand frequently several compounds are found, which differ in the ratio between the inorganic and organic part. During our investigations we have found that most of the ligand richer compounds lose their ligands stepwise on heating, forming ligand poorer intermediate compounds [1–8]. In most cases these intermediates can be isolated in a very pure form and in almost 100% yield. Hence, the thermal decomposition of suitable CuX precursor compounds is an alternative route for the preparation of new CuX coordination polymers which cannot be prepared in solution or which are otherwise only obtained as mixtures.

Starting from these findings we have investigated if the preparation of ligand poorer coordination compounds is limited to copper(I) halide coordination polymers or if it can be expanded to other classes of coordination compounds. Because in the ligand rich and ligand poor copper(I) halide coordination polymers in most cases different CuX substructures like *e. g.* monomers, or single and double chains are found, ligand rich and ligand poor compounds can be expected for those metal halides, which shows a similar structural behaviour. Since metal halide substructures are also found in compounds on the basis of zinc(II) halides and donor ligands, these compounds should be good candidates for further investigations [9–13]. Therefore, we have started systematic investigations on the preparation, structures and thermal properties of zinc(II) halide coordination compounds. In the beginning we tried to prepare compounds with some pyrazine derivatives as ligand like *e. g.* 2-chloropyrazine, which we have also used in

the preparation of the copper(I) coordination polymers. During these investigations we have synthesized and structurally characterized the coordination compounds $ZnX_2(2\text{-chloropyrazine})_2$ ($X = \text{Cl, Br, I}$) [14]. In order to prove if there are several compounds of different stoichiometry we reacted different amounts of the zinc halides in acetonitrile. In one of these batches we obtained a mixture of the 1 : 2 compound $ZnBr_2(2\text{-chloropyrazine})_2$ and two polymorphic modifications of $ZnBr_2(\text{acetonitrile})_2$. The phenomenon of polymorphism is of interest from several points of view. First of all the structural aspects of polymorphism provide information on intermolecular interactions in crystals, and therefore, can be used for a more rational crystal design [15]. Because the structure is different while the chemical composition is identical, structure property relationships can be investigated [16]. Moreover, investigations on the thermodynamic and kinetic aspects of polymorphism provide important information on the stability of the modifications and their transformation behavior [17]. In addition, even though some examples of polymorphic modifications of coordination compounds have been reported in literature, this is a very rare phenomenon in this area [18–21]. Therefore, we have structurally characterized and investigated both forms.

Results and Discussion

Crystal structures

Form I of dibromo-bis(acetonitrile-N) zinc(II) crystallizes in the orthorhombic primitive space group $Pnma$ with four formula units in the unit cell (Table 2). The asymmetric unit consists of one zinc cation and two bromide anions which are located on a crystallographic mirror plane, and one acetonitrile ligand which occupies a general position. Each zinc cation is coordinated by two bromide anions and two nitrogen atoms of symmetry related acetonitrile ligands within a distorted tetrahedron forming discrete complexes (Fig. 1). The Zn-Br distances of 2.336 and 2.338 Å as well as the Zn-N distance of 2.046 Å are comparable to distances retrieved from the CSD data base (Conquest; Version 1.6, 2005) (Table 1) [22]. The N-Zn-N angles of 95.9° as well as the Br-Zn-Br angles of 119.85° deviate strongly from the ideal tetrahedral values, whereas the N-Zn-Br angles are close to 109° (Table 1).

Form II of dibromo-bis(acetonitrile-N)-zinc(II) crystallizes in the orthorhombic C -centered space

Table 1. Selected bond lengths (Å) and angles ($^\circ$) for form I and form II.

Form I		Form II	
Zn1-Br1	2.338(1)	Zn1-Br1	2.336(1)
Zn1-Br2	2.336(1)	Zn1-Br1 ⁱ	2.336(1)
Zn1-N1	2.036(5)	Zn1-N1	2.034(6)
Zn1-N1 ⁱ	2.036(5)	Zn1-N1 ⁱⁱ	2.034(6)
N1-Zn1-N1 ⁱ	95.9(3)	N1 ⁱⁱ -Zn1-N1	96.0(4)
N1-Zn1-Br2	109.6(2)	N1 ⁱⁱ -Zn1-Br1 ⁱ	109.5(1)
N1 ⁱ -Zn1-Br2	109.6(2)	N1-Zn1-Br1 ⁱ	109.5(1)
N1-Zn1-Br1	109.6(2)	N1 ⁱ -Zn1-Br1	109.5(1)
N1 ⁱ -Zn1-Br1	109.6(2)	N1-Zn1-Br1	109.5(1)
Br2-Zn1-Br1	119.85(4)	Br1 ⁱ -Zn1-Br1	120.2(1)
Cl1-N1-Zn1	171.7(5)	Cl1-N1-Zn1	172.0(6)

Symmetry transformations used to generate equivalent atoms for form I (ⁱ $x, -y + 1/2, z$) and form II (ⁱ $-x, y, -z + 1/2$, ⁱⁱ $x, y, -z + 1/2$).

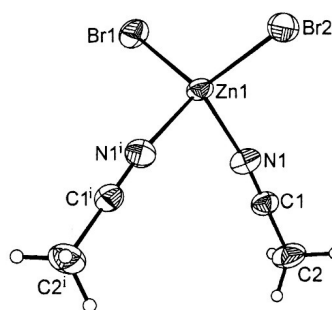


Fig. 1. Crystal structure of form I with labelling and displacement ellipsoids drawn at the 50% probability level (symmetry codes: ⁱ $x, -y + 1/2, z$).

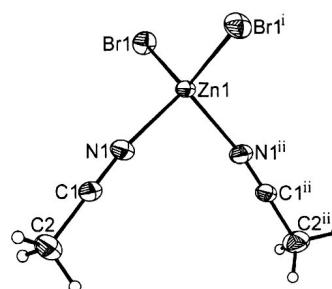
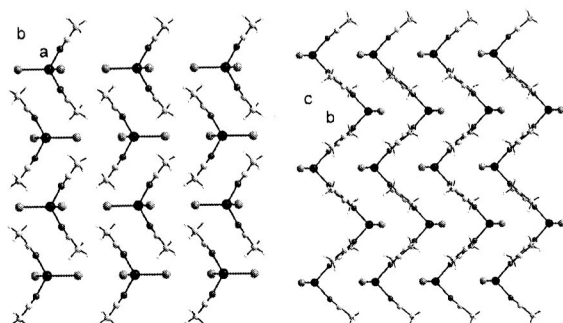


Fig. 2. Crystal structure of form II with labelling and displacement ellipsoids drawn at the 50% probability level (the disorder of the hydrogen atoms is not shown for clarity; symmetry codes: ⁱ $-x, y, -z + 1/2$; ⁱⁱ $x, y, -z + 1/2$).

group $Cmcm$ with four formula units in the unit cell (Table 2). The asymmetric unit consists of one zinc cation located on a position with site symmetry $m2m$ as well as one bromide anion and one acetonitrile ligand which are located on a crystallographic mirror plane. Because of symmetry, the hydrogen atoms of the acetonitrile ligand are disordered in two orientations. The zinc cations are each coordinated by two symmetry related bromide anions and the nitrogen atoms of two symmetry related acetonitrile ligands within a distorted tetrahedron (Fig. 2). As in form I, discrete molecular complexes are formed. The Zn-Br distance of 2.336 Å and the Zn-N distance of 2.034 Å are comparable to those in form I and agree well with those retrieved

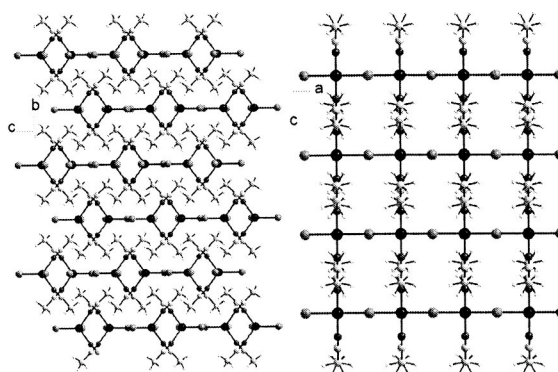
Table 2. Selected crystal data and results of the structure refinements for form I and II.

Compound	Form I	Form II
Formula	C ₄ H ₆ Br ₂ N ₂ Zn	C ₄ H ₆ Br ₂ N ₂ Zn
MW [g·mol ⁻¹]	307.30	307.30
Crystal colour	colourless	colourless
Crystal size [mm ⁻¹]	0.40 × 0.35 × 0.30	0.45 × 0.30 × 0.25
Crystal system	orthorhombic	orthorhombic
Space group	<i>Pnma</i>	<i>Cmcm</i>
<i>a</i> [Å]	13.101(2)	8.0734(8)
<i>b</i> [Å]	10.210(1)	11.012(1)
<i>c</i> [Å]	6.8078(7)	10.204(1)
<i>V</i> [Å ³]	910.6(2)	907.2(3)
Temperature [K]	200	200
<i>Z</i>	4	4
<i>D</i> _{calc.} g·cm ⁻³	2.241	2.250
2θ-Range [°]	3–56	3–56
<i>h</i> / <i>k</i> / <i>l</i> Ranges	–17/17 –13/10 –8/7	–10/10 –14/13 –13/13
μ(Mo-Kα) [mm ⁻¹]	11.4	11.4
Min./max. transm.	0.110/0.205	0.104/0.380
Measured reflections	4746	4265
<i>R</i> _{int.}	0.0794	0.1294
Independent refl.	1137	614
Refl. with <i>I</i> > 2σ(<i>I</i>)	828	548
Parameters	48	31
<i>R</i> ₁ [<i>I</i> > 2σ(<i>I</i>)]	0.0437	0.0447
<i>wR</i> ₂ [all data]	0.1103	0.1275
Goof	0.993	1.036
Residual electron density [e·Å ⁻³]	1.51/–1.14	1.34/–0.84

Fig. 3. Crystal structure of form I with view along the crystallographic *c*-axis (left) and of form II with view along the crystallographic *a*-axis (right).

from the CSD data base (Table 1) [22]. The distortion of the polyhedra is comparable to that in form I (N–Zn–N angles = 96.0°; Br–Zn–Br angles = 120.2°) (Table 1).

The crystal structures of both forms are completely different. In form I the discrete complexes are stacked in the direction of the *c*-axis, with the bromide anions pointing in the direction of the *a*-axis, the neigh-

Fig. 4. Crystal structure of form I with view along the crystallographic *a*-axis (left) and of form II with view along the crystallographic *b*-axis (right).

boring stacks being related by inversion symmetry in the direction of the *b*-axis (Fig. 3: left). The stacks are packed in a way that one stack fits perfectly into the aperture formed by the surrounding stacks. The organic ligands as well as the ZnBr₂ units are arranged in layers, which are stacked perpendicular to the *b*-axis (Fig. 4: left). The shortest intermolecular Br···Br distances amount to 3.947 and 4.045 Å. There is one short intermolecular C–H···Br contact with an H···Br distance of 3.145 Å and a C–H···Br angle of 166.0° indicative of weak hydrogen bonding.

In contrast to form I, in the crystal structure of form II the discrete complexes are shifted in the *b*-*c*-plane and therefore, no stacks are found (Fig. 3: right). Additionally, the methyl groups are not arranged in separate layers as in form I (Fig. 4: right). The shortest intermolecular Br···Br distances of 4.024 and 4.049 Å are slightly longer than in form I. The shortest intermolecular H···Br contact amounts to 3.131 Å but the angle C–H···Br of 137.5° deviates strongly from linearity and therefore, this should not correspond to any significant stabilizing interaction. This could be the reason for the disorder of the methyl hydrogen atoms and besides other reasons for the lower stability of this form.

Crystallization experiments

As mentioned in the experimental part, both forms were isolated for the first time by serendipity in one batch which contained 2-chloropyrazine as a ligand. Therefore, we tried to prepare both forms from acetonitrile. However, all crystals investigated consists only of form I. In the following we determined which of

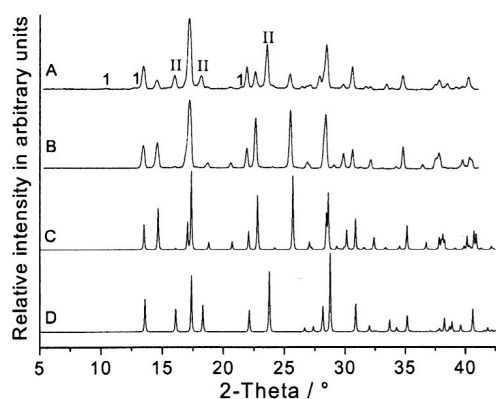


Fig. 5. Experimental X-ray powder pattern of a residue obtained by fast crystallization of a mixture of ZnBr_2 with 2-chloropyrazine in acetonitrile (A), after stirring a suspension of crystalline ZnBr_2 in acetonitrile for 2 d leading to the thermodynamically most stable form II (B), and theoretical X-ray powder patterns calculated for form I (C) and form II (D) from single crystal data (II indicates reflections which originate from modification II and 1 indicates reflections which originates from the 1:2 compound $\text{ZnBr}_2(2\text{-chloropyrazine})_2$).

the two forms represents the thermodynamically most stable form at r. t. Therefore, we stirred suspensions of crystalline zinc(II) bromide in acetonitrile for two days and investigated the residue obtained by X-ray powder measurements. By comparing the experimental pattern with those calculated for forms I and II from single crystal data, it was obvious that only modification I had formed phase pure (Fig. 5: B–D). Therefore, this form represents the thermodynamically most stable form at r. t. To investigate the stability range of form I, we have performed additional experiments, in which suspensions were stirred at -40 and 80 °C and the residues were immediately investigated by X-ray powder diffraction. In all of these experiments we obtained only form I as a phase pure compound and therefore, this modification represents the thermodynamically most stable forms within this temperature range. However, these experiments indicated that modification II was formed only by kinetic control. Therefore, we have added clear solutions of zinc(II) bromide in acetonitrile to tetrachloromethane in which this compound is insoluble. The precipitates formed were isolated immediately and investigated by X-ray powder measurements. However, the powder pattern can be explained successfully only with the presence of the stable form I. Because the crystals of modification II were formed in the presence of 2-chloropyrazine (see Experimental Section), we assumed that this ligand is needed for the

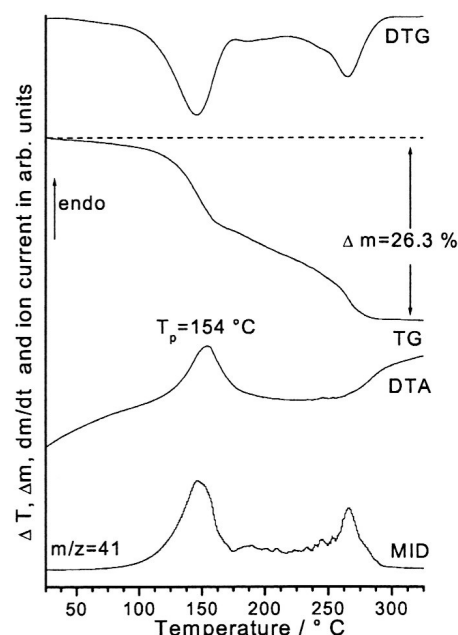


Fig. 6. DTA-, TG-, DTG and MS trend scan curve for form I (T_p = peak temperature; $m/z = 41$ corresponds to acetonitrile).

crystallization of the metastable form. It is well known that in different solvents or in the presence of some additives crystal growth of some thermodynamically stable forms is prevented and a metastable form may be observed. Therefore, we have performed crystallization experiments in the presence of 2-chloropyrazine and we have found in some batches mixtures which consisted of large amounts of the stable form I and small amounts of $\text{ZnBr}_2(2\text{-chloropyrazine})_2$ as well as of form II (Fig. 5: A), but we have to mention that in some batches only form I appeared. Therefore, the preparation of form II is difficult to reproduce and depends on the experimental conditions. This is not an unusual phenomenon and several of such observations have been described in the literature [23].

Form I was additionally investigated by simultaneous differential thermoanalysis and thermogravimetry coupled to mass spectroscopy in order to investigate if the decomposition of this compound directly leads to the formation of zinc bromide or if some ligand poor intermediate compound can be observed (Fig. 6). During the thermogravimetric analysis of form I only a single mass loss is observed in the TG curve which is accompanied by an endothermic event at 154 °C in the DTA curve. This mass loss is finished at about 300 °C and the MS measurements show clearly that only ace-

Table 3. Atomic coordinates [$\cdot 10^4$] and equivalent isotropic displacement parameters [$\text{\AA}^2 \cdot 10^3$] for form I.

Atom	Wyckoff position	x	y	z	U_{eq}
Zn(1)	4c	5109(1)	2500	5388(1)	27(1)
Br(1)	4c	5782(1)	2500	2207(1)	38(1)
Br(2)	4c	3342(1)	2500	5848(1)	36(1)
N(1)	8d	5746(3)	3981(6)	6972(7)	36(1)
C(1)	8d	6157(4)	4688(6)	7977(7)	31(1)
C(2)	8d	6677(5)	5598(7)	9276(9)	45(2)

Equivalent isotropic U_{eq} calculated as a third of the trace of the orthogonalized U_{ij} tensors.

tonitrile ($m/z = 41$) is emitted. In addition, the experimental mass loss of 26.3% is in very good agreement with that calculated for the removal of all ligands ($\Delta m_{\text{theo}} = -26.7\%$). From the nature of the TG curve there is some hint for the formation of a ligand poor intermediate phase at about 150 °C. Therefore, we performed further DTA-TG measurements in which the reaction was stopped at about 150 °C, where the DTG curve exhibits a minimum. The residue isolated at this temperature was investigated later by X-ray powder measurements. The experimental powder pattern was in perfect agreement with that calculated for form I and therefore, the presence of a ligand poor compound can be excluded.

Conclusion

In the present work two polymorphic modifications of dibromo-bis(acetonitrile-N)-zinc(II) were found by serendipity. Both forms consists of discrete complexes built up of zinc cations which are coordinated by two bromide anions and two acetonitrile ligands within distorted tetrahedra. The crystallization experiments have shown that form I represents the thermodynamically most stable form at r. t., whereas form II must be metastable. The reason for the higher stability of form I compared to form II is difficult to analyze. However, in contrast to form II, intermolecular C-H...Br and Br...Br interactions are observed in the stable modification I. In addition, in the stable form the methyl groups of the acetonitrile ligands are arranged in layers and therefore, van der Waals interactions might also contribute to the stabilization of this form. Additionally, crystallization experiments reveal that form I should also be the thermodynamically most stable form between -40 and 80 °C. However, it might be that both forms behave monotropically and that form I is the thermodynamically most stable form over the complete temperature range. It might also be that they

Table 4. Atomic coordinates [$\cdot 10^4$] and equivalent isotropic displacement parameters [$\text{\AA}^2 \cdot 10^3$] for form II.

Atom	Wyckoff position	x	y	z	U_{eq}
Zn(1)	4c	0	4764(1)	2500	18(1)
Br(1)	8g	-2508(1)	5822(1)	2500	29(1)
N(1)	8f	0	3528(5)	3981(6)	26(1)
C(1)	8f	0	2743(6)	4692(7)	24(1)
C(2)	8f	0	1715(7)	5582(8)	39(2)

Equivalent isotropic U_{eq} calculated as a third of the trace of the orthogonalized U_{ij} tensors.

behave enantiotropically, but in this case form II must be the most stable form at lower temperatures which would be in accordance with the higher density of this form.

Finally, our investigations have shown that the phenomenon of polymorphism is sometimes hard to investigate and especially the preparation of metastable forms is very often difficult to reproduce.

Experimental Section

Preparation of form I

Forms I and II were originally prepared by the reaction of equivalent amounts of zinc(II) bromide with 2-chloropyrazine in an large excess of non-dried commercial available acetonitrile, which leads to a mixture of both forms and of $\text{ZnBr}_2(2\text{-chloropyrazine})_2$. However, form I can simply be prepared by stirring suspensions of crystalline zinc(II) bromide in acetonitrile at r. t. Single crystals of form I were prepared by slow evaporation of the solvent from a solution of zinc(II) bromide in acetonitrile. In this case very brittle colorless crystals of irregular shape were obtained. Most of them were grown together and decomposed on storage. $\text{C}_4\text{H}_6\text{Br}_2\text{N}_2\text{Zn}$ (307.30): calcd. C 15.63, H 1.97, N 9.12; found C 15.45, H 1.89, N 9.01.

Crystals of form II were initially obtained in a batch where 2-chloropyrazine was present. Small amounts could also be prepared as the crystallization was performed in the presence of 2-chloropyrazine under kinetic control, but it was not possible to obtain form II as a phase pure product.

Single crystal structure analysis

All data were measured using an Imaging Plate Diffraction System from STOE & CIE. Structure solutions were performed with direct methods using SHELXS-97 [24]. Structure refinement was carried out against F^2 using SHELXL-97 [24]. All non-hydrogen atoms were refined with anisotropic displacement parameters. The C-H hydrogen atoms were positioned with idealised geometry, allowed to rotate but not tip, and refined with isotropic displacement

parameters using the riding model. For both forms a numerical absorption correction was performed using X-RED and X-SHAPE [25]. In form **II** the methyl hydrogen atoms are disordered in two orientations with equal s.o.f.'s due to symmetry. The low reliability factors for both structure determinations originate from very low crystal quality. Selected crystal data and results of the structure refinements are shown in Table 2, atomic coordinates and equivalent isotropic displacement parameters are given in Tables 3 and 4.

Crystallographic data (excluding structure factors) have been deposited with the Cambridge Crystallographic Data Centre as supplementary publication no. CCDC-600157 (form **I**), CCDC-600158 (form **II**). Copies of the data can be obtained, free of charge, on application to CCDC, 12 Union Road, Cambridge CB2 1 EZ, UK. (fax: +44-(0)1223-336033 or e-mail: deposit@ccdc.cam.ac.uk).

X-ray powder diffraction

X-ray powder diffraction experiments were performed using a STOE STADI P transmission powder diffractometer

equipped with a 4° PSD (position sensitive detector) using Cu-K α radiation ($\lambda = 1.540598 \text{ \AA}$).

Differential thermal analysis, thermogravimetry and mass spectrometry

DTA-TG-MS measurements were performed using the STA-409CD instrument with heating rates of 4 °C/min in flowing nitrogen atmosphere (purity: 5.0), which is connected to a mass spectrometer from Balzers by skimmer coupling from Netzsch. All measurements were performed with a flow rate of 75 ml/min and were corrected for buoyancy and current effects. The instrument was calibrated using standard reference materials.

Acknowledgements

This work was supported by the State of Schleswig-Holstein and the Deutsche Forschungsgemeinschaft (Projekt No.: NA 720/1-1). We are very thankful to Professor Dr. Wolfgang Bensch for financial support and for access to his equipment.

-
- [1] C. Näther, J. Greve, I. Jeß, *Polyhedron* **20**, 1017 (2001).
[2] C. Näther, I. Jeß, H. Studzinski, *Z. Naturforsch.* **56b**, 997 (2001).
[3] C. Näther, I. Jeß, *J. Solid State Chem.* **169**, 103 (2002).
[4] C. Näther, J. Greve, I. Jeß, *Solid State Sci.* **4**, 813 (2002).
[5] C. Näther, M. Wriedt, I. Jeß, *Inorg. Chem.* **42**, 2391 (2003).
[6] C. Näther, I. Jeß, N. Lehnert, D. Hinz-Hübner, *Solid State Sci.* **5**, 1343 (2003).
[7] C. Näther, J. Greve, I. Jeß, C. Wickleder, *Solid State Sci.* **5**, 1167 (2003).
[8] T. Kromp, W. S. Sheldrick, C. Näther, *Z. Anorg. Allg. Chem.* **629**, 45 (2003).
[9] S. A. Bourne, M. Kilkenny, L. R. Nassimbeni, *J. Chem. Soc. Dalton Trans.* 1176 (2001).
[10] S. M. Godfrey, C. A. McAuliffe, R. G. Pritchard, J. M. Sheffield, *Inorg. Chim. Acta* **292**, 213 (1999).
[11] F. Bottomley, E. C. Ferris, P. S. White, *Acta Crystallogr.* **C45**, 816 (1989).
[12] J. Pickardt, B. Staub, *Z. Naturforsch.* **51**, 947 (1996).
[13] Chunhua Hu, U. Englert, *Cryst. Eng. Com.* **3**, 91 (2001).
[14] G. Bhosekar, C. Näther, unpublished results.
[15] J. Bernstein, *J. Phys.* **B66**, 26 (1993).
[16] G. R. Desiraju (ed.): "Crystal Engineering" *Mat. Sci. Monogr.*, Elsevier, Amsterdam (1989) and references cited therein.
[17] J. Bernstein, R. Davey, O. Henck, *Angew. Chem.* **111**, 3646 (1999) and *Angew. Chem. Int. Ed. Engl.* **38**, 3440 (1999).
[18] S. A. Barnett, A. J. Blake, N. R. Champness, C. Wilson, *Chem. Commun.* 1640 (2002).
[19] B. Moulton, M. Zaworotko, *J. Chem. Soc. Rev.* **101**, 1629 (2001).
[20] S. R. Batten, K. S. Murray, *K. S. Aust. J. Chem.* **54**, 605 (2001).
[21] D. Braga, L. Maini, M. Polito, L. Scaccianoce, G. Cozzazzi, F. Grepioni, *Coordination Chem. Rev.* **216**, 783 (2001).
[22] F. Allen, O. Kennard, *Chem. Des. Autom. News* **8**, 31 (1993).
[23] J. D. Dunitz, J. Bernstein *Acc. Chem. Res.* **28**, 193 (1995).
[24] W. S. Sheldrick, *SHELXS-97 and SHELXL-97*; programs for the solution and the refinement of crystal structures; University of Göttingen (1997).
[25] STOE & CIE, *X-Shape and X-Red*; programs for absorption correction.

Supplemental material

Table 1. Crystal data and structure refinement for ZnBr₂(acetonitrile-N) at 200 K in Cmc_m.

Identification code	gb137	
Empirical formula	C ₄ H ₆ Br ₂ N ₂ Zn	
Formula weight	307.30	
Temperature	200(2) K	
Wavelength	0.71073 Å	
Crystal system	trigonal	
Space group	Cmc _m	
Unit cell dimensions	a = 8.0734(16) Å	α = 90°.
	b = 11.012(2) Å	β = 90°.
	c = 10.204(2) Å	γ = 90°.
Volume	907.2(3) Å ³	
Z	4	
Density (calculated)	2.250 Mg/m ³	
Absorption coefficient	11.442 mm ⁻¹	
F(000)	576	
Crystal size	0.2 x 0.13 x 0.05 mm ³	
Theta range for data collection	3.13 to 28.04°.	
Index ranges	-10 ≤ h ≤ 10, -14 ≤ k ≤ 14, -13 ≤ l ≤ 13	
Reflections collected	4265	
Independent reflections	614 [R(int) = 0.1294]	
Completeness to theta = 28.04°	99.4 %	
Refinement method	Full-matrix least-squares on F ²	
Data / restraints / parameters	614 / 0 / 31	
Goodness-of-fit on F ²	1.036	
Final R indices [I > 2σ(I)]	R1 = 0.0447, wR2 = 0.1229	
R indices (all data)	R1 = 0.0503, wR2 = 0.1275	
Extinction coefficient	0.0182(19)	
Largest diff. peak and hole	1.337 and -0.835 e.Å ⁻³	

Remarks:

All non-hydrogen atoms were refined using anisotropic displacement parameters. The hydrogen atoms were positioned with idealized geometry and were refined isotropic · U_{eq}(C_{aromatic}) = 1.2 using a riding model with C-H = 0.98 Å for aliphatic hydrogen atoms. There is one crystallographically independent molecule into the asymmetric unit, which is located in a special positions

2 Publications

Table 2. Atomic coordinates ($\times 10^4$) and equivalent isotropic displacement parameters ($\text{\AA}^2 \times 10^3$). $U(\text{eq})$ is defined as one third of the trace of the orthogonalized U_{ij} tensor.

	x	y	z	$U(\text{eq})$
Zn(1)	0	4764(1)	2500	18(1)
Br(1)	-2508(1)	5822(1)	2500	29(1)
N(1)	0	3528(5)	3981(6)	26(1)
C(1)	0	2743(6)	4692(7)	24(1)
C(2)	0	1715(7)	5582(8)	39(2)

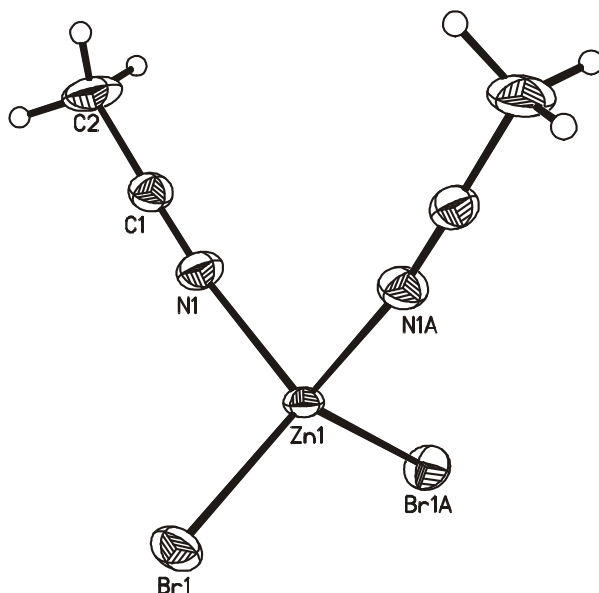


Table 3. Bond lengths [\AA] and angles [$^\circ$].

Zn(1)-N(1A)	2.034(6)	N(1A)-Zn(1)-Br(1B)	109.49(7)
Zn(1)-N(1)	2.034(6)	N(1)-Zn(1)-Br(1B)	109.49(7)
Zn(1)-Br(1B)	2.3359(8)	N(1A)-Zn(1)-Br(1)	109.49(7)
Zn(1)-Br(1)	2.3359(8)	N(1)-Zn(1)-Br(1)	109.49(7)
N(1)-C(1)	1.128(9)	Br(1B)-Zn(1)-Br(1)	120.17(5)
C(1)-C(2)	1.452(10)	C(1)-N(1)-Zn(1)	172.0(6)
N(1A)-Zn(1)-N(1)	96.0(4)	N(1)-C(1)-C(2)	178.8(8)

Symmetry transformations used to generate equivalent atoms: A: $x, y, -z+1/2$, B: $-x, y, -z+1/2$

Table 4. Anisotropic displacement parameters ($\text{\AA}^2 \times 10^3$). The anisotropic displacement factor exponent takes the form: $-2\pi^2 [h^2 a^{*2} U_{11} + \dots + 2 h k a^* b^* U_{12}]$

	U_{11}	U_{22}	U_{33}	U_{23}	U_{13}	U_{12}
Zn(1)	19(1)	13(1)	21(1)	0	0	0
Br(1)	20(1)	29(1)	38(1)	0	0	7(1)
N(1)	33(3)	18(3)	28(3)	3(2)	0	0
C(1)	29(3)	17(3)	25(3)	-2(3)	0	0
C(2)	62(6)	26(4)	30(4)	7(3)	0	0

Table 5. Hydrogen coordinates ($\times 10^4$) and isotropic displacement parameters ($\text{\AA}^2 \times 10^3$)

	x	y	z	$U(\text{eq})$
H(2A)	583	1032	5175	59
H(2B)	-1144	1478	5775	59
H(2C)	562	1941	6398	59

2 Publications

Table 1. Crystal data and structure refinement for dibromo bis (N-acetonitrile) zinc(II) in Pnma.

Identification code	gb137a
Empirical formula	C ₄ H ₆ Br ₂ N ₂ Zn
Formula weight	307.30
Temperature	170(2) K
Wavelength	0.71073 Å
Crystal system	orthorhombic
Space group	Pnma
Unit cell dimensions	a = 13.1011(17) Å α = 90° b = 10.2102(10) Å β = 90° c = 6.8078(7) Å γ = 90°
Volume	910.64(18) Å ³
Z	4
Density (calculated)	2.241 Mg/m ³
Absorption coefficient	11.398 mm ⁻¹
F(000)	576
Crystal size	0.07 x 0.1 x 0.13 mm ³
Theta range for data collection	3.11 to 27.92°.
Index ranges	-17 ≤ h ≤ 17, -13 ≤ k ≤ 10, -8 ≤ l ≤ 7
Reflections collected	4746
Independent reflections	1137 [R(int) = 0.0794]
Completeness to theta = 27.92°	99.0 %
Refinement method	Full-matrix least-squares on F ²
Data / restraints / parameters	1137 / 0 / 48
Goodness-of-fit on F ²	0.993
Final R indices [I > 2σ(I)]	R1 = 0.0437, wR2 = 0.1001
R indices (all data)	R1 = 0.0678, wR2 = 0.1103
Extinction coefficient	0.0041(12)
Largest diff. peak and hole	1.506 and -1.141 e.Å ⁻³

Remarks:

All non-hydrogen atoms were refined using anisotropic displacement parameters. The hydrogen atoms were positioned with idealized geometry and were refined isotropic · Ueq(C_{aliphatic}) = 1.5 using a riding model with C-H = 0.98 Å for aromatic hydrogen atoms. There is one crystallographically independent molecule into the asymmetric unit, which is located in a special positions

2 Publications

Table 2. Atomic coordinates ($\times 10^4$) and equivalent isotropic displacement parameters ($\text{\AA}^2 \times 10^3$)

U(eq) is defined as one third of the trace of the orthogonalized U_{ij} tensor.

	x	y	z	U(eq)
Br(1)	5782(1)	2500	2207(1)	38(1)
Br(2)	3342(1)	2500	5848(1)	36(1)
Zn(1)	5109(1)	2500	5388(1)	27(1)
N(1)	5746(3)	3981(6)	6972(7)	36(1)
C(1)	6157(4)	4688(6)	7977(7)	31(1)
C(2)	6677(5)	5598(7)	9276(9)	45(2)

Table 3. Bond lengths [\AA] and angles [$^\circ$].

Br(1)-Zn(1)	2.3383(11)	N(1)-Zn(1)-Br(2)	109.59(13)
Br(2)-Zn(1)	2.3359(11)	N(1A)-Zn(1)-Br(2)	109.59(13)
Zn(1)-N(1)	2.036(5)	N(1)-Zn(1)-Br(1)	109.62(14)
Zn(1)-N(1A)	2.036(5)	N(1A)-Zn(1)-Br(1)	109.62(14)
N(1)-C(1)	1.131(8)	Br(2)-Zn(1)-Br(1)	119.85(4)
C(1)-C(2)	1.453(8)	C(1)-N(1)-Zn(1)	171.7(5)
N(1)-Zn(1)-N(1A)	95.9(3)	N(1)-C(1)-C(2)	179.6(6)

Symmetry transformations used to generate equivalent atoms: A: x,-y+1/2,z

Table 4. Anisotropic displacement parameters ($\text{\AA}^2 \times 10^3$). The anisotropic

displacement factor exponent takes the form: $-2\pi^2 [h^2 a^{*2} U_{11} + \dots + 2 h k a^* b^* U_{12}]$

	U_{11}	U_{22}	U_{33}	U_{23}	U_{13}	U_{12}
Br(1)	43(1)	51(1)	21(1)	0	7(1)	0
Br(2)	29(1)	48(1)	29(1)	0	1(1)	0
Zn(1)	30(1)	33(1)	16(1)	0	-2(1)	0
N(1)	41(3)	37(3)	29(2)	-3(2)	-4(2)	-5(2)
C(1)	33(3)	38(4)	23(3)	1(2)	1(2)	-2(2)
C(2)	58(4)	38(4)	38(3)	-10(3)	-15(3)	-7(3)

Table 5. Hydrogen coordinates ($\times 10^4$) and isotropic displacement parameters ($\text{\AA}^2 \times 10^3$)

	x	y	z	U(eq)
H(2A)	6187	6240	9781	67
H(2B)	7217	6052	8548	67
H(2C)	6979	5115	10376	67

Acta Crystallographica Section E
Structure Reports
Online

ISSN 1600-5368

Gaurav Bhosekar, Inke Jess and
Christian Näther*

Institut für Anorganische Chemie, Christian-
Albrechts-Universität Kiel, Olshausenstr. 40,
D-24098 Kiel, Germany

Correspondence e-mail:
cnaether@ac.uni-kiel.de

Key indicators

Single-crystal X-ray study
T = 220 K
Mean $\sigma(\text{C}-\text{C}) = 0.008 \text{ \AA}$
R factor = 0.032
wR factor = 0.088
Data-to-parameter ratio = 23.5

For details of how these key indicators were
automatically derived from the article, see
<http://journals.iucr.org/e>.

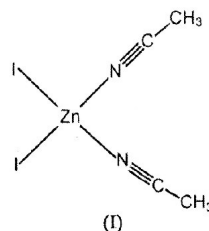
A redetermination of (acetonitrile- κN)diiodo- zinc(II)

Received 10 May 2006
Accepted 12 May 2006

In the title compound, $[\text{Zn}(\text{C}_2\text{H}_3\text{N})_2\text{I}_2]$ each Zn atom is coordinated by two symmetry-related I atoms and two symmetry-related acetonitrile ligands within a distorted tetrahedron to form a discrete complex. All non-H atoms are located in special positions, that for Zn having $m2m$ symmetry.

Comment

Recently, we have reported two polymorphs of dibromobis(acetonitrile- N)zinc(II) (Bhosekar, Jess & Näther, 2006). Form 1 crystallizes in the orthorhombic space group $Pnma$, whereas form 2 crystallizes in space group $Cmcm$. We have proven that form 2 is the thermodynamically more stable form between 233 and 353 K and that form 1 is metastable. In continuation of this work, we have investigated the reaction of zinc(II) iodide with acetonitrile. Surprisingly, only one form can be prepared, which is isotopic with the more stable form 2 of dibromobis(acetonitrile- N)zinc(II). A search of the CSD database [Version 1.8; Allen, 2002 using *ConQuest* (Version 1.8; Bruno *et al.*, 2002)] showed that this structure is known, but was reported in space group $P2_1/m$ (Raubacher & Weller, 1996). However, this structure can easily be transformed into the orthorhombic cell and space group $Cmcm$ was used in the refinement of the present compound.



The asymmetric unit of the title compound, (I), consists of one zinc cation located on a position of site symmetry $m2m$, as well as one iodide anion and one acetonitrile ligand which are located on perpendicular crystallographic mirror planes. The zinc cations are each coordinated by two symmetry-related iodide anions and two N atoms of two symmetry-related acetonitrile ligands within a distorted tetrahedron (Fig. 1). The Zn–I distance of 2.5315 (6) Å and the Zn–N distance of 2.046 (5) Å are comparable to those in related structures retrieved from the CSD. The crystal packing is shown in Fig. 2.

Experimental

ZnI_2 was obtained from Acros and acetonitrile from Fluka. Large amounts of crystalline powder can be prepared if a crystalline

metal-organic papers

suspension of 1 mmol (319.2 mg) of zinc(II) iodide is stirred in 1 ml of acetonitrile for 2 d. Single crystals are obtained if 1 mmol (319.2 mg) zinc(II) iodide is dissolved in 6.0 ml acetonitrile and 0.3 ml of water. After slow evaporation of the solvent, colourless plates formed. The homogeneity of the product was checked by X-ray powder diffraction.

Crystal data

$[\text{Zn}(\text{C}_2\text{H}_3\text{N})_2\text{I}_2]$	$Z = 4$
$M_r = 401.28$	$D_x = 2.557 \text{ Mg m}^{-3}$
Orthorhombic, $Cmcm$	Mo $K\alpha$ radiation
$a = 8.7049 (7) \text{ \AA}$	$\mu = 8.22 \text{ mm}^{-1}$
$b = 11.3913 (11) \text{ \AA}$	$T = 220 (2) \text{ K}$
$c = 10.5121 (11) \text{ \AA}$	Plate, colourless
$V = 1042.38 (17) \text{ \AA}^3$	$0.15 \times 0.10 \times 0.04 \text{ mm}$

Data collection

Stoe IPDS-1 diffractometer	4886 measured reflections
φ scans	704 independent reflections
Absorption correction: numerical <i>X-SHAPE</i> (Stoe & Cie, 1998)	628 reflections with $I > 2\sigma(I)$
$T_{\min} = 0.381$, $T_{\max} = 0.725$	$R_{\text{int}} = 0.065$
	$\theta_{\max} = 28.0^\circ$

Refinement

Refinement on F^2	$w = 1/[\sigma^2(F_o^2) + (0.059P)^2]$
$R[F^2 > 2\sigma(F^2)] = 0.032$	where $P = (F_o^2 + 2F_c^2)/3$
$wR(F^2) = 0.088$	$(\Delta/\sigma)_{\max} = 0.001$
$S = 1.06$	$\Delta\rho_{\max} = 1.86 \text{ e \AA}^{-3}$
704 reflections	$\Delta\rho_{\min} = -1.06 \text{ e \AA}^{-3}$
30 parameters	Extinction correction: <i>SHELXL97</i>
H-atom parameters constrained	Extinction coefficient: 0.0041 (5)

Table 1

Selected geometric parameters (\AA , $^\circ$).

Zn1–N1	2.046 (5)	Zn1–I1	2.5316 (5)
N1 ⁱ –Zn1–N1	96.3 (3)	I1 ⁱⁱ –Zn1–I1	120.50 (3)
N1–Zn1–I1	109.33 (5)		

Symmetry codes: (i) $x, y, -z + \frac{1}{2}$; (ii) $-x, y, -z + \frac{1}{2}$.

One of the H atoms was located in a difference map and its bond length was set to ideal values. Afterwards the positions of the two missing H atoms were calculated. In the end, all H atoms were treated as riding, with C–H = 0.97 \AA and with $U_{\text{iso}}(\text{H}) = 1.5U_{\text{eq}}(\text{C})$.

Data collection: *IPDS Software* (Stoe & Cie, 1998); cell refinement: *IPDS Software*; data reduction: *IPDS Software*; program(s) used to solve structure: *SHELXS97* (Sheldrick, 1997); program(s) used to refine structure: *SHELXL97* (Sheldrick, 1997); molecular graphics: *XP* in *SHELXTL* (Bruker, 1998); software used to prepare material for publication: *CIFTAB* in *SHELXTL* (Bruker, 1998).

This work is supported by the state of Schleswig-Holstein and the Deutsche Forschungsgemeinschaft (Projekt No. NA 720/1–1). We are very grateful to Professor Dr. Wolfgang Bensch for the opportunity to use his experimental equipment.

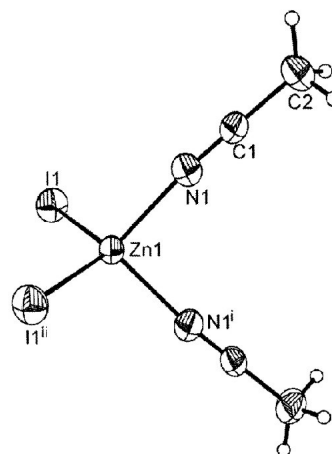


Figure 1 The structure of (I) with the atom-labelling and displacement ellipsoids drawn at the 50% probability level. [Symmetry codes: (i) $x, y, -z + \frac{1}{2}$; (ii) $-x, y, -z + \frac{1}{2}$.

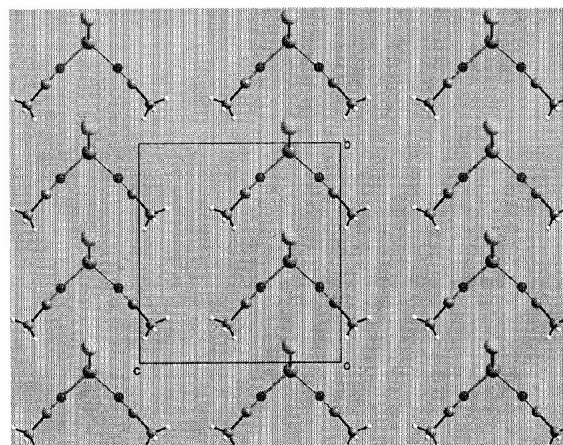


Figure 2 Packing of (I), viewed along the a axis.

References

- Allen, F. H. (2002). *Acta Cryst.* **B58**, 380–388.
 Bhosekar, G., Jess, I. & Näther, C. (2006). *Z. Naturforsch. Teil B* In the press.
 Bruker (1998). *SHELXTL*. Version 5.1. Bruker AXS Inc., Madison, Wisconsin, USA.
 Bruno, I. J., Cole, J. C., Edgington, P. R., Kessler, M., Macrae, C. F., McCabe, P., Pearson, J. & Taylor, R. (2002). *Acta Cryst.* **B58**, 389–397.
 Raubacher, F. & Weller, F. (1996). *Z. Kristallogr.* **211**, 576.
 Sheldrick, G. M. (1997). *SHELXS97* and *SHELXL97*. University of Göttingen, Germany.
 Stoe & Cie (1998). *X-SHAPE* (Version 1.03) and *IPDS* (Version 2.89). Stoe & Cie, Darmstadt, Germany.

Supplemental material

Table 1. Crystal data and structure refinement for GB273.

Identification code	gb273	
Empirical formula	C ₄ H ₆ I ₂ N ₂ Zn	
Formula weight	401.28	
Temperature	220(2) K	
Wavelength	0.71073 Å	
Crystal system	orthorhombic	
Space group	Ccca	
Unit cell dimensions	a = 8.7049(7) Å	α = 90°.
	b = 11.3913(11) Å	β = 90°.
	c = 10.5121(11) Å	γ = 90°.
Volume	1042.38(17) Å ³	
Z	4	
Density (calculated)	2.557 Mg/m ³	
Absorption coefficient	8.215 mm ⁻¹	
F(000)	720	
Crystal size	0.04 x 0.10 x 0.15 mm ³	
Theta range for data collection	2.95 to 27.97°.	
Index ranges	-11 ≤ h ≤ 11, -14 ≤ k ≤ 14, -13 ≤ l ≤ 13	
Reflections collected	4886	
Independent reflections	704 [R(int) = 0.0651]	
Completeness to theta = 27.97°	99.7 %	
Refinement method	Full-matrix least-squares on F ²	
Data / restraints / parameters	704 / 0 / 30	
Goodness-of-fit on F ²	1.059	
Final R indices [I > 2σ(I)]	R1 = 0.0324, wR2 = 0.0858	
R indices (all data)	R1 = 0.0363, wR2 = 0.0877	
Extinction coefficient	0.0041(5)	
Largest diff. peak and hole	1.857 and -1.061 e.Å ⁻³	

Remarks:

All non-hydrogen atoms were refined using anisotropic displacement parameters. The hydrogen atoms were positioned with idealized geometry and were refined isotropic ($U_{eq}(H) = 1.2 \cdot U_{eq}(C)$) using a riding model with C-H = 0.95 Å for aromatic hydrogen atoms. The complex is located in a special position.

Table 2. Atomic coordinates ($\times 10^4$) and equivalent isotropic displacement parameters ($\text{\AA}^2 \times 10^3$).
 $U(\text{eq})$ is defined as one third of the trace of the orthogonalized U_{ij} tensor.

	x	y	z	$U(\text{eq})$
Zn(1)	0	4647(1)	2500	26(1)
I(1)	-2525(1)	5750(1)	2500	39(1)
N(1)	0	3449(4)	3950(4)	36(1)
C(1)	0	2733(5)	4677(5)	34(1)
C(2)	0	1787(5)	5595(6)	50(2)

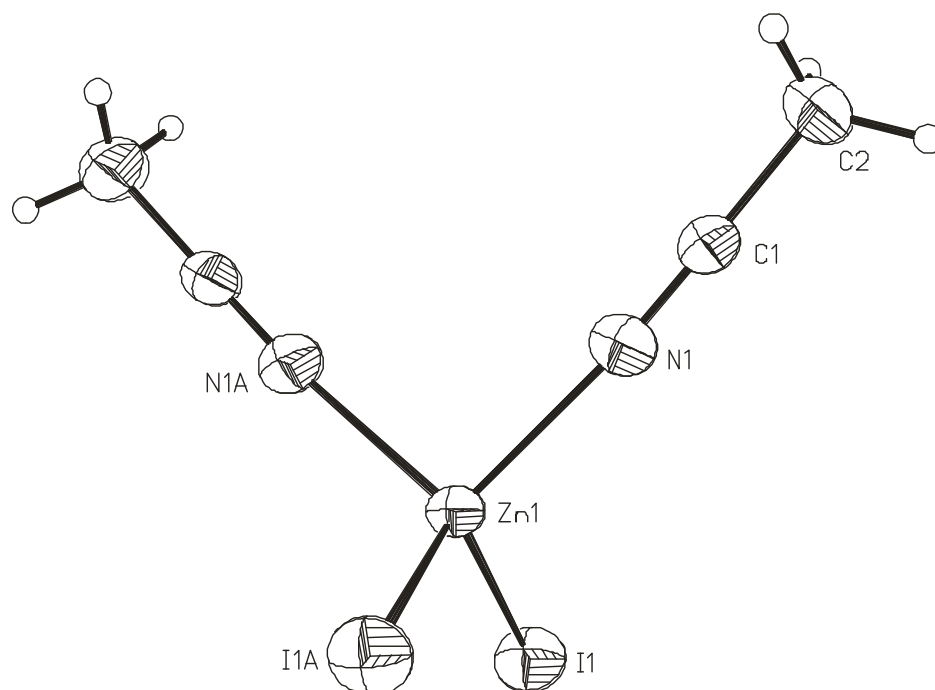


Table 3. Bond lengths [\AA] and angles [$^\circ$].

Zn(1)-N(1A)	2.046(5)	Zn(1)-I(1B)	2.5316(5)
Zn(1)-N(1)	2.046(5)	Zn(1)-I(1)	2.5316(5)
C(1)-N(1)-Zn(1)	175.0(4)	N(1A)-Zn(1)-I(1)	109.33(5)
N(1A)-Zn(1)-N(1)	96.3(3)	N(1)-Zn(1)-I(1)	109.33(5)
N(1A)-Zn(1)-I(1B)	109.33(5)	I(1B)-Zn(1)-I(1)	120.50(3)
N(1)-Zn(1)-I(1B)	109.33(5)		

Symmetry transformations used to generate equivalent atoms: A: $x, y, -z+1/2$; B: $-x, y, -z+1/2$

2 Publications

Table 4. Anisotropic displacement parameters ($\text{\AA}^2 \times 10^3$). The anisotropic displacement factor exponent takes the form: $-2\pi^2 [h^2 a^{*2} U_{11} + \dots + 2 h k a^* b^* U_{12}]$

	U_{11}	U_{22}	U_{33}	U_{23}	U_{13}	U_{12}
Zn(1)	30(1)	21(1)	28(1)	0	0	0
I(1)	28(1)	39(1)	49(1)	0	0	6(1)
N(1)	42(3)	30(2)	35(2)	3(2)	0	0
C(1)	47(3)	25(2)	29(2)	-4(2)	0	0
C(2)	82(6)	33(3)	35(3)	8(2)	0	0

Table 5. Hydrogen coordinates ($\times 10^4$) and isotropic displacement parameters ($\text{\AA}^2 \times 10^3$)

	x	y	z	U(eq)
H(2A)	0	2064	6458	60
H(2B)	899	1319	5395	75

Synthesis, Crystal Structure and Thermal Reactivity of [ZnX₂(2-chloropyrazine)] (X = Cl, Br, I) Coordination Compounds

Gaurav Bhosekar,^[a] Inke Jeß,^[a] Nicolai Lehnert,^[b] and Christian Näther*^[a]

Keywords: Coordination compounds / Synthesis / Crystal structure / Thermal reactivity / Zinc / Halides

Reaction of zinc(II) halides with 2-chloropyrazine in different solvents leads to the formation of five new coordination compounds that contain either only 2-chloropyrazine or additional water molecules as donor ligands. In the ligand-rich 1:2 compound catena[bis(2-chloropyrazine-N)]di-μ-chlorozinc(II) (1) the zinc atom is coordinated by two 2-chloropyrazine ligands and four chlorine atoms in an octahedral fashion. The zinc atoms are connected by the chloride atoms forming linear chains. In the isotypic ligand-rich 1:2 compounds bis(2-chloropyrazine-N)dibromozinc(II) (2) and bis(2-chloropyrazine-N)diiodozinc(II) (3) discrete complexes are found in which each zinc atom is coordinated by two 2-chloropyrazine ligands and two halide atoms within distorted tetrahedra. The 1:1 compounds aqua-(2-chloropyrazine-N)di-

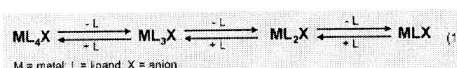
bromozinc(II) (4) and aqua-(2-chloropyrazine-N)diiodozinc(II) (5) are also isotypic and form discrete complexes in which the zinc atoms are surrounded by two halide atoms, one 2-chloropyrazine ligand and one water molecule. Upon heating, compounds 1–5 form ligand-deficient 1:1 and 2:1 compounds of composition [ZnX₂(2-chloropyrazine)] (X = halide) and [(ZnX₂)₂(2-chloropyrazine)]. X-ray powder diffraction shows that identical ligand-deficient intermediates are obtained on decomposition of either [ZnX₂L₂] (L = 2-chloropyrazine) or the [ZnX₂L(H₂O)] complexes. DFT calculations suggest that the formation of the [ZnX₂L(H₂O)] complex is energetically favoured for the heavier halide anions. © Wiley-VCH Verlag GmbH & Co. KGaA, 69451 Weinheim, Germany, 2007

Introduction

Recently the preparation of new coordination compounds like coordination polymers, inorganic–organic hybrid compounds or metal organic frameworks has become of increasing interest because of their potential applications as conducting, porous, magnetic, catalytic or NLO materials.^[1–11] For any application or investigation of the properties of such compounds, pure samples are required in large amounts, which sometimes can be difficult to achieve if the syntheses are performed in solution. Different stable and metastable compounds exist in equilibria in solution, often leading to mixtures of different compounds. In view of stability constraints, certain compounds cannot be prepared or metastable compounds are overlooked in solution.

In recent work we have demonstrated that novel coordination compounds can be conveniently prepared by the thermal decomposition reactions of suitable ligand-rich precursor compounds based on Cu^I or Zn^{II} halides and mostly aromatic diazine ligands like pyrazine or substituted pyrazines. In this method several ligand-deficient intermediates can be obtained in phase pure form in quantitative

yields.^[12–21] During the thermal reaction the equilibrium is shifted irreversibly in the direction of the ligand-deficient compounds, leading to the isolation of metastable compounds, which normally cannot be prepared in solution or which are always obtained as mixtures otherwise (Scheme 1).



Scheme 1.

It is to be noted that in all thermal reactions ligand-rich precursor compounds are transformed into ligand-deficient products and that a part of the ligand is irreversibly emitted. In certain cases, depending on the stability of the intermediate phases, some of the mass steps are not well resolved, indicating that not all of the compounds can be prepared in phase pure form. Therefore, we have started investigations on the thermal decomposition reactions of precursors that contain additional volatile sacrificial donors like CH₃CN, which can be removed first such that the desired amine ligands are retained, as shown previously.^[22] In this context it must be pointed out that ligand-rich precursor compounds that contain additional water molecules as donors can also be prepared. We have found this, for example, for the compounds based on Zn^{II} halides and 2-chloropyrazine. Upon thermal decomposition the water is removed first and, therefore, the stoichiometry of the ligand-

[a] Institut für Anorganische Chemie der Christian-Albrechts-Universität zu Kiel, Olshausenstraße 40, 24098 Kiel, Germany
E-mail: cnaether@ac.uni-kiel.de

[b] Department of Chemistry, The University of Michigan, 930 N. University Ave., Ann Arbor, MI 48109, USA
Supporting information for this article is available on the WWW under <http://www.eurjic.org> or from the author.

FULL PAPER

G. Bhosekar, I. Jeß, N. Lehnert, C. Näther

deficient coordination compound is predefined in the precursor compound. The product of this reaction is the same as expected for the decomposition of a ligand-rich precursor compound that contains only 2-chloropyrazine as ligand, as shown in this work.

Results and Discussion

Crystal Structures

The ligand-rich 1:2 compound **1** crystallizes in the monoclinic space group $P2_1/n$ with $Z = 2$ with the zinc atoms in special and all other atoms in general positions. In the crystal structure the zinc atoms are coordinated by four symmetry-equivalent chloride atoms and two nitrogen atoms of two symmetry-equivalent 2-chloropyrazine ligands within slightly distorted octahedra (Figure 1, top, and Table 1). Bond lengths and angles are in rough agreement with those retrieved from the literature for hexacoordinate zinc(II) atoms (Zn–Cl: 2.476–2.516 Å and Zn–N: 2.145–2.188 Å).^[23–25] Interestingly, two of the four Zn–Cl bond lengths are significantly elongated (Table 1).

The zinc atoms are connected by the chloride atoms by common edges to form linear chains (Figure 1, mid), which elongate in the direction of the crystallographic a axis (Figure 1, bottom). The 2-chloropyrazine ligands are coordinated to the zinc atoms through the nitrogen atom, which is away from the bulky chlorine, and thus function as monodentate terminal ligands.

The ligand-rich 1:2 compounds bis(2-chloropyrazine-*N*)-dibromozinc(II) (**2**) and bis(2-chloropyrazine-*N*)-diiodozinc(II) (**3**) are isotopic and crystallize in the monoclinic space group $C2/c$ with four formula units in the unit cell. The halide atoms and the 2-chloropyrazine ligands are located in general positions whereas the zinc atoms occupy special positions. In contrast to compound **1**, discrete complexes are found, with the zinc atoms coordinated by two symmetry-related halide atoms and two nitrogen atoms of two symmetry-related 2-chloropyrazine ligands. As in compound **1**, the 2-chloropyrazine ligand coordinates with the nitrogen atom, which is away from the bulky chlorine substituent (Figure 2, top, and Table 1). The Zn–N bond lengths in compounds **2** and **3** are comparable and significantly shorter than in compound **1**. In the crystal structure the discrete complexes are stacked into columns that elongate in the direction of the b axis (Figure 2, bottom).

The 1:1 compounds aqua-(2-chloropyrazine-*N*)-dibromozinc(II) (**4**) and aqua-(2-chloropyrazine-*N*)-diiodozinc(II) (**5**) are isotopic and crystallize in the orthorhombic space group $Pbca$ with eight formula units in the unit cell and all atoms in general positions. Their crystal structures are similar to those of compounds **2** and **3**, but one of the two 2-chloropyrazine ligand is exchanged by a water molecule. Discrete complexes are found, with the zinc tetrahedrally coordinated by two halide atoms, one 2-chloropyrazine ligand and one water molecule (Figure 3, top, and Table 2). The Zn–N and Zn–X bond lengths are comparable to those in compounds **2** and **3**, but the tetrahedra are more dis-

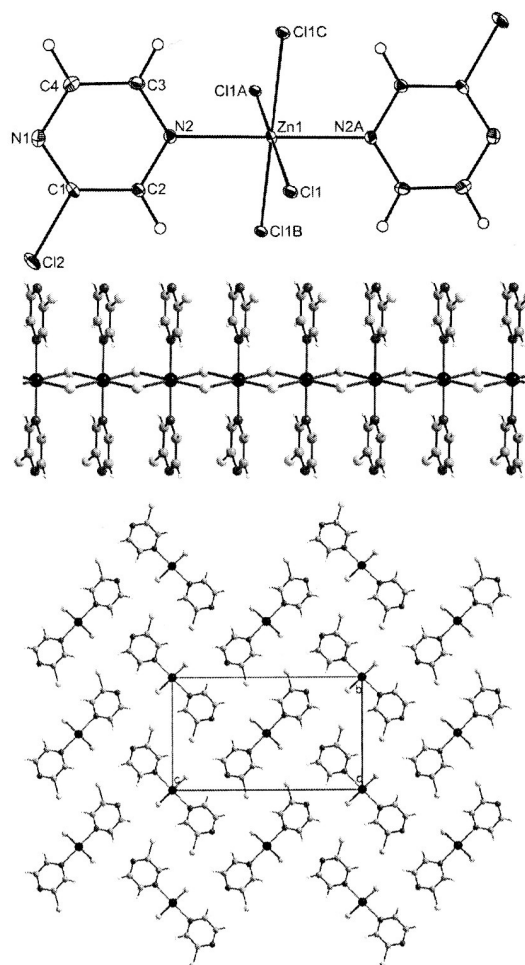


Figure 1. Crystal structure of compound **1** with a view of the coordination sphere of the zinc atoms with labelling and displacement ellipsoids drawn at the 50% probability level (top), with a view of the linear $ZnCl_2(2\text{-chloropyrazine})$ chains (mid) and with a view along the crystallographic a axis (bottom). Symmetry codes: A: $-x + 1, -y + 1, -z + 1$; B: $-x + 2, -y + 1, -z + 1$; C: $3x - 1, y, z$.

Table 1. Bond lengths [Å] and angles [°] for compounds **1**, **2** and **3**.

Compound	1 (X = Cl)	2 (X = Br)	3 (X = I)
Zn1–N2	2.2055(12)	2.076(3)	2.091(2)
Zn1–X1A	2.4388(4)	2.3380(5)	2.5324(3)
Zn1–X1	2.4388(4)	2.3380(5)	2.5324(3)
Zn1–X1C	2.5001(4)	–	–
N2–Zn1–N2A	180.000(1)	99.82(17)	96.96(12)
N2–Zn1–X1A	89.29(3)	105.21(9)	107.33(6)
N2–Zn1–X1	90.71(3)	108.92(9)	109.64(6)
X1A–Zn1–X1	180.000(12)	125.82(3)	122.88(2)
X1–Zn1–X1B	86.662(12)	–	–
N2–Zn1–X1C	89.74(3)	–	–
X1–Zn1–X1C	93.338(12)	–	–
X1B–Zn1–X1C	180.0	–	–
N2–Zn1–X1B	90.26(3)	–	–

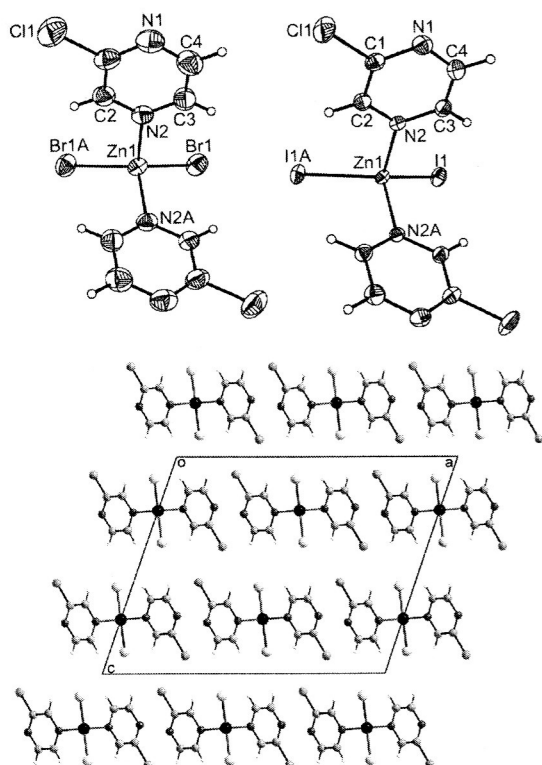


Figure 2. Crystal structure of compounds **2** (top left) and **3** (top right) with a view of the coordination sphere of the zinc atoms with labelling and displacement ellipsoids drawn at the 50% probability level and a view of the structure along the crystallographic *b* axis for compound **3** as a representative (bottom). Symmetry codes: A: $-x + 1, y, -z + 5/2$.

torted than those in the anhydrous compounds (compare Tables 1 and 2).

In the crystal structure the discrete complexes are connected through O–H \cdots N hydrogen bonds between the water molecules and the nitrogen atoms of the 2-chloropyrazine ligands, which are not involved in metal coordination (Table 3). Additional hydrogen bonding is also found between the water hydrogen atoms and the halide atoms (Table 3 and Figure 3).

Differential Thermoanalysis and Thermogravimetry (DTA-TG)

Compounds **1–5** are suitable ligand-rich precursor compounds for the preparation of new ligand-deficient intermediate compounds. Thus, their thermal reactivity was investigated using simultaneous differential thermoanalysis and thermogravimetry (DTA-TG).

The ligand-rich 1:2 dichloro compound **1** exhibits three mass steps up to 400 °C in the TG curves accompanied with endothermic events in the DTA curve (Figure 4). The experimental mass loss in the first TG step of 31.2% is in good agreement with that calculated for the removal of a 2-

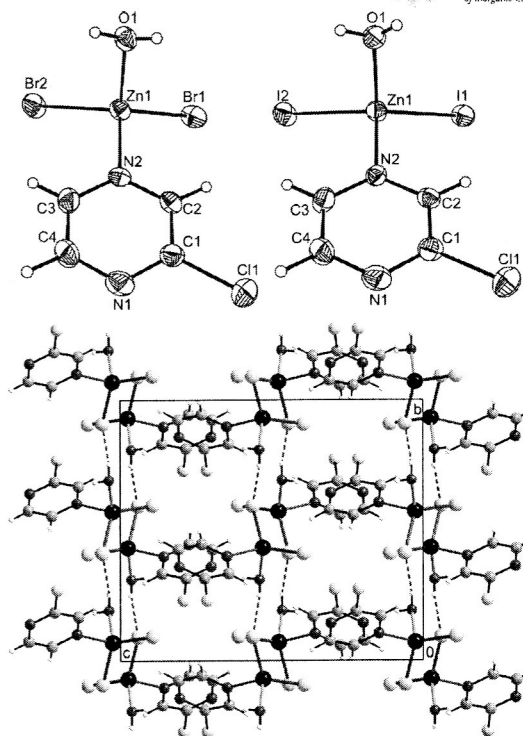


Figure 3. Crystal structure of compounds **4** (top left) and **5** (top right) with a view of the coordination sphere of the zinc atoms with labelling and displacement ellipsoids drawn at the 50% probability level and a view of the structure along the crystallographic *a* axis (bottom). Hydrogen bonding is shown as dashed lines.

Table 2. Bond lengths [Å] and angles [°] for compounds **4** and **5**.

Compound	4 (X = Br)	5 (X = I)
Zn1–N2	2.074(3)	2.084(3)
Zn1–X1	2.3273(7)	2.5219(4)
Zn1–X2	2.3576(7)	2.5468(5)
Zn1–O1	2.034(3)	2.026(3)
N2–Zn1–X1	109.34(10)	109.22(8)
O1–Zn1–N2	99.25(13)	99.43(10)
O1–Zn1–X1	111.17(8)	110.47(6)
O1–Zn1–X2	104.32(9)	104.34(7)
N2–Zn1–X2	106.13(10)	106.57(8)
X1–Zn1–X2	123.79(3)	123.99(2)

Table 3. Hydrogen-bonding parameters for compounds **4** and **5**.

D–H \cdots A	<i>d</i> (D–H)	<i>d</i> (H \cdots A)	\angle (DH \cdots A)	<i>d</i> (D \cdots A)
Compound 4				
O1–H1O1 \cdots N1A ^[a]	0.840	1.983	169.33	2.812
O1–H2O1 \cdots Br2B	0.840	2.523	163.37	3.337
Compound 5				
O1–H1O1 \cdots N1A	0.840	1.993	171.78	2.827
O1–H2O1 \cdots I2B	0.840	2.855	143.60	3.566

[a] A = $x + 1/2, y, -z + 1/2$; B = $-x + 3/2, y + 1/2, z$.

chloropyrazine ligand [$\Delta m_{\text{theo1}}(-1 \text{ 2-chloropyrazine}) = 31.3\%$], whereas the second mass loss corresponds to the

FULL PAPER

G. Bhosekar, I. Jeß, N. Lehnert, C. Näther

emission of two-thirds of a 2-chloropyrazine ligand [$\Delta m_{\text{theo}}(-2/3 \text{ 2-chloropyrazine}) = 20.9\%$] (Figure 4, left). Similar observations were made for the corresponding 1:2 dibromo compound **2** [$\Delta m_{\text{theo}}(-1 \text{ 2-chloropyrazine}) = 25.2\%$; $\Delta m_{\text{theo}}(-2/3 \text{ 2-chloropyrazine}) = 16.8\%$] and the diiodo compound **3** [$\Delta m_{\text{theo}}(-1 \text{ 2-chloropyrazine}) = 20.9\%$; $\Delta m_{\text{theo}}(-2/3 \text{ 2-chloropyrazine}) = 13.9\%$], but for the latter the second TG step is not well resolved (Figure 4). The final products at the end of this reaction were identified as ZnCl_2 , ZnBr_2 and ZnI_2 . The above data can be attributed to the formation of the new ligand-deficient 1:1 compounds $\text{ZnX}_2(\text{2-chloropyrazine})$ ($X = \text{Cl, Br, I}$) in the first TG step. In the second TG step a transformation of the 1:1 compounds into more ligand-deficient products of composition $(\text{ZnX}_2)_3(\text{2-chloropyrazine})$ ($X = \text{Cl, Br, I}$) occurs. This is in agreement with the results from elemental analysis (see Experimental Section).

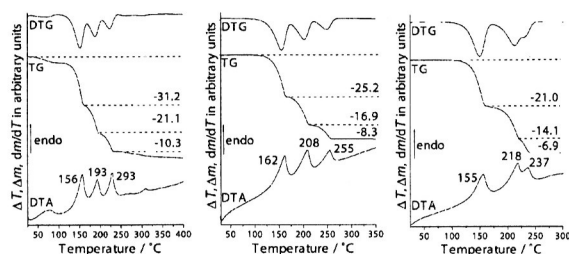


Figure 4. DTA, TG and DTG curves for compounds **1**, **2** and **3** (the mass loss in % and the peak temperatures in °C are given).

The TG-DTA thermogram of the 1:1 compound $[\text{ZnBr}_2(\text{2-chloropyrazine})(\text{H}_2\text{O})]$ (**4**) exhibits three TG steps. The first step corresponds to the removal of the water molecule [$\Delta m_{\text{theo}}(-\text{H}_2\text{O}) = 5.0\%$], whereas the mass loss in the second step agrees with the emission of two-thirds of the 2-chloropyrazine ligands [$\Delta m_{\text{theo}}(-2/3 \text{ 2-chloropyrazine}) = 21.3\%$] (Figure 5).

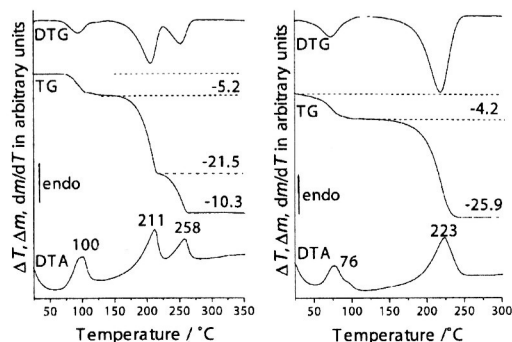


Figure 5. DTA, TG and DTG curves for compounds **4** and **5** (% mass loss and peak temperatures [°C] are given).

In contrast, for $[\text{ZnI}_2(\text{2-chloropyrazine-N})(\text{H}_2\text{O})]$ (**5**) only two mass steps are observed, the first of which corresponds to the emission of the water molecules [$\Delta m_{\text{theo}}(-\text{H}_2\text{O}) = 4.0\%$], whereas the second TG step agrees with

the removal of the 2-chloropyrazine ligands [$\Delta m_{\text{theo}}(-2 \text{ 2-chloropyrazine}) = 26.2\%$] (Figure 5). Based on these results it can be rationalized that in the first TG step the 1:1 compounds $[\text{ZnX}_2(\text{2-chloropyrazine})]$ ($X = \text{Br, I}$) are formed, which in the case of the dibromide transforms into a ligand-deficient compound of composition $[(\text{ZnBr}_2)_3(\text{2-chloropyrazine})]$. The elemental analyses add further credence to these findings (see Experimental Section).

In order to prove the formation of ligand-deficient compounds, additional TG experiments were performed, which were stopped after the first mass loss. The residues obtained in this way were then investigated by X-ray powder diffraction (Figure 6). These investigations clearly show that new ligand-deficient 1:1 compounds of composition $[\text{ZnX}_2(\text{2-chloropyrazine})]$ have formed. All powder patterns are different from those calculated for compounds **1**–**5**. It is interesting to note that the decomposition of the $[\text{ZnX}_2\text{L}_2]$ compounds ($X = \text{Br, I}$; $L = \text{2-chloropyrazine}$) as well as the $[\text{ZnX}_2\text{LH}_2\text{O}]$ compounds leads to the formation of the same 1:1 compound (compare parts B/C and D/E of Figure 6). The low crystallinity of the 1:1 compounds as well as the hygroscopic nature of the ligand-deficient dibromo and diiodo compounds preclude further investigations.

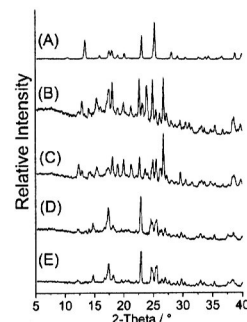


Figure 6. Experimental X-ray powder pattern of the residues obtained after the first TG step in the thermal decomposition reaction of compounds **1** (A), **2** (B), **3** (D), **4** (C) and **5** (E).

The residues formed in the second TG step, which correspond to ligand-deficient 3:1 compounds, are extremely hygroscopic and transform into a liquid within a few minutes. Therefore, elemental analysis was not performed. However, X-ray powder diffraction clearly shows that the patterns are different from those of the 1:1 compounds and from those of the pure Zn^{II} halides.

Calculations

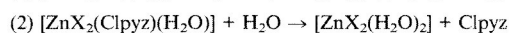
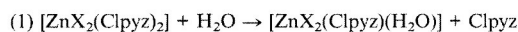
As mentioned above, $[\text{ZnX}_2(\text{2-chloropyrazine})(\text{H}_2\text{O})]$ compounds were obtained for $X = \text{Br}$ and I in which one 2-chloropyrazine ligand is replaced by a water molecule. In contrast, for $X = \text{Cl}$ such a compound cannot be prepared. These results suggest that the exchange of 2-chloropyrazine against water is energetically favoured for the ZnBr_2 - and ZnI_2 -based coordination compounds. To get more insight into this phenomenon, theoretical calculations on the

B3LYP/TZVP level were performed for the two following reactions, in which all species were fully optimized (Table 4):

Table 4. Results of the calculations for reactions 1 and 2.

Complex	ΔE [kcal/mol]	ΔH [kcal/mol]	ΔG [kcal/mol]	K_{eq} (r.t.) ^[a]
		Reaction 1		
X = Cl ⁻	+1.70	+1.94	0.00	1.00
X = Br ⁻	+0.95	+1.19	-0.78	3.73
X = I ⁻	+0.40	+0.59	-1.46	11.77
		Reaction 2		
X = Cl ⁻	+3.8	+3.9	+1.4	0.094
X = Br ⁻	+3.2	+3.2	+0.9	0.22
X = I ⁻	+2.7	+2.8	+0.2	0.71

[a] $\Delta G = -RT \ln K = -592.183 \ln K$ ($T = 298$ K).



In these calculations, solvation effects were neglected, because it can be assumed that the solvation energies should only affect the absolute reaction energies (ΔE), but not the relative energies of the different systems ($\Delta\Delta E$). In other words, addition of solvation energies will cause a linear shift of all three reaction energies by approximately the same amount.

From Table 4, an interesting trend can be derived where the exchange of the first 2-chloropyrazine against water (reaction 1) becomes more favourable with increasing size of the anion X. This means that in aqueous solution, the equilibrium according to reaction 1 is more and more shifted toward the water-containing species with increasing size of X (cf. K_{eq} values in Table 4, top). Although the energy differences are small, this can at least be counted as evidence to explain the experimental observation that the water-containing species can be prepared for X = Br and I, whereas this compound cannot be obtained for X = Cl. In addition, whereas the first exchange of 2-chloropyrazine against water (reaction 1) is thermodynamically neutral to exergonic, the exchange of the second 2-chloropyrazine against water (reaction 2) becomes unfavourable. Correspondingly, the 2-chloropyrazine-free compounds with two water molecules bound could not be accessed from the solutions. Interestingly, the same trend is observed for reaction 2, that is, the exchange of water is more favourable with increasing size of the halide anion X (cf. Table 4, bottom). In summary, the calculations provide some evidence to understand the experimental observation that with ZnBr₂ and ZnI₂, 2-chloropyrazine coordination compounds are accessible with one additional water in the coordination sphere, whereas for ZnCl₂, this species seems less stable.

Conclusions

In the present work we have prepared several new coordination compounds of Zn halides with 2-chloropyrazine, which form ligand-deficient zinc(II)halide compounds upon thermal decomposition. The same ligand-deficient com-

pounds are obtained irrespective of the thermal decomposition of $[\text{ZnX}_2\text{L}_2]$ (L = 2-chloropyrazine) or the $[\text{ZnX}_2\text{L}(\text{H}_2\text{O})]$ complexes. In this context the $[\text{ZnX}_2\text{L}(\text{H}_2\text{O})]$ complexes are of special interest because by thermal decomposition the water is removed first and the N-donor ligand is retained. Although not all of the ligand-deficient compounds can be obtained in a pure form, our investigations clearly show that such compounds can be prepared. It must be noted that the water-containing complexes can only be prepared with ZnBr₂ or ZnI₂ and 2-chloropyrazine. These experimental observations are in agreement with our theoretical calculations, which indicate that the formation of the $[\text{ZnX}_2\text{L}(\text{H}_2\text{O})]$ complexes is energetically favoured only for the bromide and iodide compounds.

Experimental Section

Synthesis of Compounds 1–3: ZnCl₂, ZnBr₂ or ZnI₂ (1.0 mmol) and 2-chloropyrazine (2.0 mmol, 216.28 mg) were stirred in hexane (2.0 mL) for 2 d. The colorless precipitates were filtered off and washed with diethyl ether. C₈H₆Cl₄N₄Zn (1): calcd. C 26.30, H 1.66, N 15.33; found C 26.1, H 1.69, N 15.40. C₈H₆Br₂Cl₂N₄Zn (2): calcd. C 21.15, H 1.33, N 12.33; found C 21.12, H 1.36, N 12.45. C₈H₆Cl₂I₂N₄Zn (3): calcd. C 17.53, H 1.10, N 10.22; found C 17.47, H 1.05, N 10.16. Single crystals were prepared by dissolving ZnCl₂, ZnBr₂ or ZnI₂ (0.25 mmol) and 2-chloropyrazine (0.25 mmol) in ethanol (1.0 mL). On slow evaporation of the solvent, single crystals of compounds 1, 2 and 3 grew within 1 week.

Synthesis of Compounds 4 and 5: ZnBr₂ or ZnI₂ (1.0 mmol) and 2-chloropyrazine (1.0 mmol) were stirred in hexane (2.0 mL) for 2 d. The colorless precipitates were filtered off and washed with diethyl ether. C₄H₅Br₂ClN₂OZn (4): calcd. C 13.43, H 1.41, N 7.83; found C 13.36, H 1.32, N 7.75. C₄H₅ClI₂N₂OZn (5): calcd. C 10.64, H 1.12, N 6.20; found C 10.57, H 1.09, N 6.11. Single crystals were prepared by dissolving ZnBr₂ or ZnI₂ (0.25 mmol) and 2-chloropyrazine (0.25 mmol) in ethanol (2.0 mL) (4) or acetonitrile (0.5 mL) and water (0.2 mL) (5). On slow evaporation of the solvent, single crystals of compounds 4 and 5 grew within 1 week.

Single-Crystal Structure Analysis: The data were measured using an IPDS-1 from STOE, Germany. All structure solutions were performed with direct methods using SHELXS-97.^[26] Structure refinement was done against F^2 using SHELXL-97.^[27] All non-hydrogen atoms were refined with anisotropic displacement parameters. The C–H hydrogen atoms were positioned with idealized geometry and were refined with isotropic displacement parameters using a riding model. The data were corrected for absorption using X-RED^[28] and X-SHAPE.^[29] Selected crystal data and results of the structure refinement are shown in Table 5.

CCDC-662623 (for 1), -662624 (for 2), -662625 (for 3), -662626 (for 4) and -662627 (for 5) contain the supplementary crystallographic data (excluding structure factors) for this paper. These data can be obtained free of charge from The Cambridge Crystallographic Data Centre via www.ccdc.cam.ac.uk/data_request/cif.

X-ray Powder Diffraction: X-ray powder diffraction experiments were performed using a STOE STADI P transmission powder using Cu- K_{α} radiation ($\lambda = 1.540598$ Å).

Differential Thermal Analysis, Thermogravimetry and Mass Spectrometry: DTA-TG measurements were performed using the STA-409CD in Al₂O₃ crucibles under nitrogen (purity: 5.0). All mea-

FULL PAPER

Table 5. Selected crystal data and results of the structure refinements for compounds 1–5.

Compound	1	2	3	4	5
Formula	C ₈ H ₆ Cl ₄ N ₄ Zn	C ₈ H ₆ Br ₂ Cl ₂ N ₄ Zn	C ₈ H ₆ Cl ₂ I ₂ N ₄ Zn	C ₄ H ₅ Br ₂ ClN ₂ OZn	C ₄ H ₅ ClI ₂ N ₂ OZn
Formula mass [g/mol]	365.34	454.26	548.24	357.74	451.72
Crystal color	colorless	colorless	colorless	colorless	colorless
Crystal system	monoclinic	monoclinic	monoclinic	orthorhombic	orthorhombic
Space group	<i>P</i> 2 ₁ / <i>n</i>	<i>C</i> 2/ <i>c</i>	<i>C</i> 2/ <i>c</i>	<i>P</i> bca	<i>P</i> bca
<i>a</i> [Å]	3.5928(3)	17.9491(15)	16.8523(14)	11.2591(7)	11.4595(8)
<i>b</i> [Å]	9.8030(6)	5.6817(5)	6.0972(4)	12.2488(6)	12.9539(7)
<i>c</i> [Å]	16.5933(14)	14.6824(11)	15.1299(13)	14.1375(7)	14.4758(8)
<i>α</i> [°]	–	–	–	–	–
<i>β</i> [°]	94.185(10)	108.853(9)	105.413(10)	–	–
<i>γ</i> [°]	–	–	–	–	–
<i>V</i> [Å ³]	582.86(8)	1417.0(2)	1498.7(2)	1949.71(2)	2148.9(2)
Temperature [K]	170.0	220	170.0	220.0	220.0
<i>Z</i>	2	4	4	8	8
<i>D</i> _{calcd} [g/cm ³]	2.082	2.129	2.430	2.437	2.793
<i>F</i> (000)	360	864	1008	1344	1632
2 θ range [°]	4.82–56.02	4.80–56.04	5.58–56.02	5.7–56.14	5.52–56.01
<i>hkl</i> ranges	–4/4 –12/12 –21/21	–23/23 –7/7 –19/19	–21/22 –7/7 –19/19	–14/14 –16/16 –18/18	–15/11 –15/17 –19/19
μ (Mo- <i>K</i> α) [mm ^{–1}]	3.00	7.73	6.10	10.94	8.23
Absorption correction	numerical	numerical	numerical	numerical	numerical
Min./max. transmission	0.6068/0.6898	0.1065/0.4909	0.2845/0.5756	0.1111/0.3304	0.1983/0.3629
Measured reflections	5475	6595	6849	17607	13377
<i>R</i> _{int}	0.0231	0.0699	0.0373	0.0966	0.0455
Independent reflections	1366	1644	1762	2358	2581
Reflections with <i>I</i> > 2 σ (<i>I</i>)	1284	1239	1577	1874	2078
Parameters	80	79	79	101	101
<i>R</i> ₁ [<i>I</i> > 2 σ (<i>I</i>)]	0.0209	0.0354	0.0232	0.0378	0.0230
<i>wR</i> ₂ [all data]	0.0560	0.0877	0.0602	0.1013	0.0519
Gof	1.095	1.025	1.039	1.026	0.975
Residual electron density [e/Å ³]	0.384/–0.477	0.415/–0.451	0.844/–0.845	0.578/–0.904	0.643/–0.770

measurements were performed with a flow rate of 75 mL/min and were corrected for buoyancy and current effects. The instrument was calibrated using standard reference materials.

Elemental Analysis: C,H,N analysis was performed using a CHN-O-RAPID combustion analyzer from Heraeus.

CHN Analysis of the Residues Obtained in the Thermal Decomposition of Compounds 1–5: (A) Isolated after the first TG step for compound 1: C₄H₃Cl₃N₂Zn (250.82): calcd. C 19.15, H 1.21, N 11.17; found C 19.01, H 1.10, N 10.93. (B) Isolated after the first heating step for compound 2: C₄H₃Br₂ClN₂Zn (339.72): calcd. C 14.14, H 0.89, N 8.25; found C 13.98, H 0.78, N 8.14. (C) Isolated after the first heating step for compound 3: C₄H₃N₂ClI₂Zn (433.71): calcd. C 11.08, H 0.70, N 6.46; found C 10.98, H 0.62, N 6.39. (D) Isolated after the first heating step for compound 4: C₄H₃Br₂ClN₂Zn (339.72): calcd. C 14.14, H 0.89, N 8.25; found C 14.01, H 0.81, N 8.19. (E) Isolated after the first heating step for compound 5: C₄H₃ClI₂N₂Zn (433.71): calcd. for C 11.08, H 0.70, N 6.46; found C 10.93, H 0.64, N 6.32.

Calculations: Spin-unrestricted DFT calculations using Becke's three-parameter hybrid functional with the correlation functional of Lee, Yang and Parr (B3LYP)^[30] were performed with the program package Gaussian 03.^[31] For all calculations, the TZVP basis set^[32] was applied as implemented in G03. The structures of the complexes [ZnX₂(Clpyz)₂], [ZnX₂(Clpyz)(H₂O)] and [ZnX₂(H₂O)₂] (X[–] = Cl[–], Br[–], I[–]) were fully optimized. Frequency calculations performed on these structures yielded no imaginary modes, which shows that true energy minima have been located in all cases. From the calculated frequencies, the thermodynamic corrections for enthalpy and the entropies of all species have been obtained as im-

plemented in G03 (cf. Table 4). The obtained structures are in general very close to tetrahedral for all three types of complexes, which is significantly different from the crystal structures where significant distortions toward a planar geometry are observed (vide supra). These distortions can therefore be attributed to crystal packing effects in the solid state.

Supporting Information (see also the footnote on the first page of this article): Tables with atomic coordinates, isotropic and anisotropic displacement parameters, bond lengths and angles, and details of the structure determinations. Figures with experimental and calculated X-ray powder patterns for compounds 1–5. Experimental powder patterns for the 3:1 compounds.

Acknowledgments

This work was supported by the German Land Schleswig-Holstein and the Deutsche Forschungsgemeinschaft (projekt number NA 720/1-1). We thank Prof. Dr. W. Bensch for access to his equipment.

- [1] S. L. James, *Chem. Soc. Rev.* **2003**, 5, 276.
- [2] C. Janiak, *Dalton Trans.* **2003**, 2781.
- [3] A. Y. Robin, K. M. Fromm, *Coord. Chem. Rev.* **2006**, 250, 2127.
- [4] M. Eddaoudi, J. Kim, N. Rosi, D. Vodak, J. Wachter, M. O'Keefe, O. M. Yaghi, *Science* **2002**, 295, 469.
- [5] J. L. C. Rowsell, O. M. Yaghi, *Microporous Mesoporous Mater.* **2004**, 73, 3.
- [6] H. K. Chae, D. Y. Siberio-Perez, J. Kim, Y. B. Go, M. Eddaoudi, A. J. Matzger, M. O'Keefe, O. M. Yaghi, *Nature* **2004**, 427, 523.

- [7] S. Kitagawa, K. Uemura, *Chem. Soc. Rev.* **2005**, *34*, 109.
- [8] S. R. Batten, K. Murray, *Coord. Chem. Rev.* **2003**, *246*, 103.
- [9] B. Moulton, J. Lu, R. Hajndl, S. Hariharan, M. J. Zaworotko, *Angew. Chem. Int. Ed.* **2002**, *41*, 2821.
- [10] L.-X. Dai, *Angew. Chem. Int. Ed.* **2004**, *43*, 5726.
- [11] B. Paul, C. Näther, B. Walfort, K. M. Fromm, B. Zimmermann, H. Lang, C. Janiak, *CrystEngComm* **2005**, *7*, 309.
- [12] C. Näther, J. Greve, I. Jeß, *Solid State Sci.* **2002**, *4*, 813.
- [13] C. Näther, I. Jeß, *J. Solid State Chem.* **2002**, *169*, 103.
- [14] C. Näther, M. Wriedt, I. Jeß, *Inorg. Chem.* **2003**, *42*, 2391.
- [15] C. Näther, I. Jeß, *Inorg. Chem.* **2003**, *42*, 2968.
- [16] C. Näther, I. Jeß, N. Lehnert, H.-D. Hübner, *Solid State Sci.* **2003**, *5*, 1343.
- [17] C. Näther, J. Greve, I. Jeß, C. Wickleder, *Solid State Sci.* **2003**, *5*, 1167.
- [18] C. Näther, I. Jeß, *Eur. J. Inorg. Chem.* **2004**, 2868.
- [19] I. Jeß, C. Näther, *Inorg. Chem.* **2006**, *45*, 7446.
- [20] G. Bhosekar, I. Jeß, C. Näther, *Inorg. Chem.* **2006**, *43*, 6508.
- [21] C. Näther, G. Bhosekar, I. Jeß, *Inorg. Chem.* **2007**, *46*, 8079.
- [22] I. Jeß, C. Näther, *Z. Naturforsch., Teil B* **2007**, *62*, 617.
- [23] J. Pickardt, B. Staub, *Z. Naturforsch., Teil A* **1996**, *51*, 947.
- [24] H. Chunhua, U. Englert, *CrystEngComm* **2001**, *3*, 91.
- [25] H. Chunhua, U. Englert, *Angew. Chem. Int. Ed.* **2005**, *44*, 2281.
- [26] G. M. Sheldrick, *SHELXS 97*, Program for Crystal Structure Solution, University of Göttingen, Germany, **1997**.
- [27] G. M. Sheldrick, *SHELXL-97*, Program for the Refinement of Crystal Structures, University of Göttingen, Germany, **1997**.
- [28] *STOE & CIE*, X-Red Version 1.11: Program for data reduction and absorption correction, STOE & CIE GmbH, Darmstadt, Germany, **1998**.
- [29] *STOE & CIE*, X-Shape Version 1.03: Program for the crystal optimisation for numerical absorption correction, STOE & CIE GmbH, Darmstadt, Germany, **1998**.
- [30] a) A. D. Becke, *Phys. Rev. A* **1988**, *38*, 3098; b) A. D. Becke, *J. Chem. Phys.* **1993**, *98*, 1372; c) A. D. Becke, *J. Chem. Phys.* **1993**, *98*, 5648.
- [31] M. J. Frisch, G. W. Trucks, H. B. Schlegel, G. E. Scuseria, M. A. Robb, J. R. Cheeseman, J. A. Montgomery Jr, T. Vreven, K. N. Kudin, J. C. Burant, J. M. Millam, S. S. Iyengar, J. Tomasi, V. Barone, B. Mennucci, M. Cossi, G. Scalmani, N. Rega, G. A. Petersson, H. Nakatsuji, M. Hada, M. Ehara, K. Toyota, R. Fukuda, J. Hasegawa, M. Ishida, T. Nakajima, Y. Honda, O. Kitao, H. Nakai, M. Klene, X. Li, J. E. Knox, H. P. Hratchian, J. B. Cross, C. Adamo, J. Jaramillo, R. Gomperts, R. E. Stratmann, O. Yazyev, A. J. Austin, R. Cammi, C. Pomelli, J. W. Ochterski, P. Y. Ayala, K. Morokuma, G. A. Voth, P. Salvador, J. J. Dannenberg, V. G. Zakrzewski, S. Dapprich, A. D. Daniels, M. C. Strain, O. Farkas, D. K. Malick, A. D. Rabuck, K. Raghavachari, J. B. Foresman, J. V. Ortiz, Q. Cui, A. G. Baboul, S. Clifford, J. Cioslowski, B. B. Stefanov, G. Liu, A. Liashenko, P. Piskorz, I. Komaromi, R. L. Martin, D. J. Fox, T. Keith, M. A. Al-Laham, C. Y. Peng, A. Nanayakkara, M. Challacombe, P. M. W. Gill, B. Johnson, W. Chen, M. W. Wong, C. Gonzalez, J. A. Pople, *Gaussian 03*, Gaussian, Inc., Pittsburgh, PA, **2003**.
- [32] A. Schaefer, H. Horn, R. Ahlrichs, *J. Chem. Phys.* **1992**, *97*, 2571.

Received: September 7, 2007

Supplemental material

Synthesis, Crystal Structure and Thermal Reactivity of ZnX₂(2-Chloropyrazine) (X = Cl, Br, I) Coordination Compounds

Gaurav Bhosekar, Inke Jeß, Nicolai Lehnert and Christian Näther

- Selected crystal data and details on the single crystal structure determinations for compounds **1-5**
- Experimental and calculated X-ray powder patterns for compounds **1-5**

2 Publications

Compound 1

Table 1. Crystal data and structure refinement for dichloro-bis(2-chloropyrazine-N) zinc(II)

Identification code	gb26	
Empirical formula	C ₈ H ₆ Cl ₄ N ₄ Zn	
Formula weight	365.34	
Temperature	170(2) K	
Wavelength	0.71073 Å	
Crystal system	monoclinic	
Space group	<i>P</i> 2 ₁ / <i>n</i>	
Unit cell dimensions	<i>a</i> = 3.5928(3) Å	$\alpha = 90^\circ.00$
	<i>b</i> = 9.8030(6) Å	$\beta = 94.185(10)^\circ$
	<i>c</i> = 16.5933(14) Å	$\gamma = 90^\circ.00$
Volume	582.86(8) Å ³	
<i>Z</i>	2	
Density (calculated)	2.082 Mg/m ³	
Absorption coefficient	3.001 mm ⁻¹	
<i>F</i> (000)	360	
Crystal size	0.12 x 0.09 x 0.06 mm ³	
Theta range for data collection	2.41 to 28.01°.	
Index ranges	-4 ≤ <i>h</i> ≤ 4, -12 ≤ <i>k</i> ≤ 12, -21 ≤ <i>l</i> ≤ 21	
Reflections collected	5475	
Independent reflections	1366 [R(int) = 0.0231]	
Completeness to theta = 28.01°	97.2 %	
Refinement method	Full-matrix least-squares on <i>F</i> ²	
Data / restraints / parameters	1366 / 0 / 80	
Goodness-of-fit on <i>F</i> ²	1.095	
Final R indices [I > 2σ(I)]	R1 = 0.0209, wR2 = 0.0553	
R indices (all data)	R1 = 0.0226, wR2 = 0.0560	
Extinction coefficient	0.042(3)	
Largest diff. peak and hole	0.384 and -0.477 e.Å ⁻³	

Remarks:

All non-hydrogen atoms were refined using anisotropic displacement parameters. The hydrogen atoms were positioned with idealized geometry and were refined isotropic with $U_{eq}(H) = 1.2 \cdot U_{eq}(C_{aromatic})$ using a riding model with C-H = 0.95 Å for aromatic hydrogen atoms. There is one crystallographically independent molecule into the asymmetric unit which is located in a special positions.

2 Publications

Table 2. Atomic coordinates ($\times 10^4$) and equivalent isotropic displacement parameters ($\text{\AA}^2 \times 10^3$)

$U(\text{eq})$ is defined as one third of the trace of the orthogonalized U_{ij} tensor.

	x	y	z	$U(\text{eq})$
Zn(1)	5000	5000	5000	8(1)
Cl(1)	9634(1)	3801(1)	4263(1)	8(1)
N(1)	5471(4)	1309(1)	7086(1)	13(1)
C(1)	4267(4)	1109(1)	6324(1)	9(1)
C(2)	4164(4)	2119(1)	5734(1)	9(1)
N(2)	5243(4)	3389(1)	5930(1)	8(1)
C(3)	6418(4)	3629(1)	6706(1)	11(1)
C(4)	6546(5)	2588(2)	7274(1)	14(1)
Cl(2)	2747(1)	-516(1)	6060(1)	14(1)

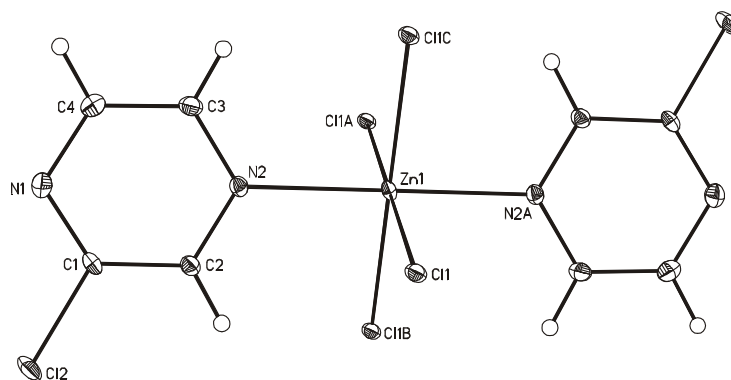


Table 3. Bond lengths [\AA] and angles [$^\circ$]

Zn(1)-N(2)	2.2055(12)	N(2)-Zn(1)-N(2A)	180.000(1)
Zn(1)-N(2A)	2.2055(12)	N(2)-Zn(1)-Cl(1A)	89.29(3)
Zn(1)-Cl(1A)	2.4388(4)	N(2A)-Zn(1)-Cl(1A)	90.71(3)
Zn(1)-Cl(1)	2.4388(4)	N(2)-Zn(1)-Cl(1)	90.71(3)
Zn(1)-Cl(1B)	2.5001(4)	N(2A)-Zn(1)-Cl(1)	89.29(3)
Zn(1)-Cl(1C)	2.5001(4)	Cl(1A)-Zn(1)-Cl(1)	180.000(12)
C(2)-N(2)-Zn(1)	120.01(10)	N(2)-Zn(1)-Cl(1B)	90.26(3)
C(3)-N(2)-Zn(1)	122.56(10)	N(2A)-Zn(1)-Cl(1B)	89.74(3)
Cl(1A)-Zn(1)-Cl(1B)	93.338(12)	Cl(1A)-Zn(1)-Cl(1C)	86.662(12)
Cl(1)-Zn(1)-Cl(1B)	86.662(12)	Cl(1)-Zn(1)-Cl(1C)	93.338(12)
N(2)-Zn(1)-Cl(1C)	89.74(3)	Cl(1B)-Zn(1)-Cl(1C)	180.0
		N(2A)-Zn(1)-Cl(1C)	90.26(3)

Symmetry transformations used to generate equivalent atoms: A: $-x+1, -y+1, -z+1$;

B: $-x+2, -y+1, -z+1$; C: $3-x, y, z$

2 Publications

Table 4. Anisotropic displacement parameters ($\text{\AA}^2 \times 10^3$). The anisotropic displacement factor exponent takes the form: $-2\pi^2 [h^2 a^{*2} U_{11} + \dots + 2 h k a^* b^* U_{12}]$

	U_{11}	U_{22}	U_{33}	U_{23}	U_{13}	U_{12}
Zn(1)	9(1)	5(1)	9(1)	2(1)	2(1)	-1(1)
Cl(1)	10(1)	6(1)	9(1)	-1(1)	1(1)	-1(1)
N(1)	16(1)	12(1)	11(1)	3(1)	0(1)	-1(1)
C(1)	8(1)	5(1)	13(1)	1(1)	2(1)	0(1)
C(2)	10(1)	7(1)	10(1)	0(1)	0(1)	0(1)
N(2)	9(1)	8(1)	9(1)	1(1)	2(1)	0(1)
C(3)	13(1)	10(1)	11(1)	-2(1)	1(1)	-2(1)
C(4)	20(1)	14(1)	9(1)	-1(1)	-1(1)	-1(1)
Cl(2)	16(1)	6(1)	20(1)	0(1)	0(1)	-3(1)

Table 5. Hydrogen coordinates ($\times 10^4$) and isotropic displacement parameters ($\text{\AA}^2 \times 10^3$)

	x	y	z	U(eq)
H(2)	3327	1907	5192	11
H(3)	7170	4523	6867	13
H(4)	7428	2787	7814	17

2 Publications

Compound 2

Table 1. Crystal data and structure refinement for dibromo bis (N-chloropyrazine) zinc (II).

Identification code	gb138	
Empirical formula	$C_8H_6Br_2Cl_2N_4Zn$	
Formula weight	454.26	
Temperature	220(2) K	
Wavelength	0.71073 Å	
Crystal system	monoclinic	
Space group	$C2/c$	
Unit cell dimensions	$a = 17.9491(15)$ Å	$\alpha = 90^\circ$.
	$b = 5.6817(5)$ Å	$\beta = 108.853(9)^\circ$.
	$c = 14.6824(11)$ Å	$\gamma = 90^\circ$.
Volume	$1417.0(2)$ Å ³	
Z	4	
Density (calculated)	2.129 Mg/m ³	
Absorption coefficient	7.732 mm ⁻¹	
F(000)	864	
Crystal size	$0.03 \times 0.09 \times 0.15$ mm ³	
Theta range for data collection	2.40 to 28.02°.	
Index ranges	$-23 \leq h \leq 23, -7 \leq k \leq 7, -19 \leq l \leq 19$	
Reflections collected	6595	
Independent reflections	1644 [R(int) = 0.0699]	
Completeness to theta = 28.02°	95.3 %	
Refinement method	Full-matrix least-squares on F ²	
Data / restraints / parameters	1644 / 0 / 79	
Goodness-of-fit on F ²	1.025	
Final R indices [I > 2σ(I)]	R1 = 0.0354, wR2 = 0.0793	
R indices (all data)	R1 = 0.0562, wR2 = 0.0877	
Extinction coefficient	0.0036(4)	
Largest diff. peak and hole	0.415 and -0.451 e.Å ⁻³	

Remark:

All non-hydrogen atoms were refined using anisotropic displacement parameters. The hydrogen atoms were positioned with idealized geometry and were refined isotropic with $U_{eq}(H) = 1.2 \cdot U_{eq}(C_{aromatic})$ using a riding model with C-H = 0.94 Å for aromatic hydrogen atoms. There is one crystallographically independent molecules into the asymmetric unit which is located in a special positions.

2 Publications

Table 2. Atomic coordinates ($\times 10^4$) and equivalent isotropic displacement parameters ($\text{\AA}^2 \times 10^3$)

U(eq) is defined as one third of the trace of the orthogonalized U_{ij} tensor.

	x	y	z	U(eq)
Zn(1)	5000	10453(1)	12500	34(1)
Br(1)	5527(1)	12327(1)	13988(1)	48(1)
N(1)	3067(2)	4638(6)	12651(3)	50(1)
C(1)	3037(2)	5717(7)	11851(3)	44(1)
C(2)	3561(2)	7431(7)	11792(3)	40(1)
N(2)	4139(2)	8100(5)	12580(2)	35(1)
C(3)	4175(3)	7064(7)	13405(3)	43(1)
C(4)	3646(3)	5344(8)	13434(4)	52(1)
Cl(1)	2298(1)	4900(2)	10819(1)	69(1)

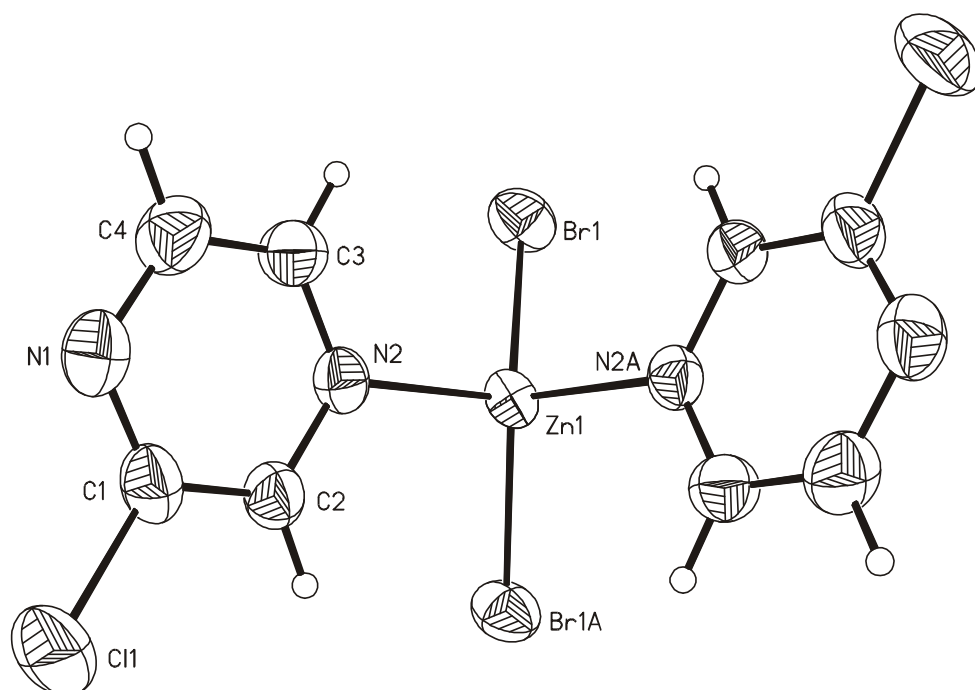


Table 3. Bond lengths [\AA] and angles [$^\circ$].

Zn(1)-N(2A)	2.076(3)	N(2A)-Zn(1)-N(2)	99.82(17)
Zn(1)-N(2)	2.076(3)	N(2A)-Zn(1)-Br(1)	105.21(9)
Zn(1)-Br(1)	2.3380(5)	N(2)-Zn(1)-Br(1)	108.92(9)
Zn(1)-Br(1A)	2.3380(5)	N(2A)-Zn(1)-Br(1A)	108.92(9)
C(3)-N(2)-Zn(1)	121.2(3)	N(2)-Zn(1)-Br(1A)	105.21(9)
C(2)-N(2)-Zn(1)	121.2(3)	Br(1)-Zn(1)-Br(1A)	125.82(3)

Symmetry transformations used to generate equivalent atoms: A: $-x+1, y, -z+5/2$

2 Publications

Table 4. Anisotropic displacement parameters ($\text{\AA}^2 \times 10^3$). The anisotropic displacement factor exponent takes the form: $-2\pi^2 [h^2 a^{*2} U_{11} + \dots + 2 h k a^* b^* U_{12}]$

	U_{11}	U_{22}	U_{33}	U_{23}	U_{13}	U_{12}
Zn(1)	27(1)	34(1)	38(1)	0	7(1)	0
Br(1)	47(1)	46(1)	46(1)	-11(1)	6(1)	0(1)
N(1)	44(2)	48(2)	60(3)	-2(2)	22(2)	-9(2)
C(1)	34(2)	45(2)	53(3)	-7(2)	14(2)	-8(2)
C(2)	35(2)	45(2)	41(2)	-7(2)	13(2)	-6(2)
N(2)	31(1)	35(2)	42(2)	-4(1)	14(2)	1(1)
C(3)	44(2)	45(2)	40(2)	1(2)	13(2)	-1(2)
C(4)	55(2)	48(2)	55(3)	5(2)	22(2)	-7(2)
Cl(1)	56(1)	76(1)	64(1)	-11(1)	6(1)	-31(1)

Table 5. Hydrogen coordinates ($\times 10^4$) and isotropic displacement parameters ($\text{\AA}^2 \times 10^3$)

	x	y	z	U(eq)
H(2)	3512	8133	11196	48
H(3)	4568	7515	13976	52
H(4)	3692	4634	14028	62

2 Publications

Compound 3

Table 1. Crystal data and structure refinement for diiodo-bis(2-chloropyrazine-N) zinc(II).

Identification code	gb11	
Empirical formula	$C_8H_6Cl_2I_2N_4Zn$	
Formula weight	548.24	
Temperature	170(2) K	
Wavelength	0.71073 Å	
Crystal system	monoclinic	
Space group	C2/c	
Unit cell dimensions	$a = 16.8523(14)$ Å	$\alpha = 90^\circ$.
	$b = 6.0972(4)$ Å	$\beta = 105.413(10)^\circ$.
	$c = 15.1299(13)$ Å	$\gamma = 90^\circ$.
Volume	1498.7(2) Å ³	
Z	4	
Density (calculated)	2.430 Mg/m ³	
Absorption coefficient	6.099 mm ⁻¹	
F(000)	1008	
Crystal size	0.06 x 0.09 x 0.12 mm ³	
Theta range for data collection	2.79 to 28.01°.	
Index ranges	-21 ≤ h ≤ 22, -7 ≤ k ≤ 7, -19 ≤ l ≤ 19	
Reflections collected	6849	
Independent reflections	1762 [R(int) = 0.0373]	
Completeness to theta = 28.01°	97.5 %	
Refinement method	Full-matrix least-squares on F ²	
Data / restraints / parameters	1762 / 0 / 79	
Goodness-of-fit on F ²	1.039	
Final R indices [I > 2σ(I)]	R1 = 0.0232, wR2 = 0.0589	
R indices (all data)	R1 = 0.0270, wR2 = 0.0602	
Extinction coefficient	0.00136(17)	
Largest diff. peak and hole	0.844 and -0.845 e.Å ⁻³	

Remarks:

All non-hydrogen atoms were refined using anisotropic displacement parameters. The hydrogen atoms were positioned with idealized geometry and were refined isotropic with $U_{eq}(H) = 1.2 \cdot U_{eq}(C_{aromatic})$ using a riding model with C-H = 0.95 Å. The complex is located on a 2-fold rotation axis.

2 Publications

Table 2. Atomic coordinates ($\times 10^4$) and equivalent isotropic displacement parameters ($\text{\AA}^2 \times 10^3$).

U(eq) is defined as one third of the trace of the orthogonalized U_{ij} tensor.

	x	y	z	U(eq)
Zn(1)	5000	10460(1)	12500	18(1)
I(1)	5394(1)	12446(1)	14025(1)	28(1)
N(1)	2893(1)	4994(4)	12489(2)	27(1)
C(1)	2971(1)	5931(5)	11732(2)	25(1)
C(2)	3554(2)	7514(4)	11705(2)	23(1)
N(2)	4069(1)	8186(4)	12493(1)	19(1)
C(3)	4003(2)	7289(4)	13272(2)	24(1)
C(4)	3416(2)	5694(5)	13259(2)	29(1)
Cl(1)	2300(1)	5099(1)	10713(1)	43(1)

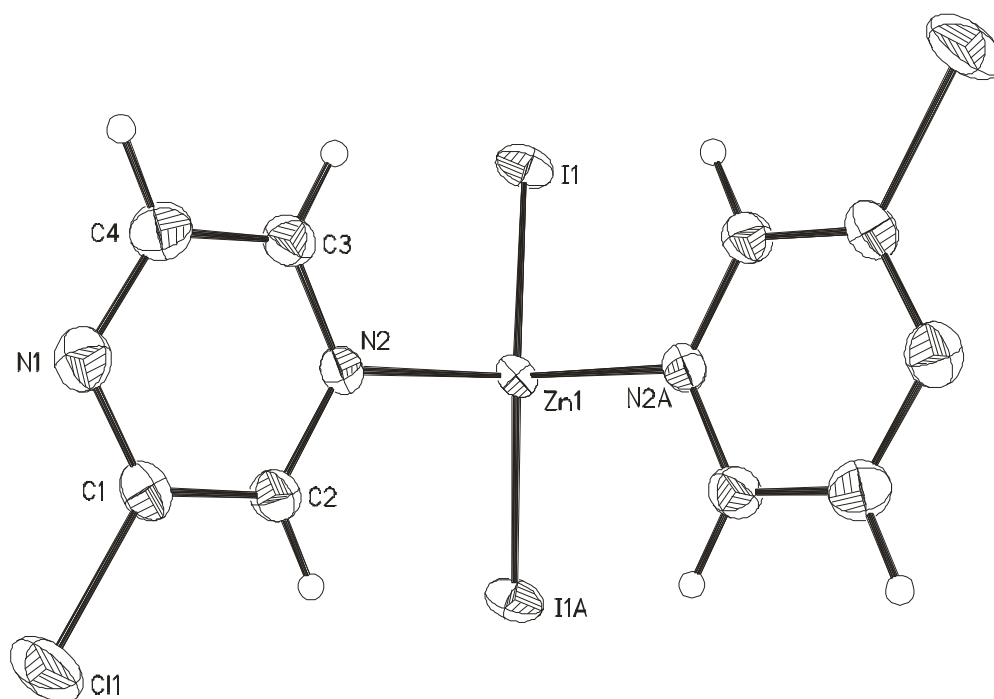


Table 3. Bond lengths [\AA] and angles [$^\circ$].

Zn(1)-N(2)	2.091(2)	Zn(1)-I(1)	2.5324(3)
Zn(1)-N(2A)	2.091(2)	Zn(1)-I(1A)	2.5324(3)
N(2)-Zn(1)-N(2A)	96.96(12)	N(2)-Zn(1)-I(1A)	107.33(6)
N(2)-Zn(1)-I(1)	109.64(6)	N(2A)-Zn(1)-I(1A)	109.64(6)
N(2A)-Zn(1)-I(1)	107.33(6)	I(1)-Zn(1)-I(1A)	122.88(2)
C(2)-N(2)-Zn(1)	121.02(18)	C(3)-N(2)-Zn(1)	120.51(18)

Symmetry transformations used to generate equivalent atoms: A: $-x+1, y, -z+5/2$

2 Publications

Table 4. Anisotropic displacement parameters ($\text{\AA}^2 \times 10^3$). The anisotropic displacement factor exponent takes the form: $-2\pi^2 [h^2 a^* 2 U_{11} + \dots + 2 h k a^* b^* U_{12}]$

	U_{11}	U_{22}	U_{33}	U_{23}	U_{13}	U_{12}
Zn(1)	15(1)	19(1)	18(1)	0	1(1)	0
I(1)	33(1)	25(1)	21(1)	-5(1)	-1(1)	2(1)
N(1)	26(1)	22(1)	32(1)	2(1)	7(1)	-3(1)
C(1)	20(1)	23(2)	28(1)	-2(1)	3(1)	-4(1)
C(2)	22(1)	23(2)	23(1)	-1(1)	5(1)	-4(1)
N(2)	16(1)	20(1)	21(1)	-1(1)	4(1)	0(1)
C(3)	22(1)	25(2)	23(1)	2(1)	4(1)	1(1)
C(4)	31(1)	29(2)	28(1)	5(1)	8(1)	0(1)
Cl(1)	42(1)	48(1)	30(1)	0(1)	-5(1)	-25(1)

Table 5. Hydrogen coordinates ($\times 10^4$) and isotropic displacement parameters ($\text{\AA}^2 \times 10^3$).

	x	y	z	U(eq)
H(2)	3587	8114	11136	27
H(3)	4360	7745	13840	29
H(4)	3385	5072	13825	35

2 Publications

Compound 4

Table 1. Crystal data and structure refinement for Dibromo-(2-chloropyrazine-N)-aqua-zinc(II)

Identification code	gb435	
Empirical formula	C ₄ H ₅ Br ₂ ClN ₂ OZn	
Formula weight	357.74	
Temperature	220(2) K	
Wavelength	0.71073 Å	
Crystal system	orthorhombic	
Space group	Pbca	
Unit cell dimensions	a = 11.2591(7) Å	α = 90°.
	b = 12.2488(6) Å	β = 90°.
	c = 14.1375(7) Å	γ = 90°.
Volume	1949.71(18) Å ³	
Z	8	
Density (calculated)	2.437 Mg/m ³	
Absorption coefficient	10.939 mm ⁻¹	
F(000)	1344	
Crystal size	0.04 x 0.09 x 0.13 mm ³	
Theta range for data collection	2.85 to 28.07°.	
Index ranges	-14 ≤ h ≤ 14, -16 ≤ k ≤ 16, -18 ≤ l ≤ 18	
Reflections collected	17607	
Independent reflections	2358 [R(int) = 0.0966]	
Completeness to theta = 28.07°	99.5 %	
Refinement method	Full-matrix least-squares on F ²	
Data / restraints / parameters	2358 / 0 / 101	
Goodness-of-fit on F ²	1.026	
Final R indices [I > 2σ(I)]	R1 = 0.0378, wR2 = 0.0946	
R indices (all data)	R1 = 0.0518, wR2 = 0.1013	
Extinction coefficient	0.0022(3)	
Largest diff. peak and hole	0.578 and -0.904 e.Å ⁻³	

Remarks:

All non-hydrogen atoms were refined using anisotropic displacement parameters. The hydrogen atoms were positioned with idealized geometry and were refined isotropic ($U_{eq}(H) = 1.2 \cdot U_{eq}(C_{aromatic}) = 1.5 \cdot U_{eq}(C_{methyl})$) using a riding model. The O-H hydrogen atoms were located in difference map, their bond lengths set to ideal values and afterwards they were refined using a riding model. This compound is located in a general position.

2 Publications

Table 2. Atomic coordinates ($\times 10^4$) and equivalent isotropic displacement parameters ($\text{\AA}^2 \times 10^3$)
 $U(\text{eq})$ is defined as one third of the trace of the orthogonalized U_{ij} tensor.

	x	y	z	$U(\text{eq})$
Br(1)	6056(1)	5924(1)	6084(1)	38(1)
Br(2)	8310(1)	4095(1)	4407(1)	39(1)
Zn(1)	7230(1)	5697(1)	4743(1)	26(1)
N(1)	4831(3)	6421(3)	1973(2)	32(1)
N(2)	6225(3)	6024(3)	3546(2)	24(1)
O(1)	8449(3)	6916(3)	4628(2)	30(1)
C(1)	4605(4)	6871(3)	2803(3)	28(1)
C(2)	5291(4)	6686(3)	3605(3)	25(1)
C(3)	6466(4)	5558(4)	2711(3)	31(1)
C(4)	5765(5)	5758(4)	1935(3)	39(1)
Cl(1)	3396(1)	7713(1)	2890(1)	46(1)

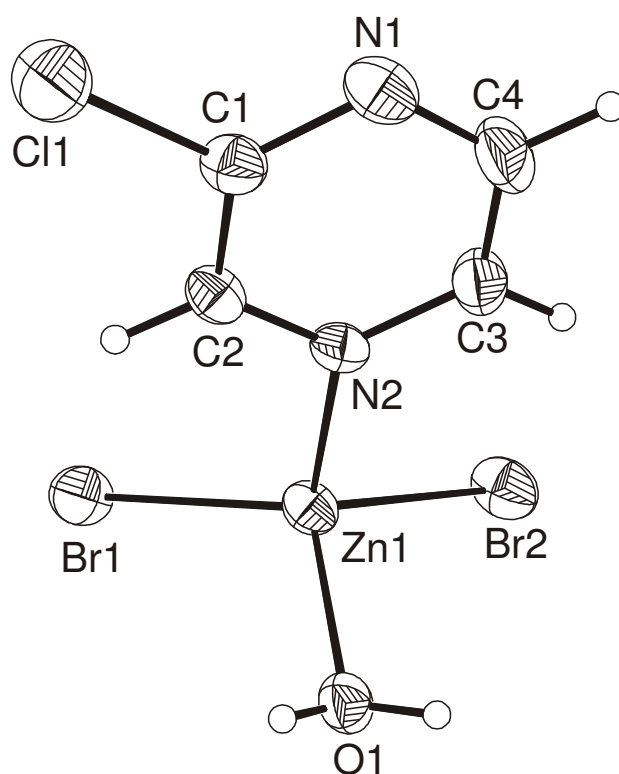


Table 3. Bond lengths [\AA] and angles [$^\circ$]

Br(1)-Zn(1)	2.3273(7)	C(2)-N(2)-Zn(1)	119.9(3)
Br(2)-Zn(1)	2.3576(7)	O(1)-Zn(1)-N(2)	99.25(13)
Zn(1)-O(1)	2.034(3)	O(1)-Zn(1)-Br(1)	111.17(8)
Zn(1)-N(2)	2.074(3)	N(2)-Zn(1)-Br(1)	109.34(10)
C(1)-N(1)-C(4)	116.3(4)	O(1)-Zn(1)-Br(2)	104.32(9)
C(2)-N(2)-C(3)	118.3(3)	N(2)-Zn(1)-Br(2)	106.13(10)
C(3)-N(2)-Zn(1)	121.7(3)	Br(1)-Zn(1)-Br(2)	123.79(3)

Table 4. Anisotropic displacement parameters ($\text{\AA}^2 \times 10^3$). The anisotropic displacement factor exponent takes the form: $-2\pi^2 [h^2 a^{*2} U_{11} + \dots + 2 h k a^* b^* U_{12}]$

	U_{11}	U_{22}	U_{33}	U_{23}	U_{13}	U_{12}
Br(1)	40(1)	46(1)	28(1)	-1(1)	7(1)	-13(1)
Br(2)	46(1)	27(1)	45(1)	-4(1)	-10(1)	8(1)
Zn(1)	31(1)	26(1)	22(1)	1(1)	-3(1)	1(1)
N(1)	39(2)	36(2)	21(2)	3(1)	-6(1)	1(2)
N(2)	25(2)	27(2)	21(1)	-1(1)	-5(1)	-2(1)
O(1)	34(2)	30(2)	25(1)	-3(1)	6(1)	-4(1)
C(1)	29(2)	27(2)	27(2)	-1(2)	-4(2)	0(2)
C(2)	31(2)	21(2)	22(2)	0(1)	-1(2)	-2(2)
C(3)	31(2)	38(2)	25(2)	-3(2)	2(2)	5(2)
C(4)	44(3)	51(3)	20(2)	-8(2)	1(2)	7(2)
Cl(1)	45(1)	43(1)	49(1)	-9(1)	-14(1)	19(1)

Table 5. Hydrogen coordinates ($\times 10^4$) and isotropic displacement parameters ($\text{\AA}^2 \times 10^3$)

	x	y	z	U(eq)
H(1O1)	8896	6852	4155	44
H(2O1)	8128	7536	4631	44
H(2)	5096	7024	4181	30
H(3)	7123	5088	2656	38
H(4)	5951	5415	1359	46

2 Publications

Compound 5

Table 1. Crystal data and structure refinement for Diiodo-(2-chloropyrazine-N)-aqua-zinc(II)

Identification code	gb410a	
Empirical formula	C ₄ H ₅ ClI ₂ N ₂ OZn	
Formula weight	451.72	
Temperature	220(2) K	
Wavelength	0.71073 Å	
Crystal system	orthorhombic	
Space group	Pbca	
Unit cell dimensions	a = 11.4595(8) Å	α = 90°.
	b = 12.9539(7) Å	β = 90°.
	c = 14.4758(8) Å	γ = 90°.
Volume	2148.9(2) Å ³	
Z	8	
Density (calculated)	2.793 Mg/m ³	
Absorption coefficient	8.235 mm ⁻¹	
F(000)	1632	
Crystal size	0.06 x 0.1 x 0.14 mm ³	
Theta range for data collection	2.76 to 28.05°.	
Index ranges	-15 ≤ h ≤ 11, -15 ≤ k ≤ 17, -19 ≤ l ≤ 19	
Reflections collected	13377	
Independent reflections	2581 [R(int) = 0.0455]	
Completeness to theta = 28.05°	99.2 %	
Refinement method	Full-matrix least-squares on F ²	
Data / restraints / parameters	2581 / 0 / 101	
Goodness-of-fit on F ²	0.975	
Final R indices [I > 2σ(I)]	R1 = 0.0230, wR2 = 0.0489	
R indices (all data)	R1 = 0.0347, wR2 = 0.0519	
Extinction coefficient	0.00078(11)	
Largest diff. peak and hole	0.643 and -0.770 e.Å ⁻³	

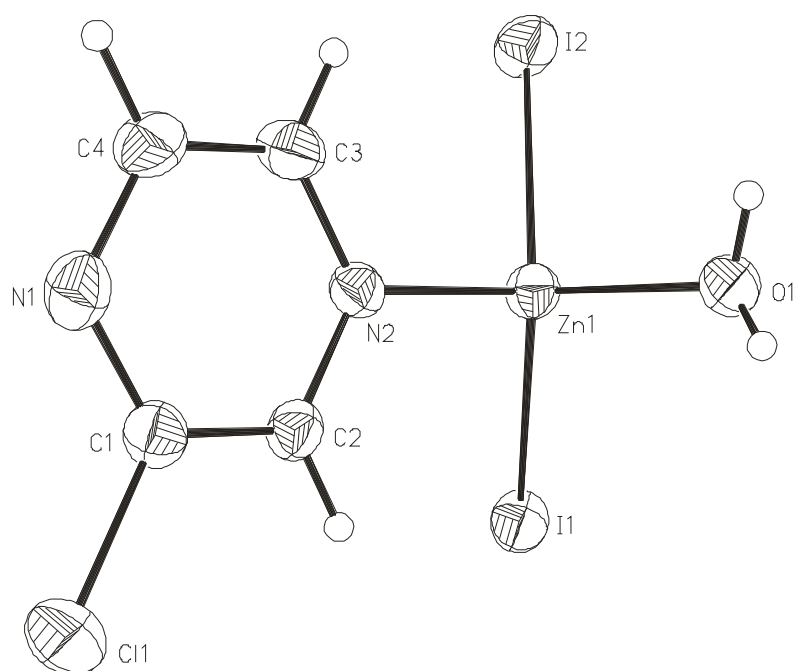
Remarks:

All non-hydrogen atoms were refined using anisotropic displacement parameters. The hydrogen atoms were positioned with idealized geometry and were refined isotropic ($U_{eq}(H) = 1.2 \cdot U_{eq}(C_{aromatic}) = 1.5 \cdot U_{eq}(C_{methyl})$) using a riding model. The O-H hydrogen atoms were located in difference map, their bond lengths set to ideal values and afterwards they were refined using a riding model. This compound is located in a general position.

Table 2. Atomic coordinates ($\times 10^4$) and equivalent isotropic displacement parameters ($\text{\AA}^2 \times 10^3$)

U(eq) is defined as one third of the trace of the orthogonalized U^{ij} tensor.

	x	y	z	U(eq)
I(1)	6037(1)	5985(1)	6124(1)	33(1)
I(2)	8377(1)	4045(1)	4360(1)	37(1)
Zn(1)	7254(1)	5700(1)	4696(1)	25(1)
N(1)	4861(3)	6385(3)	1995(2)	32(1)
N(2)	6243(2)	6003(2)	3530(2)	24(1)
O(1)	8458(2)	6834(2)	4561(1)	30(1)
C(1)	4647(3)	6811(3)	2808(2)	28(1)
C(2)	5326(3)	6628(3)	3585(2)	25(1)
C(3)	6475(3)	5563(3)	2716(2)	31(1)
C(4)	5771(3)	5745(3)	1959(2)	34(1)
Cl(1)	3475(1)	7622(1)	2900(1)	48(1)

Table 3. Bond lengths [\AA] and angles [$^\circ$]

I(1)-Zn(1)	2.5219(4)	O(1)-Zn(1)-N(2)	99.43(10)
I(2)-Zn(1)	2.5468(5)	O(1)-Zn(1)-I(1)	110.47(6)
Zn(1)-O(1)	2.026(3)	N(2)-Zn(1)-I(1)	109.22(8)
Zn(1)-N(2)	2.084(3)	O(1)-Zn(1)-I(2)	104.34(7)
C(2)-N(2)-Zn(1)	120.4(2)	N(2)-Zn(1)-I(2)	106.57(8)
C(3)-N(2)-Zn(1)	121.6(2)	I(1)-Zn(1)-I(2)	123.993(16)

2 Publications

Table 4. Anisotropic displacement parameters ($\text{\AA}^2 \times 10^3$). The anisotropic displacement factor exponent takes the form: $-2\pi^2 [h^2 a^{*2} U_{11} + \dots + 2 h k a^* b^* U_{12}]$

	U_{11}	U_{22}	U_{33}	U_{23}	U_{13}	U_{12}
I(1)	33(1)	40(1)	27(1)	-1(1)	6(1)	-8(1)
I(2)	41(1)	26(1)	43(1)	-4(1)	-8(1)	7(1)
Zn(1)	26(1)	27(1)	22(1)	0(1)	-3(1)	1(1)
N(1)	34(2)	35(2)	27(1)	1(1)	-7(1)	0(1)
N(2)	21(1)	27(1)	23(1)	0(1)	1(1)	-1(1)
O(1)	28(1)	32(1)	30(1)	-2(1)	5(1)	-4(1)
C(1)	29(2)	24(2)	30(2)	1(1)	-4(1)	2(1)
C(2)	26(2)	27(2)	21(1)	-1(1)	-2(1)	-1(1)
C(3)	27(2)	37(2)	27(2)	1(1)	3(1)	6(2)
C(4)	37(2)	46(2)	20(1)	-4(1)	0(1)	6(2)
Cl(1)	41(1)	47(1)	54(1)	-8(1)	-14(1)	20(1)

Table 5. Hydrogen coordinates ($\times 10^4$) and isotropic displacement parameters ($\text{\AA}^2 \times 10^3$)

	x	y	z	U(eq)
H(1O1)	8930	6732	4126	45
H(2O1)	8358	7470	4480	45
H(2)	5138	6947	4149	29
H(3)	7125	5125	2658	37
H(4)	5939	5407	1400	41

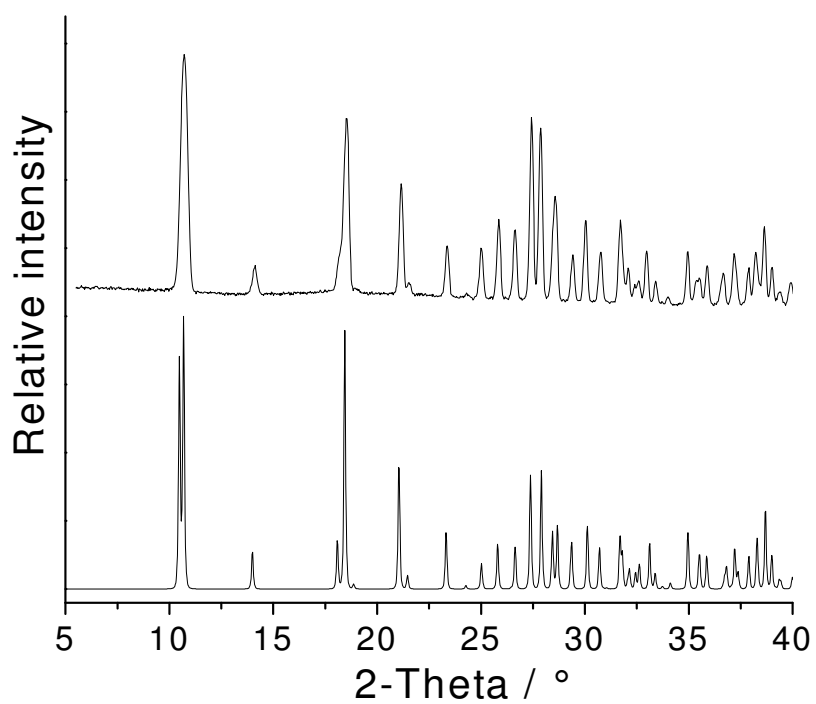


Figure S1. Experimental (top) and calculated (bottom) X-ray powder pattern of compound **1**.

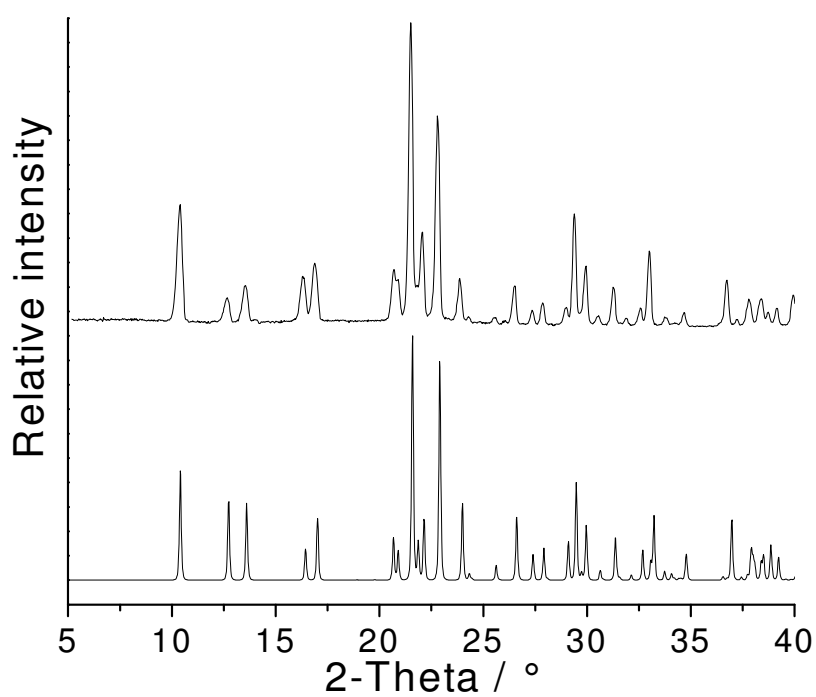


Figure S2. Experimental (top) and calculated (bottom) X-ray powder pattern of compound **2**.

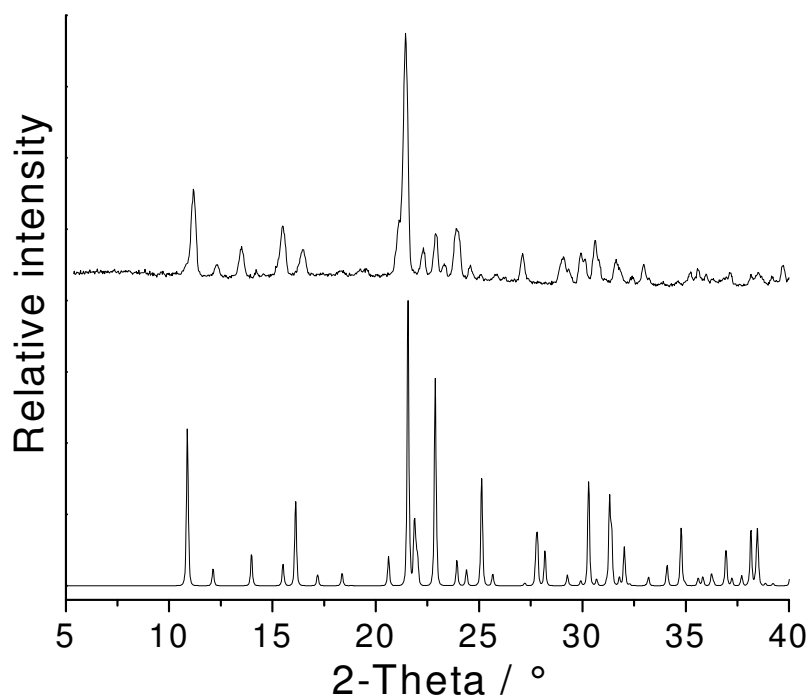


Figure S3. Experimental (top) and calculated (bottom) X-ray powder pattern of compound **3**.

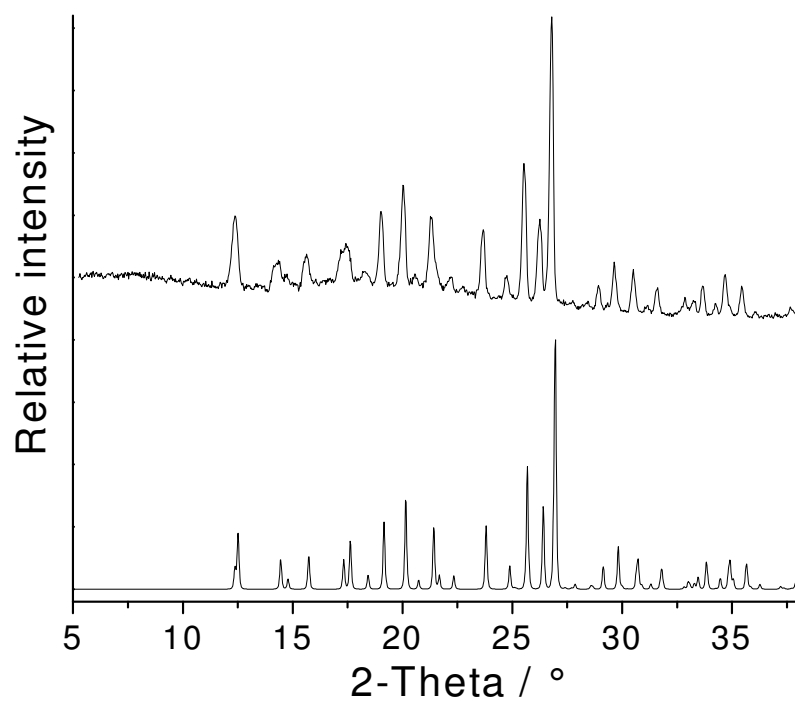


Figure S4. Experimental (top) and calculated (bottom) X-ray powder pattern of compound **4**.

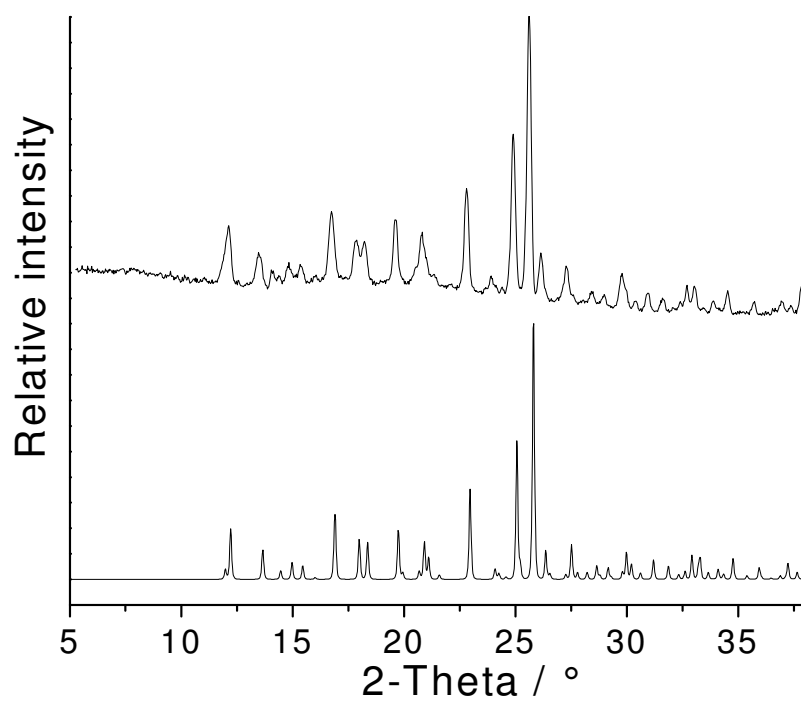


Figure S5. Experimental (top) and calculated (bottom) X-ray powder pattern of compound **5**.

3. Contribution to conferences

3.1

Synthesis, Crystal Structures and Thermal behavior of Zinc (II) halide Pyrimidine Coordination Polymers

Gaurav Bhosekar, Inke Jeß, Christian Näther*

Institut für Anorganische Chemie, CAU Kiel, Olshausenstr. 40, D-24098 Kiel

Keywords: coordination polymers; zinc; crystal structure

Recently we investigated coordination polymers on the basis of copper(I)halides and N-donor ligands. In these compounds typical CuX substructures are found, which are connected by the ligands into coordination polymers. For one definite copper(I)halide and one specific ligand several compounds are frequently found which differ in the ratio between the inorganic and organic part. We have found that the ligand-rich compounds can be transformed into ligand-poor compounds by controlled thermal decomposition. Therefore, thermal decomposition reactions are an adequate alternative for the discovery and the preparation of new coordination polymers. To prove if such reactions can also be used for the preparation of other coordination polymers we have started systematic investigations on coordination compounds on the basis of Zn(II) bromides [1,2]. Here we report on our investigations of the ZnX_2 -pyrimidine compounds ($\text{X} = \text{Br}, \text{I}$).

If ZnBr_2 is reacted with pyrimidine the most ligand-rich 1:2 compound $\text{ZnBr}_2(\text{pyrimidine})_2$ is obtained. Its structure consists of discrete complexes in which the zinc atoms are coordinated by two bromine atoms and two pyrimidine ligands. If this compound is heated in a thermobalance, three mass steps are observed which correspond to the formation of ligand-poor 2:3, 1:1 and 2:1 compounds. Not all of these compounds can be prepared phase-pure in solution but for the 2:3 and the 1:1 phases single crystals were grown and characterized by single-crystal X-ray diffraction. In the 2:3 compound discrete $(\text{ZnBr}_2)(\text{pyrimidine})_3$ units are found, whereas in the 1:1 compound ZnBr_2 single chains are observed, which are connected by the ligands into layers.

With ZnI_2 also a ligand-rich 1:2 compound was obtained which is not isotypic to that of ZnBr_2 . If this compound is investigated by thermogravimetry using heating rates of $1^\circ\text{C}/\text{min}$, two mass steps are observed which correspond to the formation of a ligand-poor 1:1 and 2:1 compound. If the heating rate is increased to $8^\circ\text{C}/\text{min}$ the first mass step splits into two equal mass steps, indicative for the formation of a ligand-poor 2:3 intermediate phase. These results show that the kinetics of all reactions involved influence the product formation in this system. The 1:1 compound was characterized by single-crystal X-ray diffraction. Its structure consists of ZnI_2 units which are connected by the pyrimidine ligands into chains.

[1] G. Bhosekar, I. Jeß, C. Näther, *Z. Naturforsch.* **2006**, *61b*, 721.

[2] G. Bhosekar, I. Jeß, C. Näther, *Inorg. Chem.*, in press.

3.2

Thermal decomposition reactions for the discovery and preparation of new stable and metastable $ZnI_2(\text{pyrimidine})$ coordination compounds

Gaurav Bhosekar, Inke Jeß and Christian Näther*

Institut für Anorganische Chemie, Universität zu Kiel, Olshausenstr. 40 (Otto-Hahn-Platz 6-7), D-24098-Kiel, Fax: +49 (0)431/880-1520, E-mail: cnaether@ac.uni-kiel.de

Recently, investigations on the synthesis, structures and properties of new coordination and inorganic-organic hybrid compounds has become of increasing interest. One major goal in this field includes the development of strategies for the preparation of new compounds which can be used as catalysts, porous frameworks, molecular magnets or nonlinear optical devices. However, one major problem in this field is the preparation of large and pure amounts of a compound, which for coordination compounds is sometimes difficult to achieve, but which is needed for any investigation of the properties. Therefore, alternatives for the pure preparation of such compounds are needed.

Several years ago we have reported that new coordination polymers based on copper(I) halides or pseudo halides CuX and N donor ligands can be prepared very pure by thermal decomposition of suitable ligand rich precursor compounds. On heating they lose their ligands stepwise, forming ligand poorer intermediate compounds which in several cases cannot be prepared in solution. Starting from these findings we have initiated systematic investigations on the thermal properties of coordination compounds in order to show if also other compounds can be transformed into ligand poorer compounds.

In the beginning we investigated Zinc(II) halide coordination polymers with pyrazine [1] and pyrimidine as ligands. If Zinc(II) iodide is reacted with pyrimidine in acetonitrile for example $ZnI_2(\text{pyrimidine})_2$ is obtained. If this compound is heated in a thermobalance, two ligand poor phases of composition $ZnI_2(\text{pyrimidine})$ (Form I) and $(ZnI_2)_2(\text{pyrimidine})$ can be isolated. Heating rate dependent measurements show, that an additional compound of composition $(ZnI_2)_3(\text{pyrimidine})_2$ is an intermediate in this reaction. If Zinc(II) iodide is reacted with pyrimidine in acetonitrile and crystallized under kinetic control, a metastable compound of composition $(ZnI_2)_4(\text{pyrimidine})_4$ -acetonitrile is isolated. If this compound is heated, a transformation into $(ZnI_2)_3(\text{pyrimidine})_3$ is observed, which on further heating undergoes a polymorphic transformation into a second modification of $ZnI_2(\text{pyrimidine})$ (Form II). All compounds were characterized by single crystal X-ray diffraction. A detailed analysis of their structures shows, that there is a strong relationship between most of the compounds. Therefore, it can be assumed that structural information is transferred from the reactants onto the products. In this lecture it will be reported in detail on the results of our investigations.

[1] G. Bhosekar, I. Jeß, C. Näther, *Inorg. Chem.*, **2006**, *45*, 6508-6515.

3.3

Synthesis, Crystal Structures and Thermal behavior of Zinc (II) halide Pyrimidine Coordination Polymers

Gaurav Bhosekar, Inke Jeß, Christian Näther*

Institut für Anorganische Chemie, CAU Kiel, Olshausenstr. 40, D-24098 Kiel

Keywords: coordination polymers; zinc; crystal structure

Recently we investigated coordination polymers on the basis of copper(I)halides and N-donor ligands. In these compounds typical CuX substructures are found, which are connected by the ligands into coordination polymers. For one definite copper(I)halide and one specific ligand several compounds are frequently found which differ in the ratio between the inorganic and organic part. We have found that the ligand-rich compounds can be transformed into ligand-poor compounds by controlled thermal decomposition. Therefore, thermal decomposition reactions are an adequate alternative for the discovery and the preparation of new coordination polymers. To prove if such reactions can also be used for the preparation of other coordination polymers we have started systematic investigations on coordination compounds on the basis of Zn(II) bromides [1,2]. Here we report on our investigations of the ZnX₂-pyrimidine compounds (X = Br, I).

If ZnBr₂ is reacted with pyrimidine the most ligand-rich 1:2 compound ZnBr₂(pyrimidine)₂ is obtained. Its structure consists of discrete complexes in which the zinc atoms are coordinated by two bromine atoms and two pyrimidine ligands. If this compound is heated in a thermobalance, three mass steps are observed which correspond to the formation of ligand-poor 2:3, 1:1 and 2:1 compounds. Not all of these compounds can be prepared phase-pure in solution but for the 2:3 and the 1:1 phases single crystals were grown and characterized by single-crystal X-ray diffraction. In the 2:3 compound discrete (ZnBr₂)(pyrimidine)₃ units are found, whereas in the 1:1 compound ZnBr₂ single chains are observed, which are connected by the ligands into layers.

With ZnI₂ also a ligand-rich 1:2 compound was obtained which is not isotopic to that of ZnBr₂. If this compound is investigated by thermogravimetry using heating rates of 1°C/min, two mass steps are observed which correspond to the formation of a ligand-poor 1:1 and 2:1 compound. If the heating rate is increased to 8°C/min the first mass step splits into two equal mass steps, indicative for the formation of a ligand-poor 2:3 intermediate phase. These results show that the kinetics of all reactions involved influence the product formation in this system. The 1:1 compound was characterized by single-crystal X-ray diffraction. Its structure consists of ZnI₂ units which are connected by the pyrimidine ligands into chains.

[1] G. Bhosekar, I. Jeß, C. Näther, *Z. Naturforsch.* **2006**, *61b*, 721.

[2] G. Bhosekar, I. Jeß, C. Näther, *Inorg. Chem.*, in press.

3.4

Investigations on the trimorphism of dichlorobis(pyridazine) zinc(II)

G. Bhosekar, I. Jeß und C. Näther

Institut für Anorganische Chemie, CAU Kiel.

gbhosekar@ac.uni-kiel.de

Recently, investigations on coordination compounds and polymers, inorganic-organic hybrid compounds or metal organic frameworks have become topics of increasing interest. For a more directed design of the structures of such solids, a specific knowledge of intermolecular interactions in crystals and their interplay is important. In this context, one has to be aware of the phenomenon of polymorphism or isomerism, which is frequently found in such compounds. If polymorphism or isomerism is detected along with the structural aspects, the thermodynamic stability and the interconversion behaviour should be investigated. It is also needed to find conditions for the preparation of each form as a phase pure compound.

In our ongoing investigations of the synthesis, structures, and properties of new coordination polymers we have started systematic investigations of their thermal behaviour, because we have demonstrated that new ligand deficient coordination polymers can be conveniently prepared by thermal decomposition of suitable ligand rich precursor compounds [1]. During these investigations we frequently obtained polymorphic modifications, which were characterized for their thermal properties, stability and transformation behaviour [2].

For coordination compounds based on zinc(II) chloride and pyridazine as the N-donor ligand we have obtained three polymorphic modifications of dichlorobis(pyridazine-N) zinc(II). All of these forms transform into a new ligand deficient compound on heating. The polymorphism of these simple coordination compounds is based predominantly on a different packing of the tetrahedral building blocks within the solid. Here we report the results of these investigations.

The reaction of zinc(II)chloride with pyridazine under different conditions leads to the formation of three polymorphic modifications of dichloro-bis(pyridazine-N) zinc(II). Form I and II crystallize in the monoclinic space group Cc (I) and P2₁/c (II) respectively, whereas form III crystallizes in the orthorhombic space group Pna2₁. In all three forms the zinc atoms are surrounded by two chloro atoms and two pyridazine ligands within distorted tetrahedra and the orientation of the pyridazine rings within these tetrahedra are different. In the crystal structure the tetrahedral building blocks are packed differently and are connected by intermolecular C-H...Cl and C-H...N interactions. Crystallization experiments clearly show that form I represents the thermodynamically most stable form at room temperature, whereas form II and form III are metastable. DTA-TG measurements reveal that all forms decompose into a new ligand deficient compound [ZnCl₂(pyridazine)], which can also be prepared in solution. On heating form I transforms into form II, which is more stable at higher temperatures as observed by DSC measurements. On some of the DSC measurements form I decompose without further transformation into form II. Both forms I and II behave enantiotropic. The DSC thermogram of form III gave no indication of a polymorphic transformation.

[1] G. Bhosekar, I. Jeß, C. Näther, C., *Inorg. Chem.* 2006, 43, 6508.

[2] G. Bhosekar, I. Jeß, C. Näther, *Z. Naturforsch.*, 2006, 61b, 721.

3.5

Polymorphic modifications of dichloro-bis(pyridazine-N) zinc(II)

Gaurav Bhosekar, Inke Jeß and Christian Näther

Institut für Anorganische Chemie der Christian-Albrechts-Universität; Otto-Hahn-Platz 6/7;
D-24098 Kiel, Germany; e-mail: gbhosekar@ac.uni-kiel.de

Polymorphism is defined as the ability of a compound to crystallize in more than one crystalline modification. It is a widespread phenomenon and frequently found in all classes of compounds. Because the properties of polymorphic modifications are different, this phenomenon is of extremely importance in a number of areas like material science or pharmaceutical development.

In our ongoing investigations on the synthesis, structures and properties of zinc(II) halide coordination compounds and polymers we frequently obtained polymorphic modifications [1,2]. Here we report on polymorphic modifications of dichlorobis(pyridazine)zinc(II), which were structurally characterized and investigated for their thermal properties, thermodynamic stability and transformation behaviour using simultaneously thermogravimetry (TG) and differential thermoanalysis (DTA), differential scanning calorimetry (DSC), X-ray powder diffraction and solvent mediated conversion experiments [3].

The reaction of zinc(II)chloride with pyridazine under different conditions leads to the formation of three polymorphic modifications of dichloro-bis(pyridazine-N) zinc(II). Form **I** and **II** crystallize in the monoclinic space group Cc (**I**) and $P2_1/c$ (**II**), whereas form **III** crystallizes in the orthorhombic space group $Pna2_1$. In all three forms the zinc atoms are surrounded by two chlorine atoms and two pyridazine ligands within distorted tetrahedra and the orientations of the pyridazine rings within these tetrahedra are different. In the crystal structure, the tetrahedral building blocks are packed differently and are connected by intermolecular C-H...Cl and C-H...N interactions. Crystallization experiments clearly show that form **I** represents the thermodynamically most stable form at room temperature, whereas form **II** and form **III** are metastable. DTA-TG measurements reveal that the all forms decompose into a new ligand deficient compound $[ZnCl_2(pyridazine)]$, which can also be prepared in solution. On heating form **I** transforms into form **II**, which is more stable at higher temperatures as observed by DSC measurements. Therefore, both forms behave enantiotropic. In some of the DSC measurements it was found that form **I** decompose without further transformation into form **II**. The DSC thermogram of form **III** gave no indication of a polymorphic transformation.

References

- [1] G. Bhosekar, I. Jeß, C. Näther, *Z. Naturforsch.*, **2006**, *61b*, 721.
- [2] C. Näther, G. Bhosekar, I. Jeß, *Inorg. Chem.* **2007**, in press.
- [3] G. Bhosekar, I. Jeß, Z. Havlas, C. Näther, *Cryst., Growth & Des.*, **2007**, in press.

4. Summary

In the present thesis, investigations on the synthesis, structures and properties of new zinc(II) halide coordination polymers has been presented. Based on the previous results of our group on the thermal properties of coordination compounds of copper(I) halides or pseudohalides and N-donor ligands we did systematic investigations in order to prove if new ligand deficient thermodynamically metastable and stable coordination zinc(II) halide compounds including polymorphic modifications can be prepared by thermal decomposition reactions.

This was investigated in the beginning for ZnX ($X = Cl, Br, I$) coordination compounds with pyrazine as ligand (chapter 2.1). In this work it was proven for the first time that new zinc(II) halide coordination compounds can be prepared by thermal decomposition reactions. Altogether, the coordination compounds poly-bis(μ_2 -pyrazine)-dichloro-zinc(II) (**1**), poly-(μ_2 -pyrazine-N,N')-dichloro-zinc(II) (**2**), poly-bis(μ_2 -pyrazine-N,N')-dibromo-zinc(II) (**3**), catena-(μ_2 -pyrazine-N,N')-dibromo-zinc(II) (**4**) and catena-(μ -pyrazine)-diiodo-zinc(II) (**5**) were prepared by the reaction of ZnX_2 ($X = Cl, Br, I$) with pyrazine in acetonitrile. In the crystal structure of compound **1** the zinc atoms are coordinated by two chlorine atoms and two pyrazine ligands within distorted tetrahedra, which are linked by the N-donor ligands into layers. The crystal structure of compound **3** is very similar to that of **1**. The structure of this compound was originally reported in space group $Ccca$ with similar a- and b-axis but we have proven that the correct space group is $I4/mmm$. The ligand deficient compound **5** is isotopic to compound **4** in which ZnX_2 units ($X=Br, I$) are connected by the pyrazine ligands into chains. This structure was originally reported in the non-centrosymmetric space group $P2_1$ but we found that the correct space group is $P2_1/m$.

If the ligand rich 1:2 compounds **1** and **3** are heated in a thermobalance different mass steps are observed. We have proven that in the first step the ligand deficient compounds **2** and **4** are formed in quantitative yields (figure 1). On further heating a second mass step occurs which leads to the formation of two new compounds of composition $(ZnCl_2)_2(\text{pyrazine})$ (**6**) and $(ZnBr_2)_2(\text{pyrazine})$ (**7**). However, the corresponding mass step are not well resolved and the new compounds are not obtained pure in this reaction. If the ligand deficient 1:1 compound **5** is investigated by thermogravimetry an unresolved single mass step is observed in which the new ligand deficient 2:1 compound $(ZnI_2)_2(\text{pyrazine})$ (**8**) is formed. On further heating all 2:1 compounds lose the remaining ligands and transform into the pure zinc(II)halides.

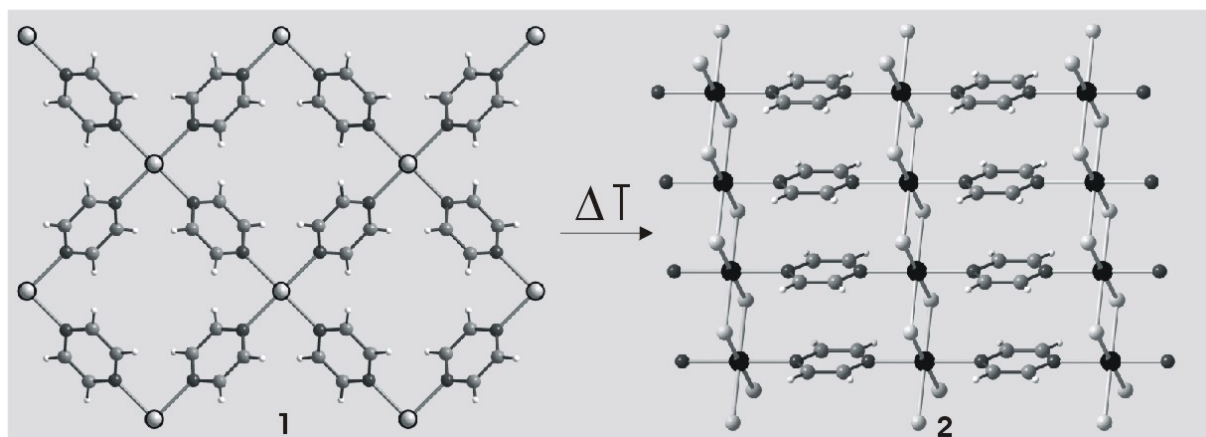


Figure 1: Structural changes during the thermal decomposition reaction of poly-bis(μ_2 -pyrazine)-dichloro-zinc(II) (**1**) into poly-(μ_2 -pyrazine-N,N')-dichloro-zinc(II) (**2**).

In further work coordination compounds based on zinc(II) iodide and pyrimidine were prepared and investigated (chapter 2.2). In this work a large number of thermodynamically stable and metastable zinc(II) coordination compounds including different polymorphic modifications were obtained for the first time. The different compounds prepared by thermal decomposition and by crystallization from solution represent a snapshot of the species in solution and thus provide deep insight into the formation of coordination compounds.

In this work ZnI_2 and pyrimidine was reacted in acetonitrile, which results in the formation of the ligand 1:2 compound $\text{ZnI}_2(\text{pyrimidine})_2$ (**1**), which consists of discrete tetrahedral complexes. Slow heating of this compound in a thermobalance at $1^\circ\text{C}/\text{min}$ leads to its transformation into the ligand deficient 1:1 compound $\text{ZnI}_2(\text{pyrimidine})$ (**3**), which on further heating decomposes into the most ligand deficient 2:1 compound $(\text{ZnI}_2)_2(\text{pyrimidine})$ (**4**) (figure 2). In contrast, the 2:3 compound $(\text{ZnI}_2)_2(\text{pyrimidine})_3$ (**2**) is formed as an intermediate by decomposing **1** using a faster heating rate of $8^\circ\text{C}/\text{min}$. Compound **2** consists of oligomeric units in which each ZnI_2 unit is connected to two iodine atoms, one bridging and one terminal pyrimidine ligand. The crystal structure of compound **3** is built up of ZnI_2 units, which are connected by the ligands into chains. For the thermal transformation of **1** into **3** via **2** as intermediate a smooth reaction pathway is found in the crystal structure, for which only small translational and rotational changes are needed.

The metastable solvated compound $(\text{ZnI}_2)(\text{pyrimidine})(\text{acetonitrile})_{0.25}$ (**5**) consisting of $(\text{ZnI}_2)_4(\text{pyrimidine})_4$ rings is obtained by quenching the reaction of ZnI_2 and pyrimidine in acetonitrile using an anti-solvent. On heating, **5** decompose into a new polymorphic 1:1 compound **6**, which consists of $(\text{ZnI}_2)(\text{pyrimidine})$ chains. On further heating **6** transforms into

4 Summary

a third polymorphic 1:1 compound **7**, which consists of $(\text{ZnI}_2)_3(\text{pyrimidine})_3$ rings and finally into the 1:1 compound **3** (figure 2). Solvent mediated conversion experiments reveal that compounds **1**, **2**, **3** and **4** are thermodynamically stable, whereas compounds **5**, **6** and **7** are metastable. Time dependent crystallization experiments unambiguously show that compound **7** is formed by kinetic control and transforms within minutes into compound **6** that finally transforms into **3**. Compound **3** represents the thermodynamically most stable 1:1 modification, whereas compounds **6** and **7** are metastable.

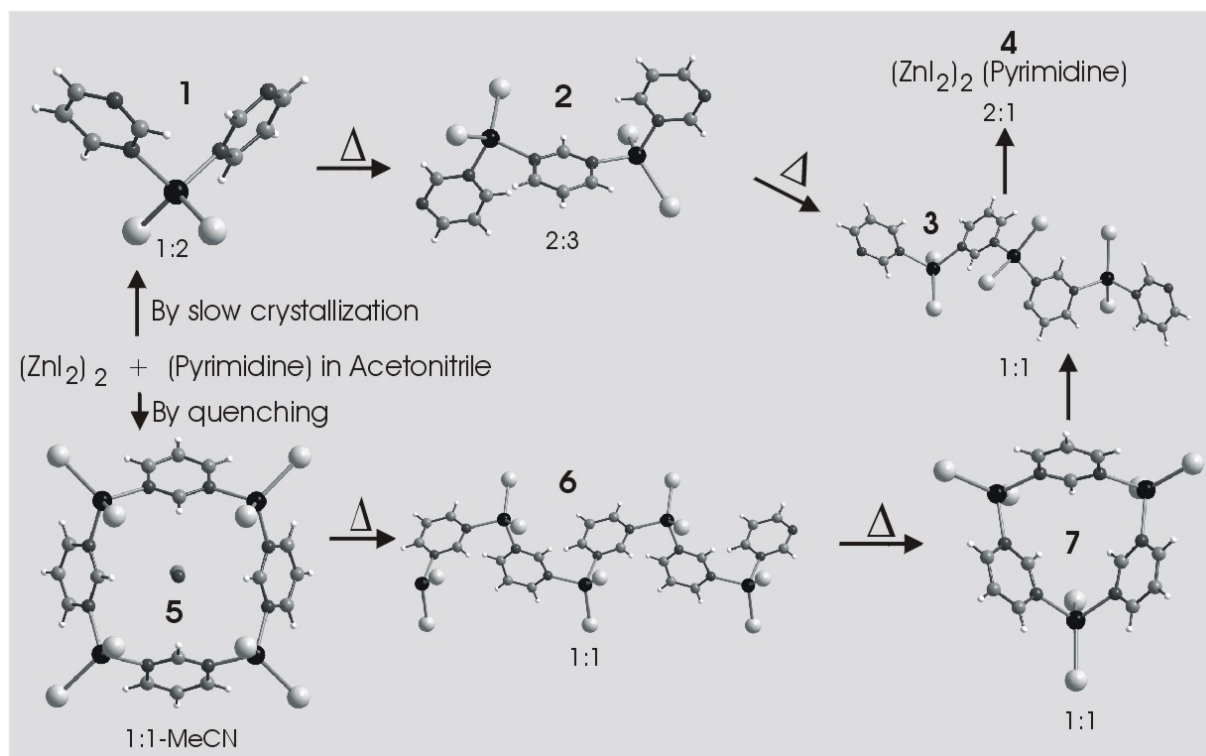


Figure 2: Schematic representation of the thermal decomposition reactions of $\text{ZnI}_2(\text{pyrimidine})$ coordination compounds.

In chapter 2.3 the corresponding compounds with zinc(II) bromide and pyrimidine were reported. In contrast to the $\text{ZnI}_2(\text{pyrimidine})$ compounds described above (chapter 2.1), no metastable compounds are obtained.

Alltogether four new zinc(II) bromide coordination compounds with pyrimidine as ligand were prepared in solution and via thermal decomposition reactions and were investigated for their thermal reactivity and thermodynamic stability. These results are compared with those for the corresponding $\text{ZnI}_2(\text{pyrimidine})$ compounds.

The ligand rich 1:2 compound dibromo-bis(pyrimidine-N) zinc(II) (**1**) crystallizes monoclinic in space group $\text{P}2_1/n$. In this structure the zinc atoms are coordinated by two bromo atoms and two pyrimidine ligands within distorted tetrahedra (figure 3). On heating, compound **1**

4 Summary

transforms into the ligand deficient 2:3 intermediate bis(dibromo-pyrimidine-N)-(μ_2 -pyrimidine-N,N')dizinc(II) (**2**), which crystallizes in the monoclinic space group C2/c. The crystal structure consists of two $\text{ZnBr}_2(\text{pyrimidine})$ subunits, which are connected by an additional pyrimidine ligand via $\mu\text{-N,N}'$ coordination. Thermal decomposition of **2** leads to the formation of the ligand deficient 1:1 compound dibromo-(μ_2 -pyrimidine-N,N') (**3**), which crystallizes in the orthorhombic space group Pmma (figure 3). In compound **3** the zinc atoms are coordinated by four bromo atoms and two pyrimidine ligands within distorted octahedra. The ZnBr_2 units are connected via common edges into chains, which are linked by the pyrimidine ligands into layers. On heating compound **3** transforms into the ligand deficient 2:1 compound $(\text{ZnBr}_2)_2(\text{pyrimidine})$ (**4**), which decompose into ZnBr_2 . Solvent mediated conversion experiments in solution shows, that not all of the compounds can be prepared by reacting ZnBr_2 and pyrimidine in a molar ratio given by the formula of the final product.

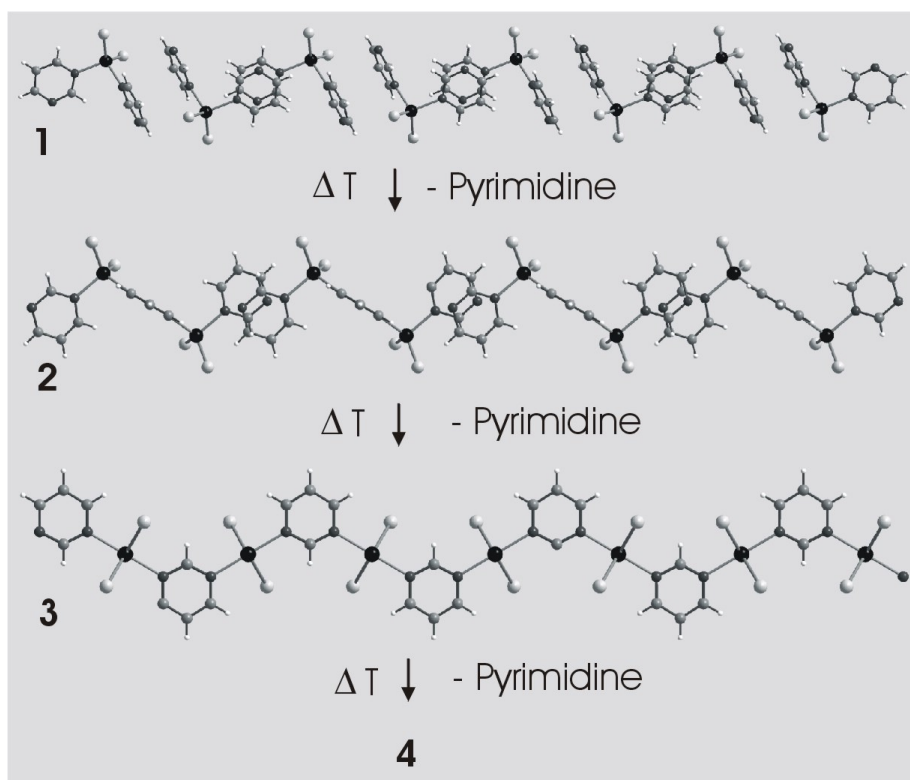


Figure 3. Structural changes in the thermal decomposition reaction of the $\text{ZnBr}_2(\text{pyrimidine})$ coordination compounds.

In further investigations, coordination compounds with zinc(II) halides and pyridazine were prepared and characterized (chapter 2.4 and 2.5). In contrast to the pyrimidine compounds no ligand deficient compounds were obtained. With zinc(II) bromide and iodide only the two ligand rich compounds Dibromo-bis(pyridazine-N)zinc(II) and Diiodo-bis(pyridazine-N)zinc(II) can be prepared (figure 4), which surprisingly decompose directly into ZnBr_2 and ZnI_2 on heating, without the formation of a ligand deficient intermediate.

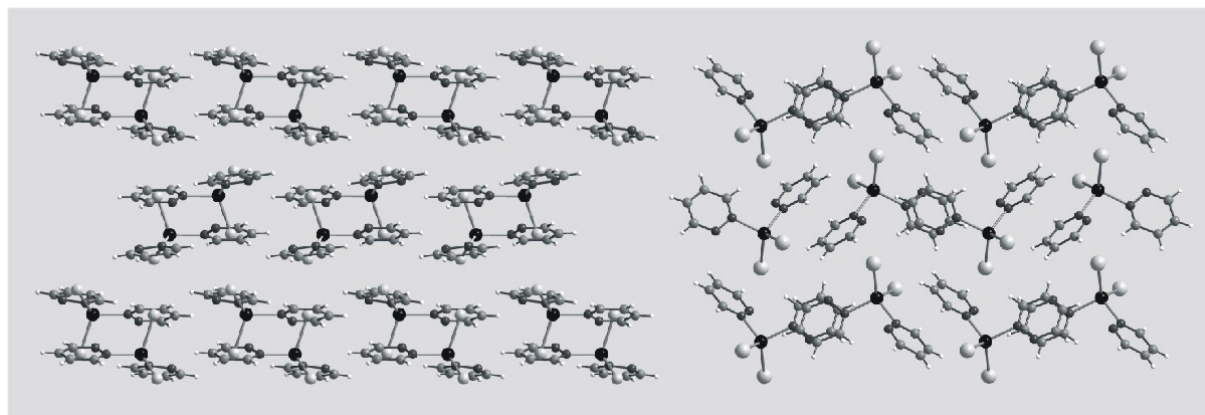


Figure 4. Crystal structure of dibromo-bis(pyridazine- κ N)zinc(II) (left) and diiodo-bis(pyridazine- κ N)zinc(II).

In contrast to the ZnI_2 and $ZnBr_2(\text{pyridazine})$ coordination compounds described in chapter 2.4 and 2.5, the corresponding ligand rich 1:2 $ZnCl_2$ compound dichloro-bis(pyridazine-N)zinc(II) decompose into a new ligand deficient 1:1 intermediate on heating (chapter 2.6). Interestingly, this compound exists in three different polymorphic modifications, which can be obtained if zinc(II)chloride is reacted with pyridazine under different conditions. Forms **1** and **2** crystallize in the monoclinic space group Cc (**1**) and $P2_1/c$ (**2**) respectively, whereas form **3** crystallizes in the orthorhombic space group $Pna2_1$. In all three forms the zinc atoms are surrounded by two chloro atoms and two pyridazine ligands within distorted tetrahedra and the orientation of the pyridazine rings within these tetrahedra are different. In the crystal structure the tetrahedral building blocks are packed differently and are connected by intermolecular $C-H\cdots Cl$ and $C-H\cdots N$ interactions.

Crystallization experiments clearly show that form **1** represents the thermodynamically most stable form at room temperature, whereas form **2** and form **3** are metastable. Theoretical calculations show, that in form **2** the most stable molecular structure is found, whereas the molecular structure in form **3** is less stable by only 8 kJ/mol. DTA-TG measurements reveal that all the forms decompose into a new ligand deficient compound $[ZnCl_2(\text{pyridazine})]$, which can also be prepared in solution. Form **1** can be transformed into form **2**, which is more stable at higher temperatures as evidenced by DSC measurements (figure 5). In some of the DSC measurements form **1** decompose without further transformation into form **2**. Both forms **1** and **2** behave enantiotropically. The DSC thermogram of form **3** gave no indication for a polymorphic transformation (figure 5).

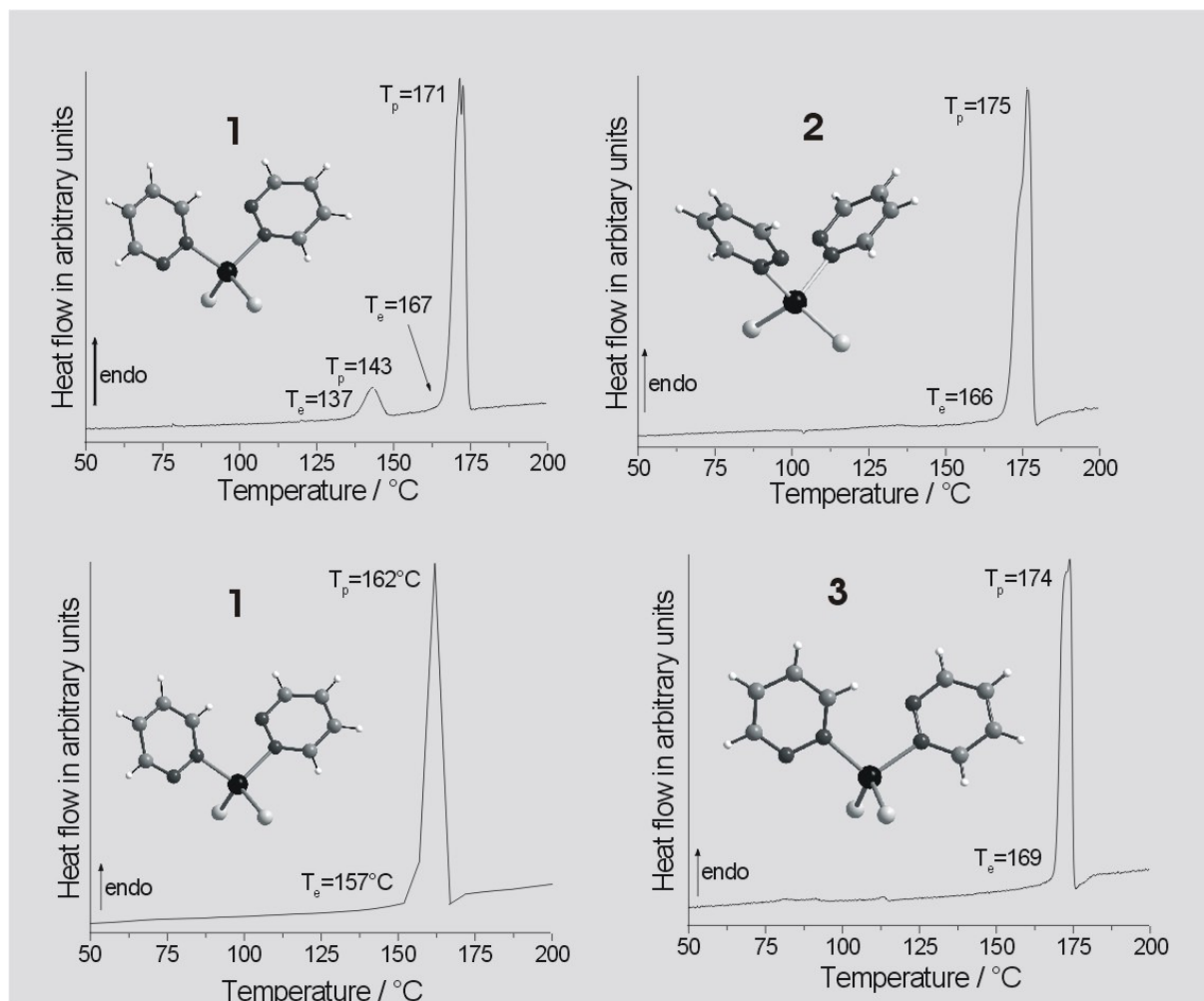


Figure 5. DSC curves of form **1** (left), **2** (top: right) and **3** (bottom right) of dichloro-bis(pyridazine-N) zinc(II).

Polymorphic modifications were also obtained for dibromo-bis(acetonitrile-N)-zinc(II) and were characterized by single crystal structure analysis and X-ray powder measurements (chapter 2.7). Form **1** crystallizes in the orthorhombic space group *Pnma* with $Z = 4$. The structure is composed of discrete molecular complexes in which each zinc cation is coordinated by two bromide anions and two acetonitrile ligands within distorted tetrahedra. Form **2** crystallizes in the orthorhombic space group *Cmcm* with $Z = 4$. In this compound also discrete complexes are found and the coordination of the zinc atoms is identical to that of form **1**. Two bromide atoms and two acetonitrile ligands coordinate to the zinc cations forming distorted tetrahedra. The packing of the discrete molecular complexes in form **2** is completely different from that in form **1** (figure 6).

Form **1** can be prepared phase pure by crystallization from acetonitrile. In contrast, form **2** was only obtained in the presence of 2-chloropyrazine if the crystallization is performed under kinetic control but it immediately transforms into form **1**. Crystallization experiments reveal that form **1** is the thermodynamically most stable form between -40 °C and 80 °C the

boiling point of acetonitrile, whereas form **2** is metastable. On storing, the thermodynamically stable form **1** at room-temperature decomposes into zinc(II) bromide within a few hours, but in a saturated acetonitrile atmosphere it is stable over a long period. On heating form **1** all ligands are emitted in one step leading to zinc bromide.

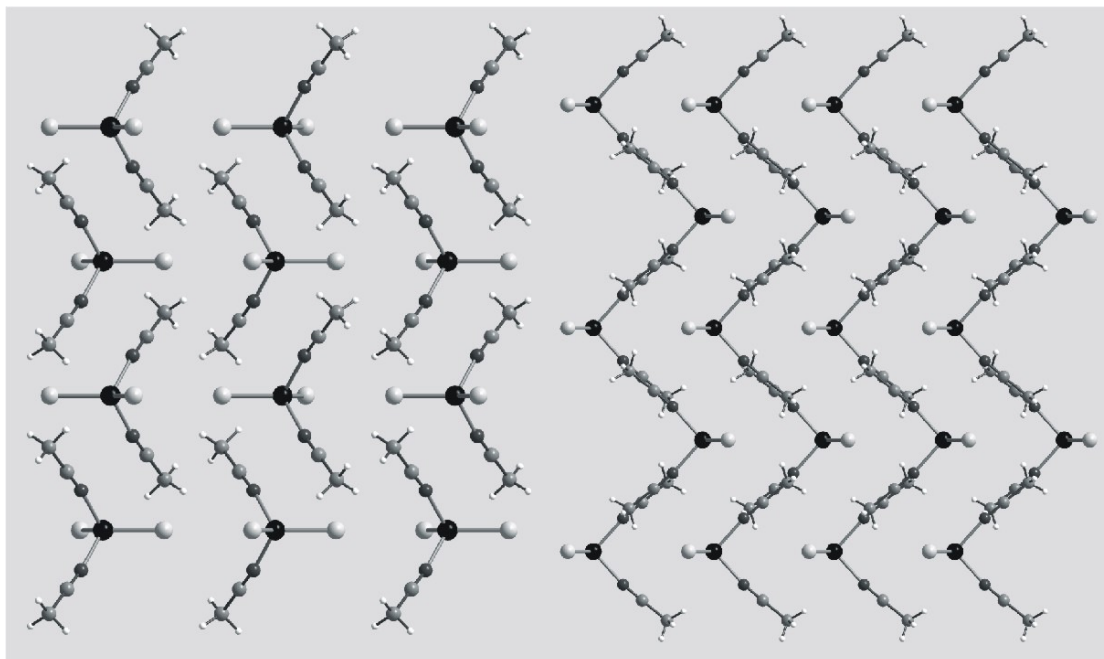


Figure 6. Crystal structures of form **1** (left) and form **2** (right) dibromo-bis(pyridazine-N) zinc(II).

In contrast the reaction of ZnI_2 and acetonitrile does not lead to the formation of polymorphic modifications of Diiodo-bis(acetonitrile-N)-zinc(II) and only one form is obtained, in which the zinc atoms are coordinated by two iodine atoms and two acetonitrile ligands (figure 7 and chapter 2.8).

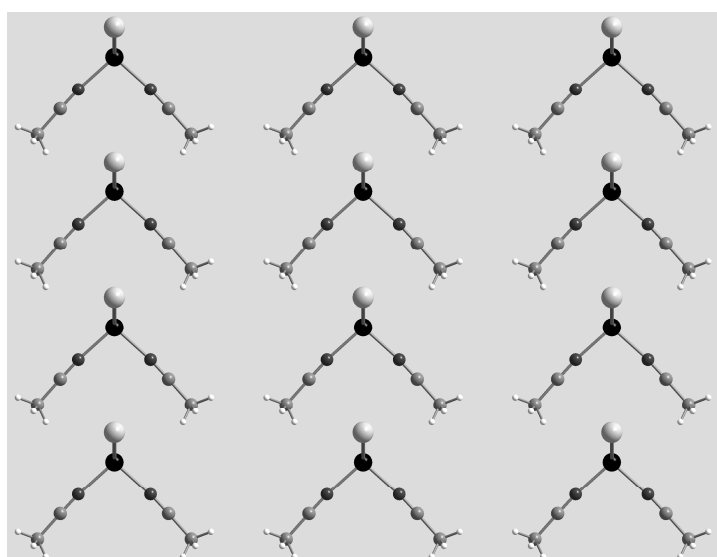


Figure 7. Crystal structure of Diiodo-bis(acetonitrile-N)-zinc(II).

One disadvantage of all the thermal decomposition reactions described above is that a part of the ligands used in the synthesis, gets irreversibly lost during decomposition. This disadvantage can be overcome by designing alternative ligand rich precursors containing additional volatile sacrificial ligands, which can be removed first, thus retaining the desired amine ligands. This was shown for the first time in the investigations described in chapter 2.6. In this work zinc(II) halides were reacted with 2-chloropyrazine in different solvents, which leads to the formation of five new coordination compounds that contain either only 2-chloropyrazine molecules as ligand or additional water molecules as donor ligands. In the ligand rich 1:2 compound di- μ -chloro-bis(2-chloropyrazine-N) zinc(II) (**1**) the zinc atom is coordinated by two 2-chloropyrazine ligands and four chloro atoms in an octahedral coordination. The zinc atoms are connected by the chloro atoms into linear chains. In the isotopic ligand rich 1:2 compounds di-bromo-bis(2-chloropyrazine-N) zinc(II) (**2**) and di-iodo-bis(2-chloropyrazine-N) zinc(II) (**3**) discrete complexes are found in which each zinc atom is coordinated by two 2-chloropyrazine ligands and two halide atoms within distorted tetrahedra (figure 8: left). The 1:1 compounds di-bromo-aqua-(2-chloropyrazine-N) zinc(II) (**4**) and di-iodo-aqua-(2-chloropyrazine-N) zinc(II) (**5**) are also isotopic and forms discrete complexes in which the zinc atoms are surrounded by two halide atoms, one 2-chloropyrazine ligand and one water molecule (figure 5: right). On heating, compounds **1** to **5** ligand deficient 1:1 and 2:1 compounds of composition $ZnX_2(2\text{-chloropyrazine})$ and $(ZnX_2)_2(2\text{-chloropyrazine})$ are observed. X-ray powder diffraction proves that the ligand deficient intermediates are the same independent if the ZnX_2L_2 ($L = 2\text{-chloropyrazine}$) or the $ZnX_2L(H_2O)$ complexes are decomposed. DFT calculations suggest that the formation of the $ZnX_2L(H_2O)$ complexes is energetically favoured and that this trend increases from chlorine to iodine.

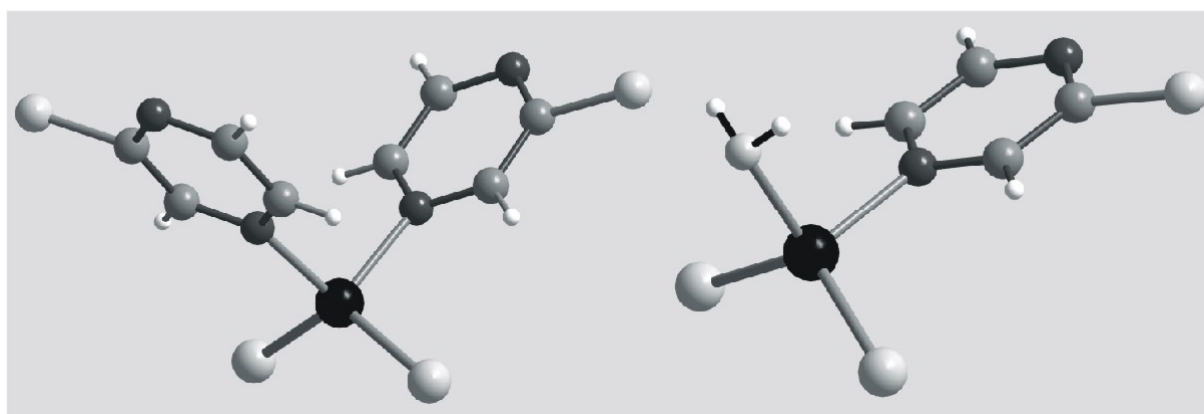


Figure 8. Crystal structure of di-bromo-bis(2-chloropyrazine-N) zinc(II) (**2**) (left) di-bromo-aqua-(2-chloropyrazine-N) zinc(II) (**4**) (right).

Summarizing, in this thesis it was proven that thermal decomposition reaction can be used as an alternative tool for the preparation of pure and quantitative amounts of ligand efficient coordination polymers and that this method can be used not only for the preparation of copper(I) halide coordination polymers.

In addition it was also shown, that thermal decomposition reactions are not only suitable to discover and prepare thermodynamic stable and metastable compounds.

One further advantage of this procedure is that practically all ligand deficient compounds can be discovered in one experiment starting from the most ligand rich compounds, which can be easily prepared if a large excess of the ligand is used in the preparation. In solution reactions, several experiments must be performed, in which different ratios of metal halide and N donor ligand are used.

The large number of compounds obtained, for example for the coordination compounds with pyrimidine, presented in chapter 2.2, clearly shows that in solution several stable and metastable species are in equilibrium which can be isolated as solids. Therefore, the rational design of new coordination polymers with defined structures is more complicated than frequently stated in the literature.

5. Appendix

5.1 List of publications

Identical Molecular Strings Woven Differently by Intermolecular Interactions in Dimorphs of *myo*-Inositol 1,3,5-Orthobenzoate.

Gaurav Bhosekar, Chebrolu Murali, Rajesh G. Gonnade, Mysore S. Shashidhar, and Mohan M. Bhadbhade. *Cryst. Growth & Design.*, 5, **2005**, 1977-1982.

Synthesis and Intramolecular Nitrile Oxide Cycloaddition of 3,5'-Ether-Linked Pseudooligosaccharide Derivatives: An Approach to Chiral Macrooxacycles.

Jhimli Sengupta, Ranjan Mukhopadhyay, Anup Bhattacharjya, Mohan M. Bhadbhade, and Gaurav V. Bhosekar. *J. Org. Chem.* **2005**, 70, 8579-8582

First enantiospecific synthesis of (+)- β -herbertenol.

Subhash P. Chavan, Mahesh Thakkar, Rajendra K. Kharul, Ashok B. Pathak, Gaurav V. Bhosekar and Mohan M. Bhadbhade *Tetrahedron*, 61, **2005**, 3873-3879.

[6+3] Cycloaddition of pentafulvenes with 3-oxidopyrylium betaine: a novel methodology toward the synthesis of 5–8 fused oxabridged cyclooctanoids

K. Syam Krishnan, V.S. Sajisha, S. Anas, C.H. Suresh, Mohan M. Bhadbhade, Gaurav V. Bhosekar and K.V. Radhakrishnan *Tetrahedron*, 62, **2006**, 5952-596.

On the Preparation of Coordination Polymers by Controlled Thermal Decomposition: Synthesis, Crystal Structures and Thermal Properties of Zinc Halide Coordination Polymers

Gaurav Bhosekar, Inke Je β and Christian Näther
Inorg. Chem., **2006**, 43, 6508-6515.

Two Polymorphic Modifications of Dibromo-bis(acetonitrile-N)-zinc(II)

Gaurav Bhosekar, Inke Je β and Christian Näther
Z. Naturforsch., **2006**, 61b, 721-726.

A redetermination of (acetonitrile- κ N)diiodozinc(II)

Gaurav Bhosekar, Inke Je β and Christian Näther
Acta Crystallogr., **2006**, E62, m315-m316.

Dibromo-bis(pyridazine-N)zinc(II)

Gaurav Bhosekar, Inke Jeß and Christian Näther
Acta Crystallogr., **2006**, E62, m1859-m1860.

Diiodo-bis(pyridazine-N)zinc(II)

Gaurav Bhosekar, Inke Jeß and Christian Näther
Acta Crystallogr., 2006, E62, m2073-m2074.

Preparation of stable and metastable coordination compounds by thermal decomposition and solution reactions: Insight into the structural, thermodynamic and kinetic aspects of the formation of coordination polymers

Christian Näther, Gaurav Bhosekar and Inke Jeß
Inorg. Chem., **2007**, 46, 8079-8087.

Synthesis, Crystal Structure and Thermal Reactivity of [ZnX₂(2-chloropyrazine)] (X = Cl, Br, I) Coordination Compounds

Gaurav Bhosekar, Inke Jeß, Nicolai Lehnert and Christian Näther
Eur. J. Inorg. Chem., **2007**, in press.

Investigations on the thermal decomposition reactions of new ZnBr₂-Pyrimidine coordination compounds

Christian Näther, Gaurav Bhosekar and Inke Jeß
Eur. J. Inorg. Chem., **2007**, in press.

Structures and Properties of three Polymorphic Modifications based on tetrahedral Building Blocks of Dichloro-bis(pyridazine-N) zinc(II)

Gaurav Bhosekar, Inke Jeß, Zdenek Havlas and Christian Näther
Cryst. Growth & Des., **2007**, in press.

5.2 Contribution to conferences

Solvent induced polymorphism in myo-inositol triols: Synthesis and X-ray structures of three triols and their polymorphs.

Gaurav Bhosekar, M. P. Sarmah, C. Murali, K. M. Sureshan Rajesh Gonnade, Mysore Shashidhar, Mohan Bhadbhade.

33rd National Seminar on Crystallography **2004**, Pune, India.

Polymorphism in Ortho Esters of *myo*- Inositol: Structures of myo-inositol 1,3,5-orthoacetate

Gaurav Bhosekar, Rajesh Gonnade, Mysore Shashidhar, Mohan Bhadbhade.

34th National Seminar on Crystallography, **2005**, Assam, India.

Synthesis, Crystal Structures and Properties of New Zinc(II) halide Coordination Polymers

Gaurav Bhosekar, Inke Jeß and Christian Näther

13th Meeting of the GDCh Section "Solid State Chemistry": Modelling in Solid State and Material Chemistry **2006**, Aachen, Germany.

Synthesis, Crystal Structures and thermal Behavior of Zn(II) halide Pyrimidine Coordination Polymers

Gaurav Bhosekar, Inke Jeß und Christian Näther

36th National Seminar on Crystallography **2007**, Chennai, India

Investigations on the trimorphism of dichlorobis(pyridazine-N)zinc(II)

Gaurav Bhosekar, Inke Jeß and Christian Näther

14th Meeting of the German Crystallographic Society, **2007**, Bremen, Germany.

Polymorphic modifications of dichloro-bis(pyridazine-N) zinc(II)

Gaurav Bhosekar, Inke Jeß and Christian Näther

10th Meeting of the North German Universities, **2007**, Bremen, Germany.

5.3 Scientific lectures

Thermal Decomposition Reactions for the Preparation of New Zinc(II) Coordination Polymers

Gaurav Bhosekar, Inke Jeß and Christian Näther

9th Meeting of the North German Universities, **2006**, Warnemünde.

5.4 Resume

GAURAV V. BHOSEKAR

Institut für Anorganische Chemie,
der Christian-Albrechts-Universität zu Kiel,
Otto-Hahn-Platz 6/7, D-24098,
Kiel, Germany.
Tel: 0049-431-880 Extn. 5546
E-mail: gbhosekar@ac.uni-kiel.de

Nationality	Indian.
July-31-1979.	Date of Birth. (Barshi, Solapur)
Marital status	Unmarried.
June 1997 - June 2000	Bachelor of Science in Chemistry, Shivaji University, Maharashtra, India.
June 2000 - June 2003	Master of Science in Industrial Chemistry, Shivaji University, Maharashtra, India.
July 2002 - June 2003	Plant operator (Industrial apprenticeship) Balaji Amines Ltd, Solapur, Maharashtra, India.
Sept. 2003 – Aug. 2005	Research Student (Project assistant). National Chemical Laboratory Pune, Maharashtra, India. Project: Guest dependent polymorphism. Supervisor: Dr. M.M. Bhadbhade.
October 2005-till date	PhD student. Christian-Albrechts Universität zu Kiel, Germany. Title of thesis: Inorganic solid state aspects of the coordination polymers: synthesis, structure and properties of new transition metal complexes. Supervisor: PD Dr. C. Näther.

5.4 Acknowledgements

Personally, I believe learning is a never-ending process. During my stay here, I have learned a lot of scientific and non-scientific things. It was a great learning experience while working with PD Dr. Christian Näther my PhD supervisor. The way he trained me in crystallography is marvellous. The scientific discussions with Dr. Näther were indeed delightful and informative. I am really glad for the efforts he took for me. For this, I would like to thank Prof. Bensch who introduced me to Dr. Näther.

This work would not have been possible without the wonderful support lent by my colleagues and friends, Viktor Suitchmezian, Beatrix Seidlhofer, Jing Wang and Elena Antonova.

I would also like to gratefully acknowledge the support of some very special people. The friendship that we all share has been immensely encouraging. I thank all these friends - Chandrashakher Kulkarni, Harun Shaikh, Dr. Amit Kulkarni, Yashodhan Gokhale, Dr. Samir Chakali, Ankush Mane, Mohan Wadekar, Dr. Atul Deshpande and Nicole Pienack.

I thank Ms. Inke Jeß for the endless effort she took during the single crystal diffraction measurements. I am also grateful to Mrs. Ute Sobotta and Mrs. Cornelia Schilz for helping me with the official paperwork. I am very thankful to State of Schleswig-Holstein and the Deutsche Forschungsgemeinschaft for the financial support they offered to this work.

I am also very pleased to thank Dr. M.M. Bhadbhade for his moral support and all the well-wishers too, from the National Chemical Laboratory, Pune.

Last but not the least, most importantly I would thank my parents whose blessings and love helped me to reach here. I am also grateful to my cousin brother Vinayak Gokhale, who has always stood by me to make my life worthier.

With the support and affection of all of you, I would surely gather more knowledge and perform better every time. *Cheers!!!*